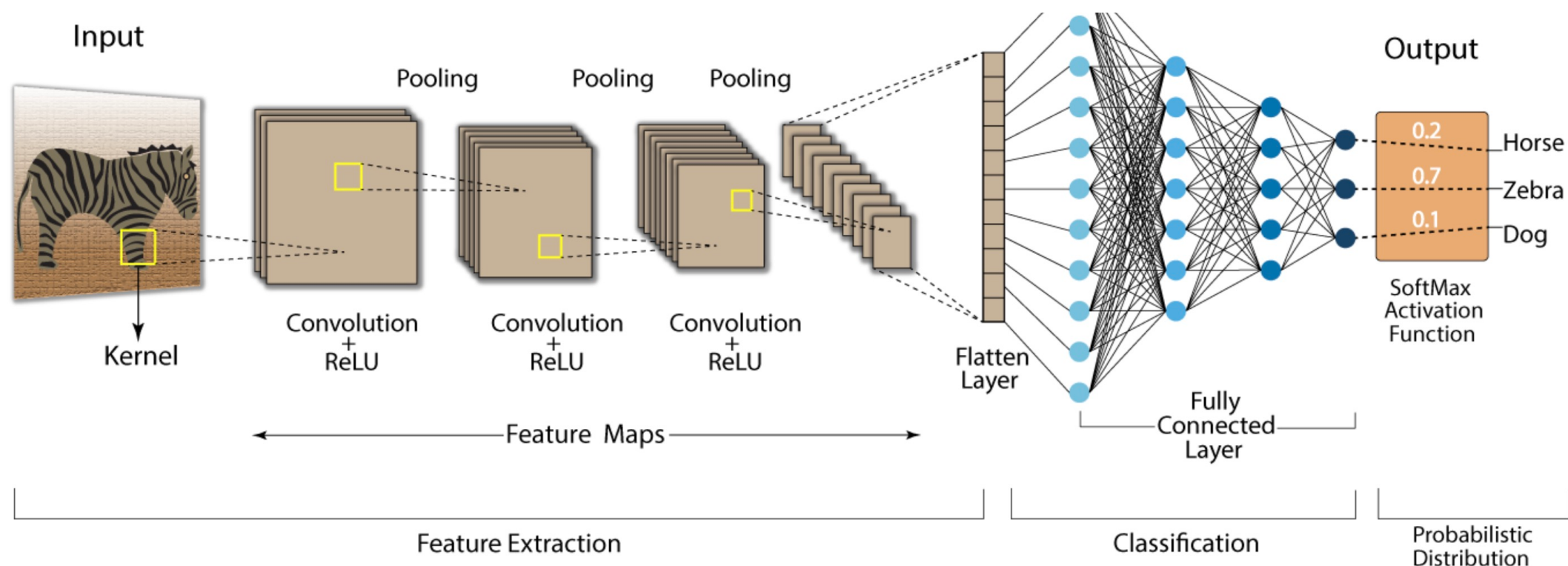


On the Shift Invariance of Max Pooling Feature Maps in CNN

joint work with H. Leterme, K. Alahari et V. Perrier

Kévin Polisano

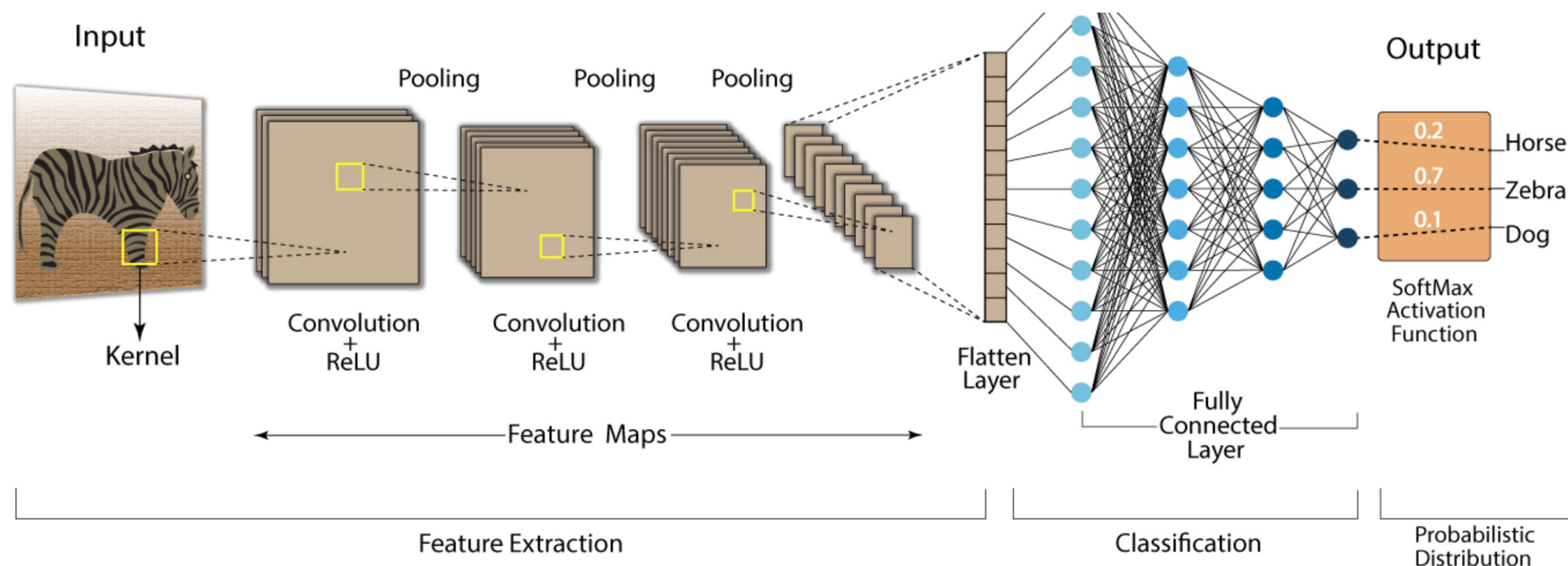
Convolutional neural networks



Source : <https://developersbreach.com/convolution-neural-network-deep-learning/>

Convolutional neural networks

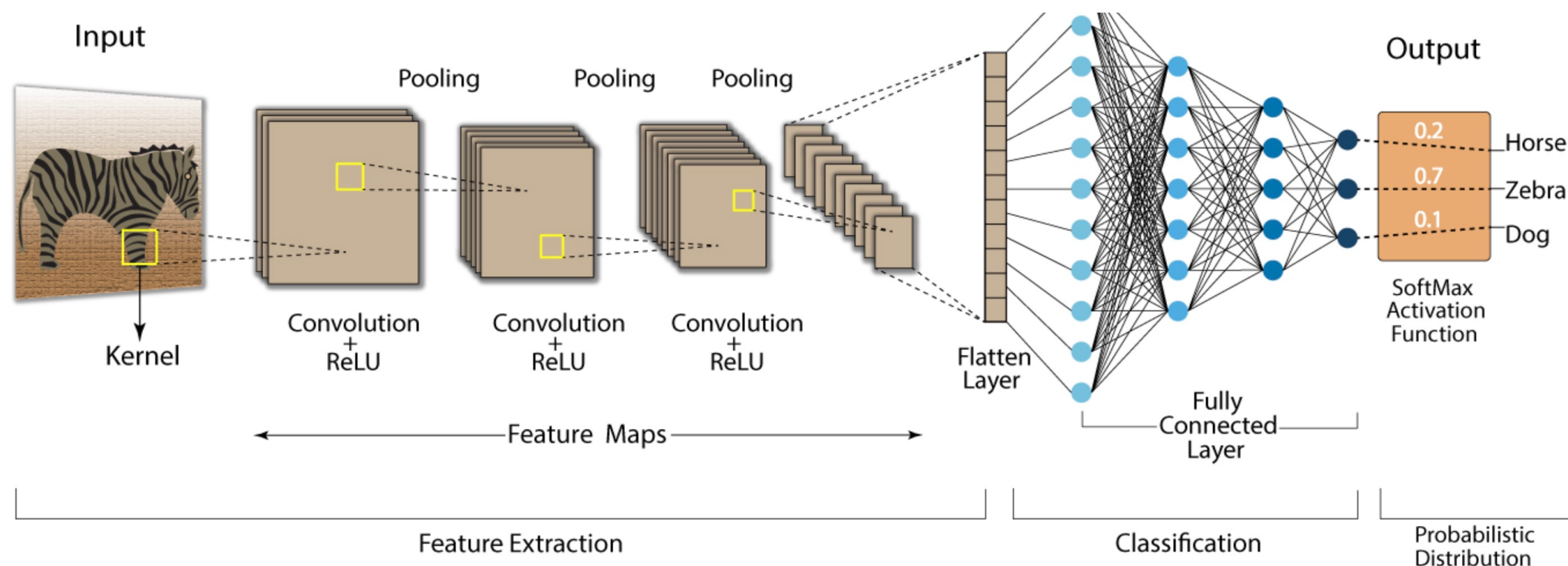
- Image classification: feature vectors are fed into a linear classifier



Source : <https://developersbreach.com/convolution-neural-network-deep-learning/>

Convolutional neural networks

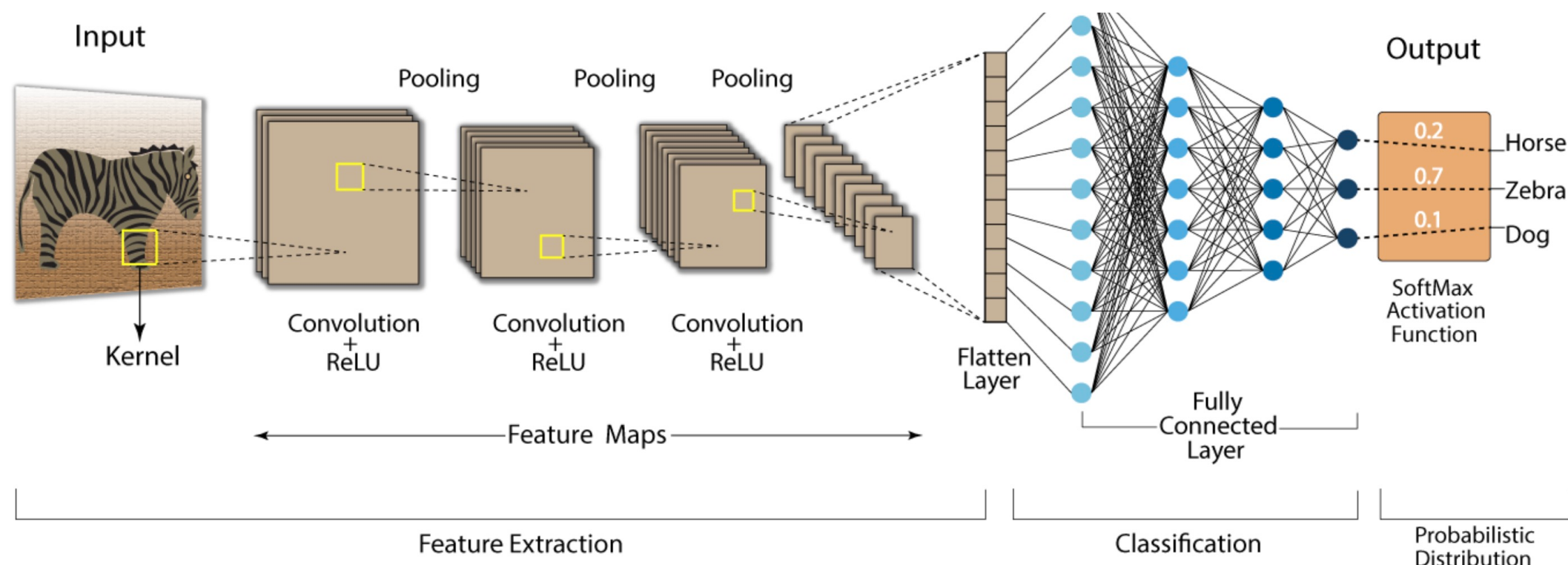
- Image classification: feature vectors are fed into a linear classifier
- Desired property of CNN: to remain invariant to small translations



Source : <https://developersbreach.com/convolution-neural-network-deep-learning/>

Convolutional neural networks

- Image classification: feature vectors are fed into a linear classifier
- Desired property of CNN: to remain invariant to small translations
- Are extracted features maps stable to translations?



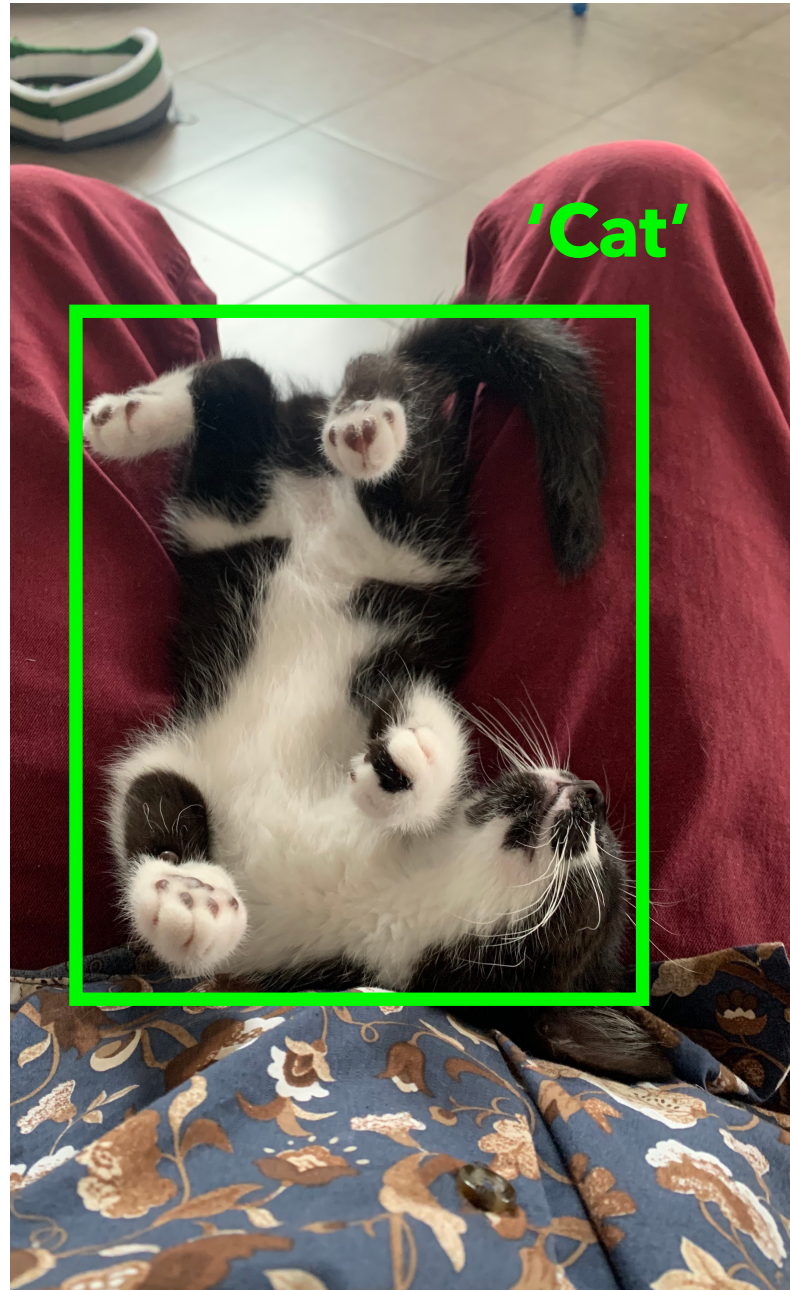
Source : <https://developersbreach.com/convolution-neural-network-deep-learning/>

Are CNNs shift-invariant?



My cat Ada

Are CNNs shift-invariant?



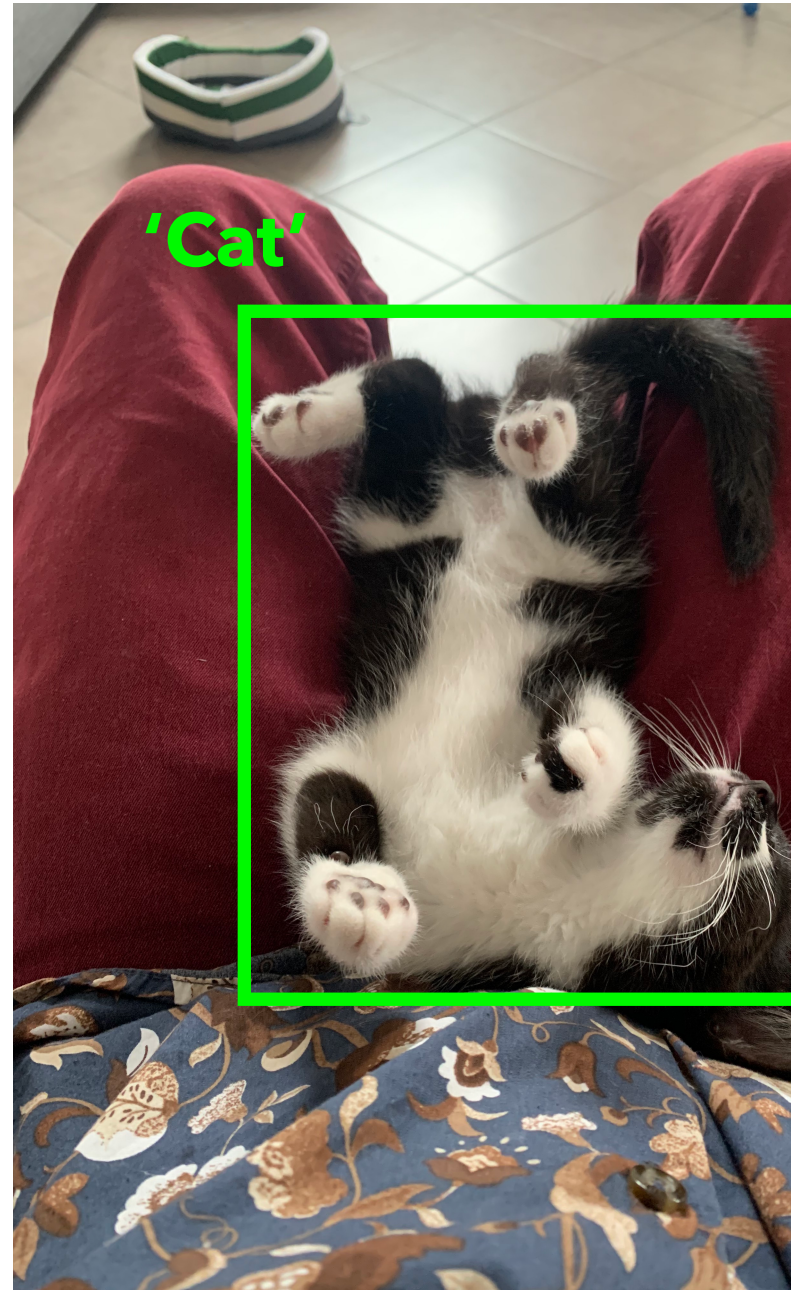
Are CNNs shift-invariant?



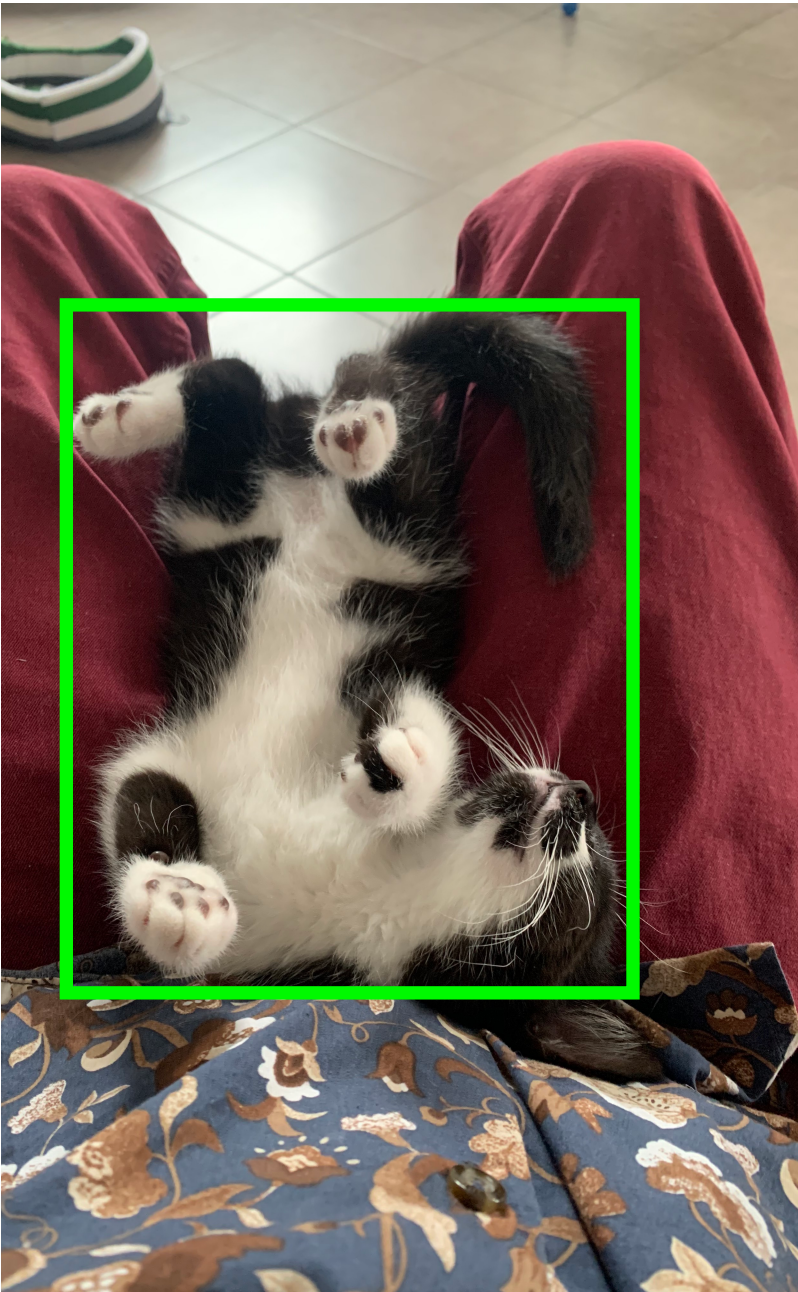
Are CNNs shift-invariant?



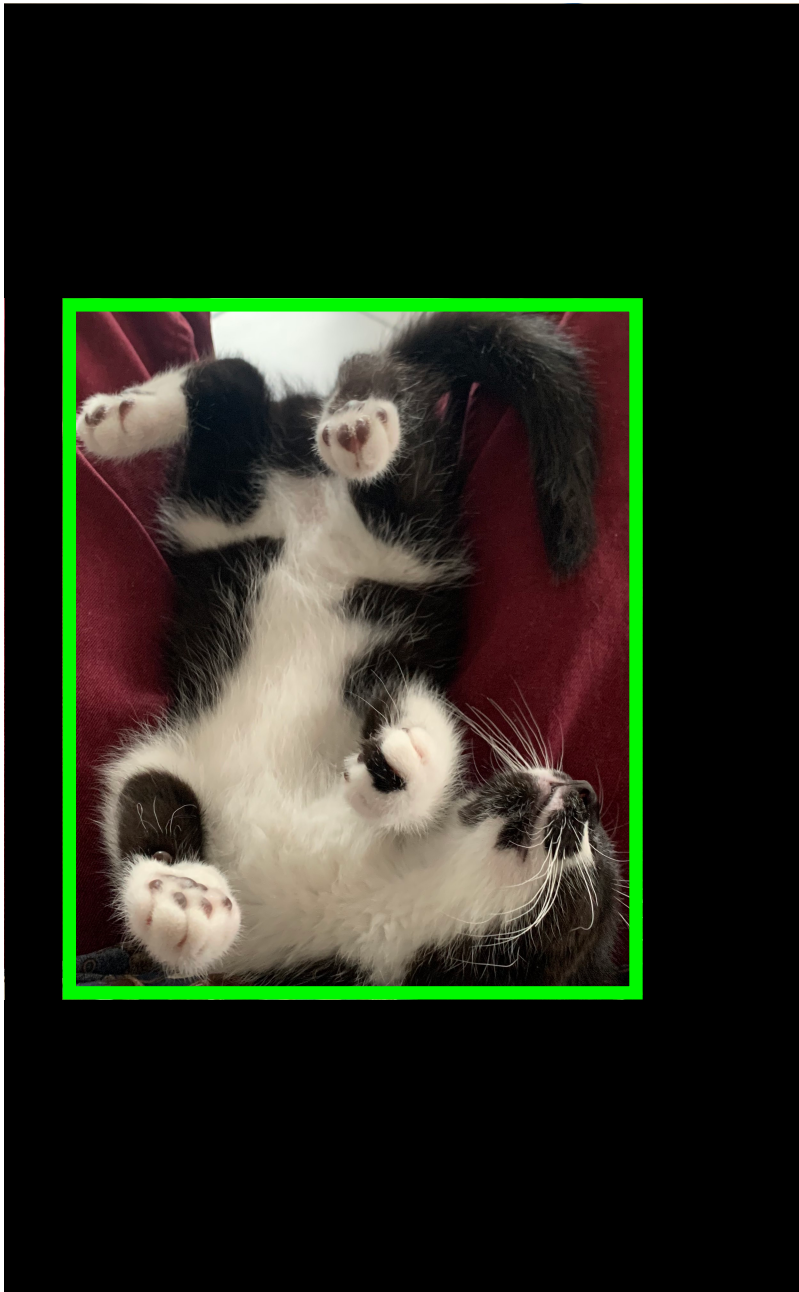
Are CNNs shift-invariant?



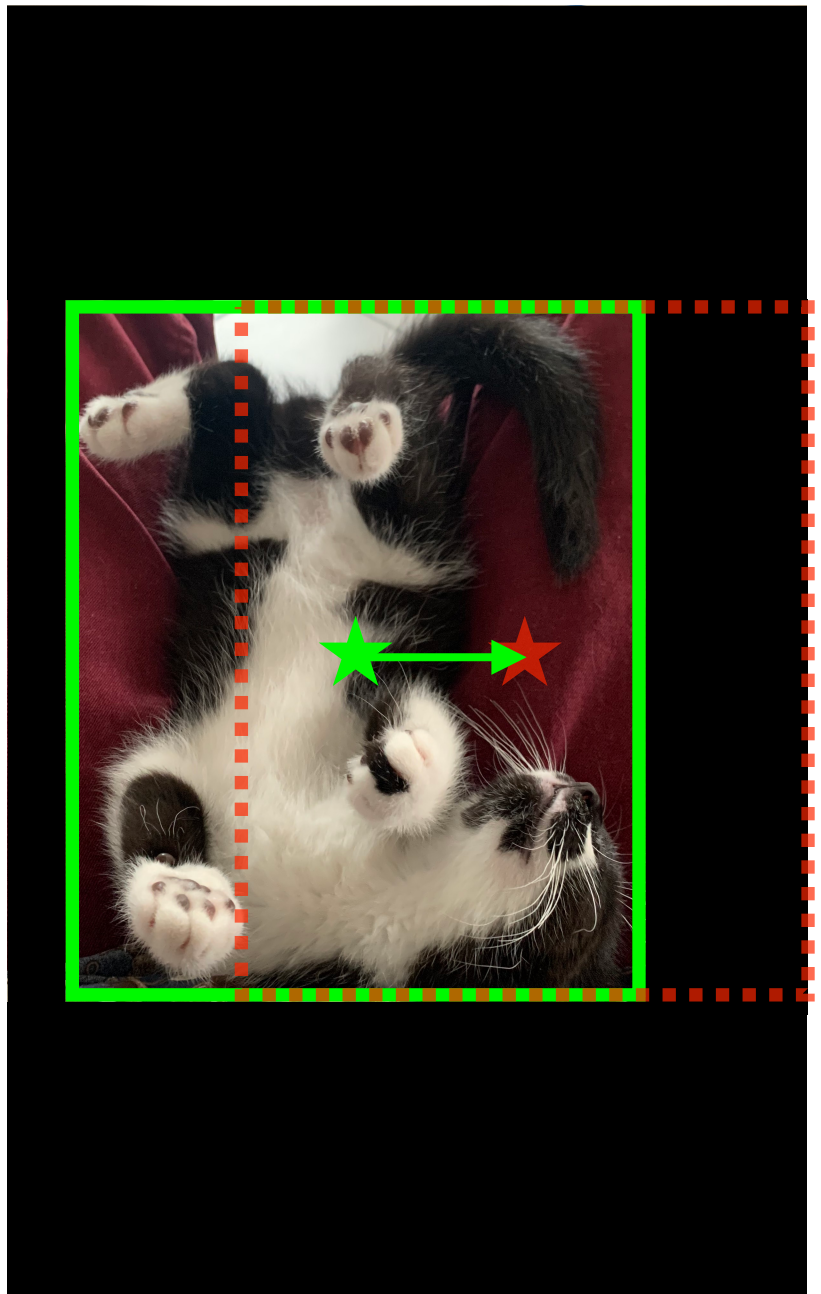
Are CNNs shift-invariant?



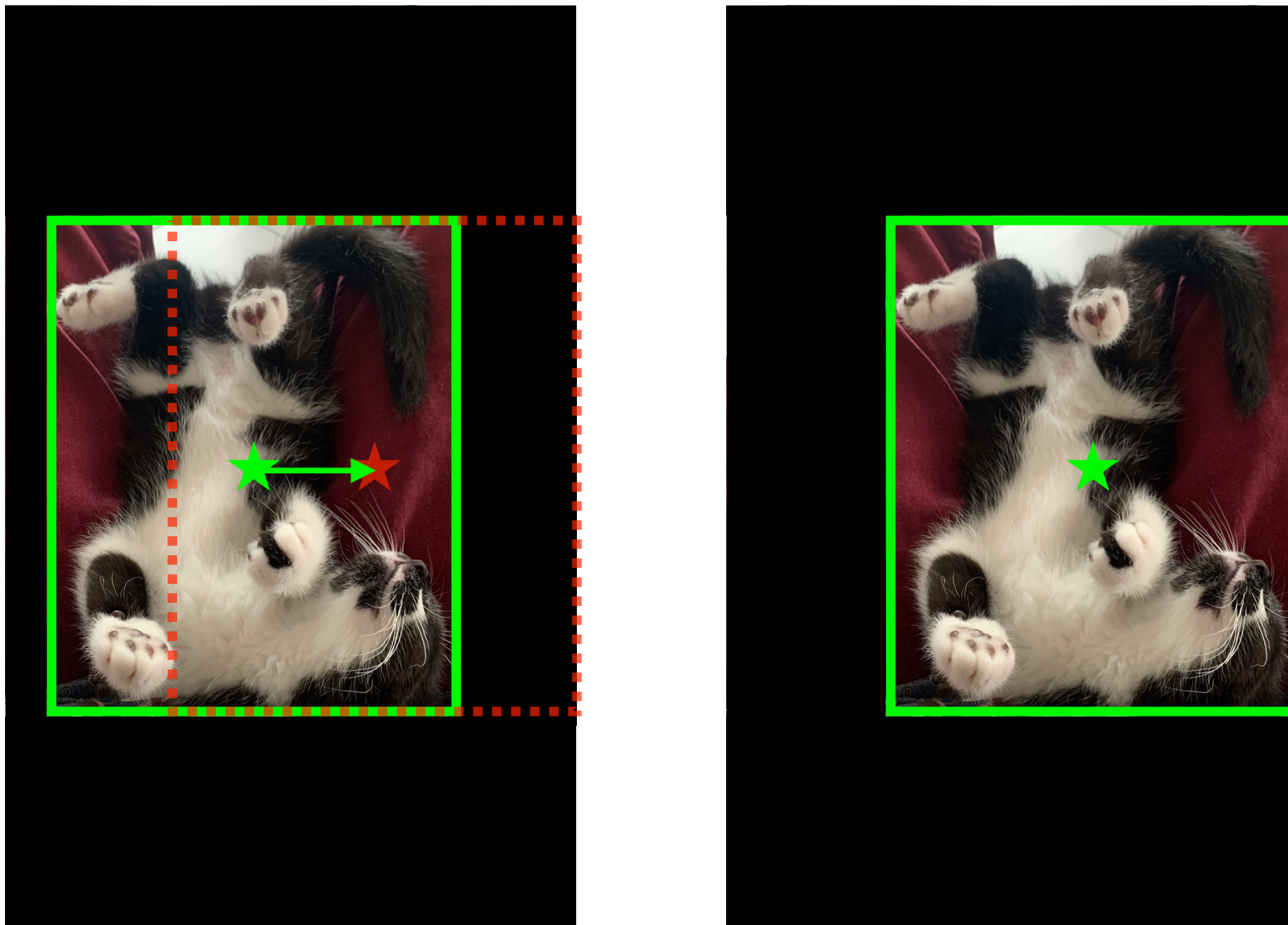
Are CNNs shift-invariant?



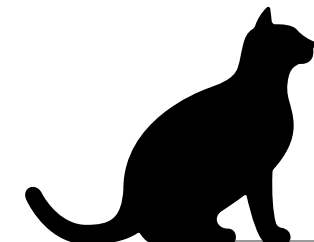
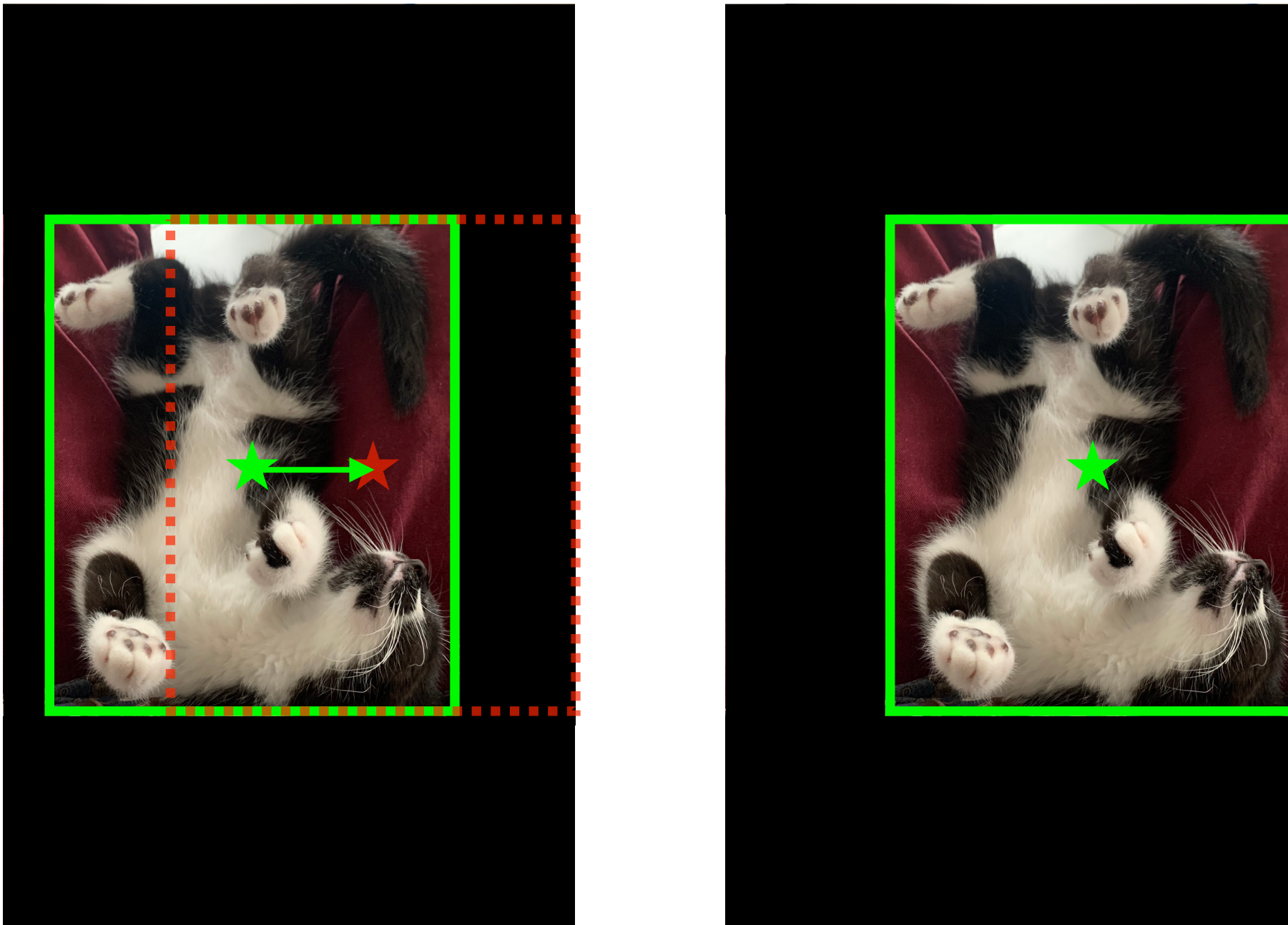
Are CNNs shift-invariant?



Are CNNs shift-invariant?

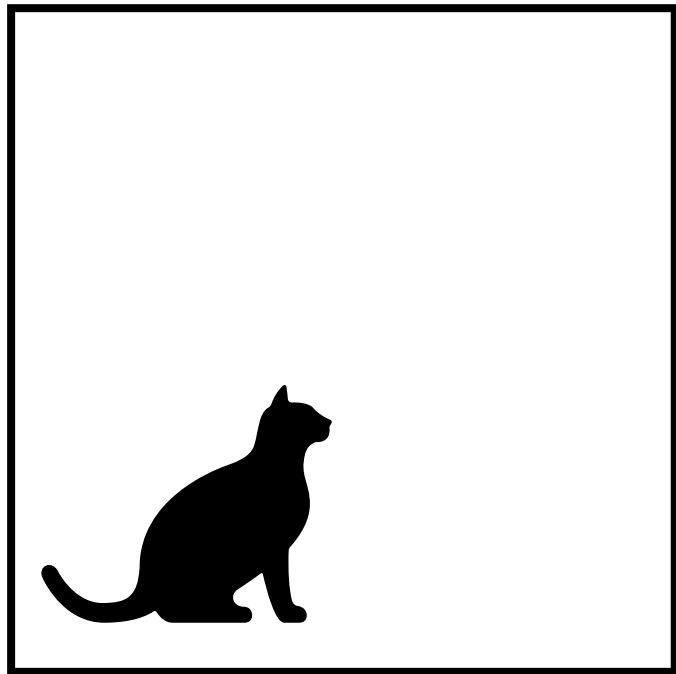


Are CNNs shift-invariant?



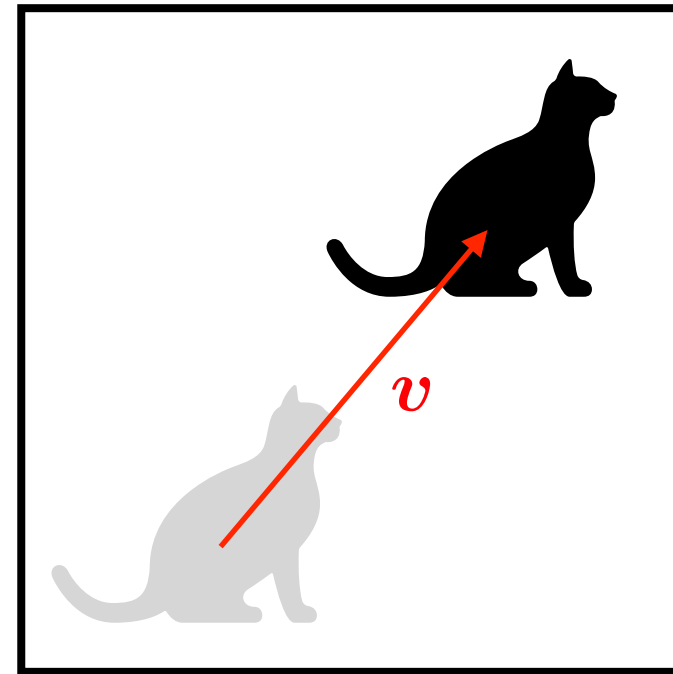
Shift invariance

Input image X



Output $f(X) = 1$

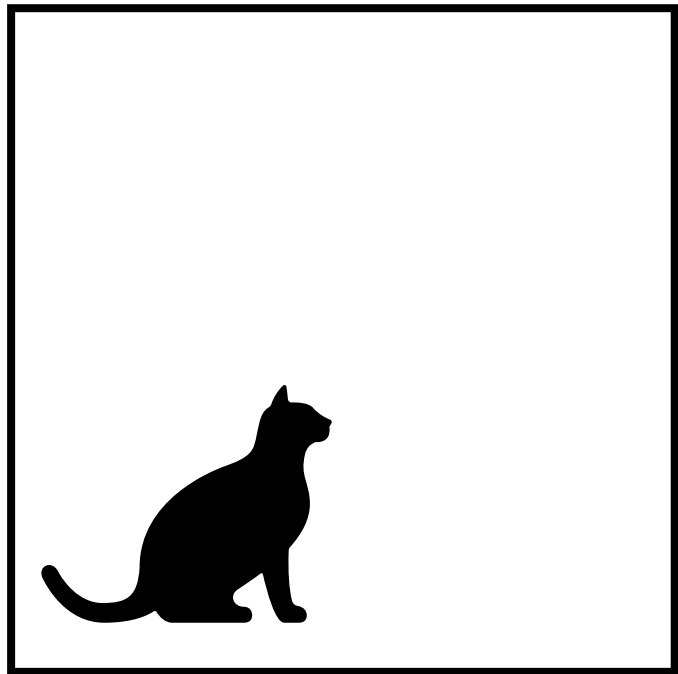
Shifted input $\mathcal{T}_v X$



Output $f(\mathcal{T}_v X) = 1$

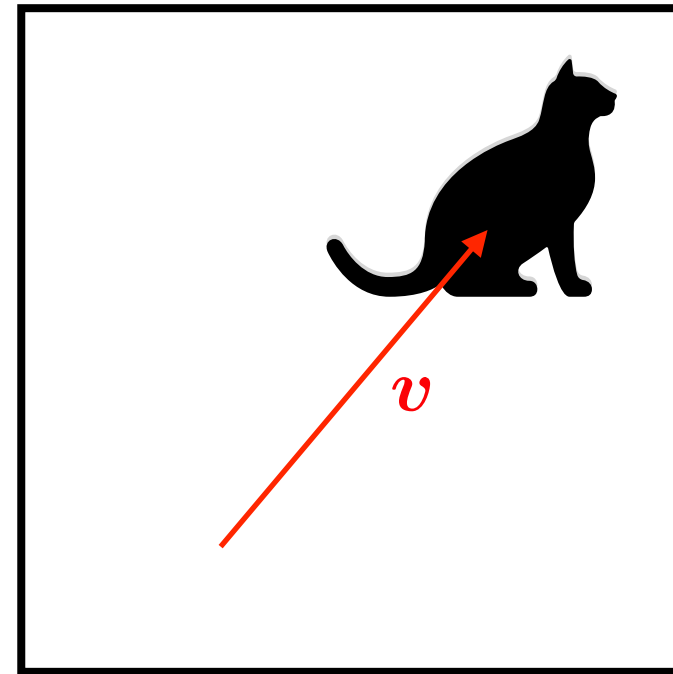
Shift invariance

Input image X



Output $f(X) = 1$

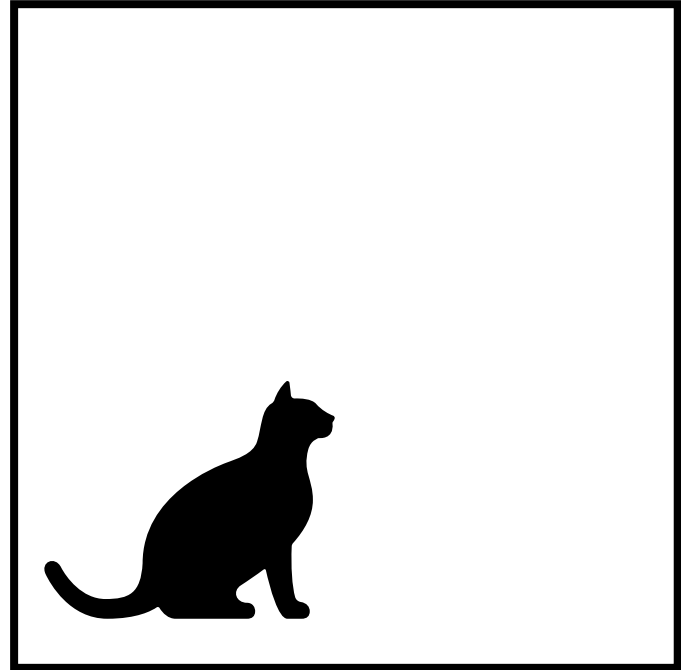
Shifted input $\mathcal{T}_v X$



Output $f(\mathcal{T}_v X) = 1$

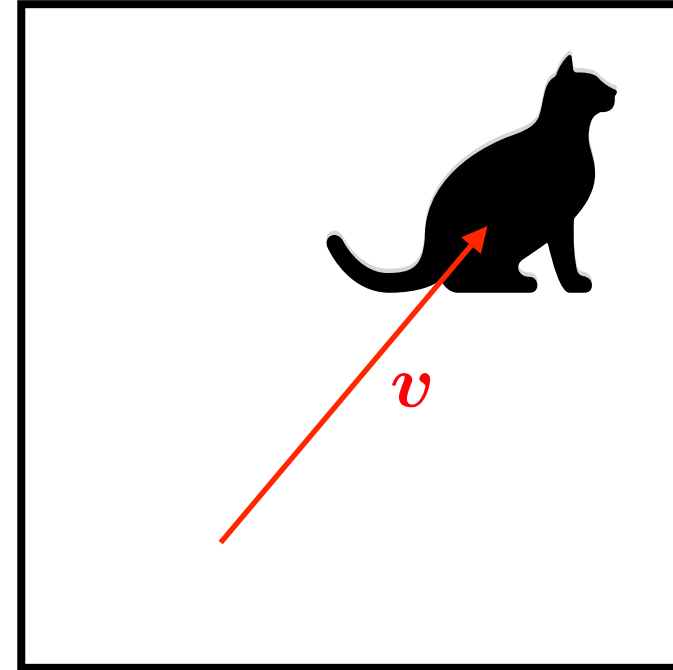
Shift invariance

Input image X



Output $f(X) = 1$

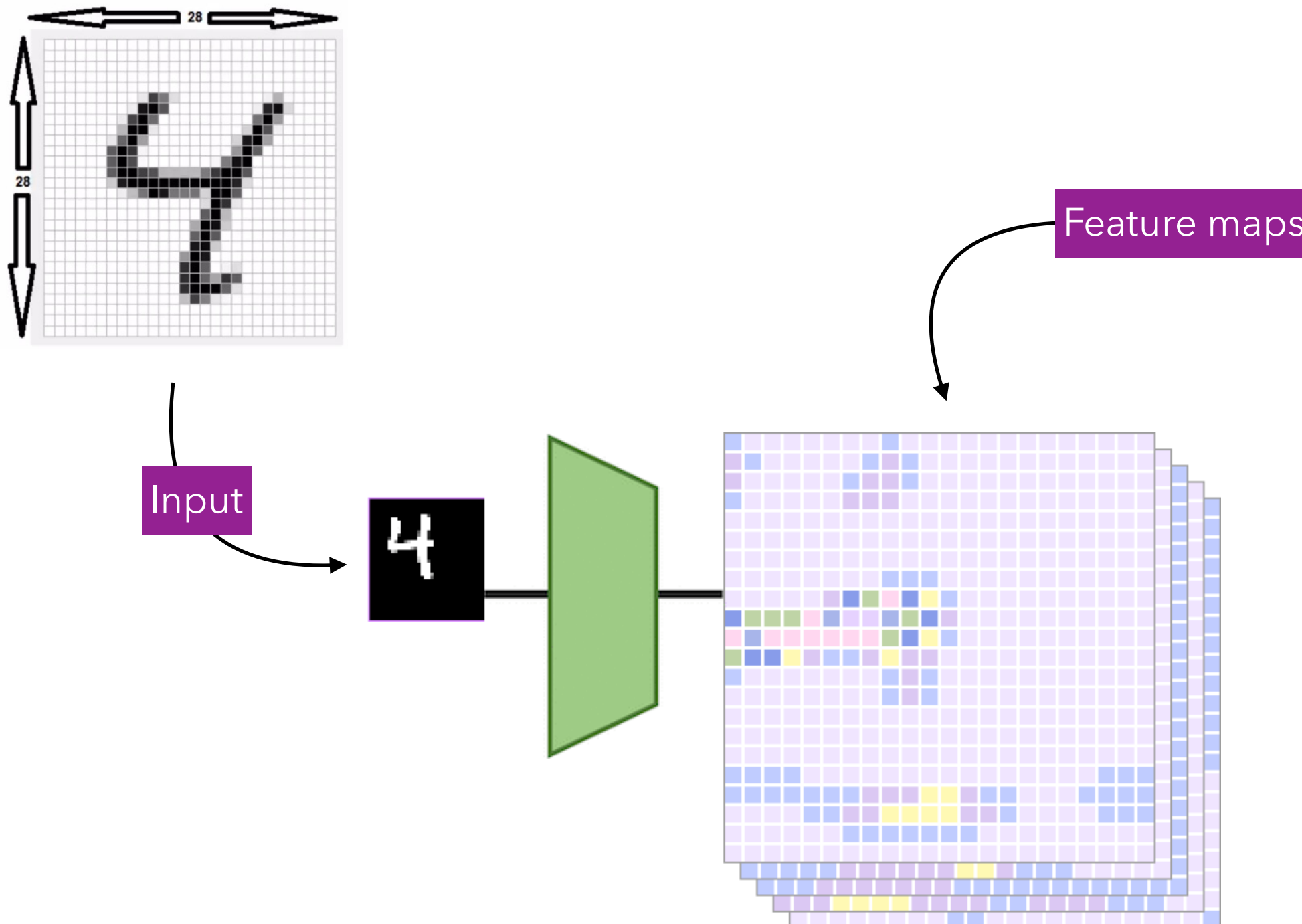
Shifted input $\mathcal{T}_v X$



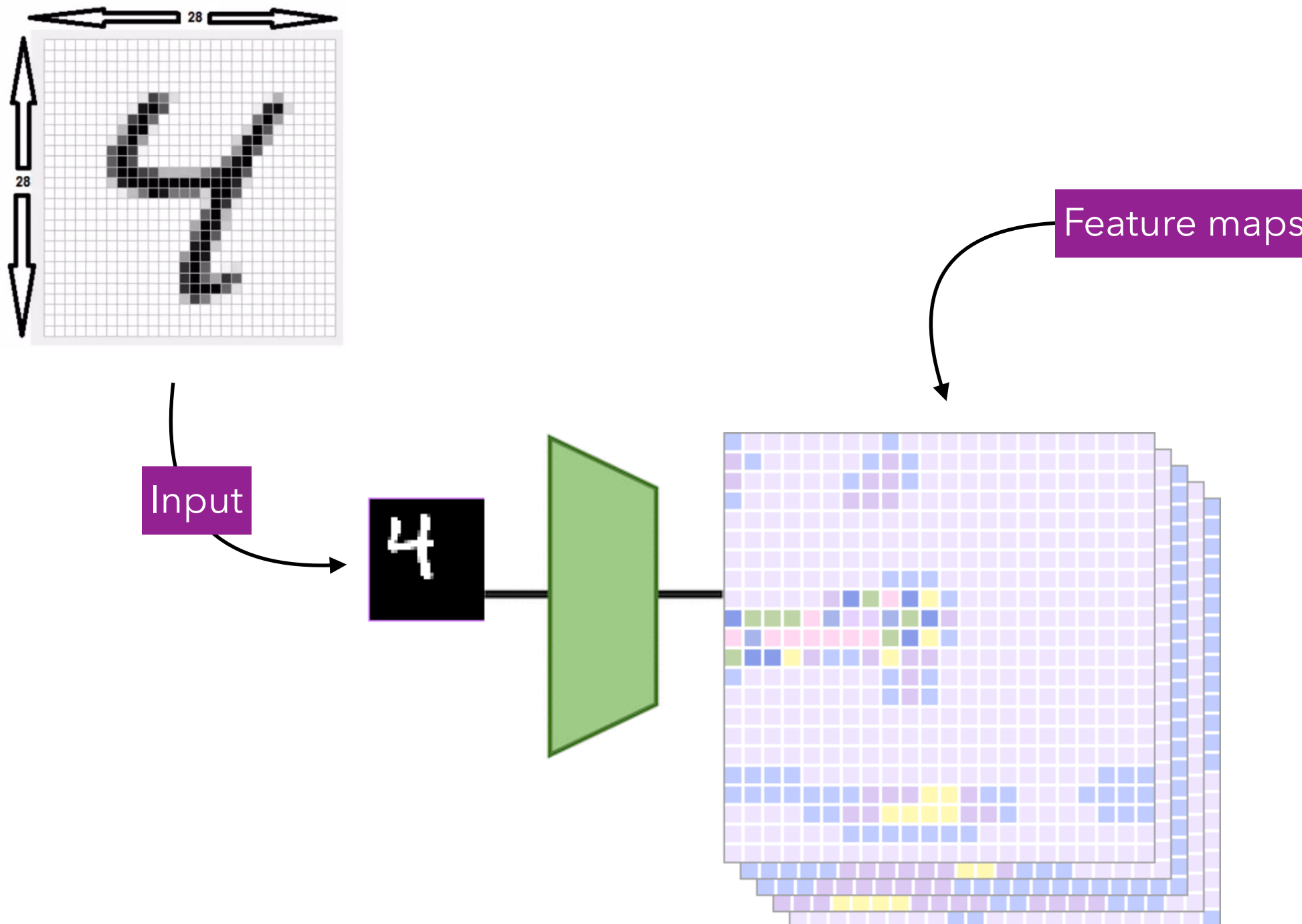
Output $f(\mathcal{T}_v X) = 1$

Shift invariance \neq Equivariance

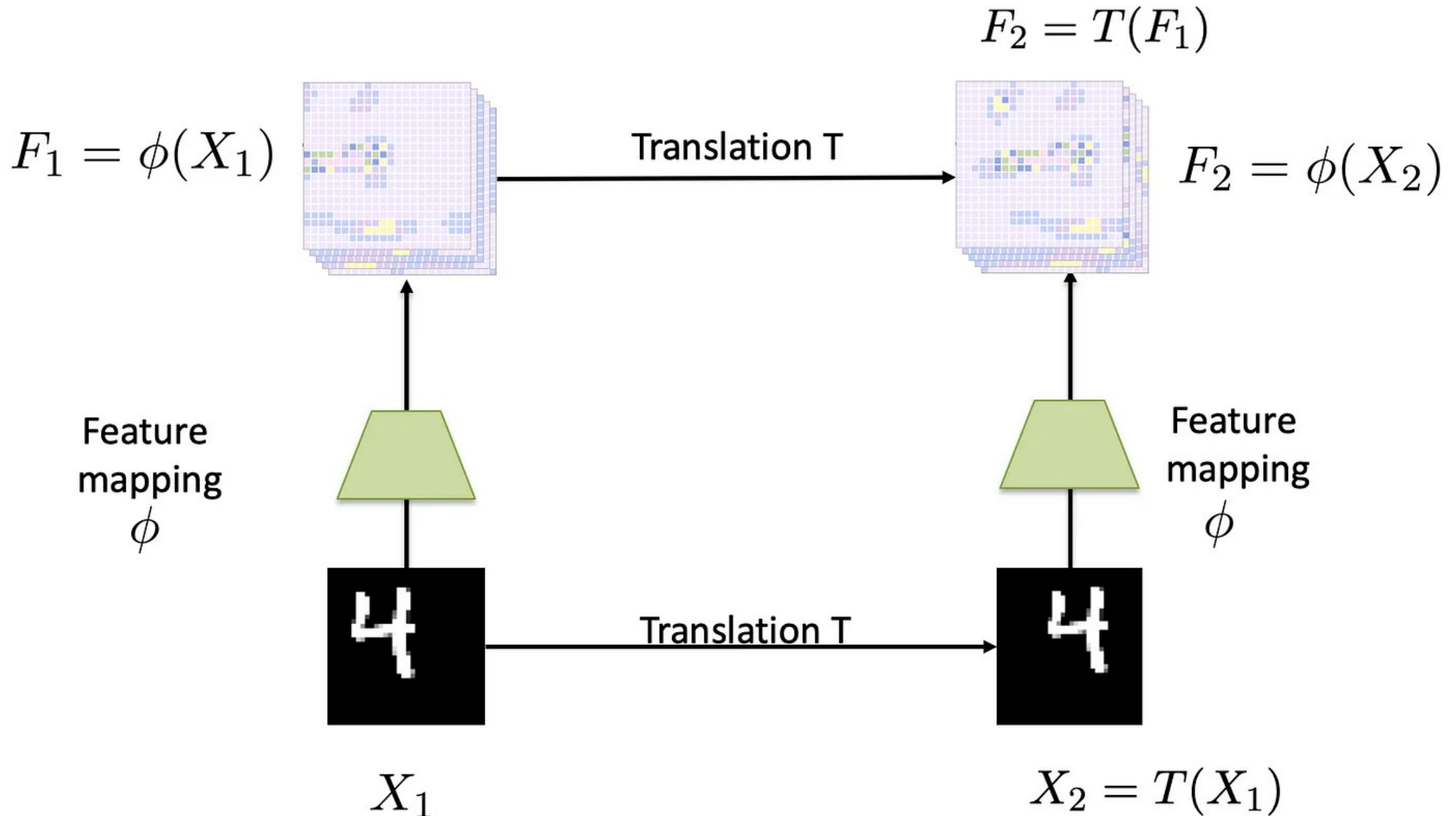
Shift equivariance



Shift equivariance

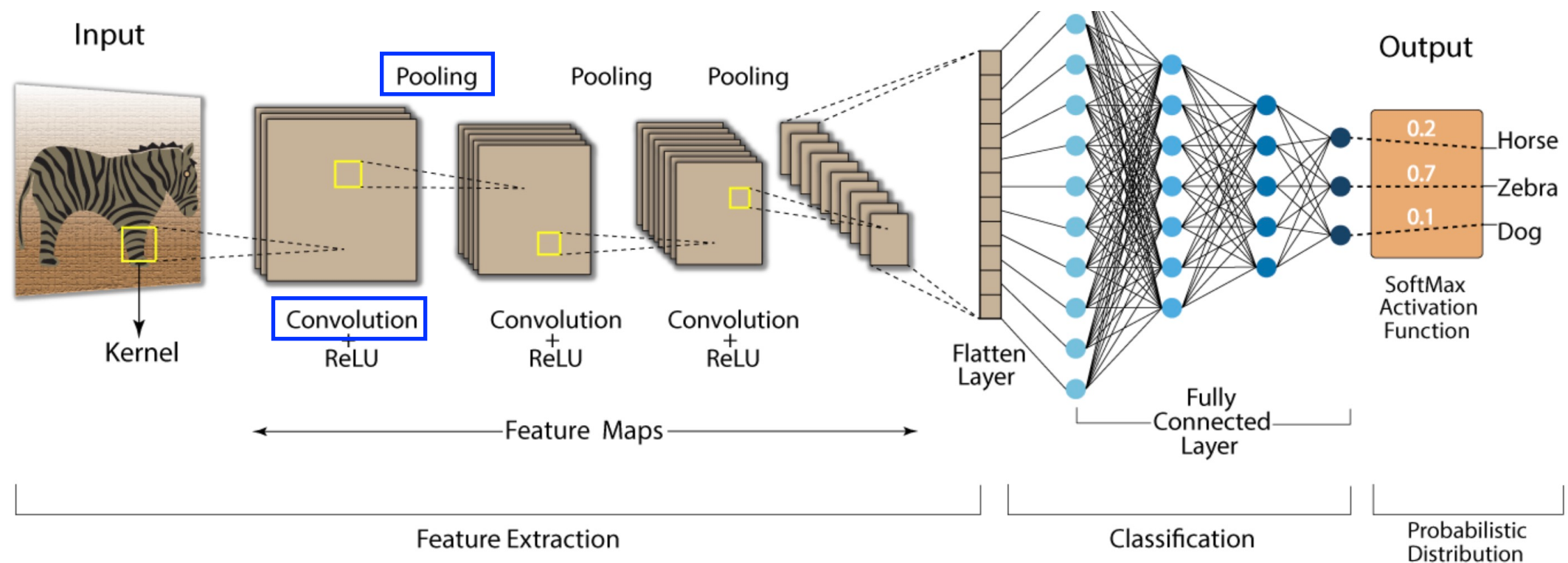


Shift equivariance



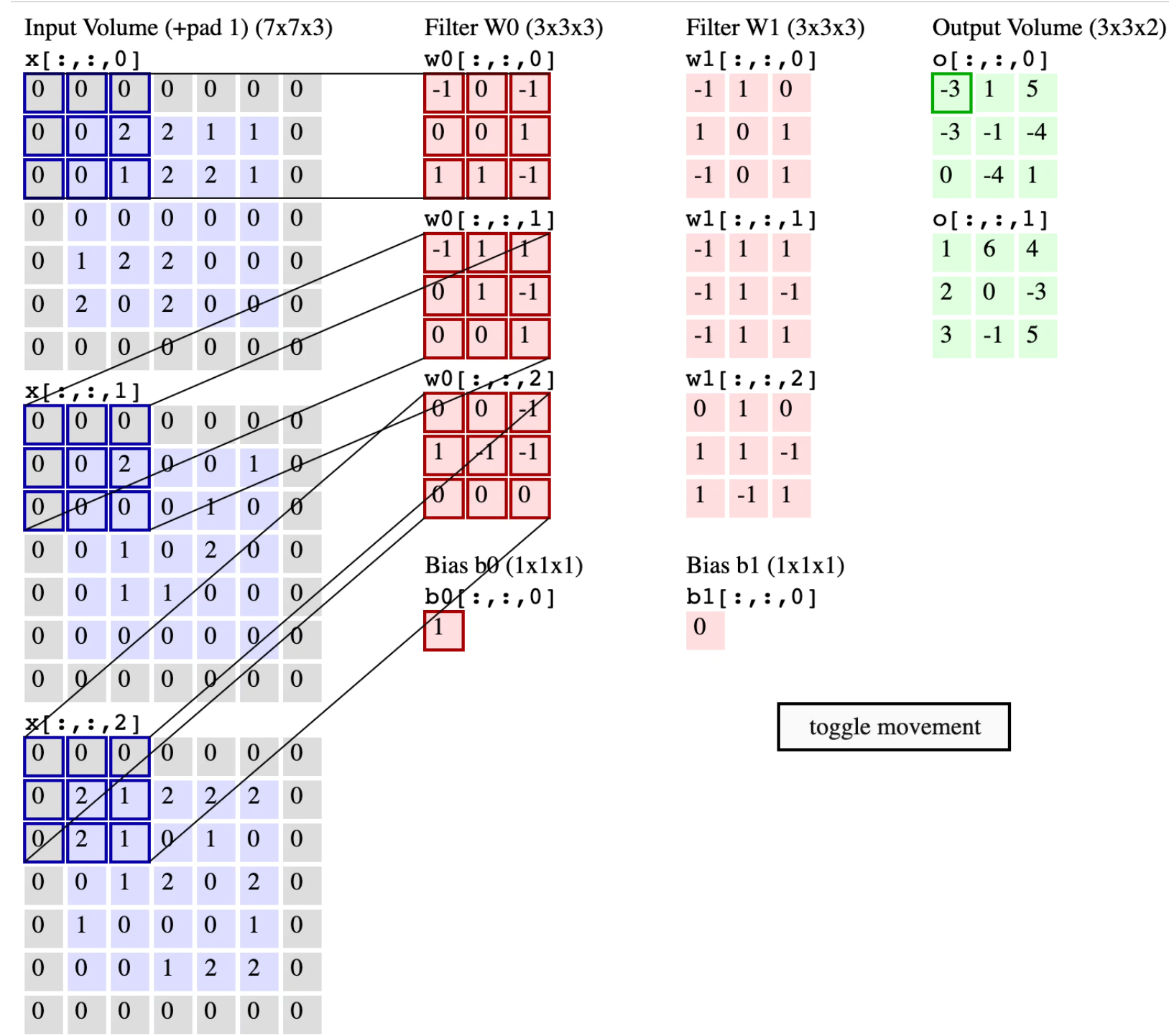
Source : <https://chriswolfvision.medium.com/what-is-translation-equivariance-and-why-do-we-use-convolutions-to-get-it-6f18139d4c59>

Convolution & Max Pooling invariance ?



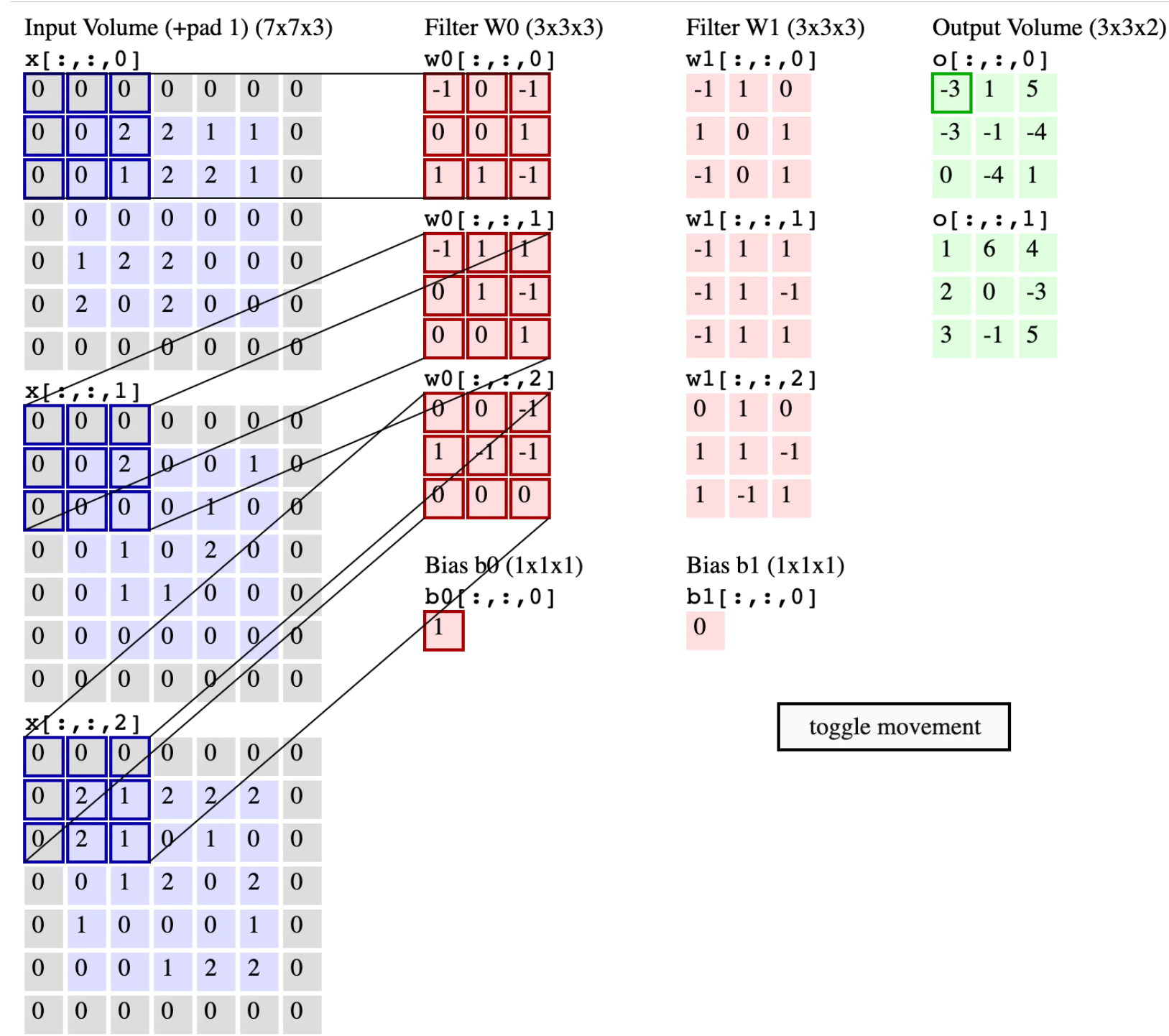
Source : <https://developersbreach.com/convolution-neural-network-deep-learning/>

Convolutional layers in CNN



Source : <https://cs231n.github.io/convolutional-networks/>

Convolutional layers in CNN

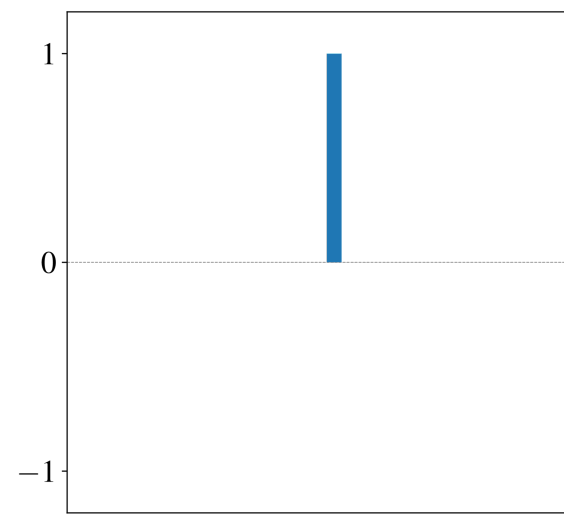


Source : <https://cs231n.github.io/convolutional-networks/>

Convolutions are shift-equivariant

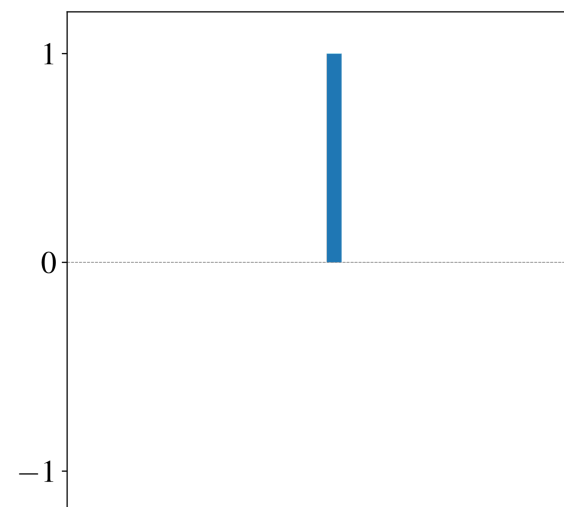


Convolutions are shift-equivariant

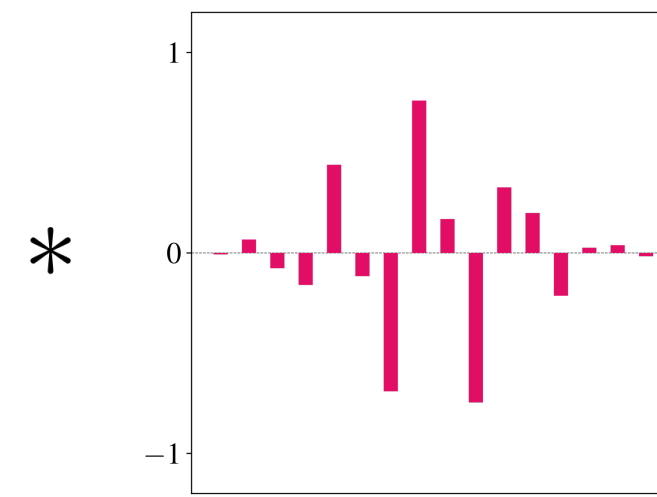


Input signal

Convolutions are shift-equivariant

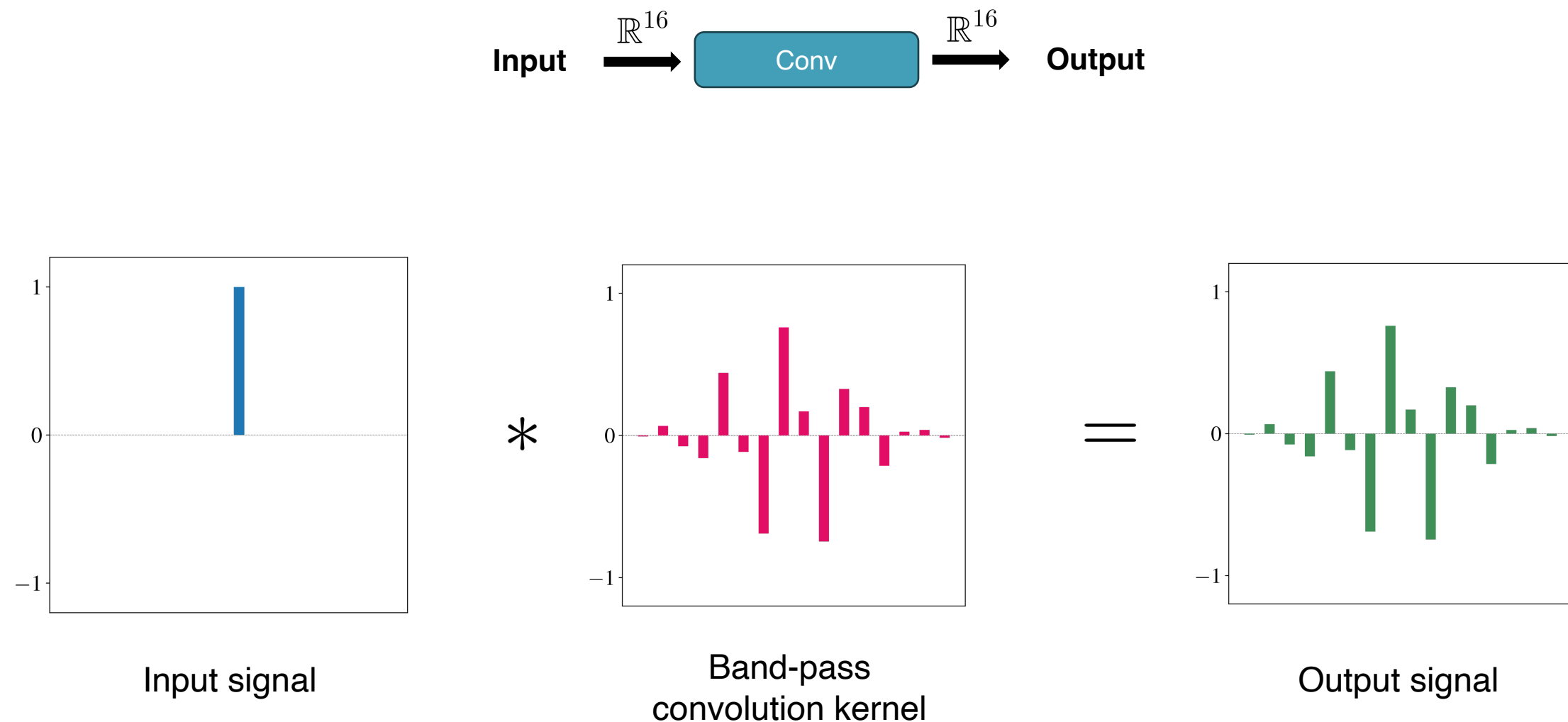


Input signal

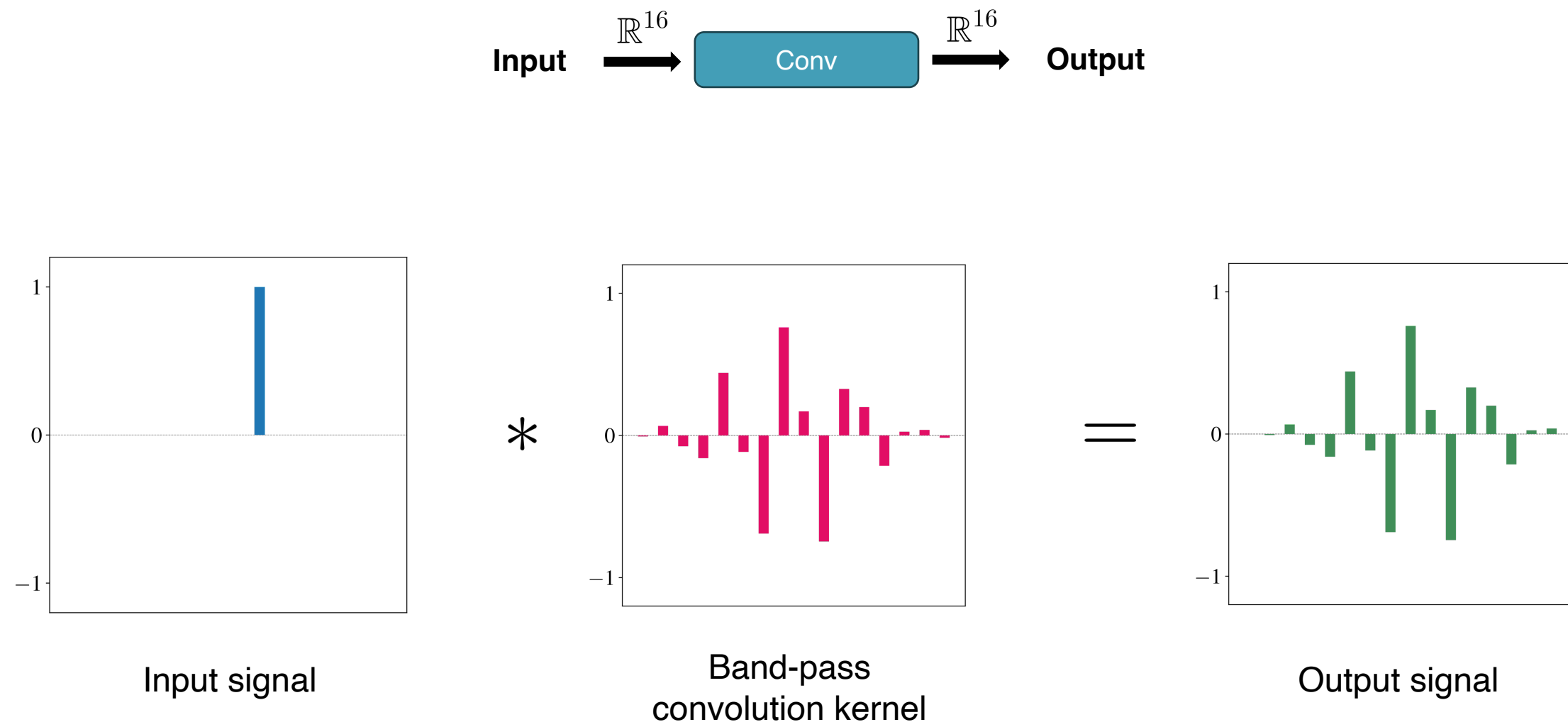


Band-pass convolution kernel

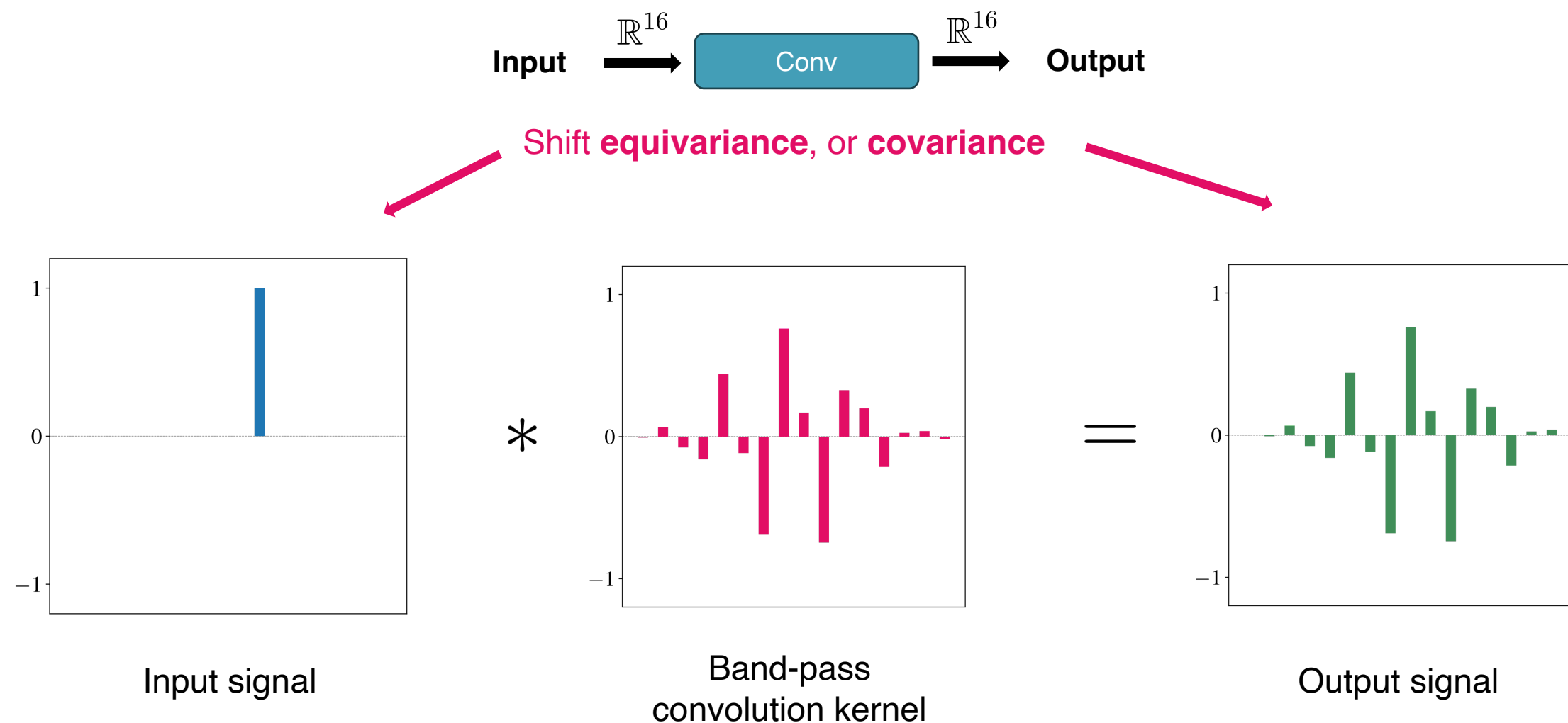
Convolutions are shift-equivariant



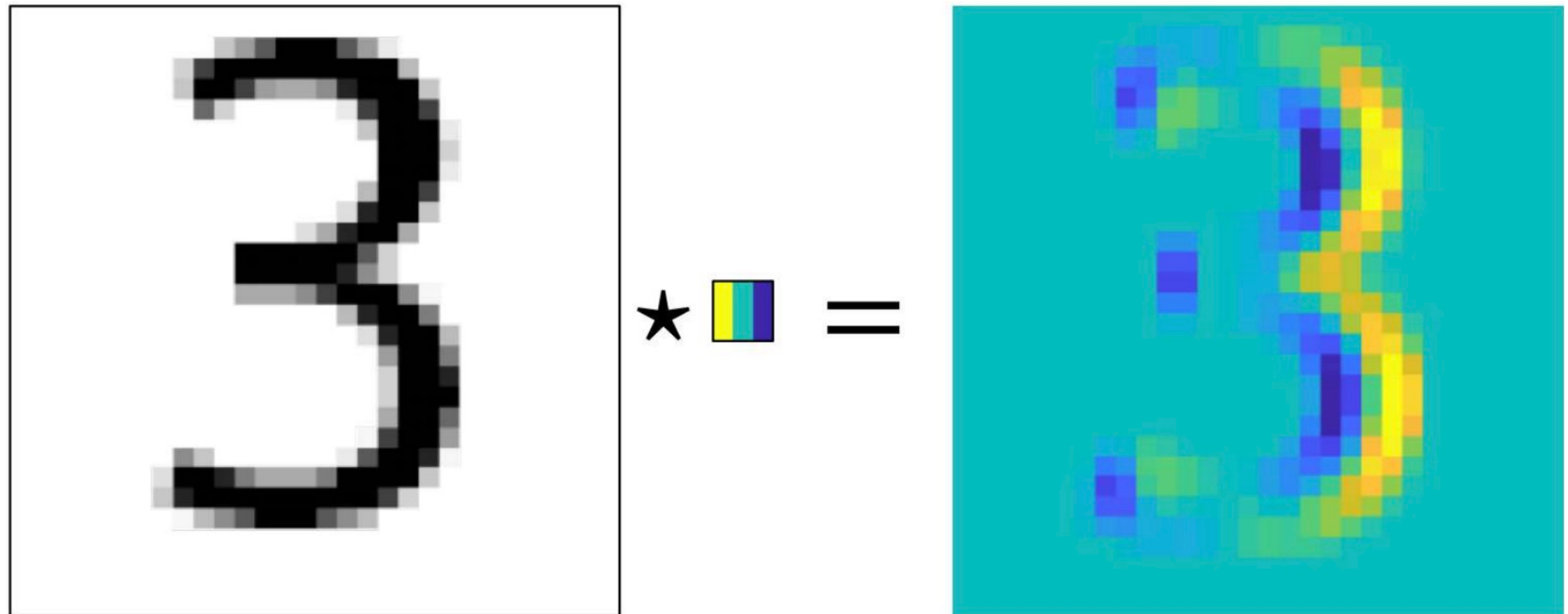
Convolutions are shift-equivariant



Convolutions are shift-equivariant

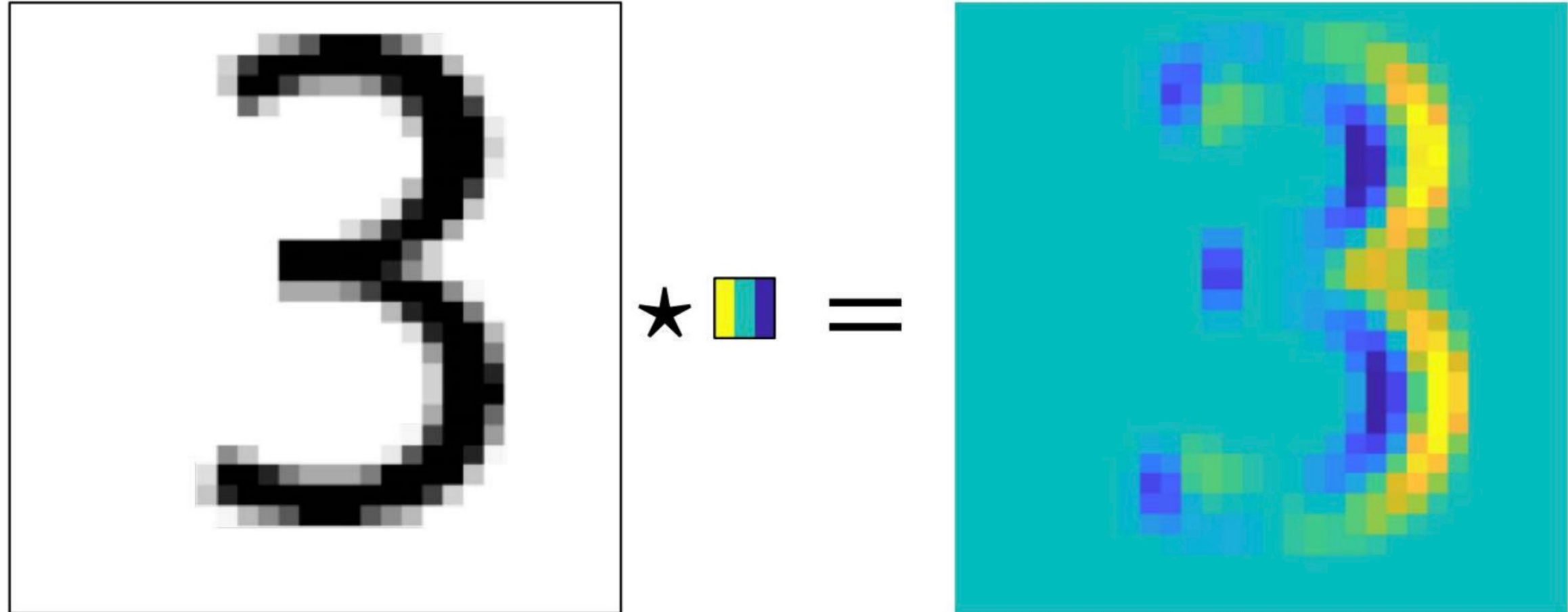


Convolutions are shift-equivariant



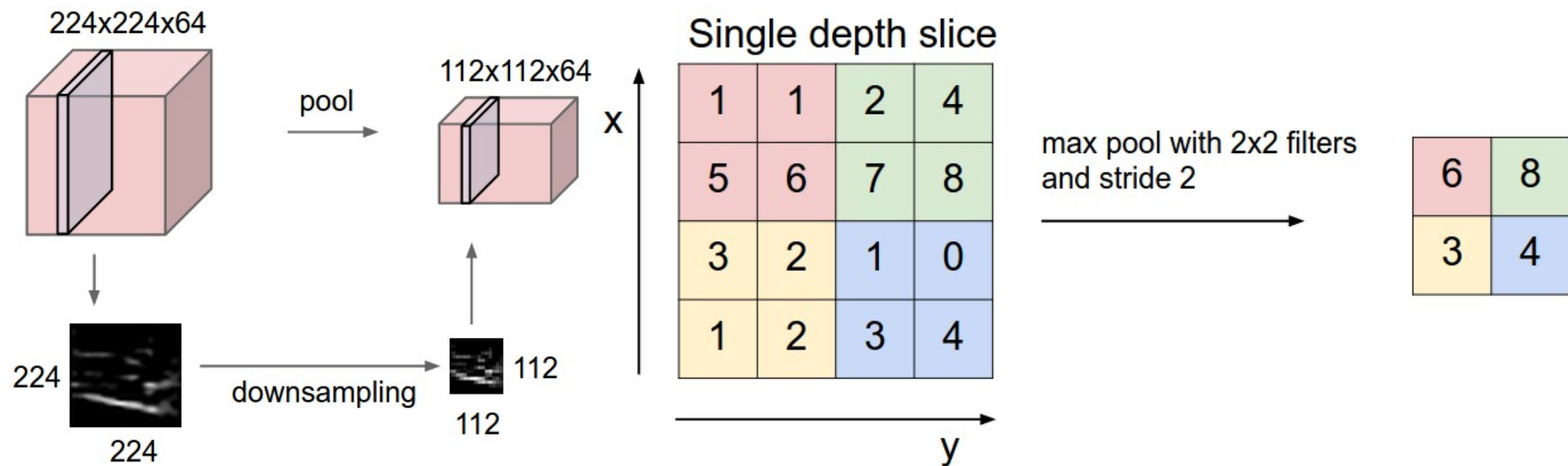
Source : <https://www.doc.ic.ac.uk/~bkainz/teaching/DL/notes/equivariance.pdf>

Convolutions are shift-equivariant

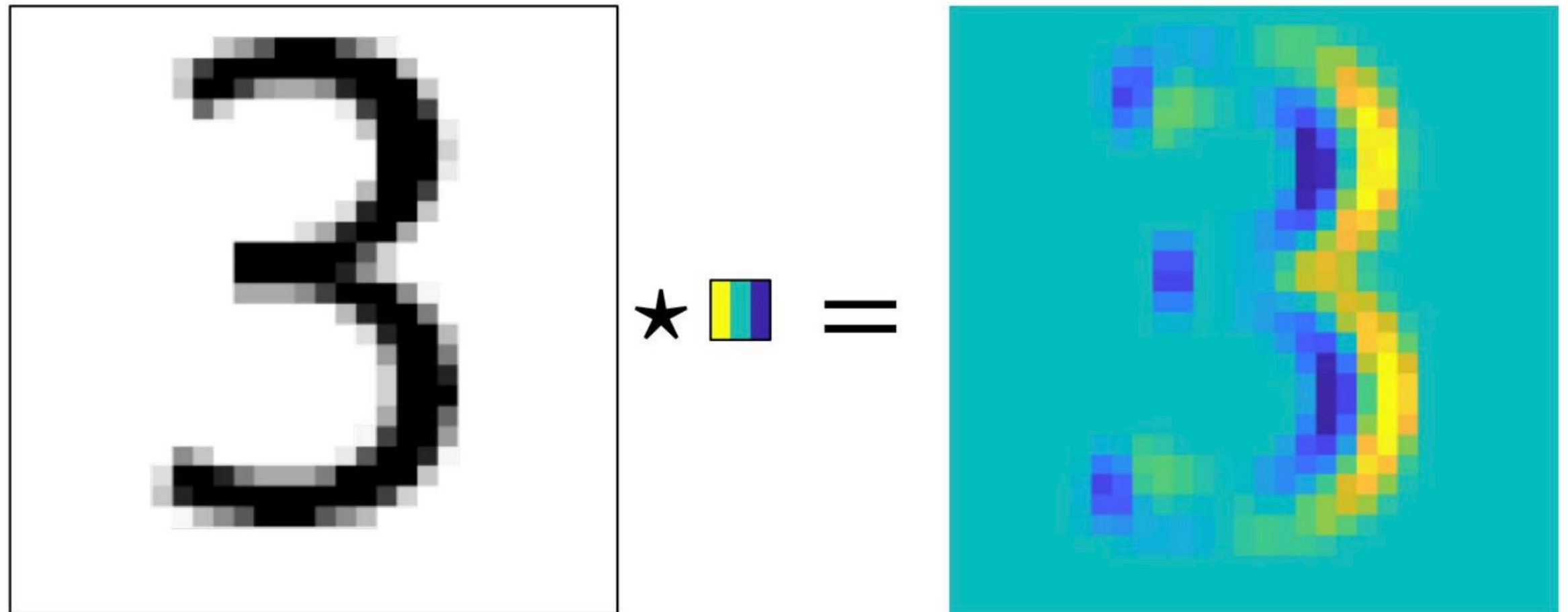


Source : <https://www.doc.ic.ac.uk/~bkainz/teaching/DL/notes/equivariance.pdf>

Max pooling layers

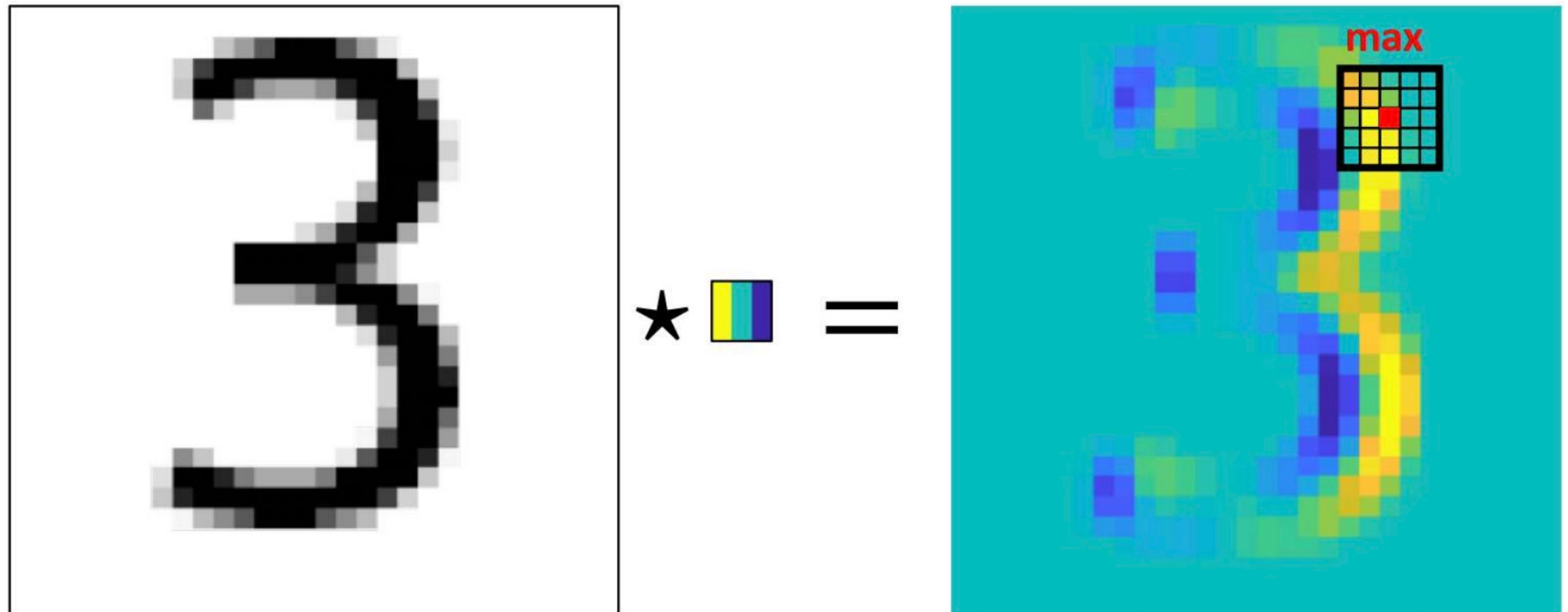


Convolutions are followed by a max pooling

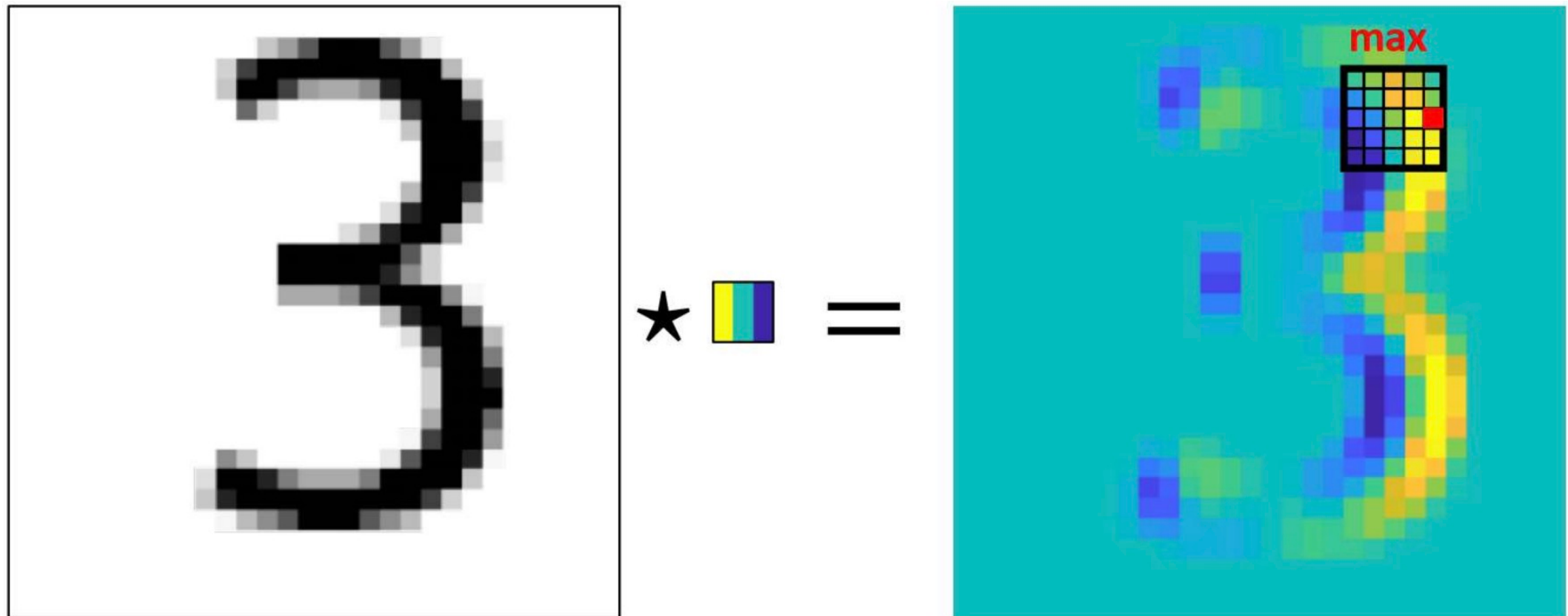


Source : <https://www.doc.ic.ac.uk/~bkainz/teaching/DL/notes/equivariance.pdf>

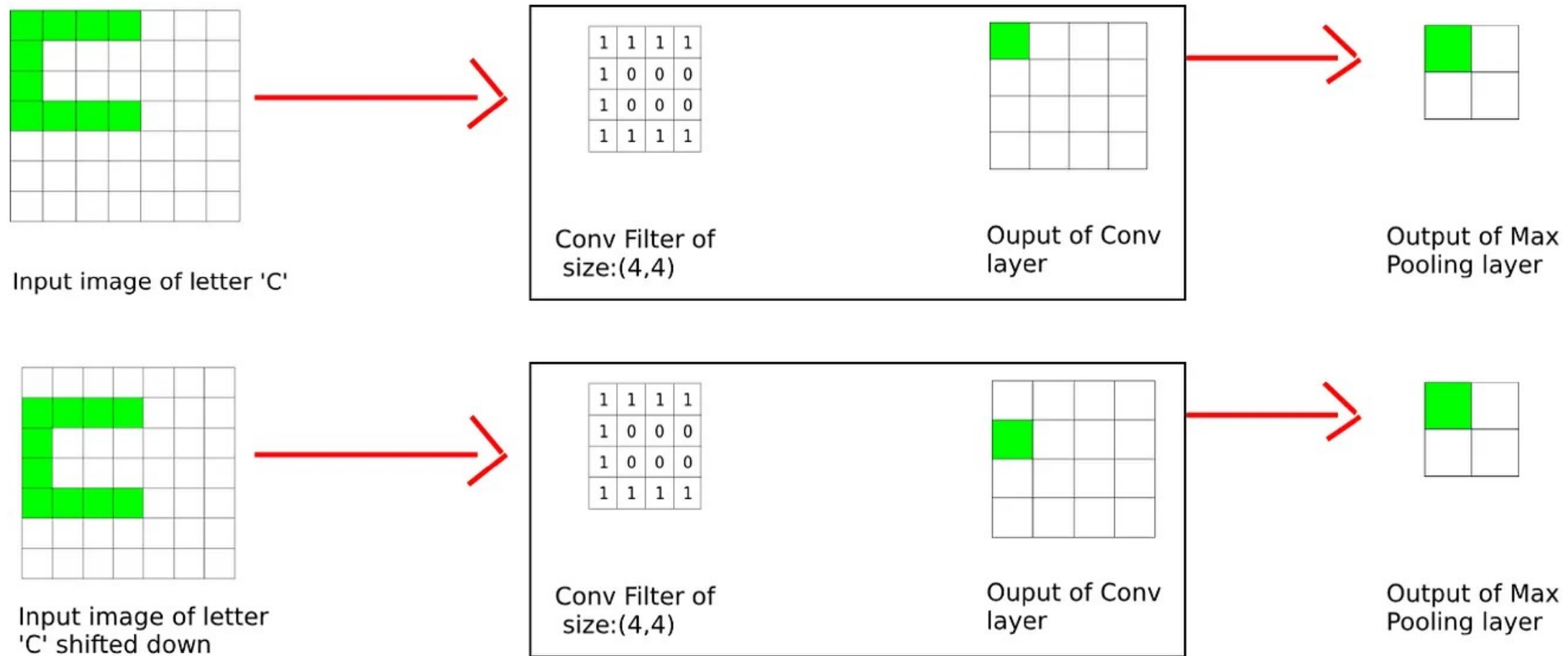
Convolutions are followed by a max pooling



Max pooling builds up shift-invariance



Max pooling builds up shift-invariance



Source : <https://divsoni2012.medium.com/translation-invariance-in-convolutional-neural-networks-61d9b6fa03df>

Invariance studies in CNN

Invariance studies in CNN

- The **scattering transform** builds shift-invariant feature vectors:

$$\Phi(x) := S_J x = \begin{pmatrix} x \star \phi_{2^J} \\ |x \star \psi_{\lambda_1}| \star \phi_{2^J} \\ |||x \star \psi_{\lambda_1}| \star \psi_{\lambda_2}| \star \phi_{2^J} \\ ||||x \star \psi_{\lambda_1}| \star \psi_{\lambda_2}| \star \psi_{\lambda_3}| \star \phi_{2^J} \\ \vdots \end{pmatrix}_{\lambda_1, \lambda_2, \lambda_3, \dots}$$

Invariance studies in CNN

- The **scattering transform** builds shift-invariant feature vectors:

$$\Phi(x) := S_J x = \begin{pmatrix} x \star \phi_{2^J} \\ |x \star \psi_{\lambda_1}| \star \phi_{2^J} \\ |||x \star \psi_{\lambda_1}| \star \psi_{\lambda_2}| \star \phi_{2^J} \\ ||||x \star \psi_{\lambda_1}| \star \psi_{\lambda_2}| \star \psi_{\lambda_3}| \star \phi_{2^J} \\ \vdots \\ \end{pmatrix}_{\lambda_1, \lambda_2, \lambda_3, \dots}$$

J. Bruna and S. Mallat, "Invariant scattering convolution networks," IEEE Trans. Pattern Anal. Mach. Intell., vol. 35, no. 8, pp. 1872–1886, 2013.

Invariance studies in CNN

- The **scattering transform** builds shift-invariant feature vectors:

$$\Phi(x) := S_J x = \begin{pmatrix} x \star \phi_{2^J} \\ |x \star \psi_{\lambda_1}| \star \phi_{2^J} \\ |||x \star \psi_{\lambda_1}| \star \psi_{\lambda_2}| \star \phi_{2^J} \\ ||||x \star \psi_{\lambda_1}| \star \psi_{\lambda_2}| \star \psi_{\lambda_3}| \star \phi_{2^J} \\ \vdots \\ \end{pmatrix}_{\lambda_1, \lambda_2, \lambda_3, \dots}$$

- General deep convolutional neural networks** also become more translation invariant with increasing network depth (proved in the *continuous framework*).

J. Bruna and S. Mallat, "Invariant scattering convolution networks," IEEE Trans. Pattern Anal. Mach. Intell., vol. 35, no. 8, pp. 1872–1886, 2013.

Invariance studies in CNN

- The **scattering transform** builds shift-invariant feature vectors:

$$\Phi(x) := S_J x = \begin{pmatrix} x \star \phi_{2^J} \\ |x \star \psi_{\lambda_1}| \star \phi_{2^J} \\ |||x \star \psi_{\lambda_1}| \star \psi_{\lambda_2}| \star \phi_{2^J} \\ ||||x \star \psi_{\lambda_1}| \star \psi_{\lambda_2}| \star \psi_{\lambda_3}| \star \phi_{2^J} \\ \vdots \\ \end{pmatrix}_{\lambda_1, \lambda_2, \lambda_3, \dots}$$

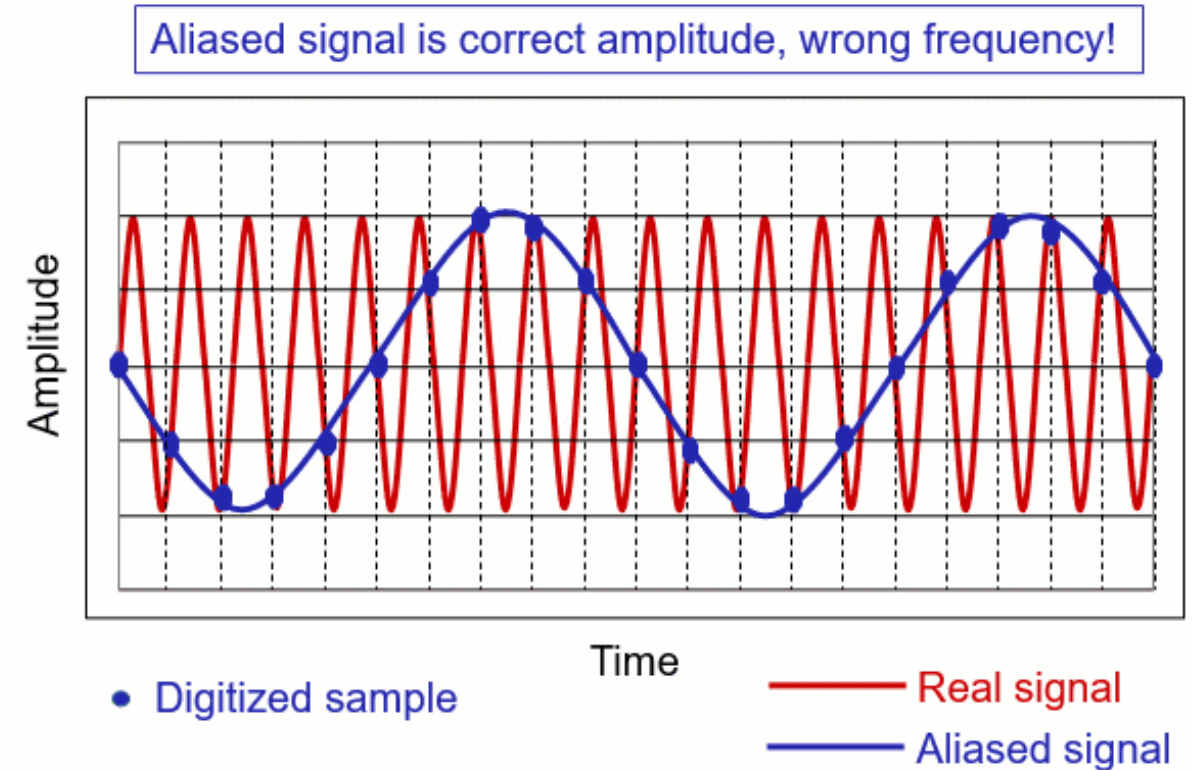
- General deep convolutional neural networks** also become more translation invariant with increasing network depth (proved in the *continuous framework*).

J. Bruna and S. Mallat, "Invariant scattering convolution networks," IEEE Trans. Pattern Anal. Mach. Intell., vol. 35, no. 8, pp. 1872–1886, 2013.

T. Wiatowski and H. Bölcskei, A Mathematical Theory of Deep Convolutional Neural Networks for Feature Extraction, IEEE Transactions on Information Theory, 64 (2018), pp. 1845-1866

Invariance studies in CNN

- These results do not fully extend to the ***discrete framework***

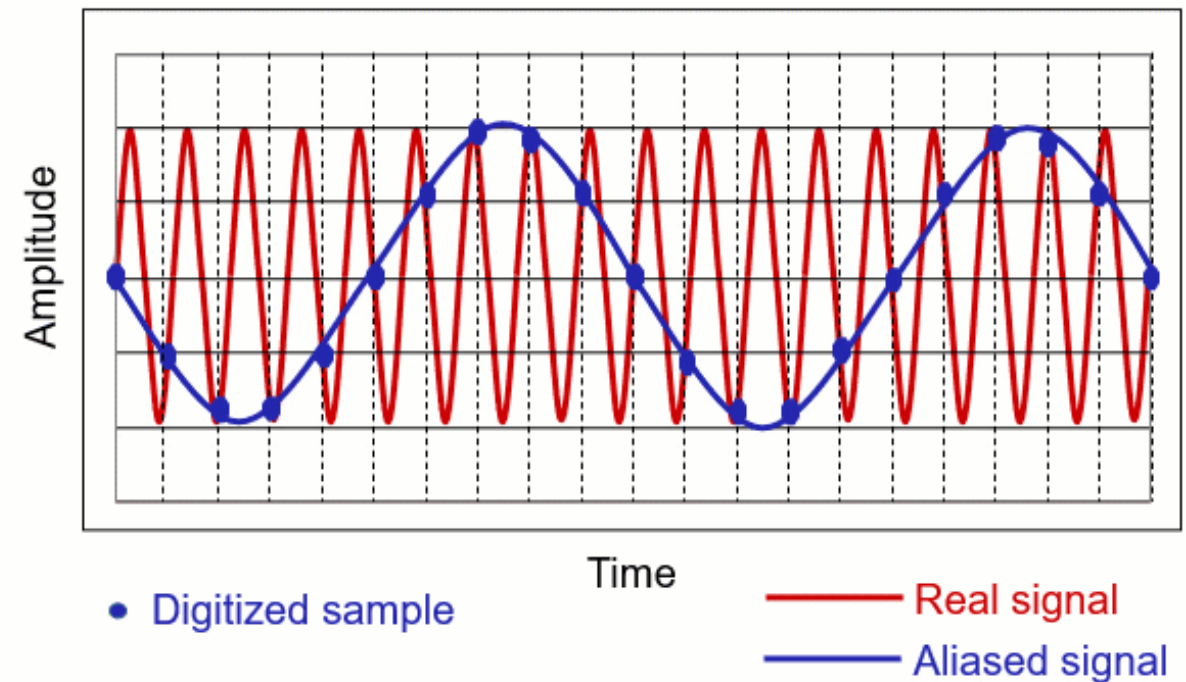


Source : [https://community.sw.siemens.com/s/article/
data-acquisition-anti-aliasing-filters](https://community.sw.siemens.com/s/article/data-acquisition-anti-aliasing-filters)

Invariance studies in CNN

- These results do not fully extend to the ***discrete framework***
- **Strided convolution** and pooling operators may greatly diverge from shift invariance, due to **aliasing** when subsampling high-frequency signals

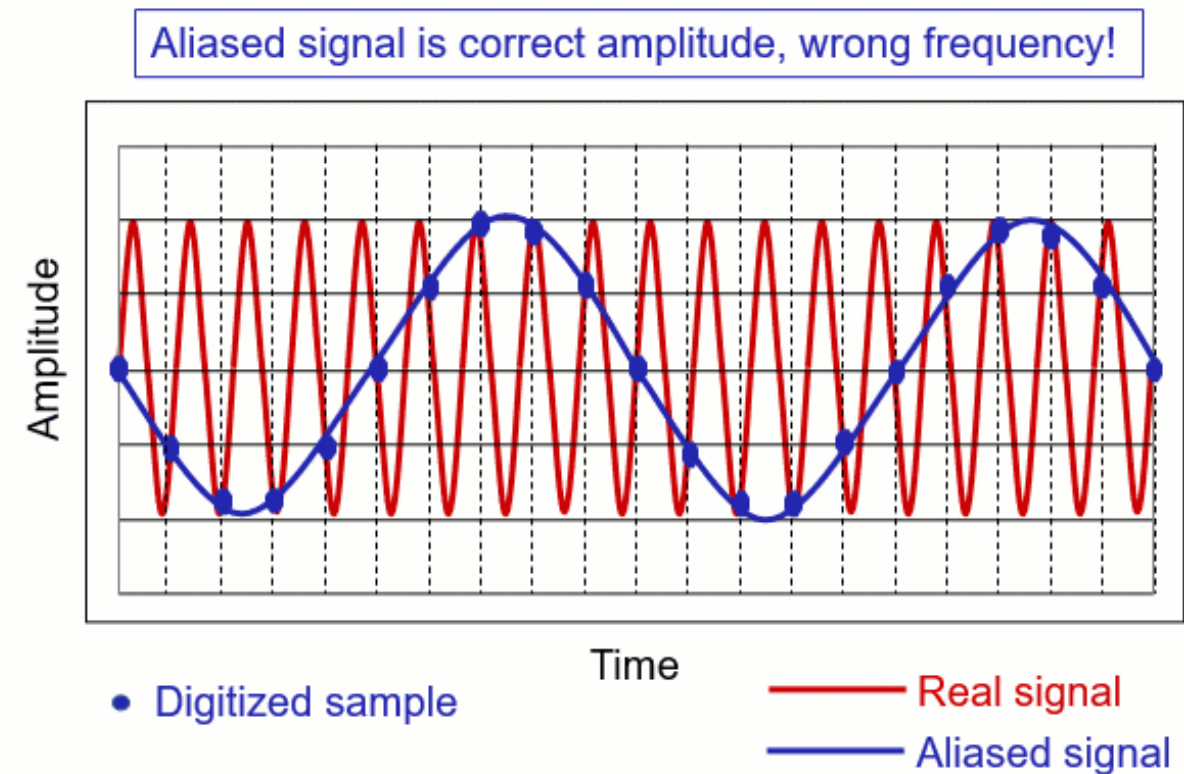
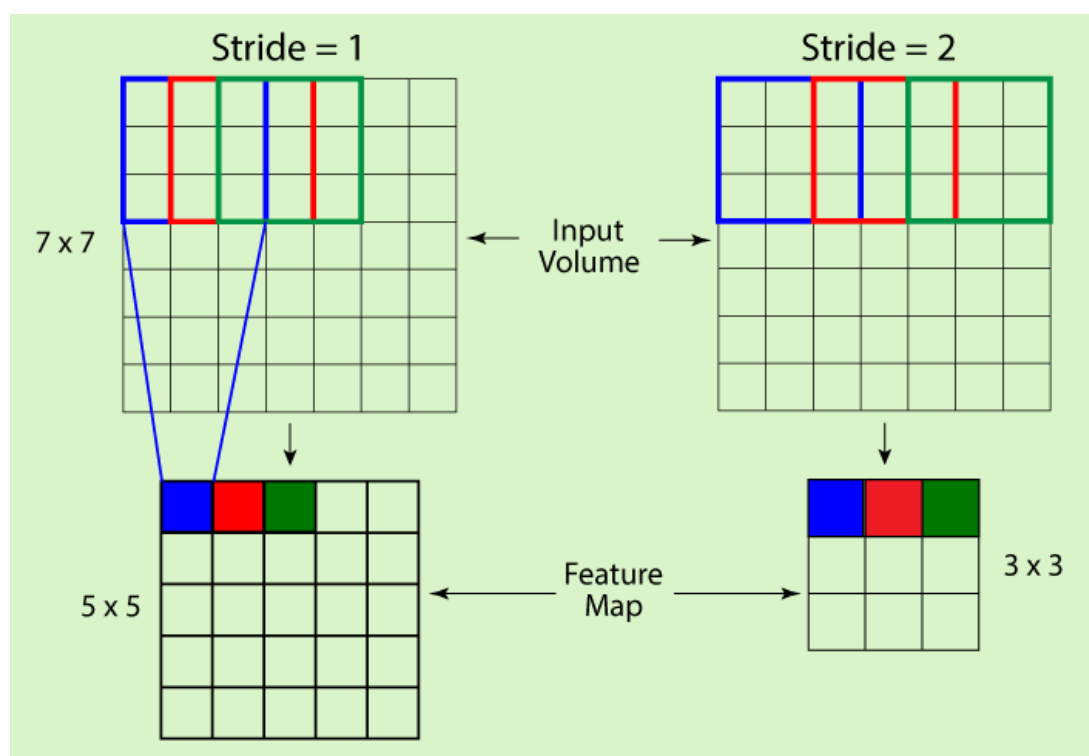
Aliased signal is correct amplitude, wrong frequency!



Source : <https://community.sw.siemens.com/s/article/data-acquisition-anti-aliasing-filters>

Invariance studies in CNN

- These results do not fully extend to the ***discrete framework***
- Strided convolution and pooling operators may greatly diverge from shift invariance, due to **aliasing** when subsampling high-frequency signals**

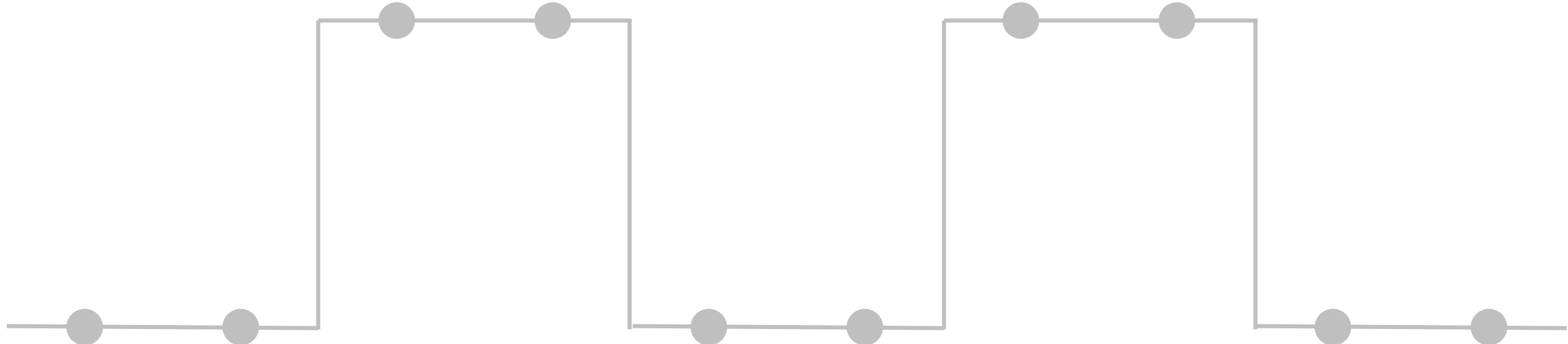


Source : <https://developersbreach.com/convolution-neural-network-deep-learning/>

Source : <https://community.sw.siemens.com/s/article/data-acquisition-anti-aliasing-filters>

Invariance studies in CNN

- These results do not fully extend to the ***discrete framework***
- **Strided convolution** and pooling operators may greatly diverge from shift invariance, due to **aliasing** when subsampling high-frequency signals

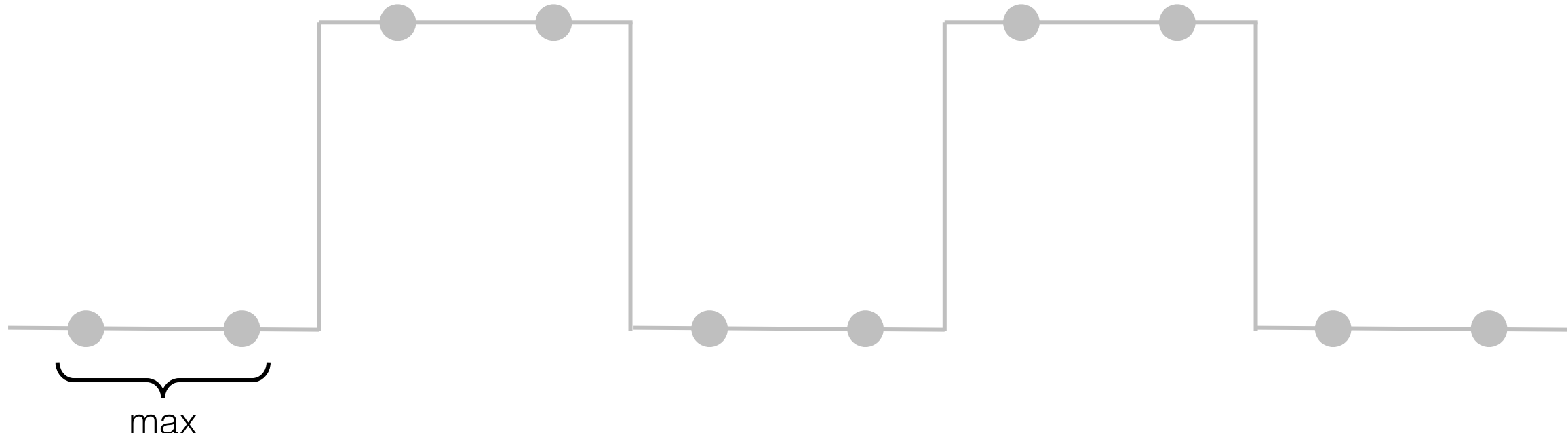


R. Zhang, Making Convolutional Networks Shift-Invariant Again, in International Conference on Machine Learning, 2019.

A. Azulay and Y. Weiss, Why do deep convolutional networks generalize so poorly to small image transformations?, Journal of Machine Learning Research, 2019.

Invariance studies in CNN

- These results do not fully extend to the ***discrete framework***
- **Strided convolution** and pooling operators may greatly diverge from shift invariance, due to **aliasing** when subsampling high-frequency signals

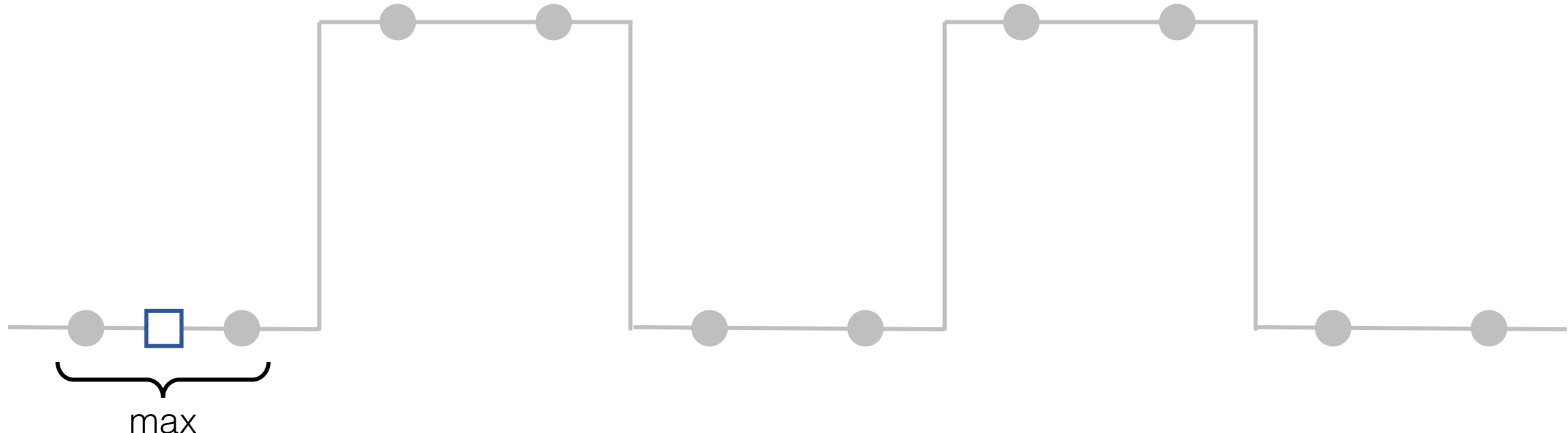


R. Zhang, **Making Convolutional Networks Shift-Invariant Again**, in International Conference on Machine Learning, 2019.

A. Azulay and Y. Weiss, Why do deep convolutional networks generalize so poorly to small image transformations?, Journal of Machine Learning Research, 2019.

Invariance studies in CNN

- These results do not fully extend to the ***discrete framework***
- **Strided convolution** and pooling operators may greatly diverge from shift invariance, due to **aliasing** when subsampling high-frequency signals

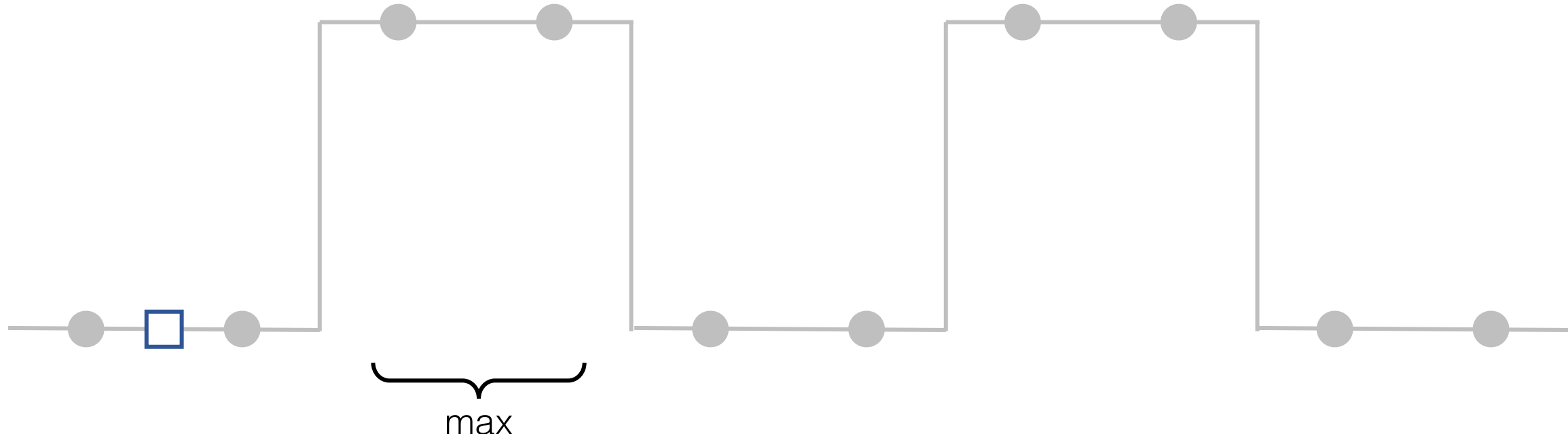


R. Zhang, **Making Convolutional Networks Shift-Invariant Again**, in International Conference on Machine Learning, 2019.

A. Azulay and Y. Weiss, Why do deep convolutional networks generalize so poorly to small image transformations?, Journal of Machine Learning Research, 2019.

Invariance studies in CNN

- These results do not fully extend to the ***discrete framework***
- **Strided convolution** and pooling operators may greatly diverge from shift invariance, due to **aliasing** when subsampling high-frequency signals

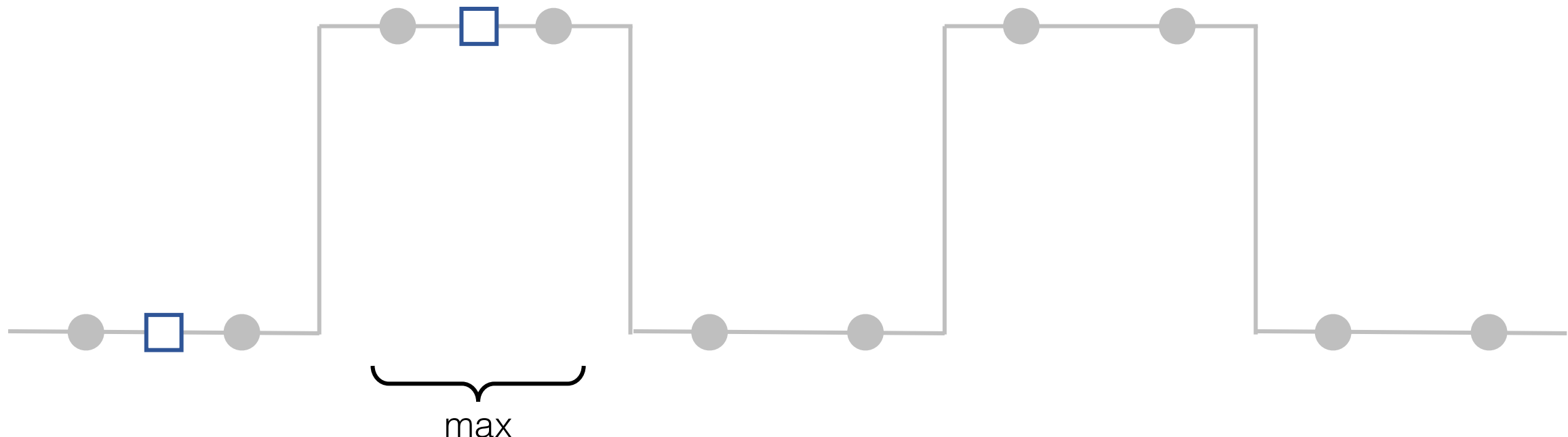


R. Zhang, **Making Convolutional Networks Shift-Invariant Again**, in International Conference on Machine Learning, 2019.

A. Azulay and Y. Weiss, Why do deep convolutional networks generalize so poorly to small image transformations?, Journal of Machine Learning Research, 2019.

Invariance studies in CNN

- These results do not fully extend to the ***discrete framework***
- **Strided convolution** and pooling operators may greatly diverge from shift invariance, due to **aliasing** when subsampling high-frequency signals

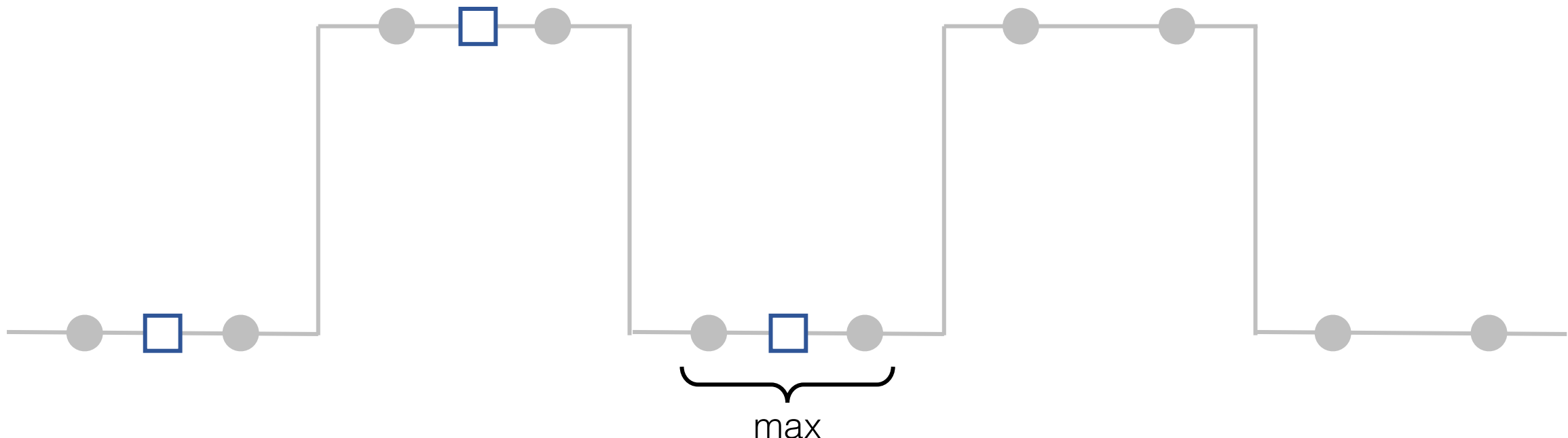


R. Zhang, **Making Convolutional Networks Shift-Invariant Again**, in International Conference on Machine Learning, 2019.

A. Azulay and Y. Weiss, Why do deep convolutional networks generalize so poorly to small image transformations?, Journal of Machine Learning Research, 2019.

Invariance studies in CNN

- These results do not fully extend to the ***discrete framework***
- **Strided convolution** and pooling operators may greatly diverge from shift invariance, due to **aliasing** when subsampling high-frequency signals

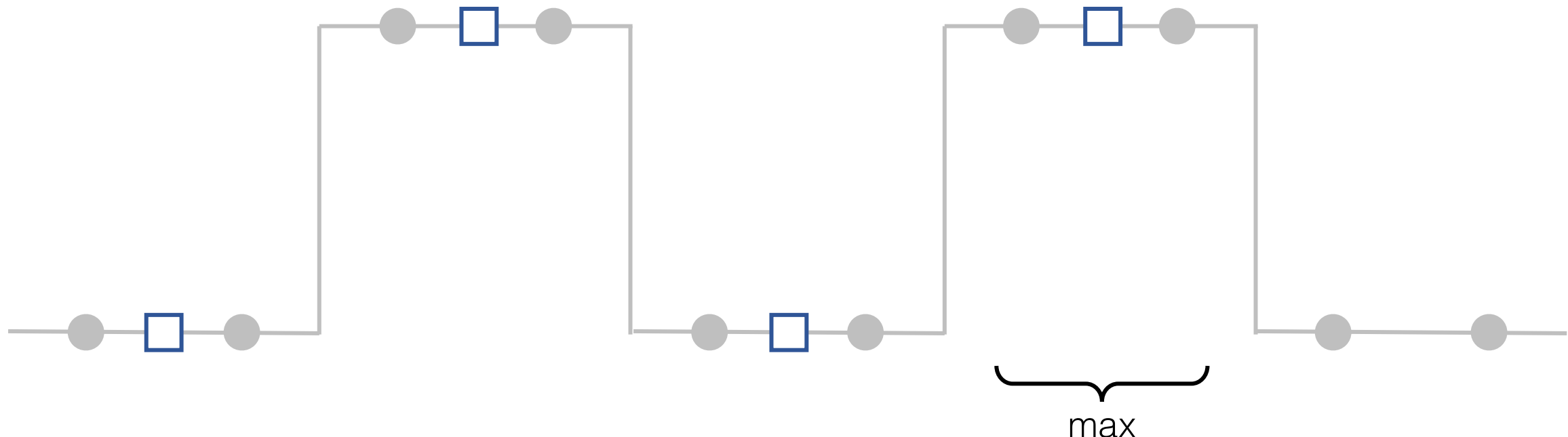


R. Zhang, **Making Convolutional Networks Shift-Invariant Again**, in International Conference on Machine Learning, 2019.

A. Azulay and Y. Weiss, Why do deep convolutional networks generalize so poorly to small image transformations?, Journal of Machine Learning Research, 2019.

Invariance studies in CNN

- These results do not fully extend to the ***discrete framework***
- **Strided convolution** and pooling operators may greatly diverge from shift invariance, due to **aliasing** when subsampling high-frequency signals

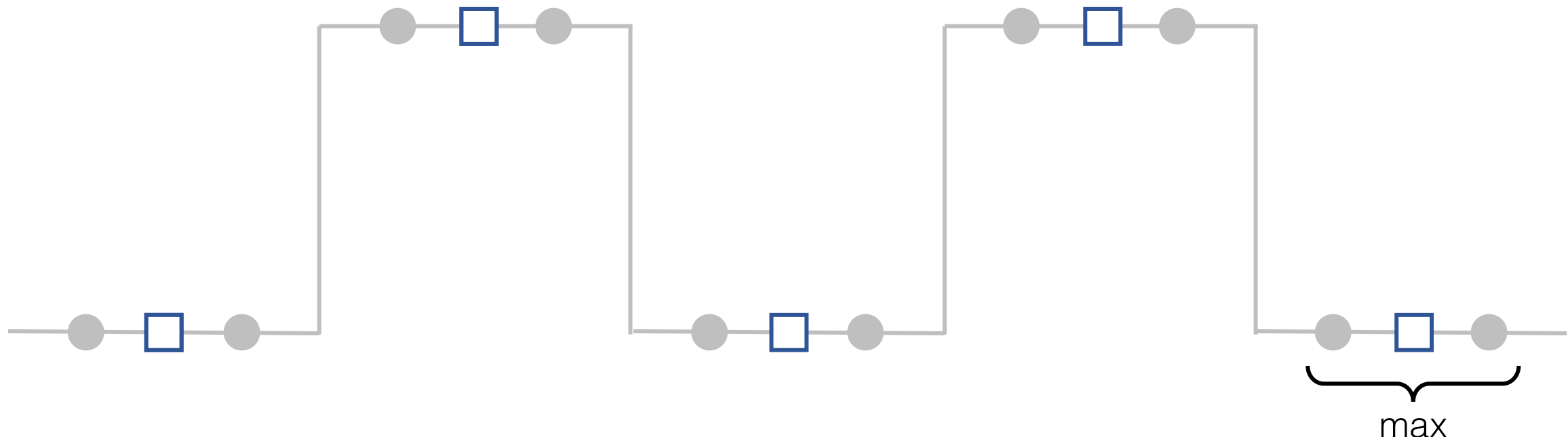


R. Zhang, Making Convolutional Networks Shift-Invariant Again, in International Conference on Machine Learning, 2019.

A. Azulay and Y. Weiss, Why do deep convolutional networks generalize so poorly to small image transformations?, Journal of Machine Learning Research, 2019.

Invariance studies in CNN

- These results do not fully extend to the ***discrete framework***
- **Strided convolution** and pooling operators may greatly diverge from shift invariance, due to **aliasing** when subsampling high-frequency signals

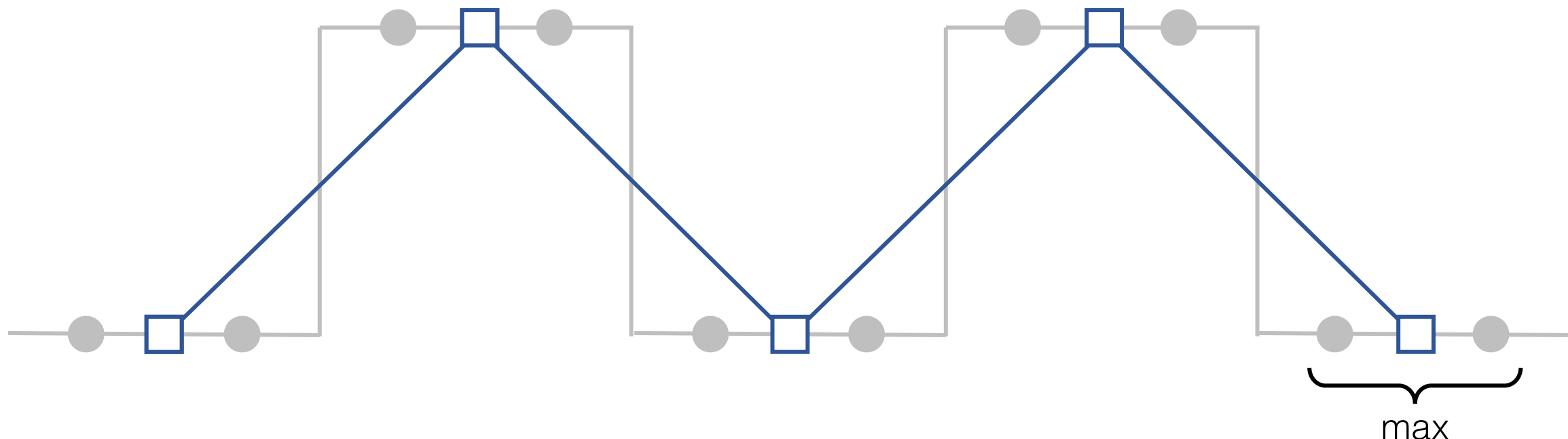


R. Zhang, **Making Convolutional Networks Shift-Invariant Again**, in International Conference on Machine Learning, 2019.

A. Azulay and Y. Weiss, Why do deep convolutional networks generalize so poorly to small image transformations?, Journal of Machine Learning Research, 2019.

Invariance studies in CNN

- These results do not fully extend to the ***discrete framework***
- **Strided convolution** and pooling operators may greatly diverge from shift invariance, due to **aliasing** when subsampling high-frequency signals

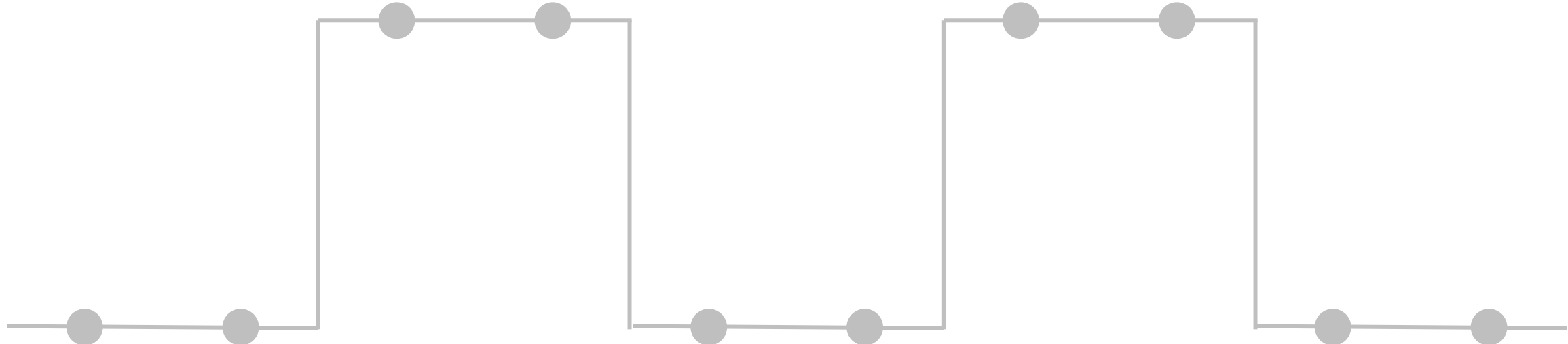


R. Zhang, **Making Convolutional Networks Shift-Invariant Again**, in International Conference on Machine Learning, 2019.

A. Azulay and Y. Weiss, Why do deep convolutional networks generalize so poorly to small image transformations?, Journal of Machine Learning Research, 2019.

Invariance studies in CNN

- These results do not fully extend to the ***discrete framework***
- **Strided convolution** and pooling operators may greatly diverge from shift invariance, due to **aliasing** when subsampling high-frequency signals

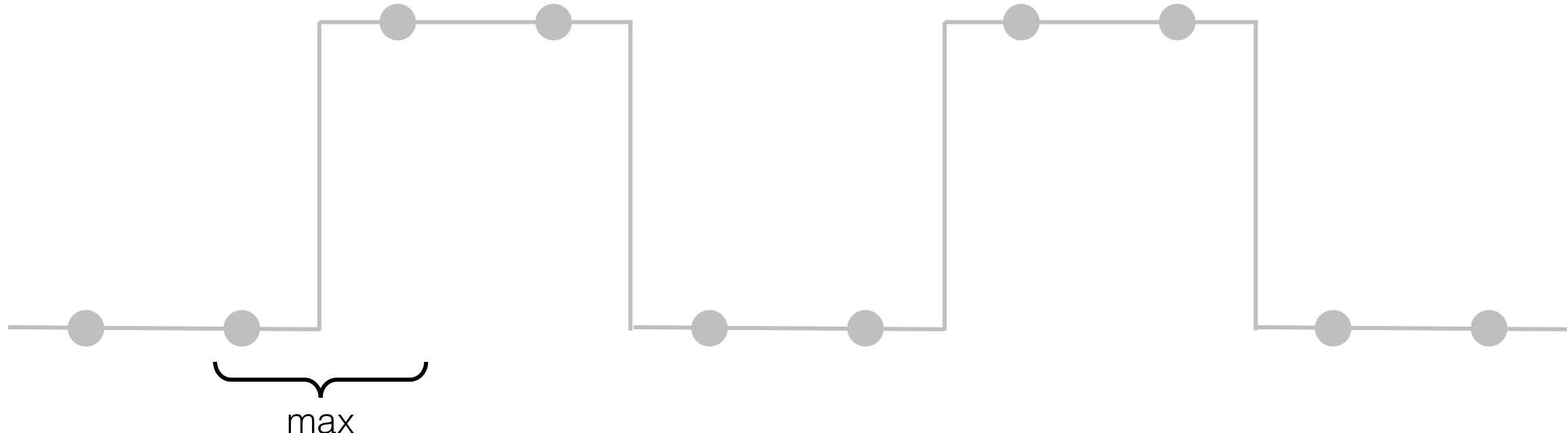


R. Zhang, **Making Convolutional Networks Shift-Invariant Again**, in International Conference on Machine Learning, 2019.

A. Azulay and Y. Weiss, Why do deep convolutional networks generalize so poorly to small image transformations?, Journal of Machine Learning Research, 2019.

Invariance studies in CNN

- These results do not fully extend to the ***discrete framework***
- **Strided convolution** and pooling operators may greatly diverge from shift invariance, due to **aliasing** when subsampling high-frequency signals

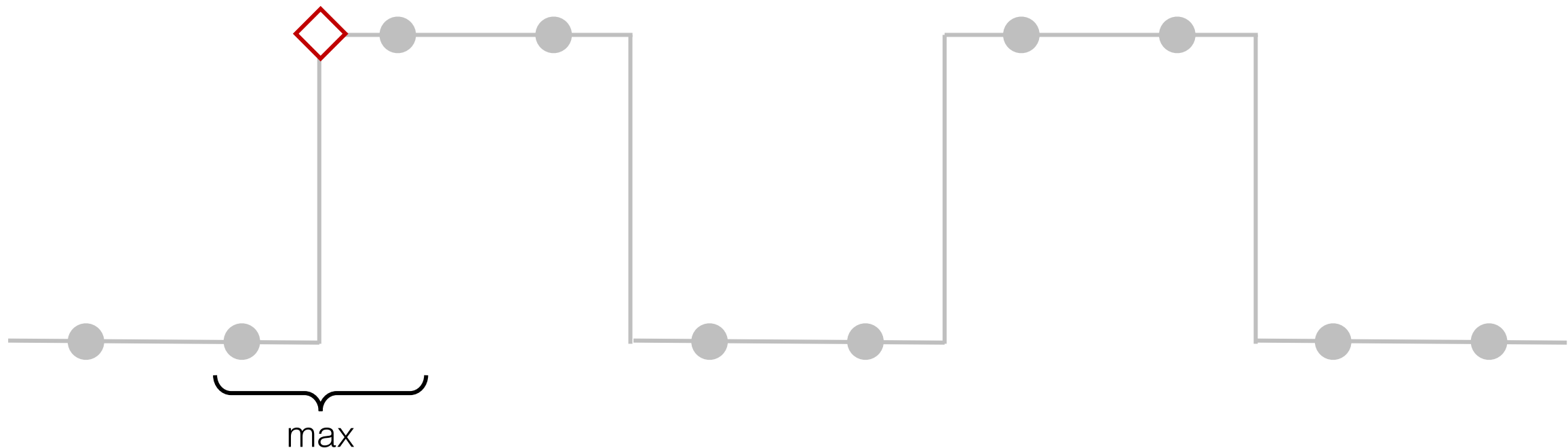


R. Zhang, **Making Convolutional Networks Shift-Invariant Again**, in International Conference on Machine Learning, 2019.

A. Azulay and Y. Weiss, Why do deep convolutional networks generalize so poorly to small image transformations?, Journal of Machine Learning Research, 2019.

Invariance studies in CNN

- These results do not fully extend to the ***discrete framework***
- **Strided convolution** and pooling operators may greatly diverge from shift invariance, due to **aliasing** when subsampling high-frequency signals

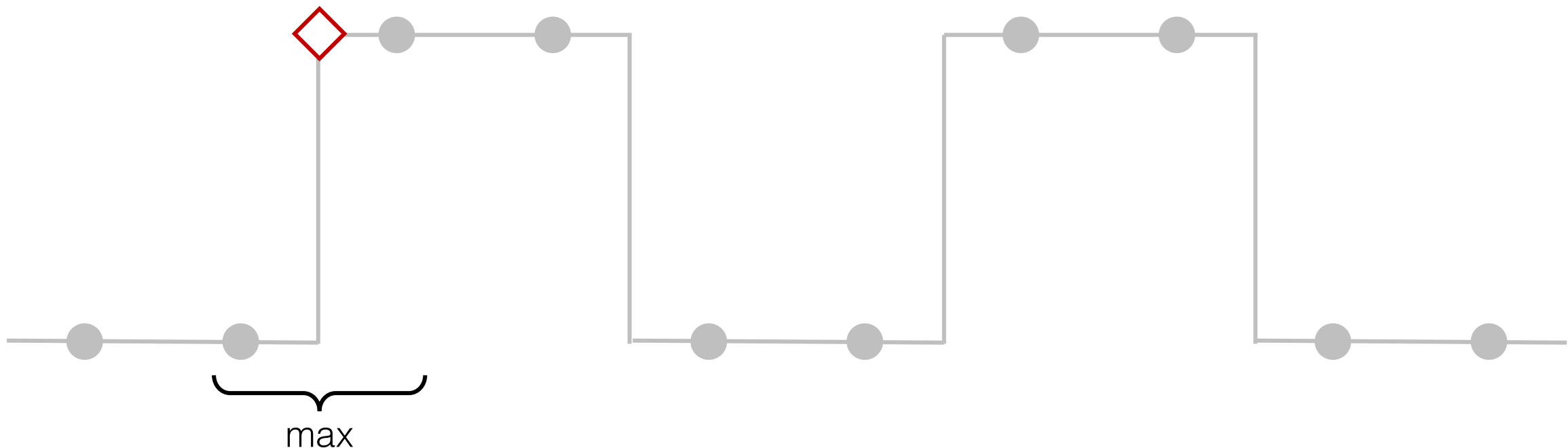


R. Zhang, **Making Convolutional Networks Shift-Invariant Again**, in International Conference on Machine Learning, 2019.

A. Azulay and Y. Weiss, Why do deep convolutional networks generalize so poorly to small image transformations?, Journal of Machine Learning Research, 2019.

Invariance studies in CNN

- These results do not fully extend to the ***discrete framework***
- **Strided convolution** and pooling operators may greatly diverge from shift invariance, due to **aliasing** when subsampling high-frequency signals

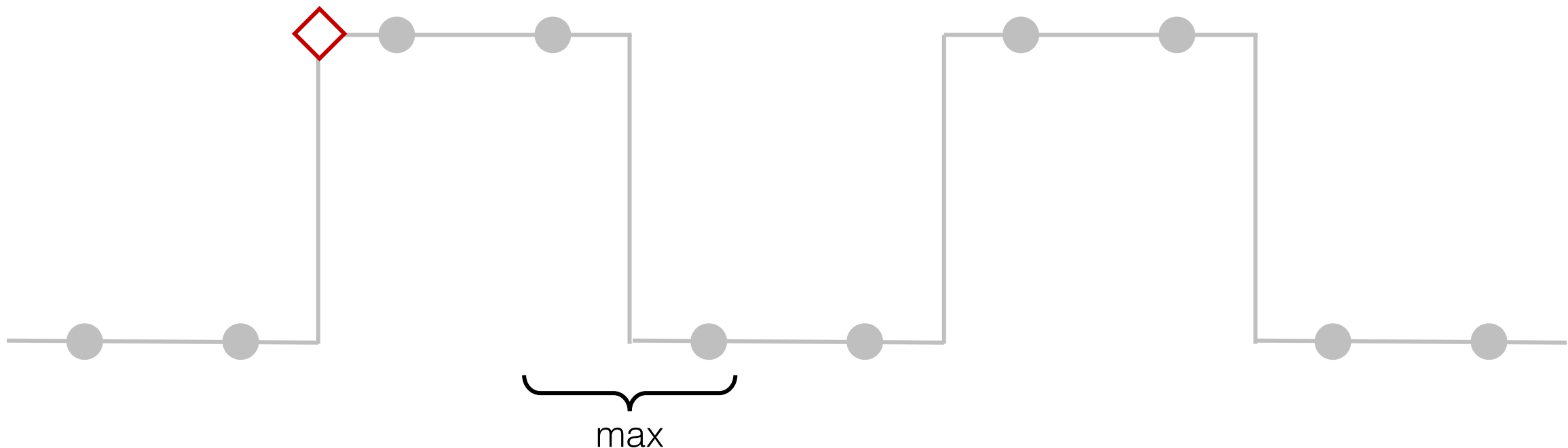


R. Zhang, **Making Convolutional Networks Shift-Invariant Again**, in International Conference on Machine Learning, 2019.

A. Azulay and Y. Weiss, Why do deep convolutional networks generalize so poorly to small image transformations?, Journal of Machine Learning Research, 2019.

Invariance studies in CNN

- These results do not fully extend to the ***discrete framework***
- **Strided convolution** and pooling operators may greatly diverge from shift invariance, due to **aliasing** when subsampling high-frequency signals

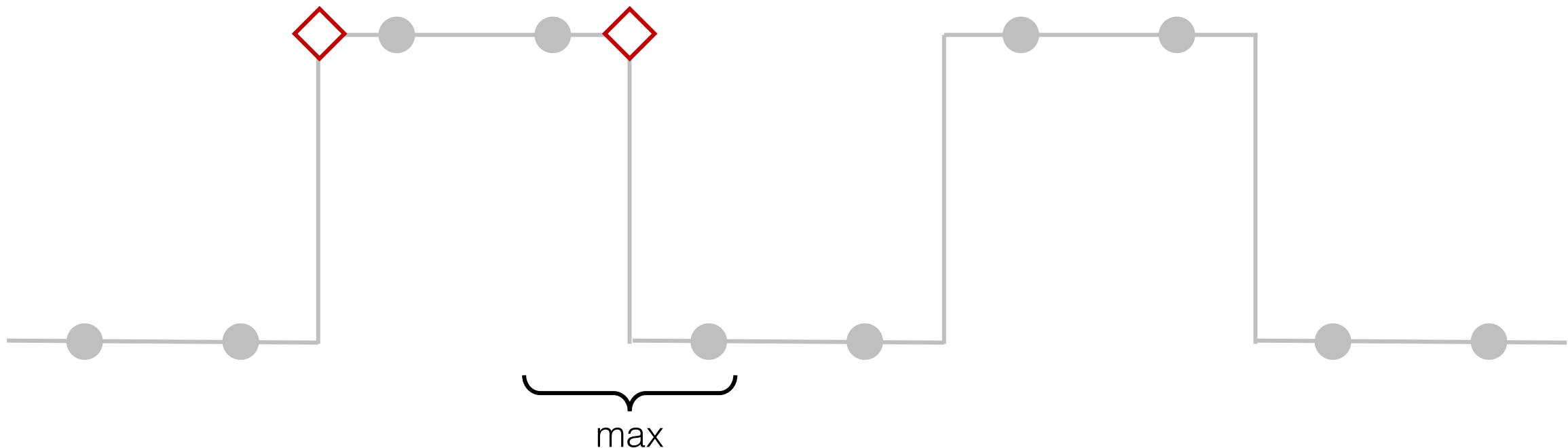


R. Zhang, **Making Convolutional Networks Shift-Invariant Again**, in International Conference on Machine Learning, 2019.

A. Azulay and Y. Weiss, Why do deep convolutional networks generalize so poorly to small image transformations?, Journal of Machine Learning Research, 2019.

Invariance studies in CNN

- These results do not fully extend to the ***discrete framework***
- **Strided convolution** and pooling operators may greatly diverge from shift invariance, due to **aliasing** when subsampling high-frequency signals

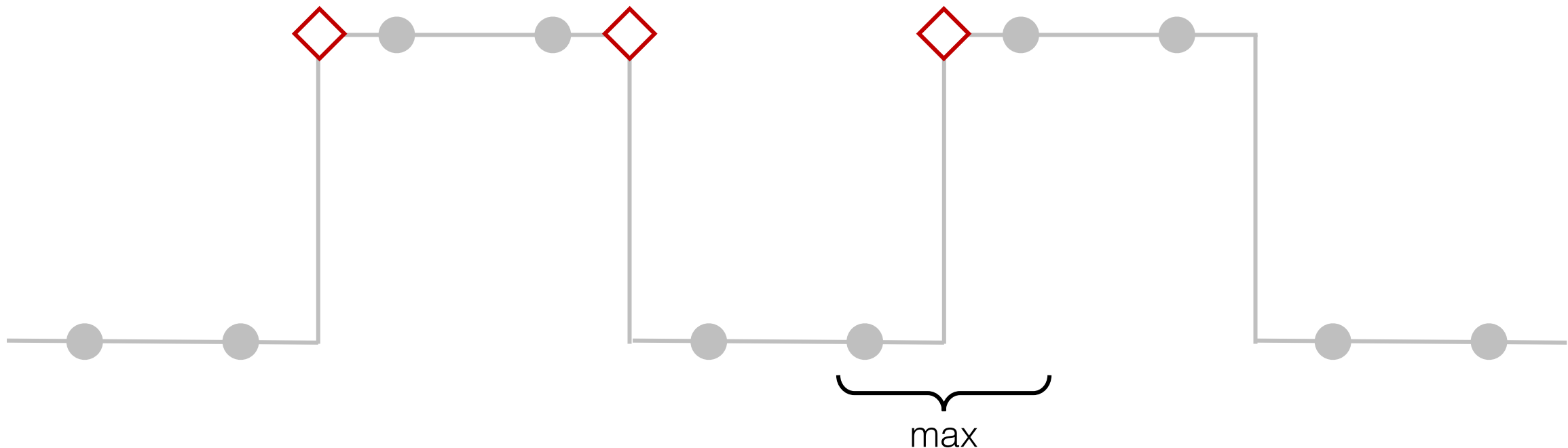


R. Zhang, **Making Convolutional Networks Shift-Invariant Again**, in International Conference on Machine Learning, 2019.

A. Azulay and Y. Weiss, Why do deep convolutional networks generalize so poorly to small image transformations?, Journal of Machine Learning Research, 2019.

Invariance studies in CNN

- These results do not fully extend to the ***discrete framework***
- **Strided convolution** and pooling operators may greatly diverge from shift invariance, due to **aliasing** when subsampling high-frequency signals

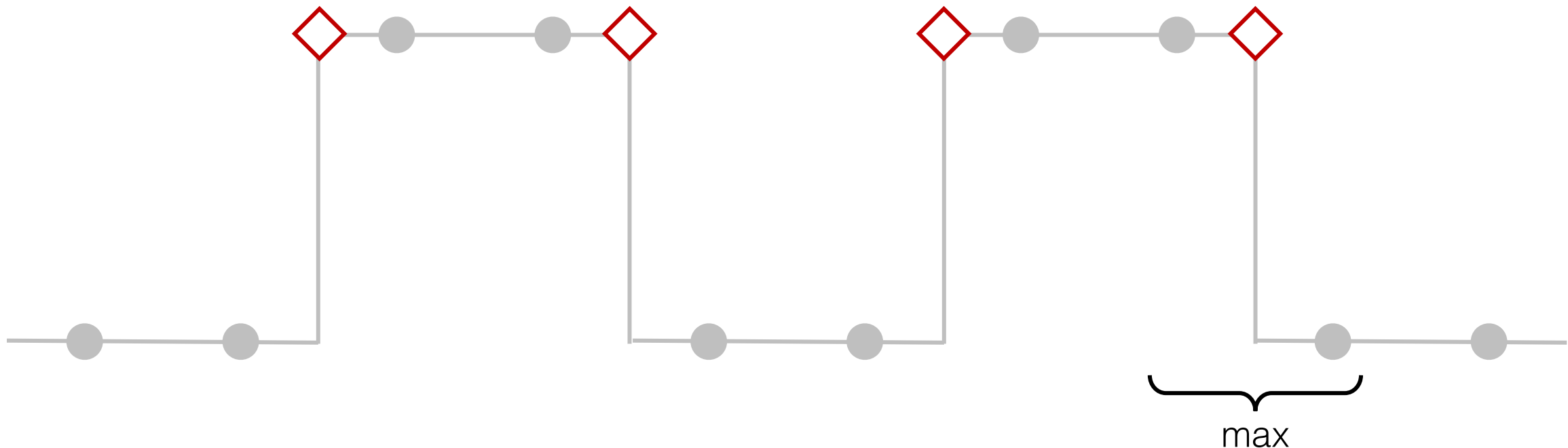


R. Zhang, **Making Convolutional Networks Shift-Invariant Again**, in International Conference on Machine Learning, 2019.

A. Azulay and Y. Weiss, Why do deep convolutional networks generalize so poorly to small image transformations?, Journal of Machine Learning Research, 2019.

Invariance studies in CNN

- These results do not fully extend to the ***discrete framework***
- **Strided convolution** and pooling operators may greatly diverge from shift invariance, due to **aliasing** when subsampling high-frequency signals

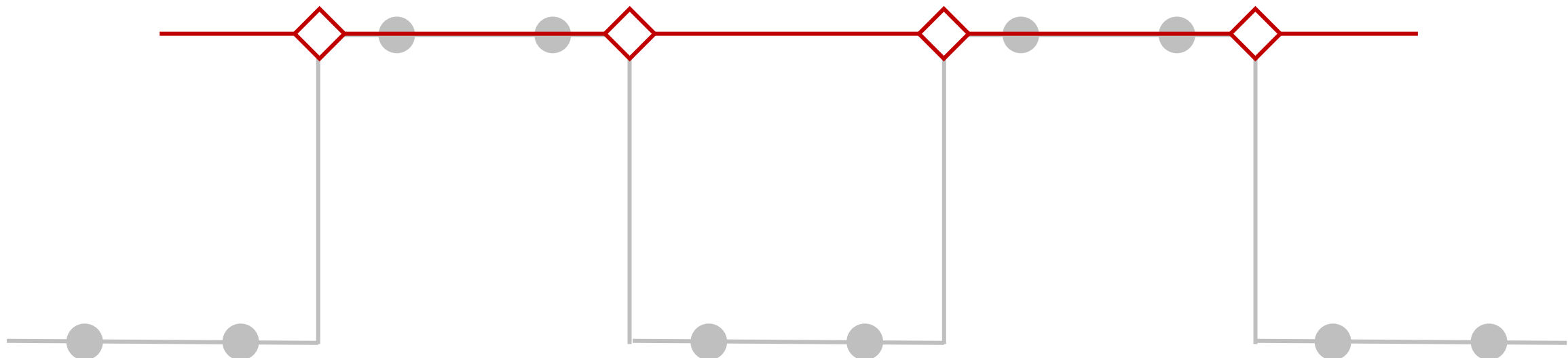


R. Zhang, **Making Convolutional Networks Shift-Invariant Again**, in International Conference on Machine Learning, 2019.

A. Azulay and Y. Weiss, Why do deep convolutional networks generalize so poorly to small image transformations?, Journal of Machine Learning Research, 2019.

Invariance studies in CNN

- These results do not fully extend to the ***discrete framework***
- **Strided convolution** and pooling operators may greatly diverge from shift invariance, due to **aliasing** when subsampling high-frequency signals

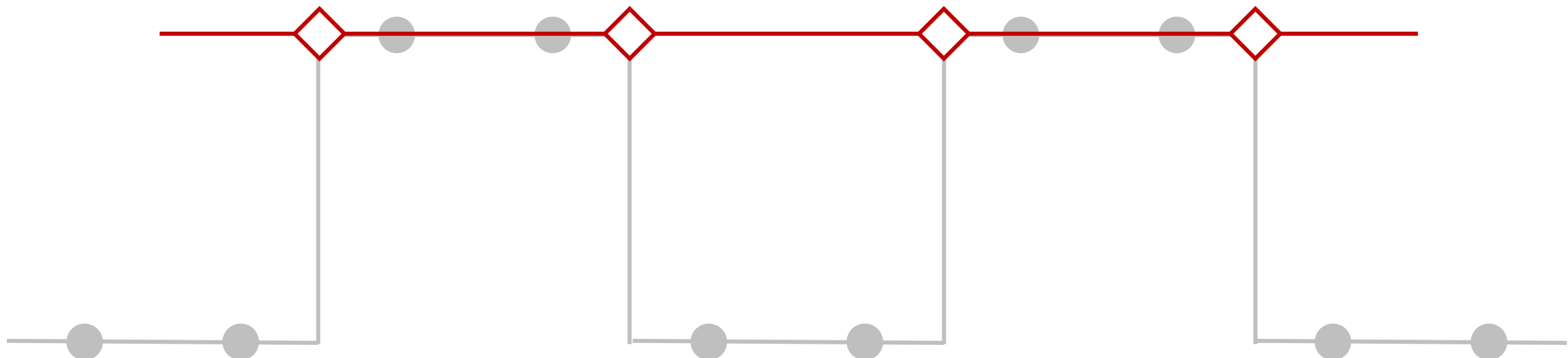


R. Zhang, **Making Convolutional Networks Shift-Invariant Again**, in International Conference on Machine Learning, 2019.

A. Azulay and Y. Weiss, Why do deep convolutional networks generalize so poorly to small image transformations?, Journal of Machine Learning Research, 2019.

Invariance studies in CNN

- These results do not fully extend to the ***discrete framework***
- **Strided convolution** and pooling operators may greatly diverge from shift invariance, due to **aliasing** when subsampling high-frequency signals

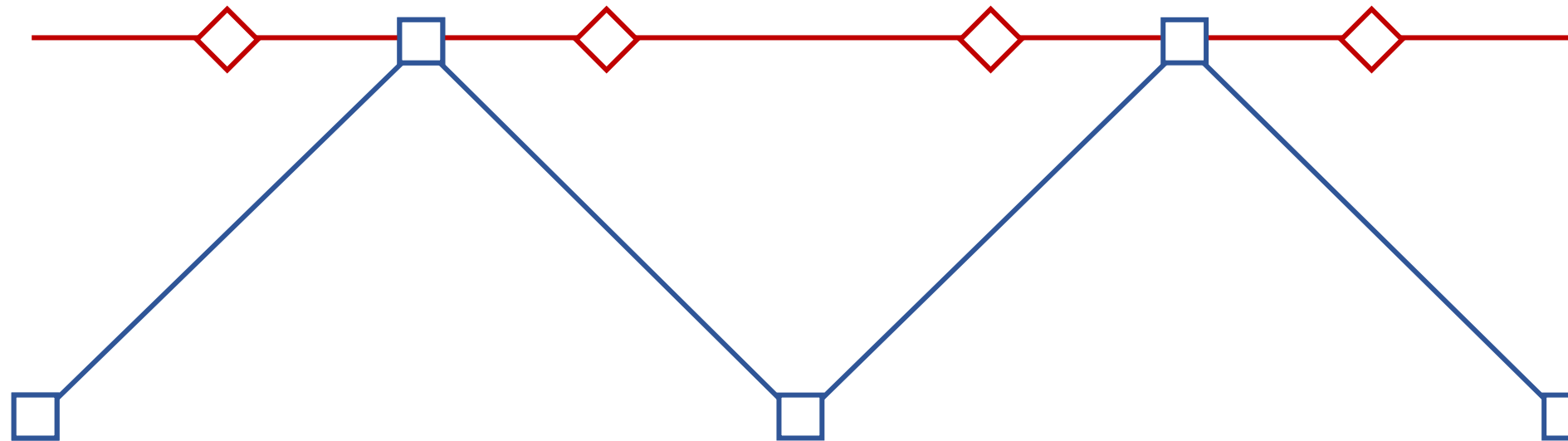


R. Zhang, **Making Convolutional Networks Shift-Invariant Again**, in International Conference on Machine Learning, 2019.

A. Azulay and Y. Weiss, Why do deep convolutional networks generalize so poorly to small image transformations?, Journal of Machine Learning Research, 2019.

Invariance studies in CNN

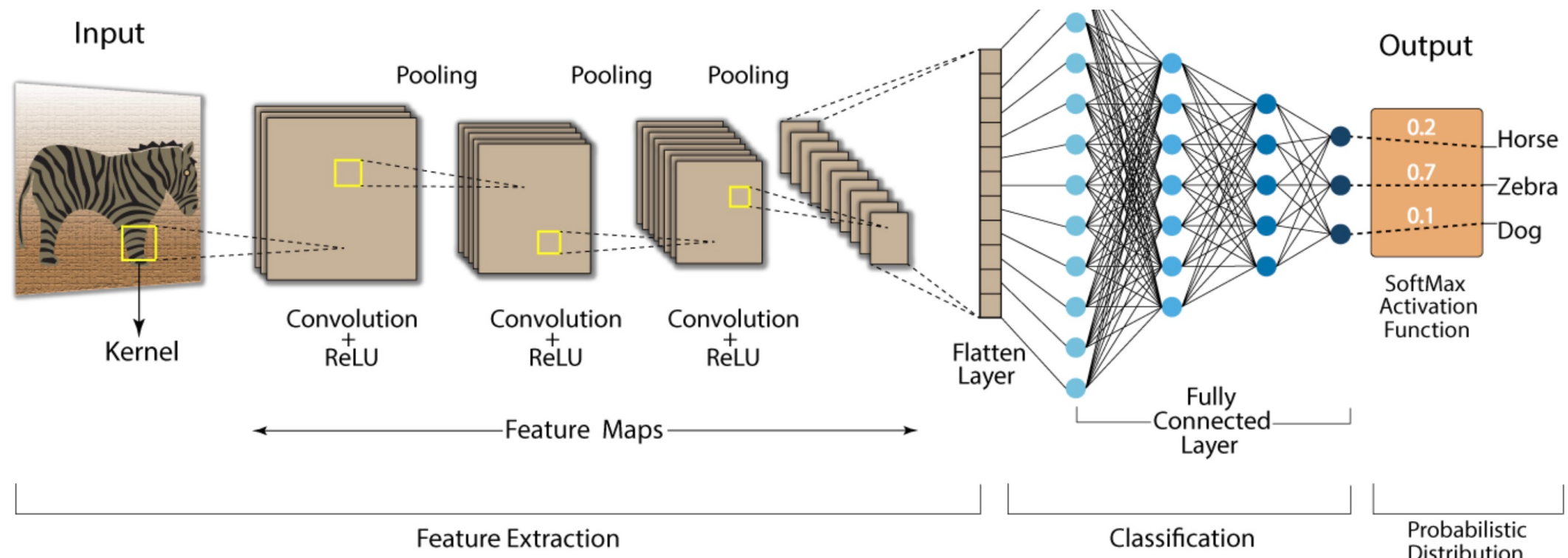
- These results do not fully extend to the ***discrete framework***
- **Strided convolution** and pooling operators may greatly diverge from shift invariance, due to **aliasing** when subsampling high-frequency signals



R. Zhang, **Making Convolutional Networks Shift-Invariant Again**, in International Conference on Machine Learning, 2019.

A. Azulay and Y. Weiss, Why do deep convolutional networks generalize so poorly to small image transformations?, Journal of Machine Learning Research, 2019.

Aliasing breaks shift-invariance

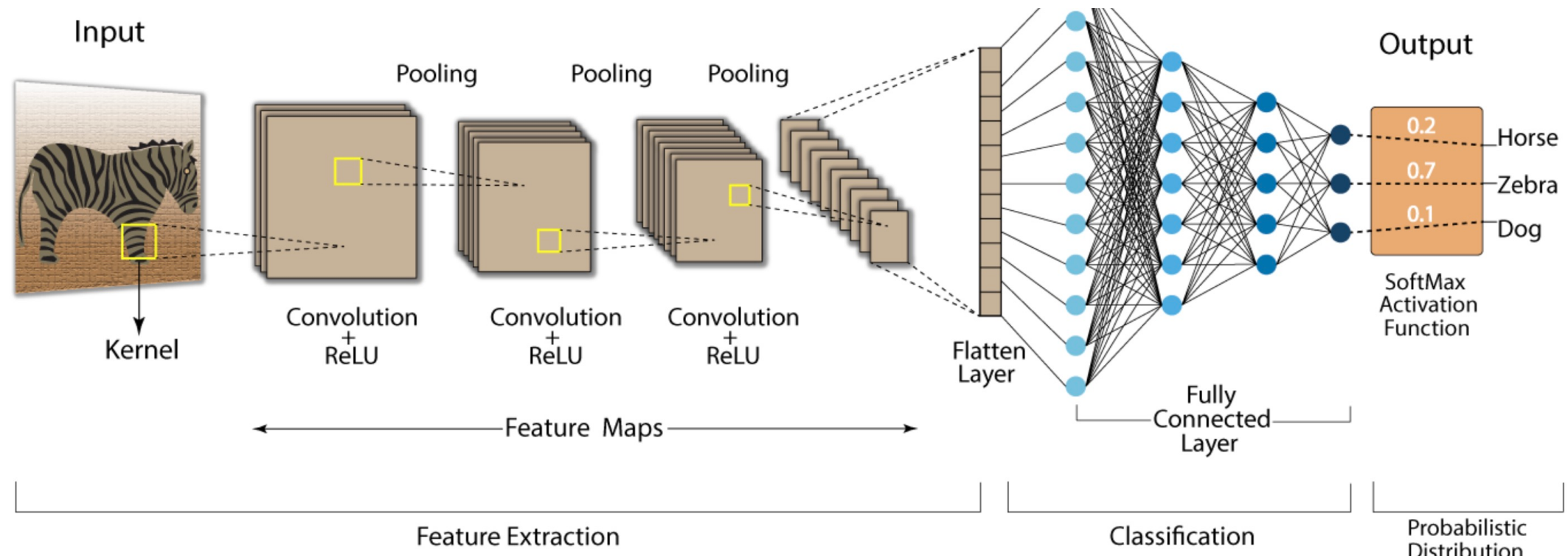


Source : <https://developersbreach.com/convolution-neural-network-deep-learning/>

86.7



Aliasing breaks shift-invariance



Source : <https://developersbreach.com/convolution-neural-network-deep-learning/>

46.3



Blind spots in the shift-invariance studies

Blind spots in the shift-invariance studies

- The effect of the max pooling operator on network stability under small input shifts has not been investigated, particularly when used in combination with Gabor-like convolutions.

Blind spots in the shift-invariance studies

- The **effect of the max pooling operator on network stability** under small input shifts has not been investigated, particularly when used in combination with Gabor-like convolutions.
- In the discrete case, the presence of subsampled convolutions with oriented band-pass filters can lead to aliasing artifacts. To our knowledge, **the literature lacks theoretical studies that take these aliasing effects into account**.

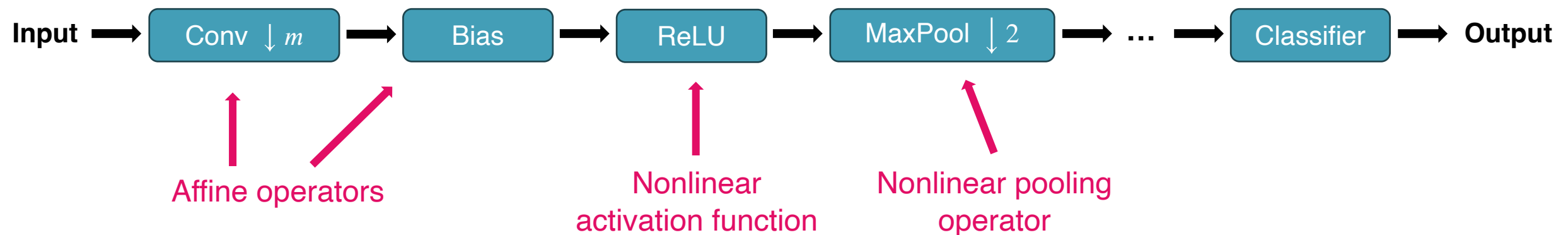
Blind spots in the shift-invariance studies

- The **effect of the max pooling operator on network stability** under small input shifts has not been investigated, particularly when used in combination with Gabor-like convolutions.
- In the discrete case, the presence of subsampled convolutions with oriented band-pass filters can lead to aliasing artifacts. To our knowledge, **the literature lacks theoretical studies that take these aliasing effects into account**.
- Although extensive studies have been conducted on complex-valued convolutions followed by modulus, **a link is missing to extend these results to standard CNNs**, which implement real-valued convolutions and spatial pooling operators.

Focus on the first layer



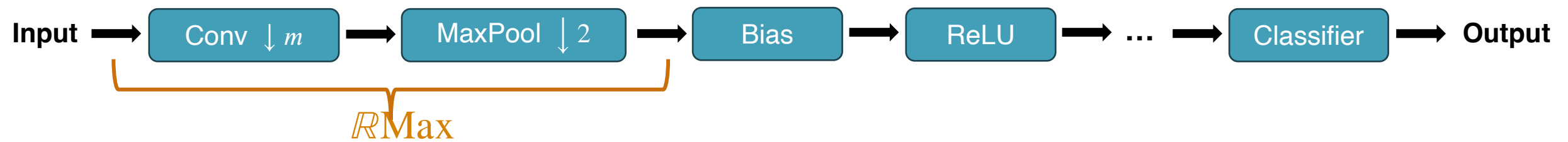
Focus on the first layer



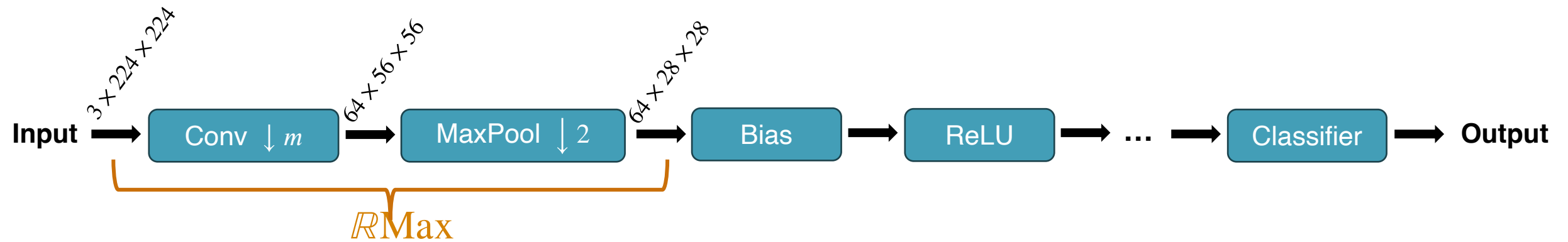
Focus on the first layer



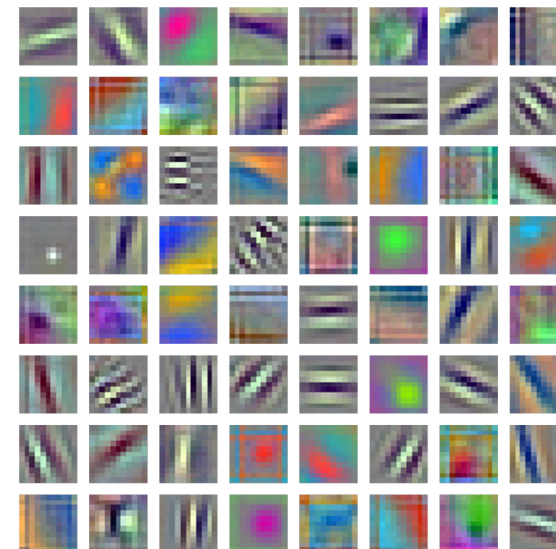
Focus on the first layer



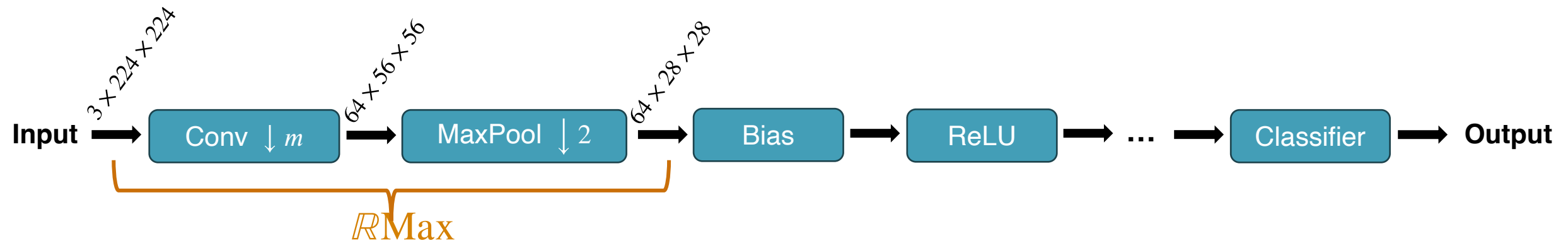
Focus on the first layer



Example: AlexNet
(2012)

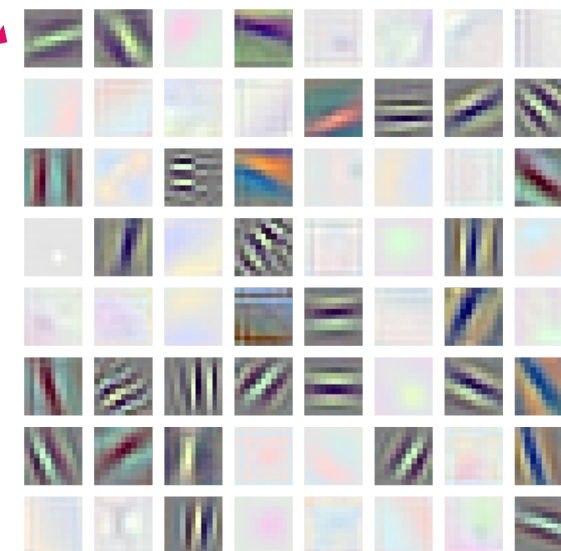


Focus on the first layer

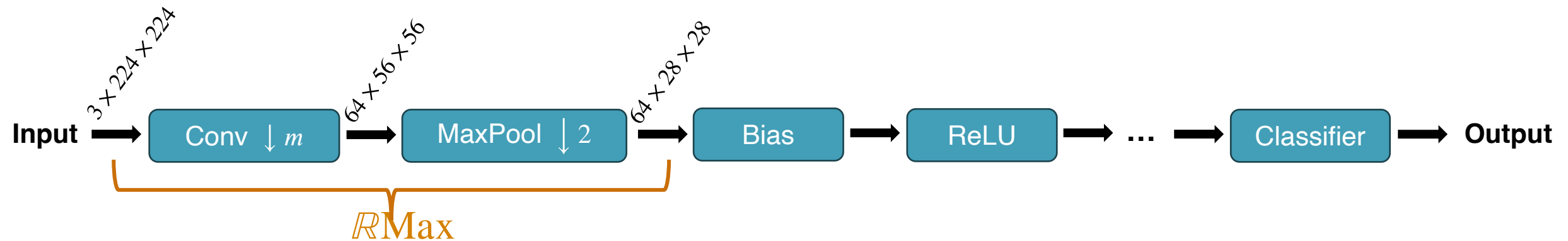


Example: AlexNet
(2012)

Band-pass “Gabor-like” filters



Focus on the first layer



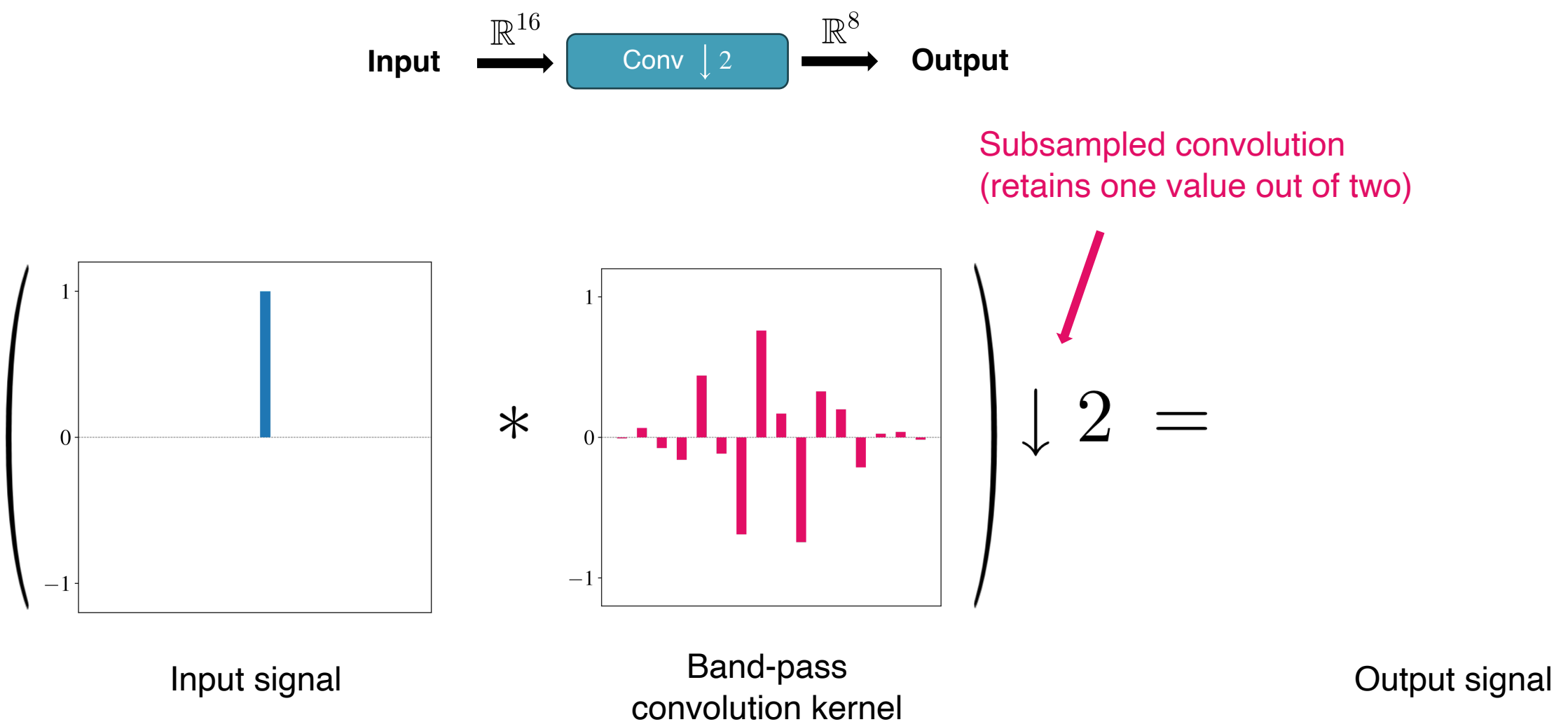
Example: AlexNet
(2012)



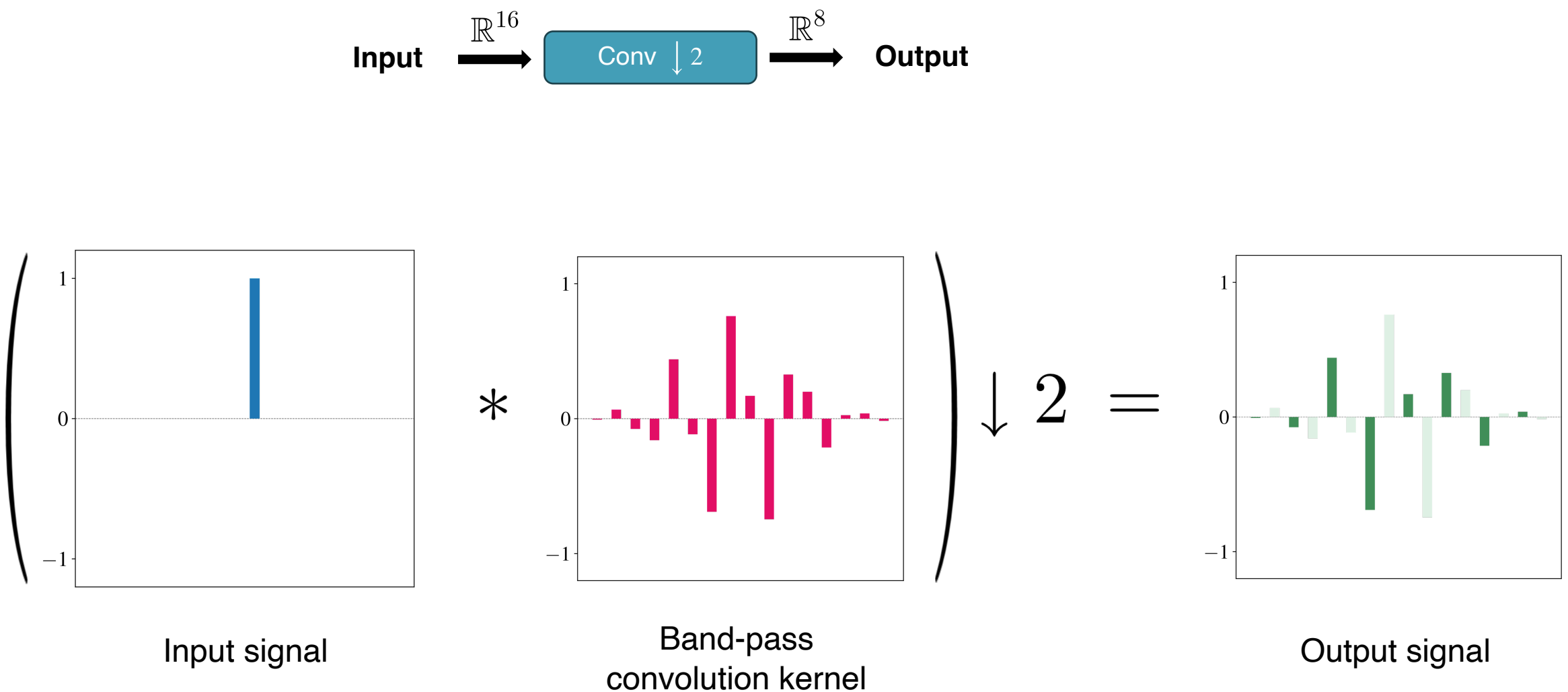
Rai, Mehang, and Pablo Rivas. "A review of convolutional neural networks and Gabor filters in object recognition." *2020 International Conference on Computational Science and Computational Intelligence (CSCI)*. IEEE, 2020.

Yosinski J, Clune J, Bengio Y, and Lipson H. How transferable are features in deep neural networks? In *Advances in Neural Information Processing Systems 27 (NIPS '14)*, NIPS Foundation, 2014.

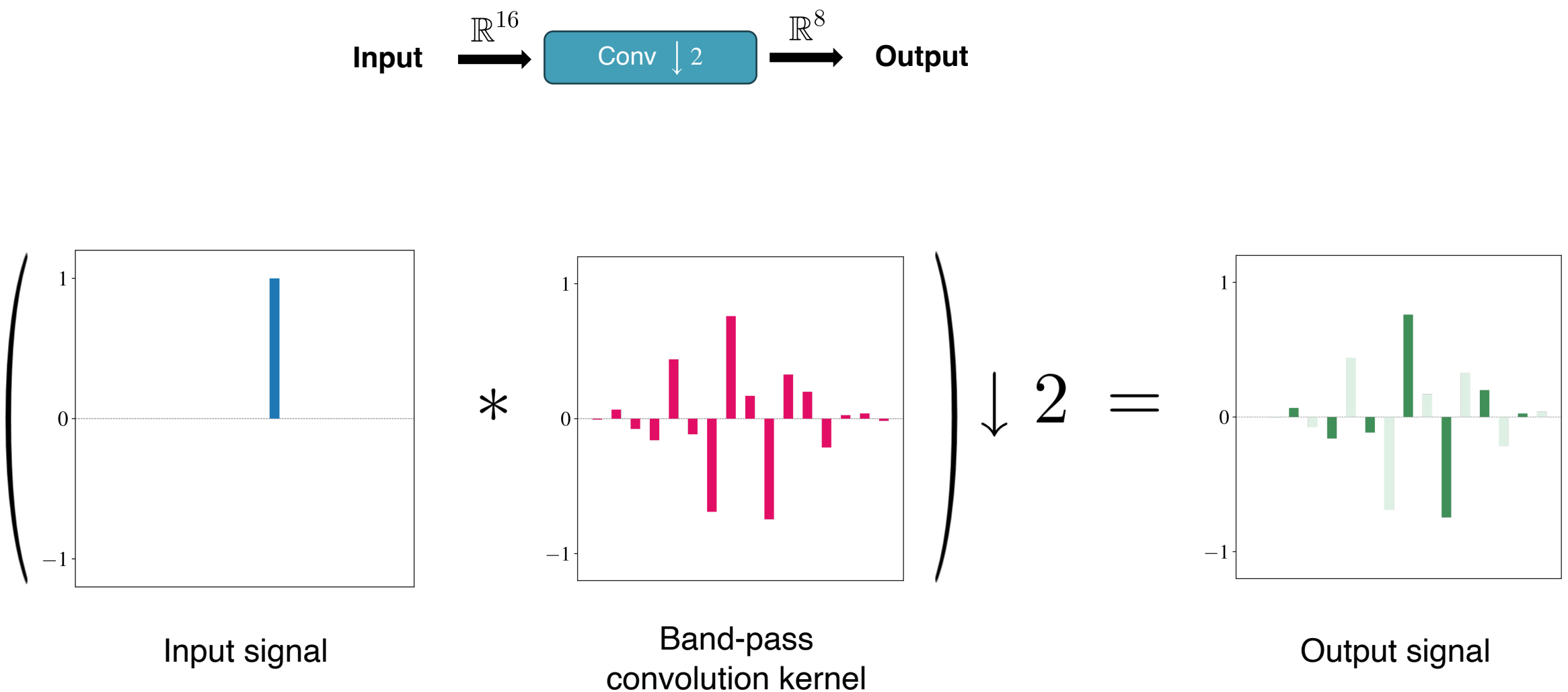
Subsampled convolutions, a real problem!



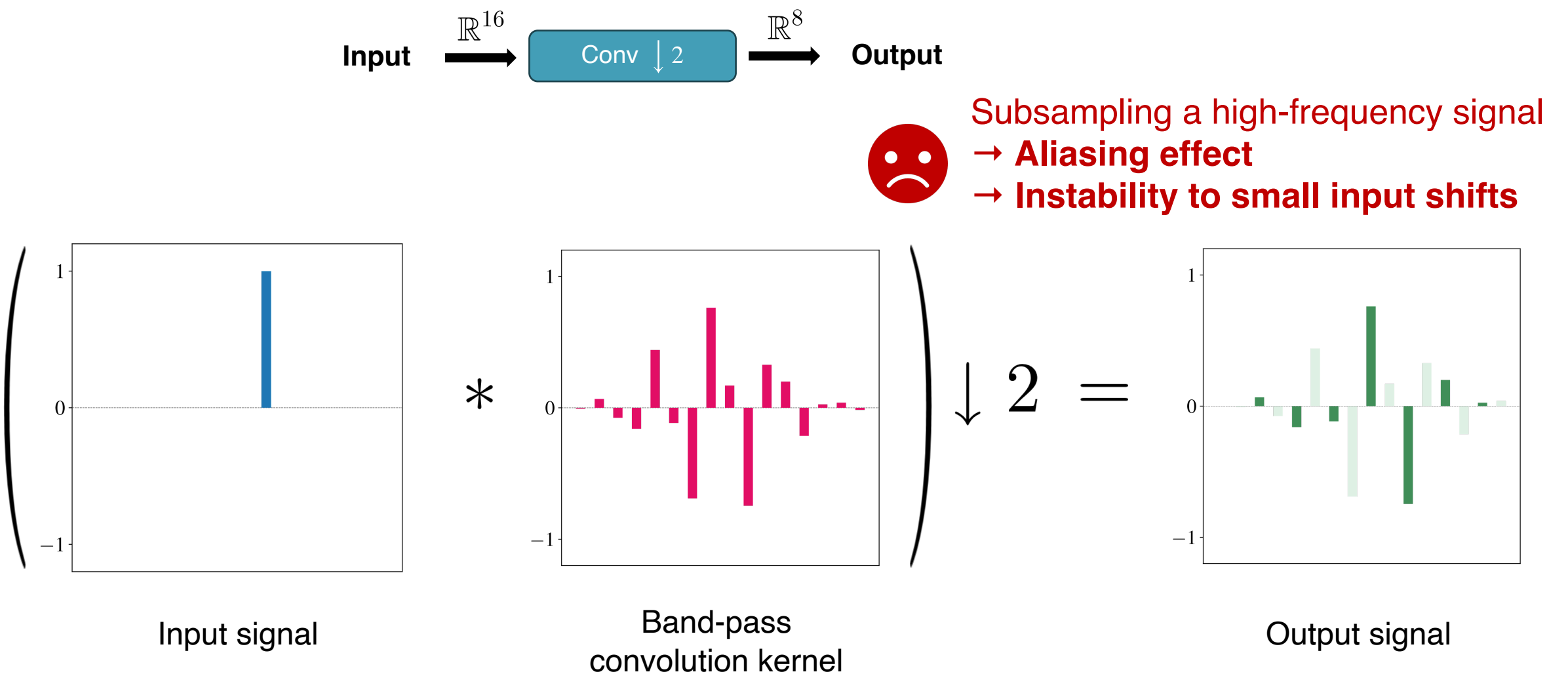
Subsampled convolutions, a real problem!



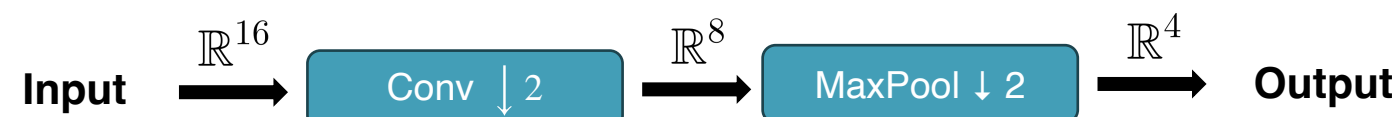
Subsampled convolutions, a real problem!



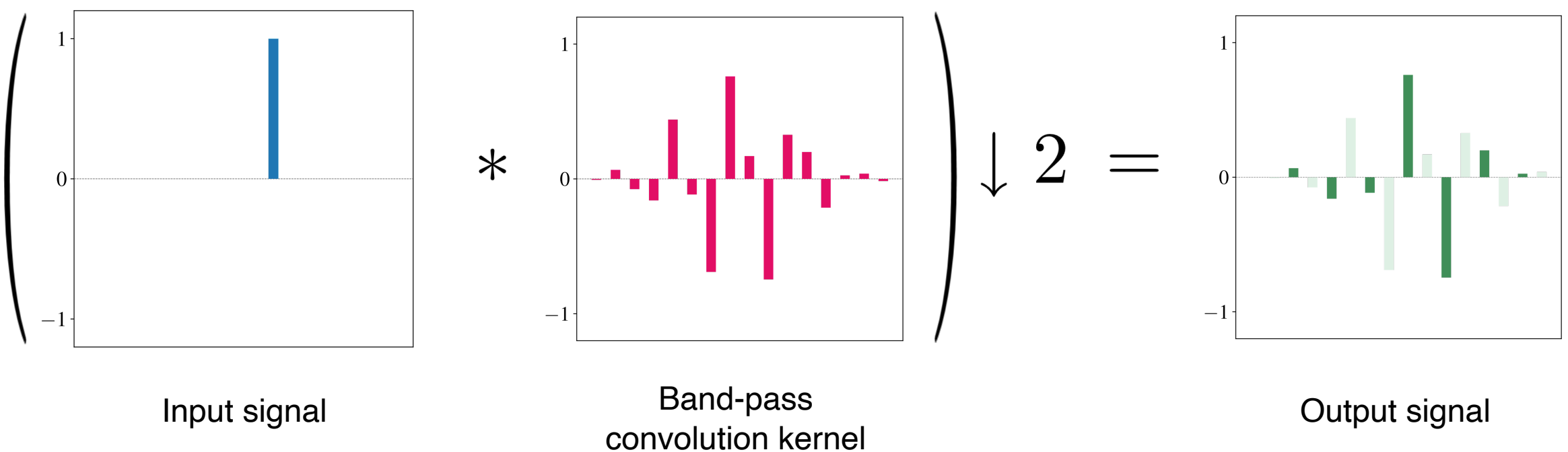
Subsampled convolutions, a real problem!



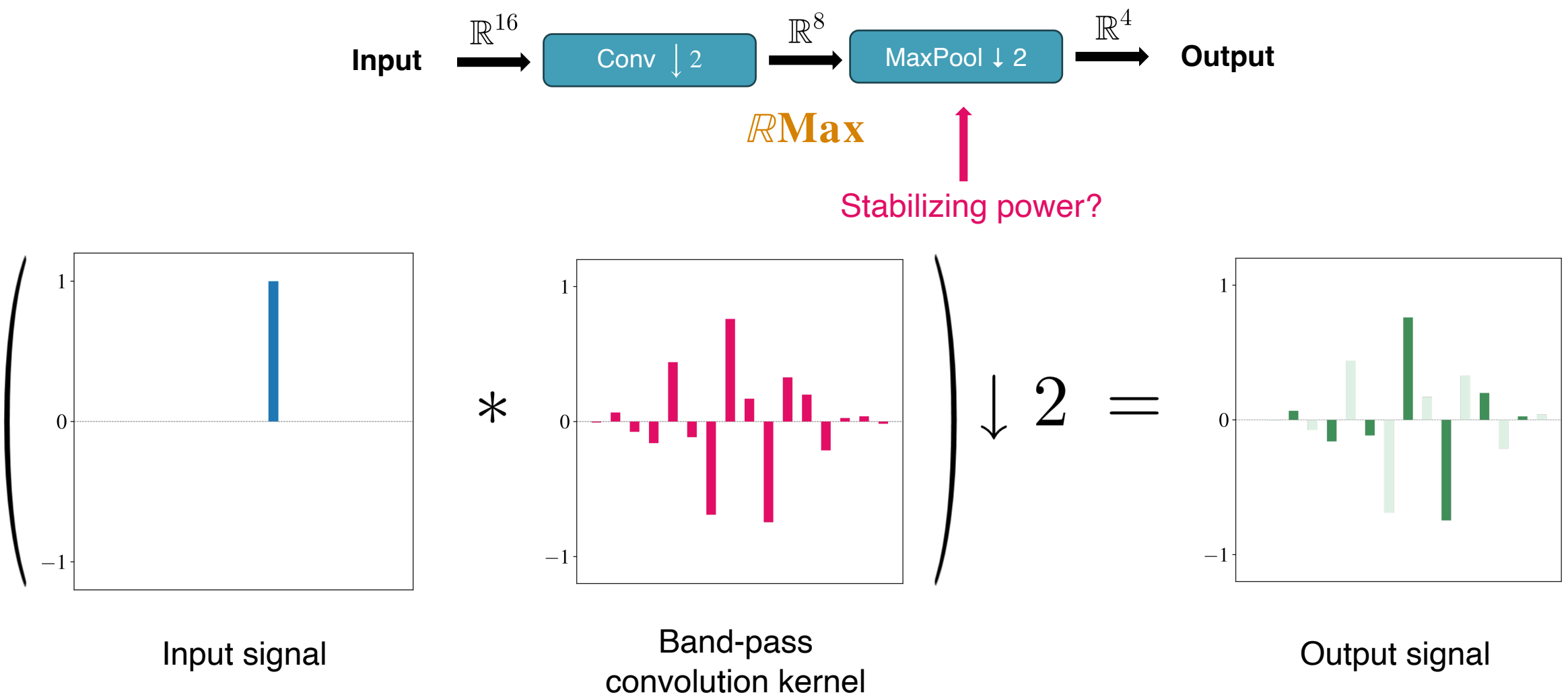
Subsampled convolutions, a real problem!



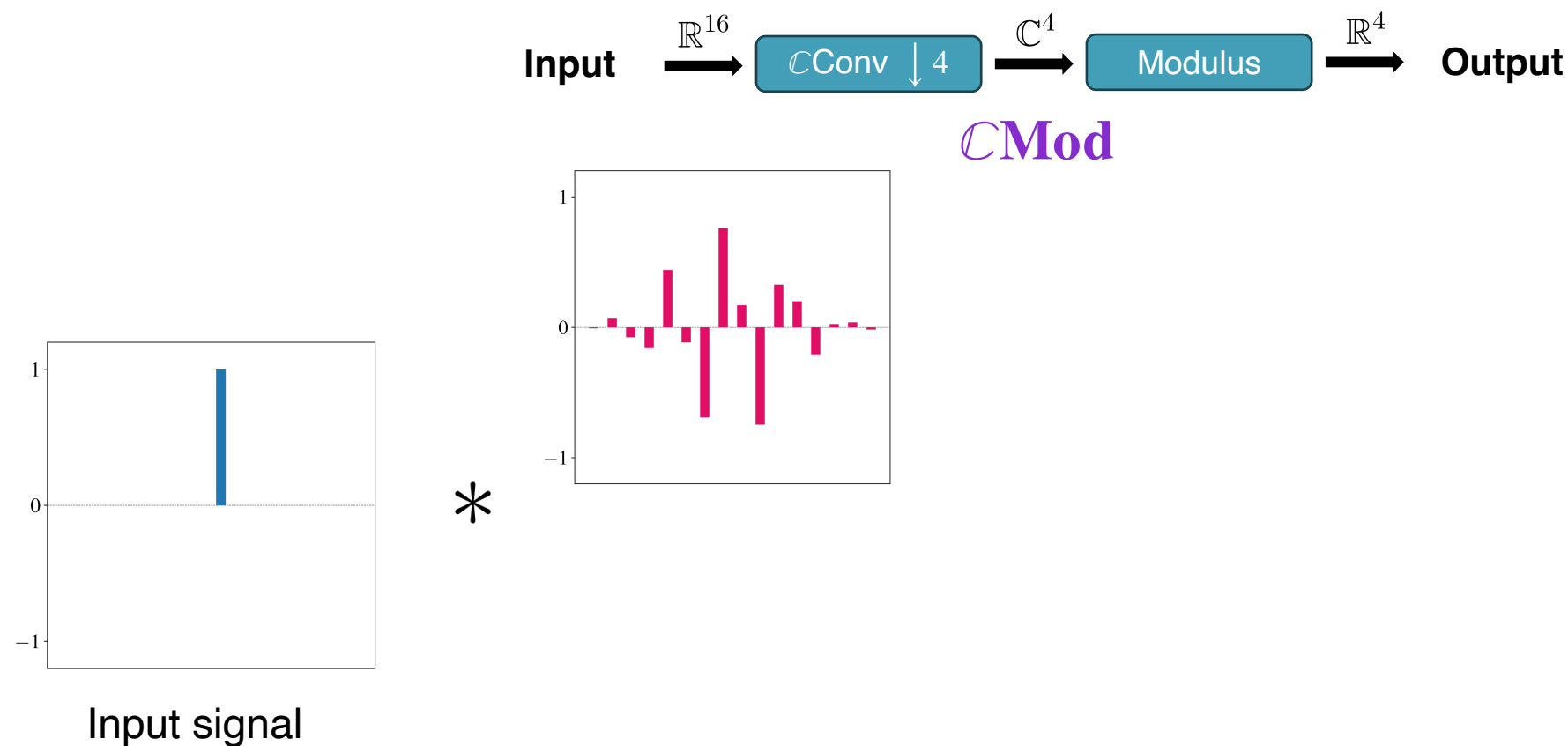
RMax



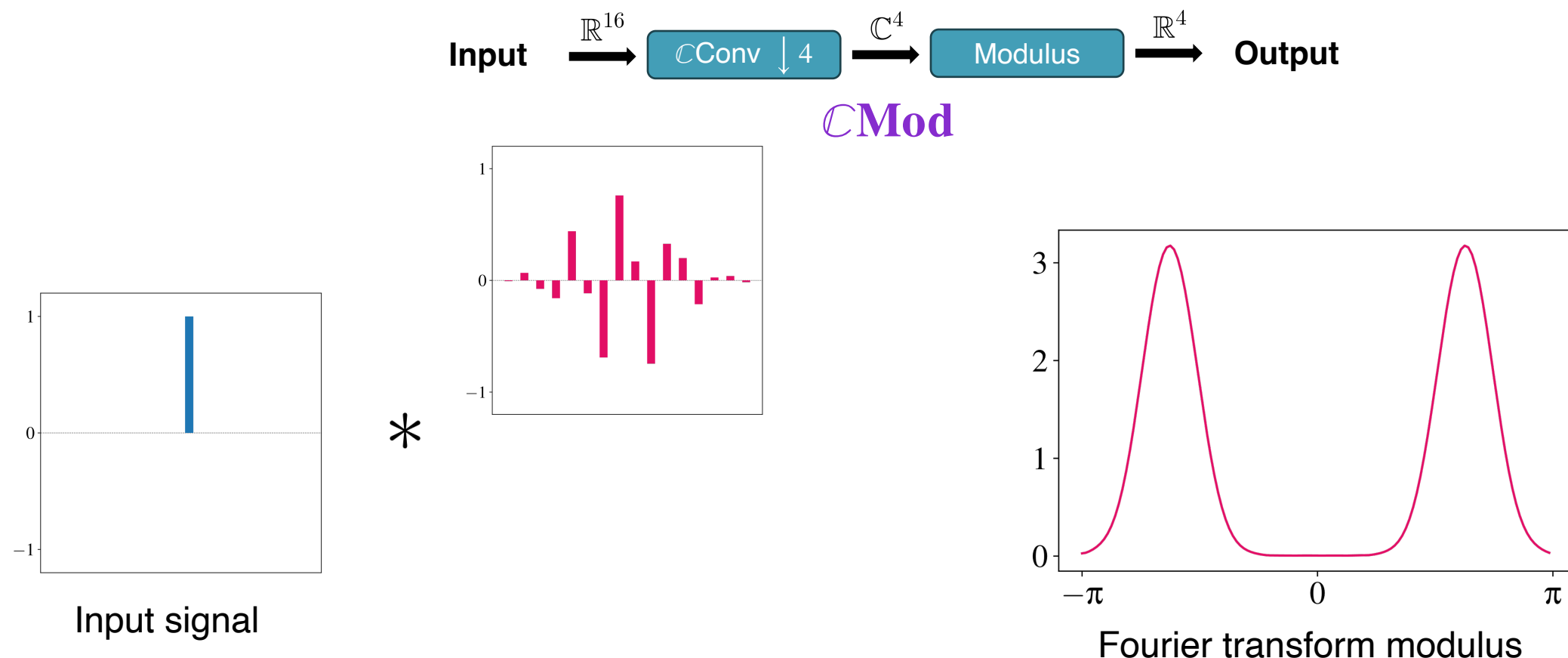
Subsampled convolutions, a real problem!



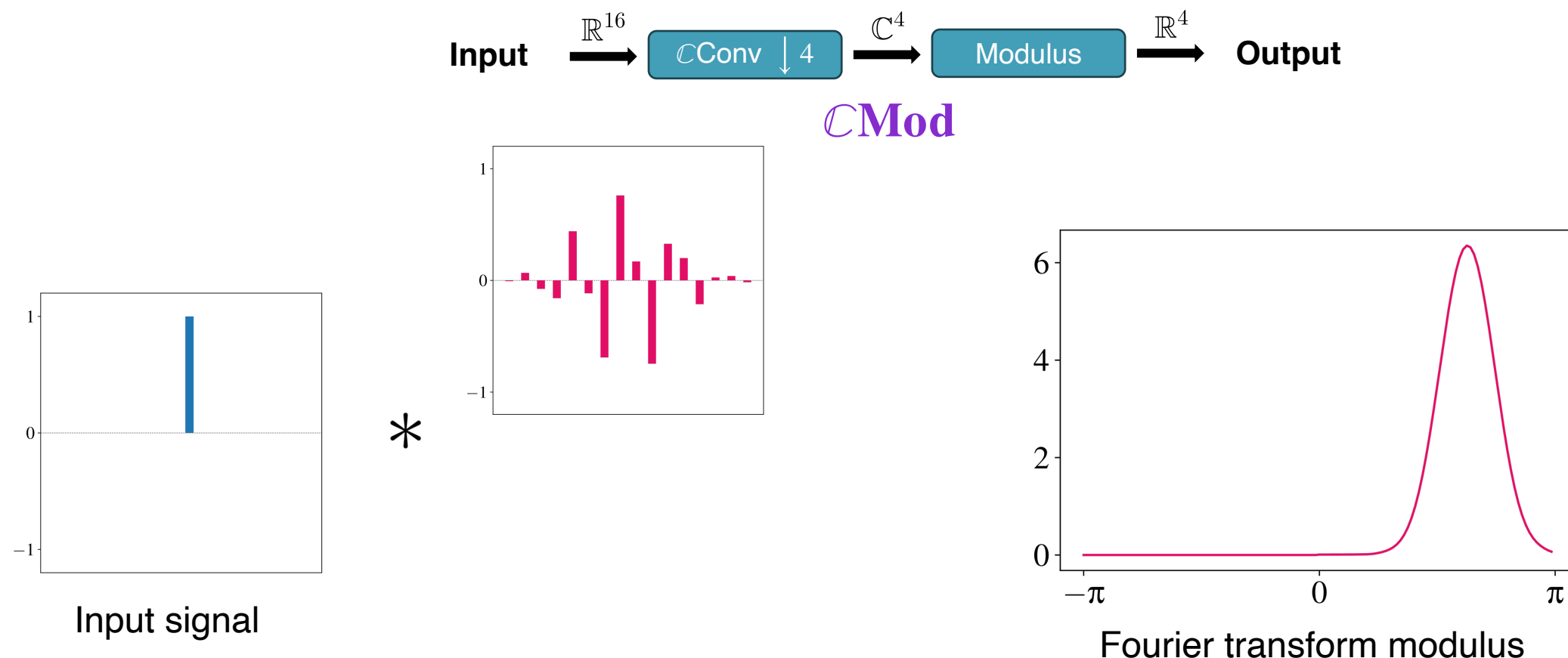
Complex-valued convolutions at rescue



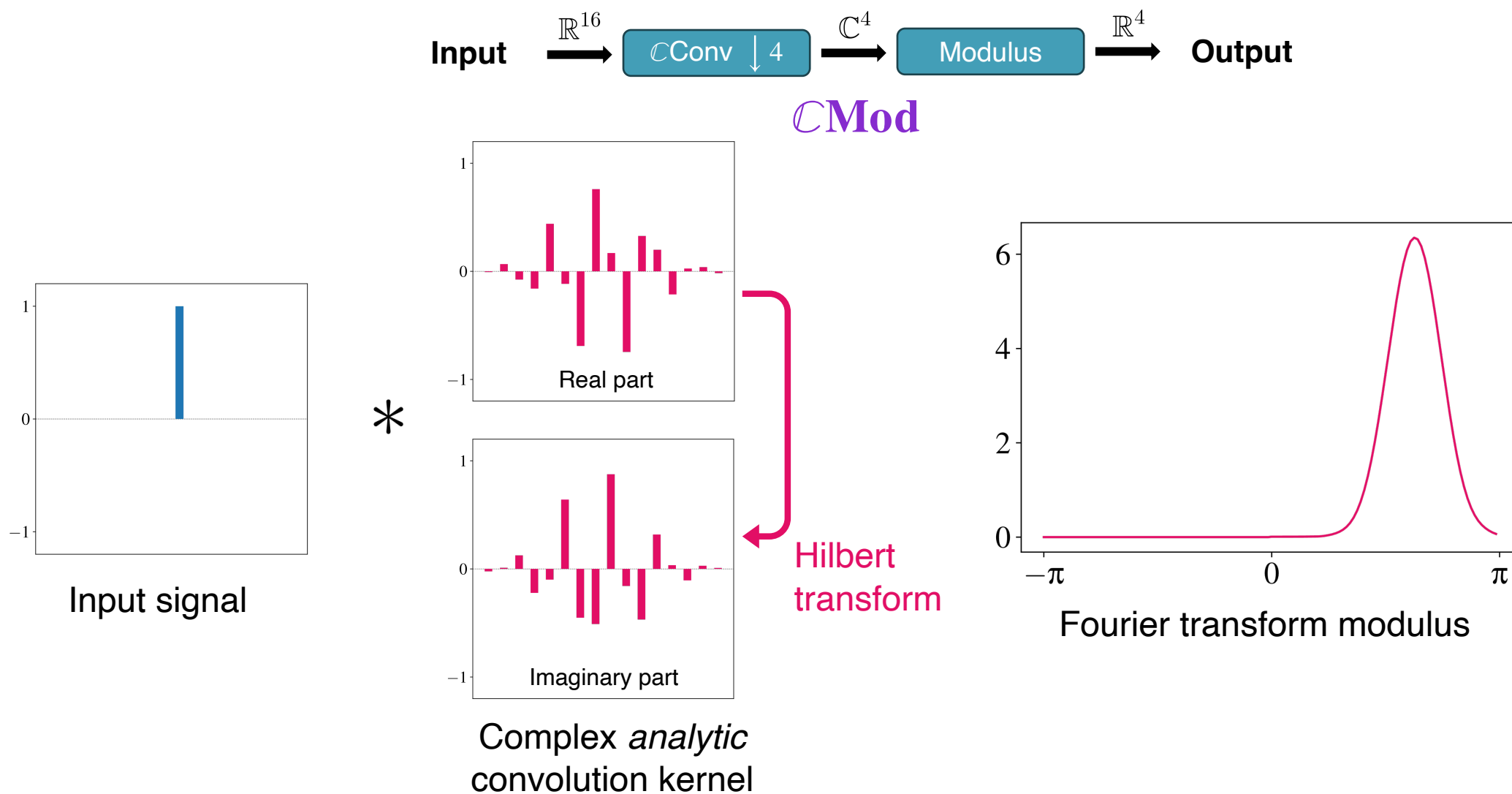
Complex-valued convolutions at rescue



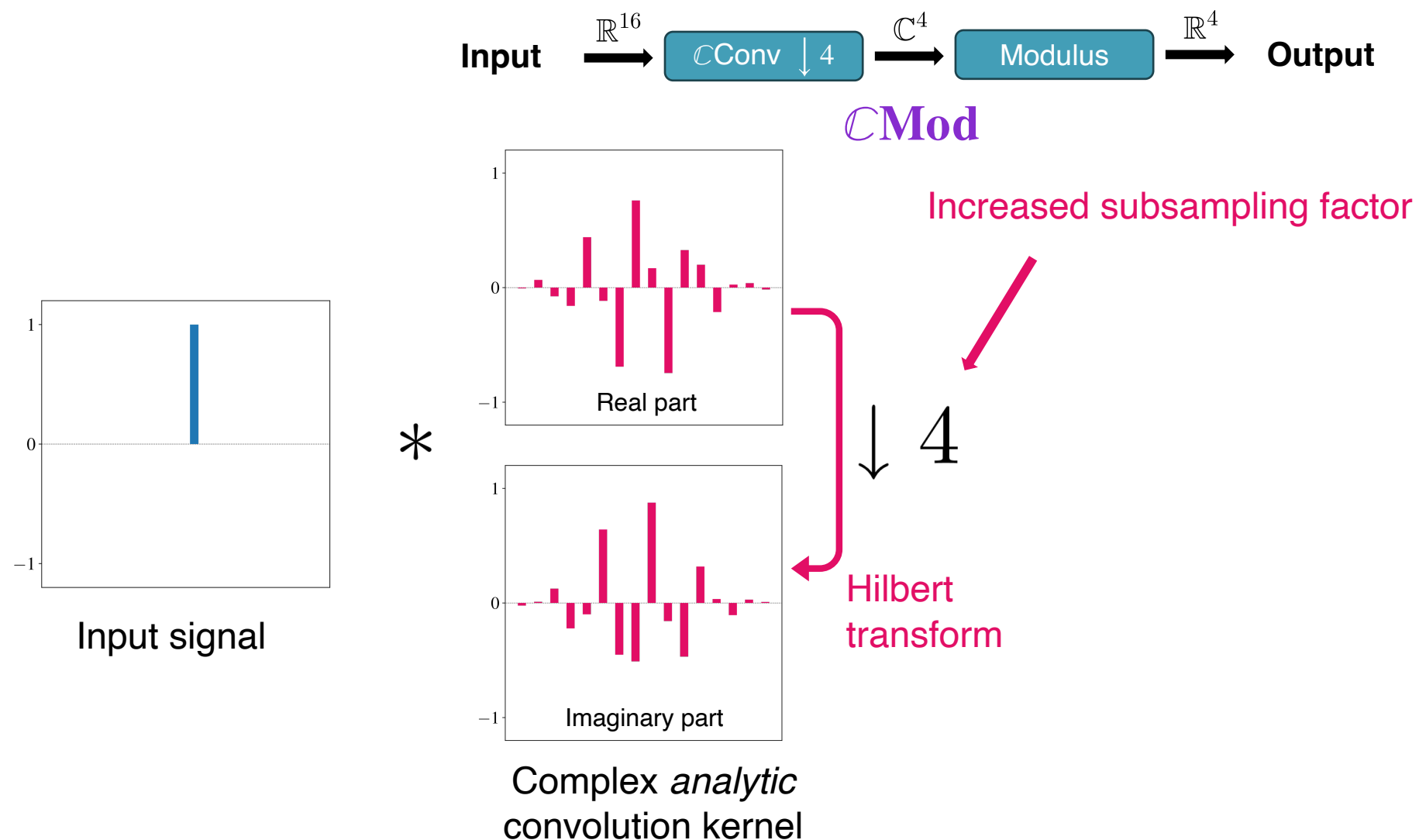
Complex-valued convolutions at rescue



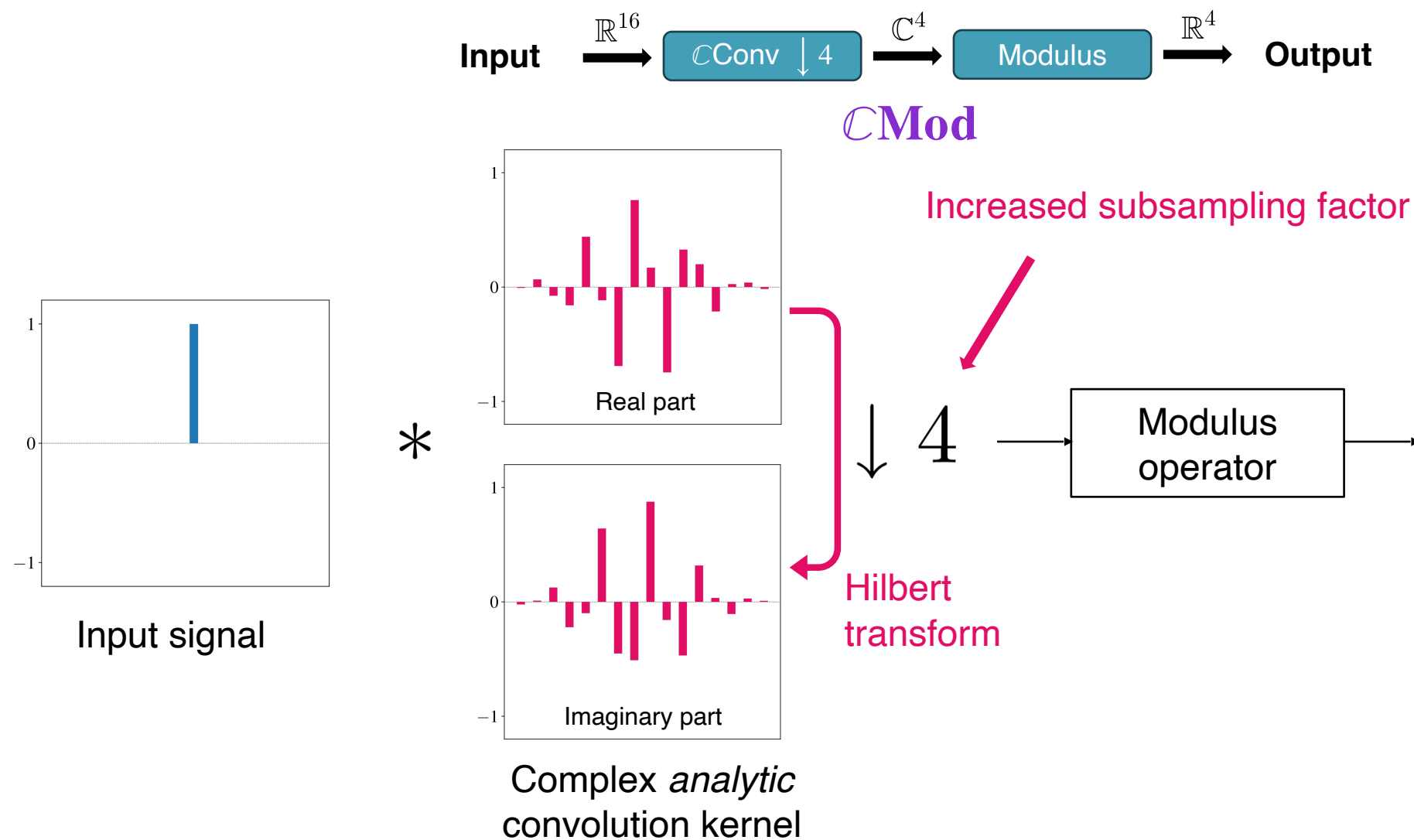
Complex-valued convolutions at rescue



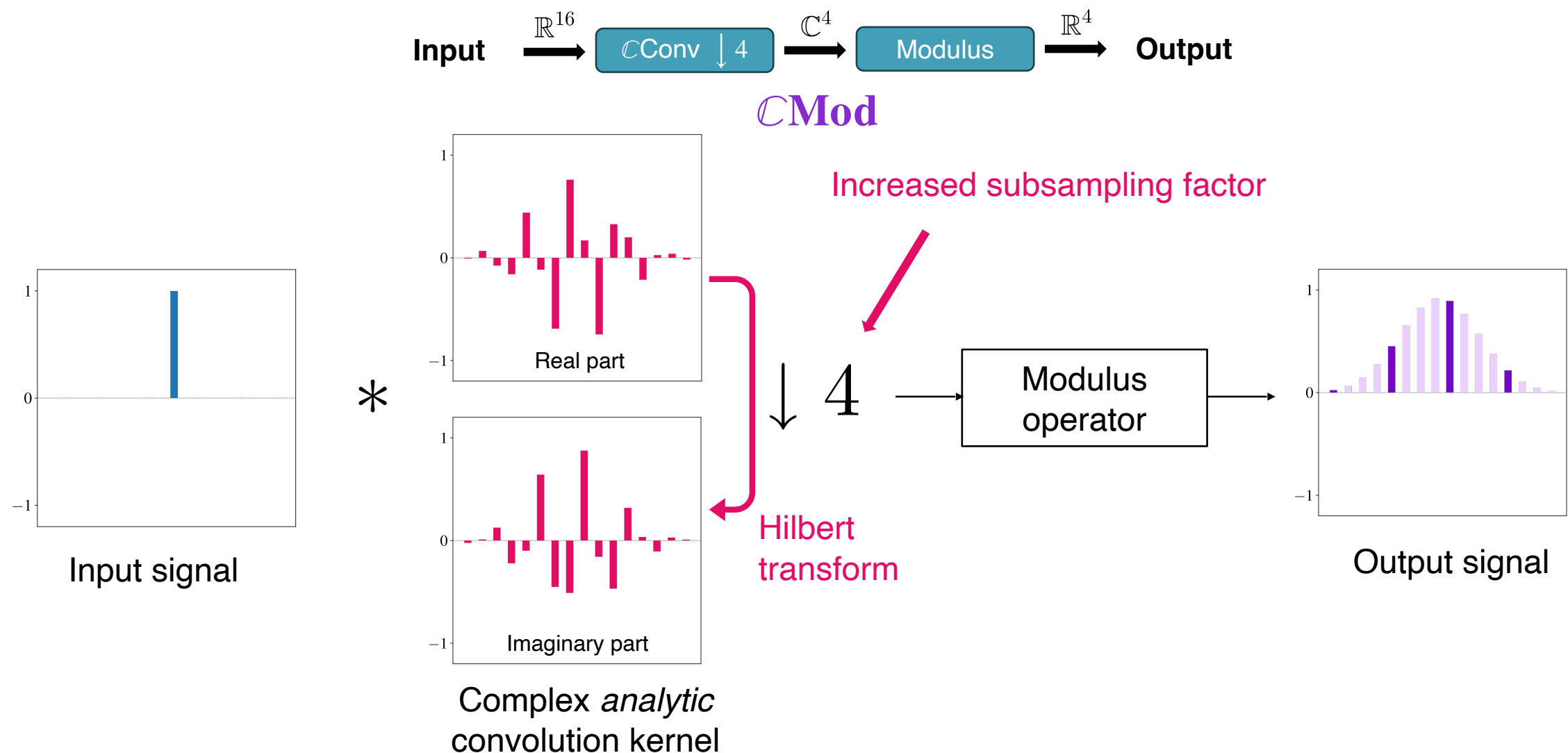
Complex-valued convolutions at rescue



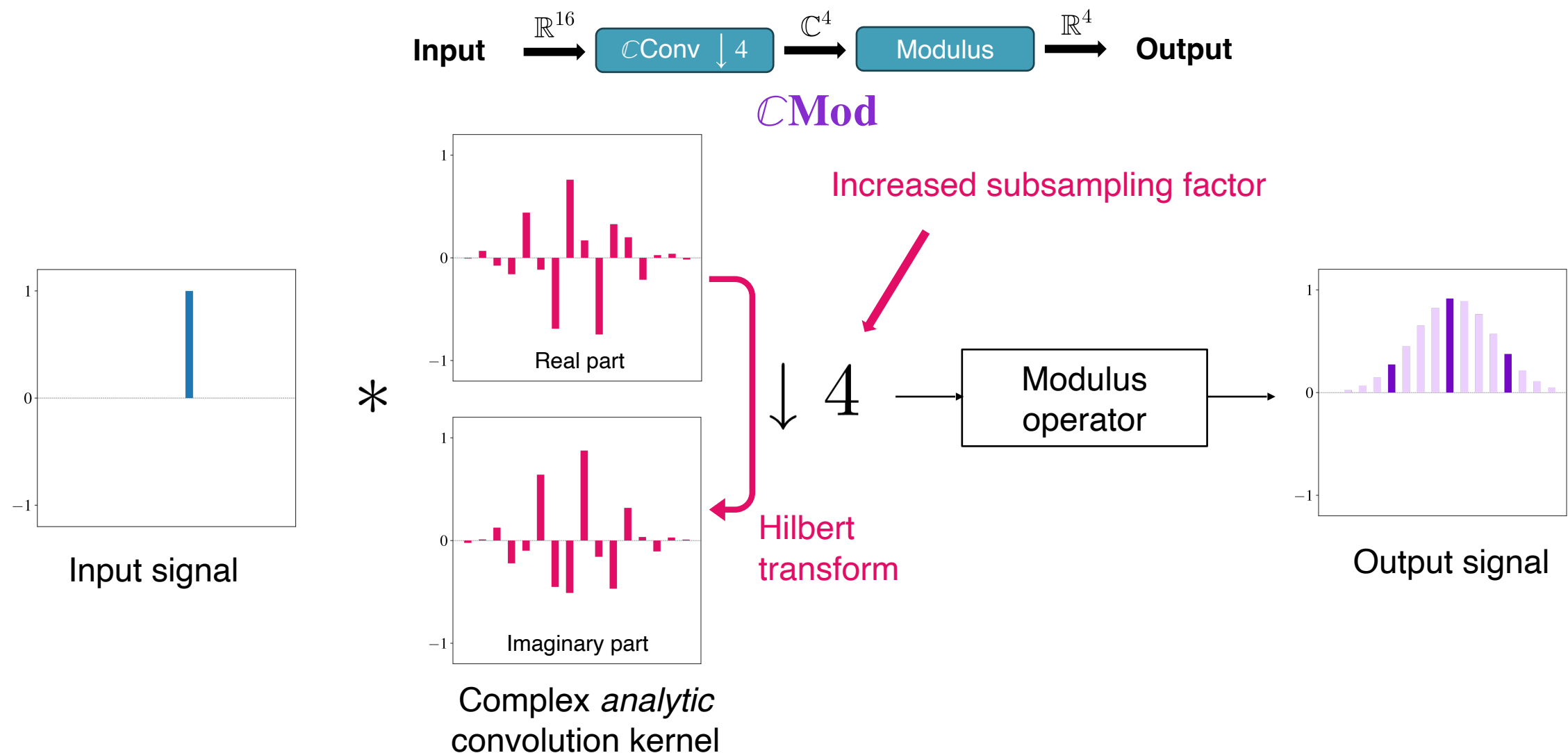
Complex-valued convolutions at rescue



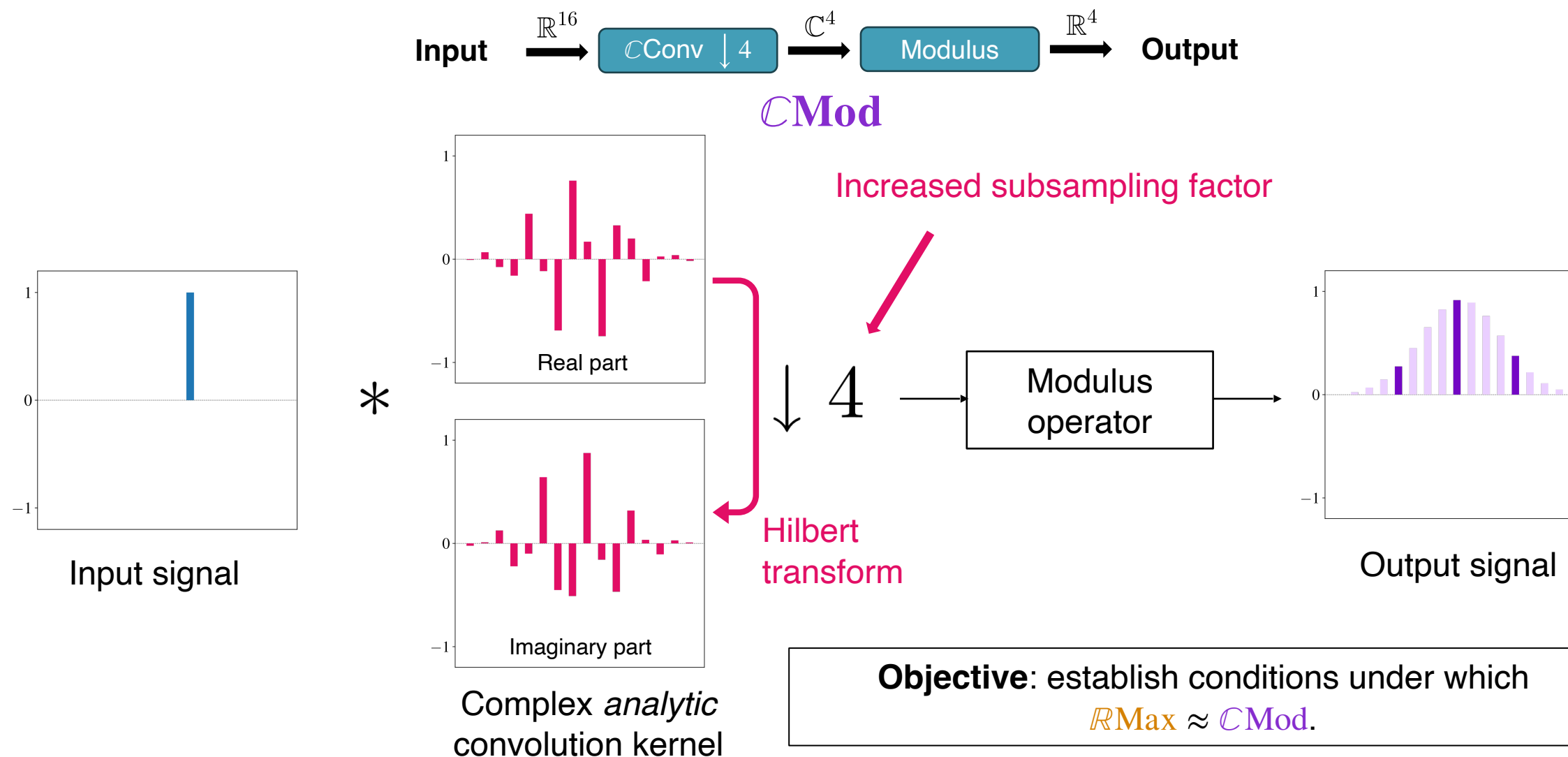
Complex-valued convolutions at rescue



Complex-valued convolutions at rescue



Complex-valued convolutions at rescue

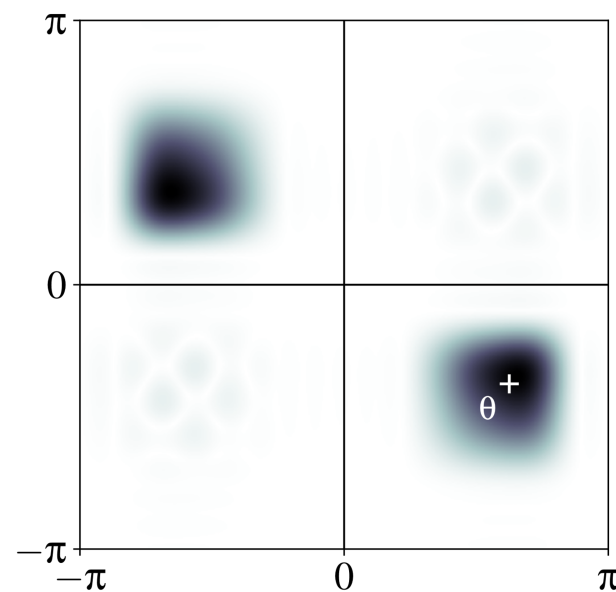
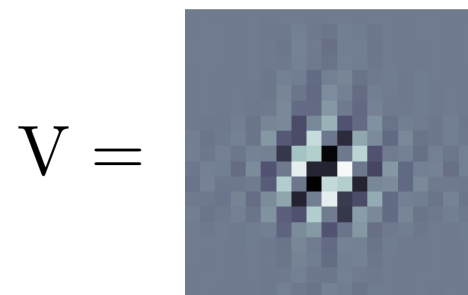


Fundamental hypothesis on filter

- Band-pass, oriented and **analytic Gabor-like** filters W

Fundamental hypothesis on filter

- Band-pass, oriented and **analytic Gabor-like** filters W

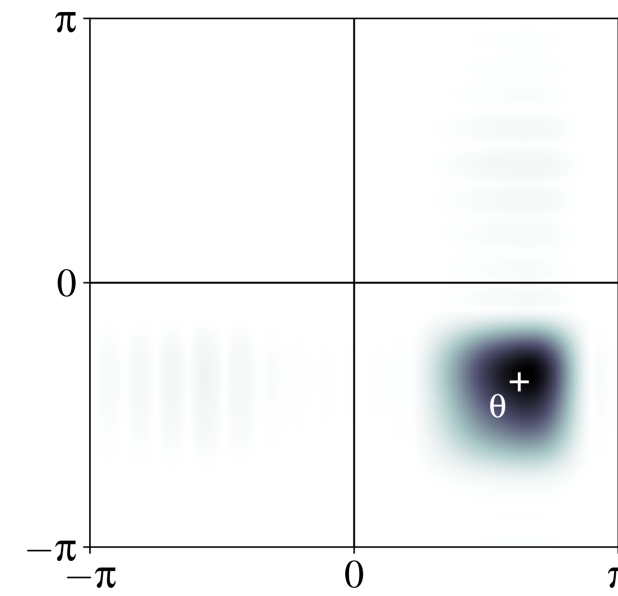
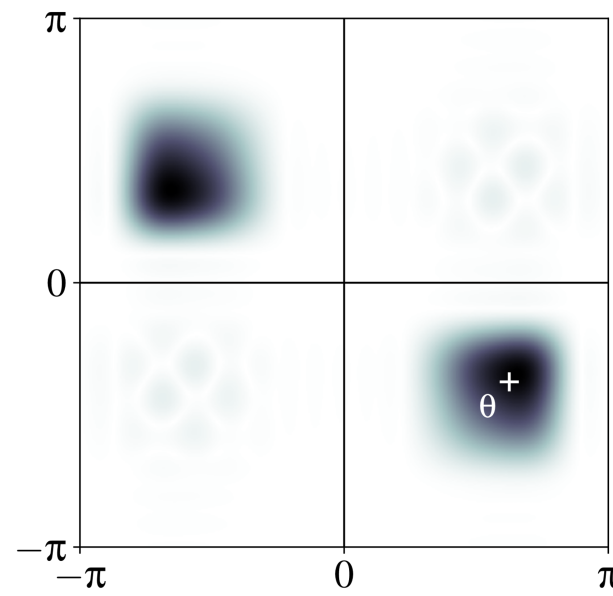


Fundamental hypothesis on filter

- Band-pass, oriented and **analytic Gabor-like** filters W

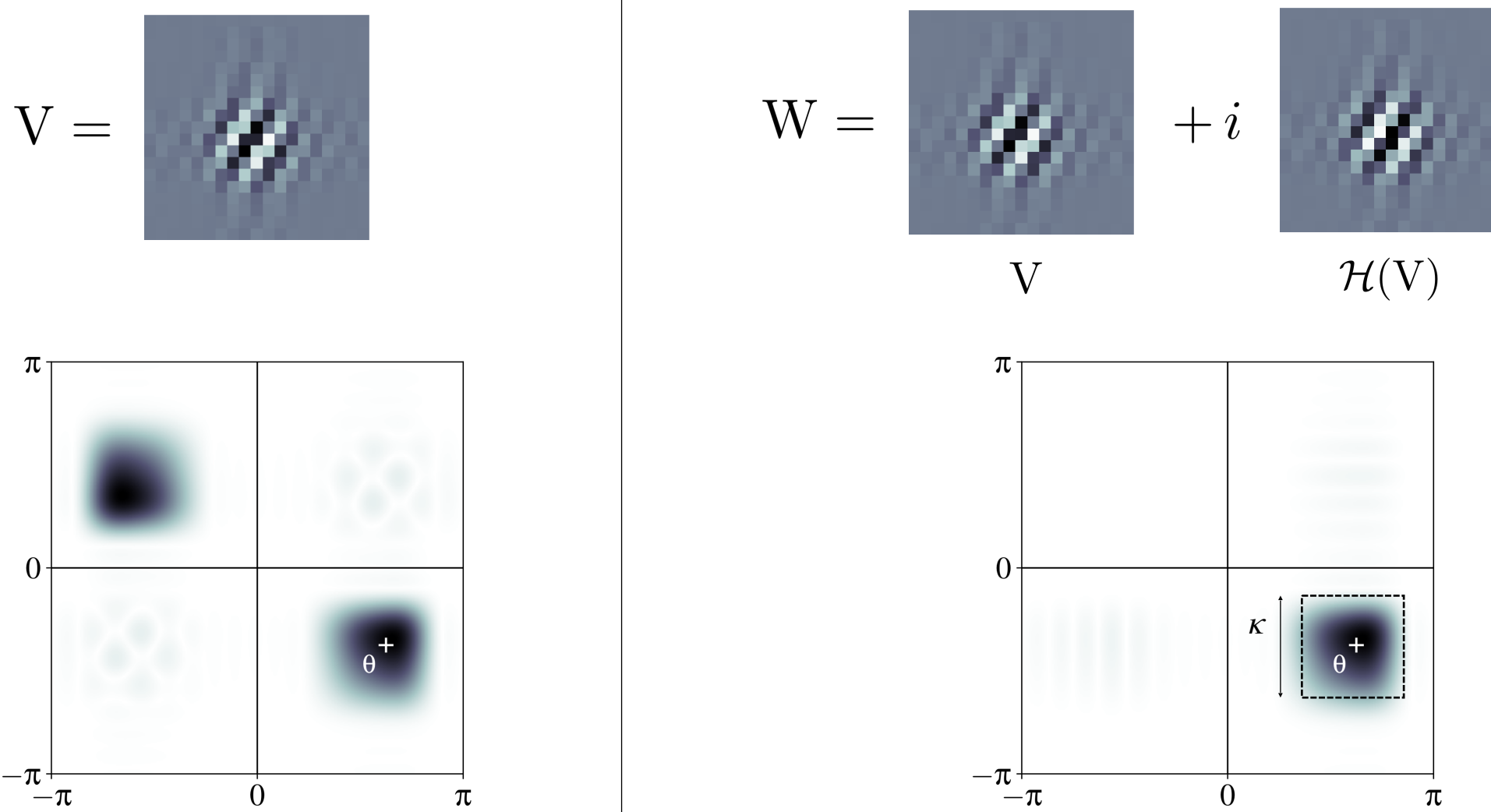
$$V = \begin{matrix} \text{Image} \end{matrix}$$

$$W = \begin{matrix} \text{Image} & + i & \text{Image} \\ V & & \mathcal{H}(V) \end{matrix}$$



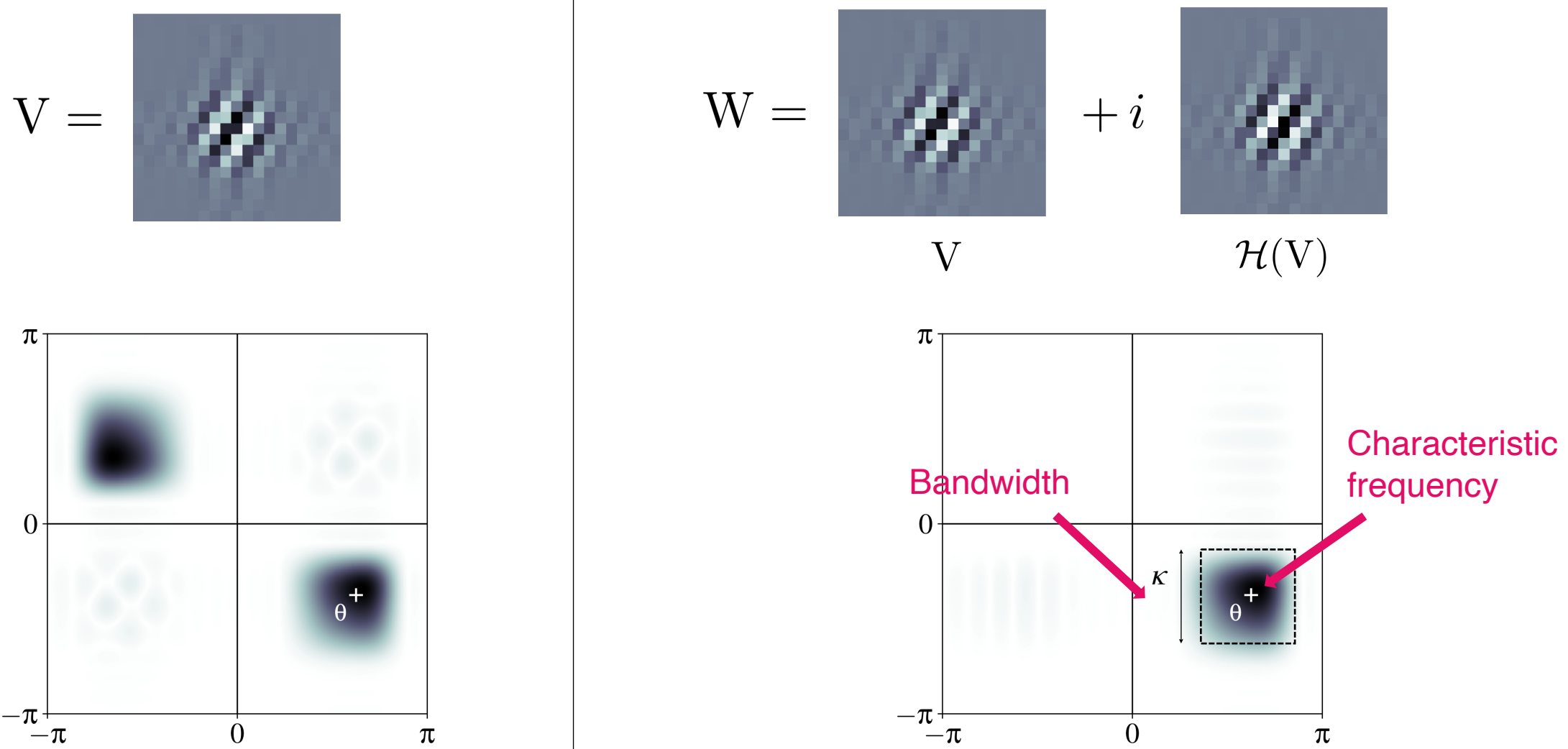
Fundamental hypothesis on filter

- Band-pass, oriented and **analytic Gabor-like** filters W



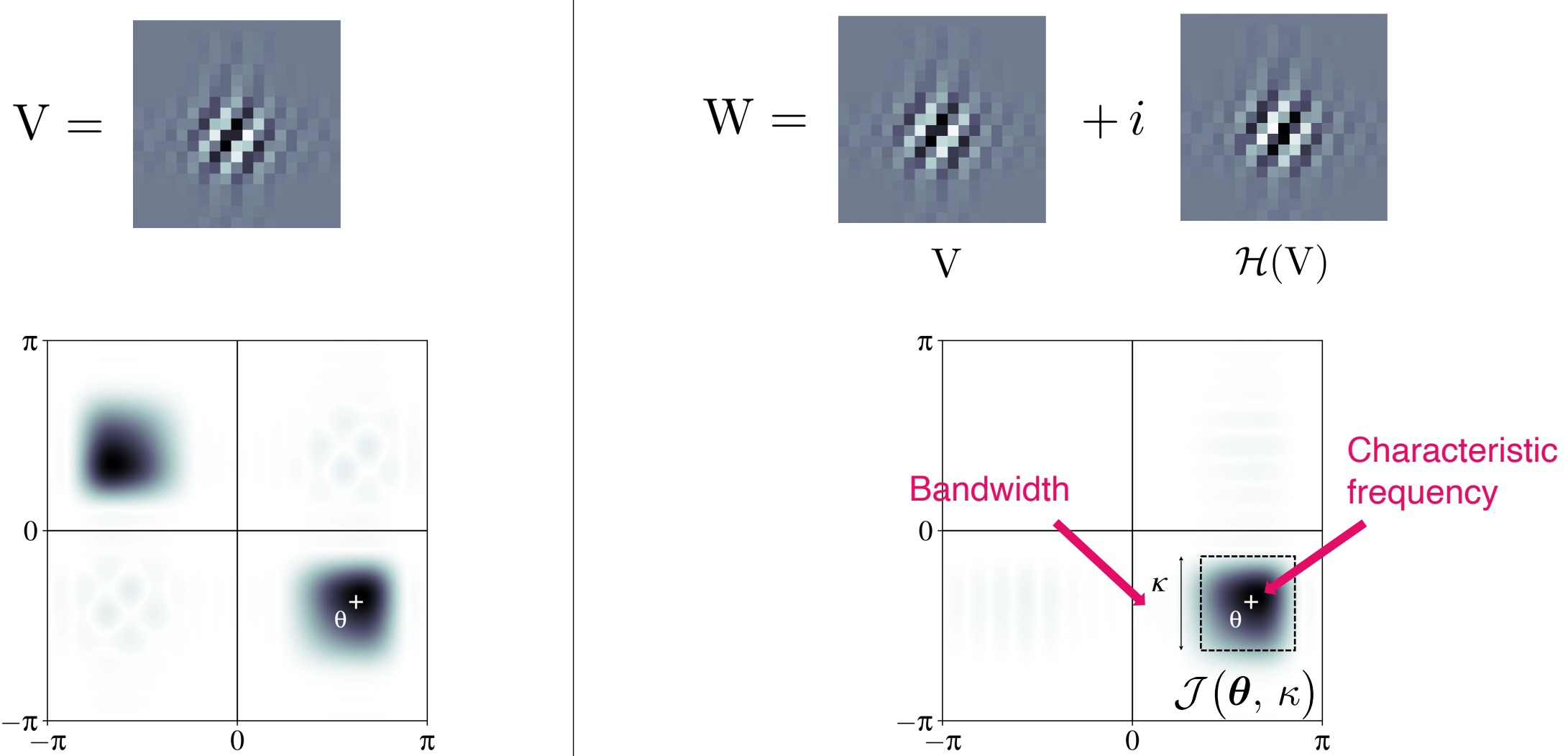
Fundamental hypothesis on filter

- Band-pass, oriented and **analytic Gabor-like filters** W

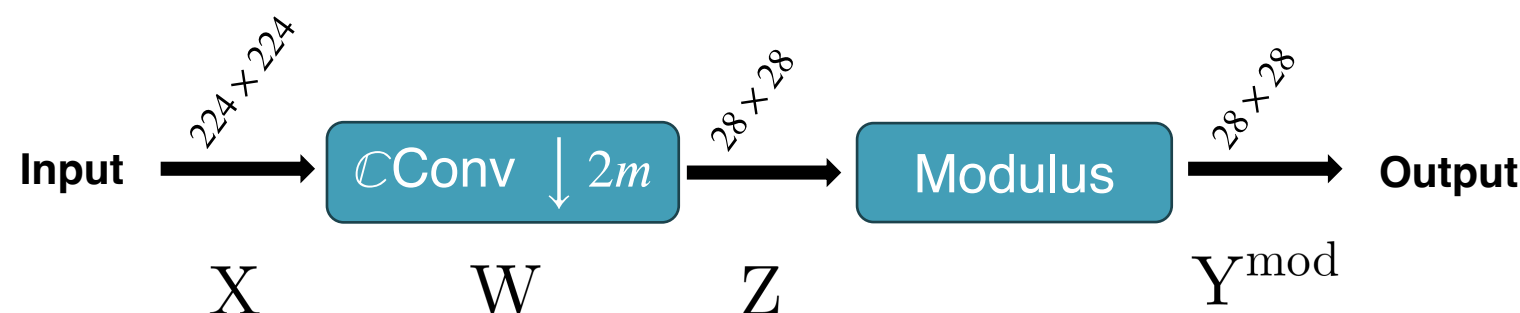
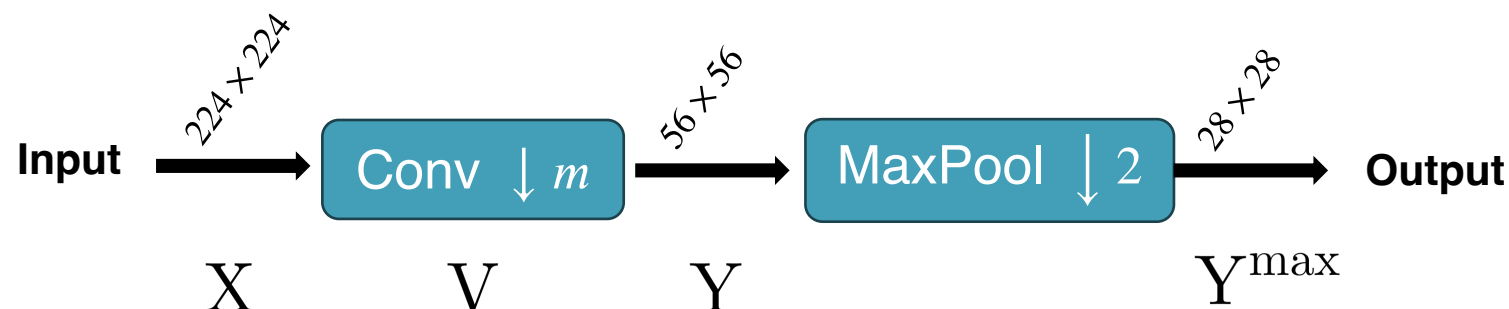


Fundamental hypothesis on filter

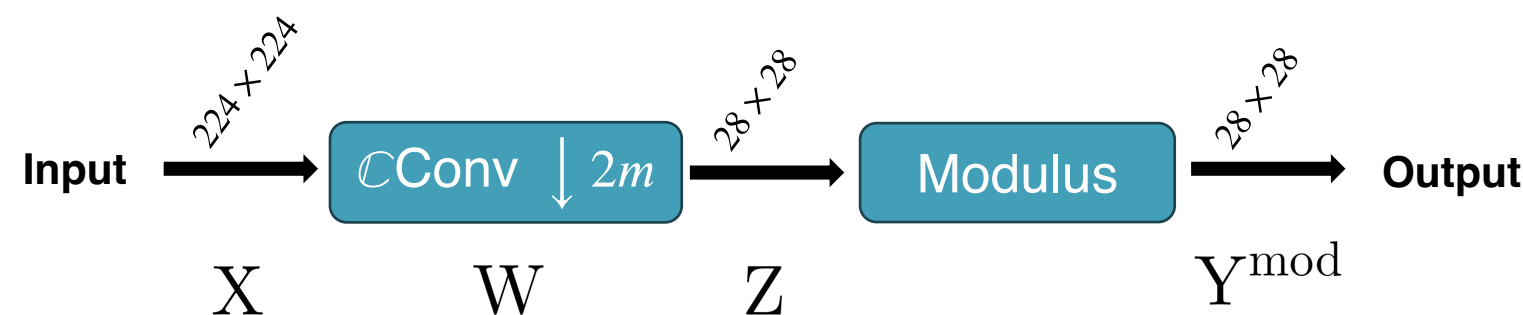
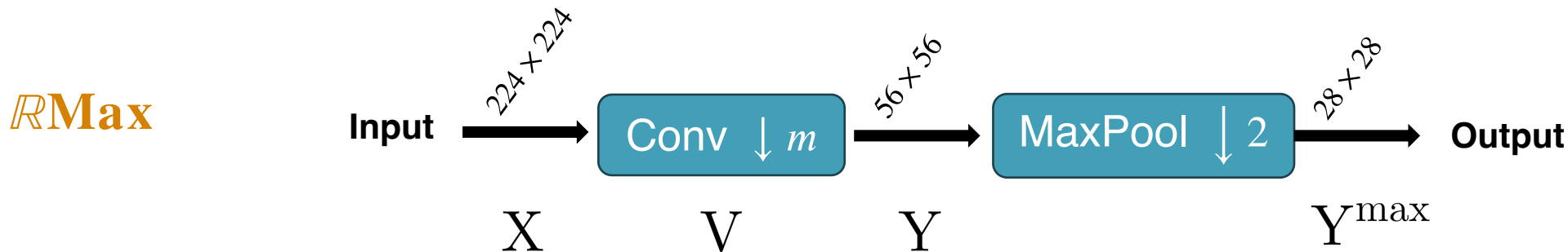
- Band-pass, oriented and **analytic Gabor-like filters** W



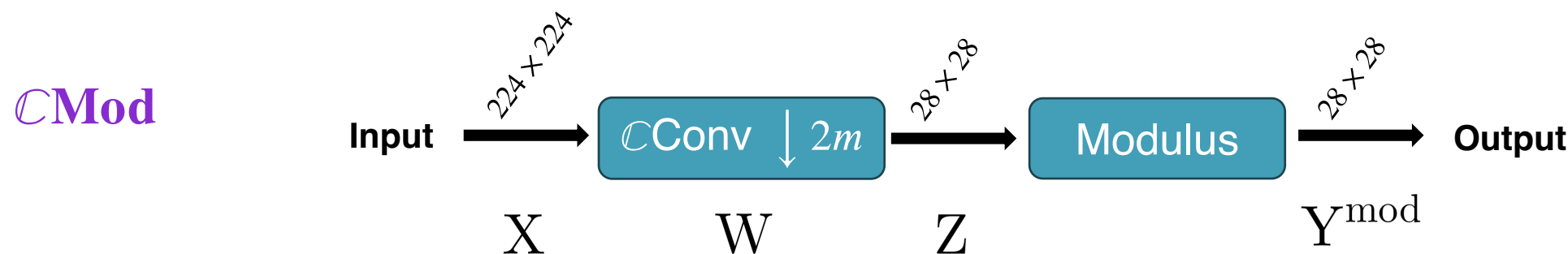
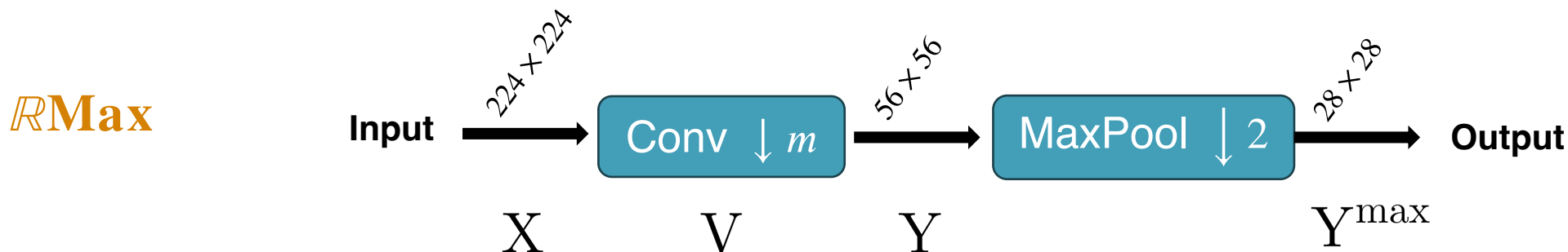
Two operators to compare



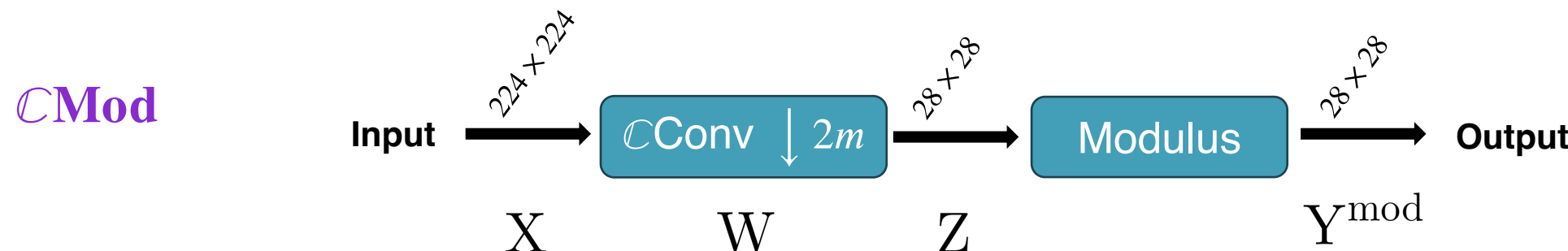
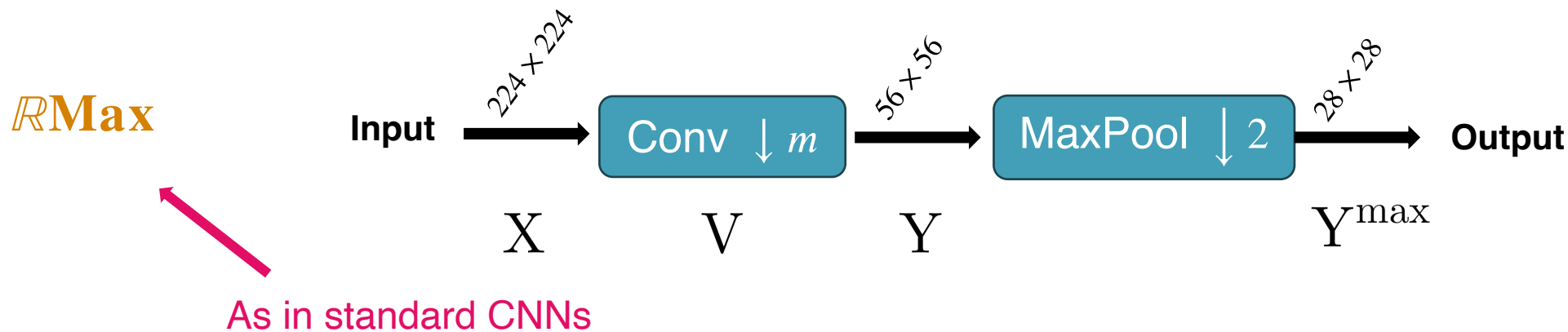
Two operators to compare



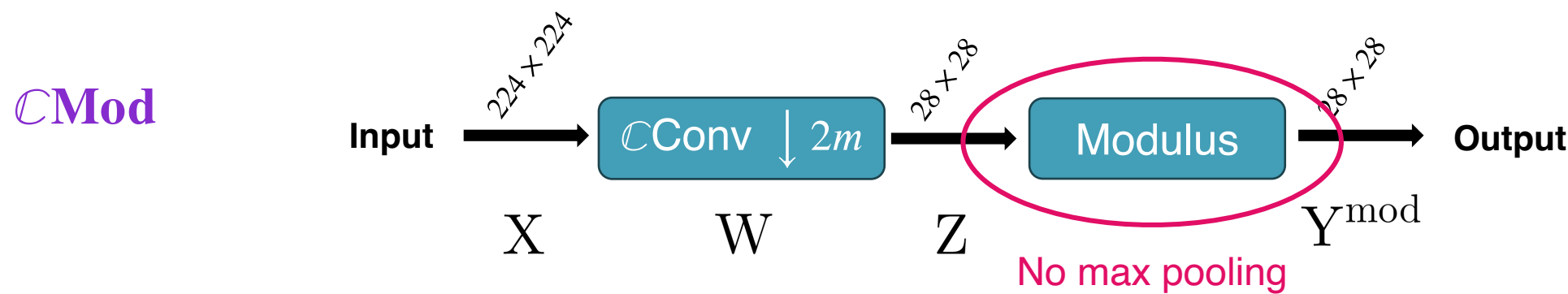
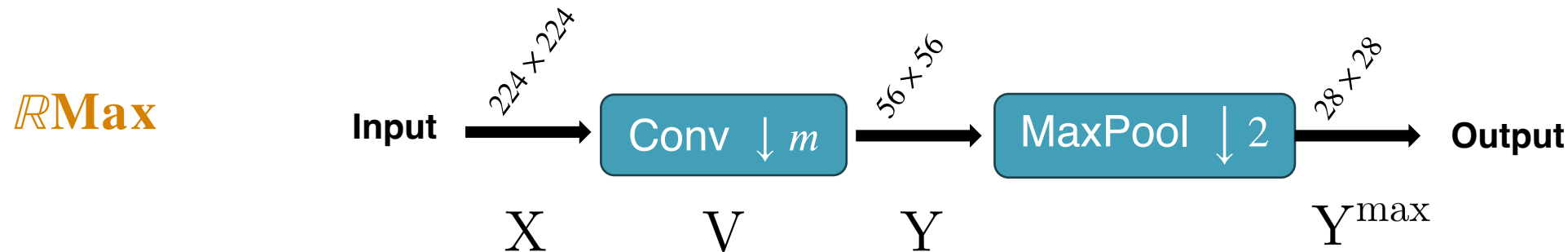
Two operators to compare



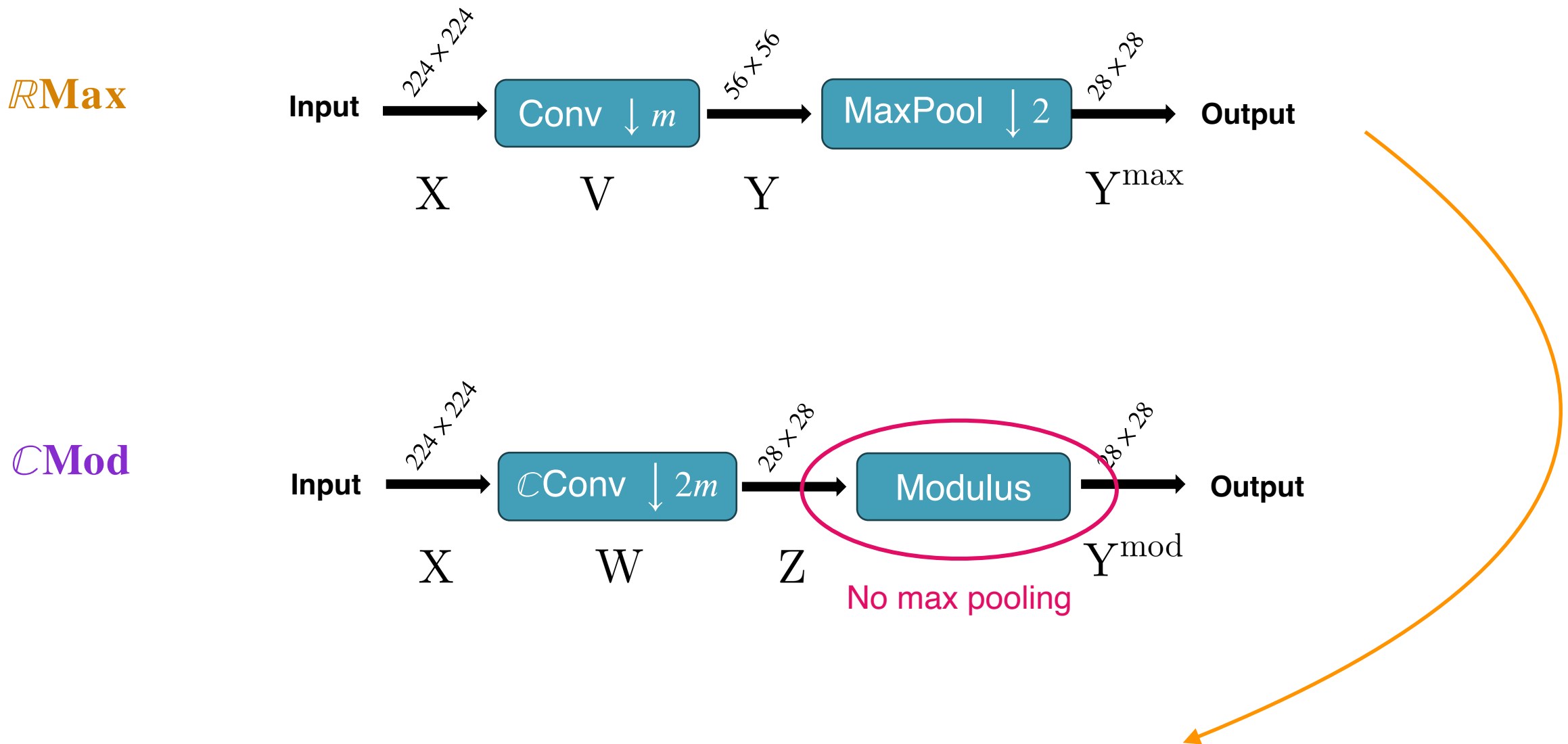
Two operators to compare



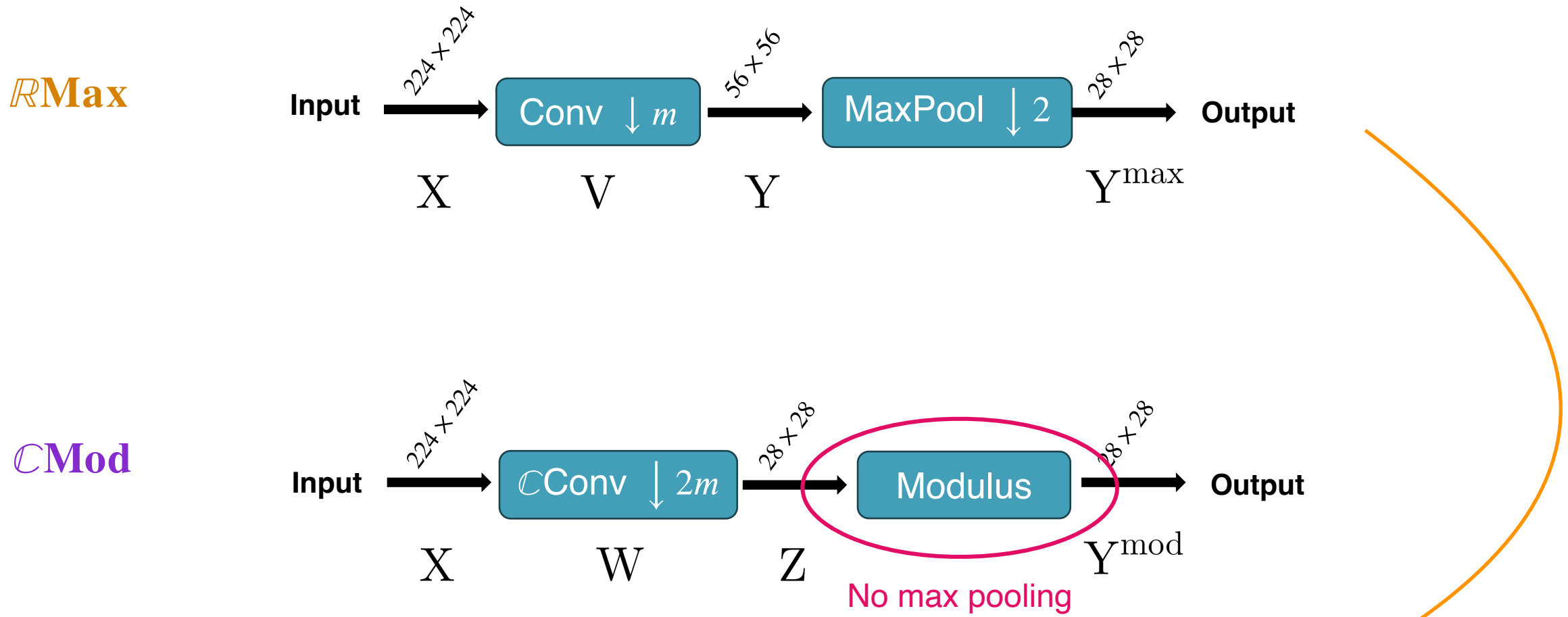
Two operators to compare



Two operators to compare

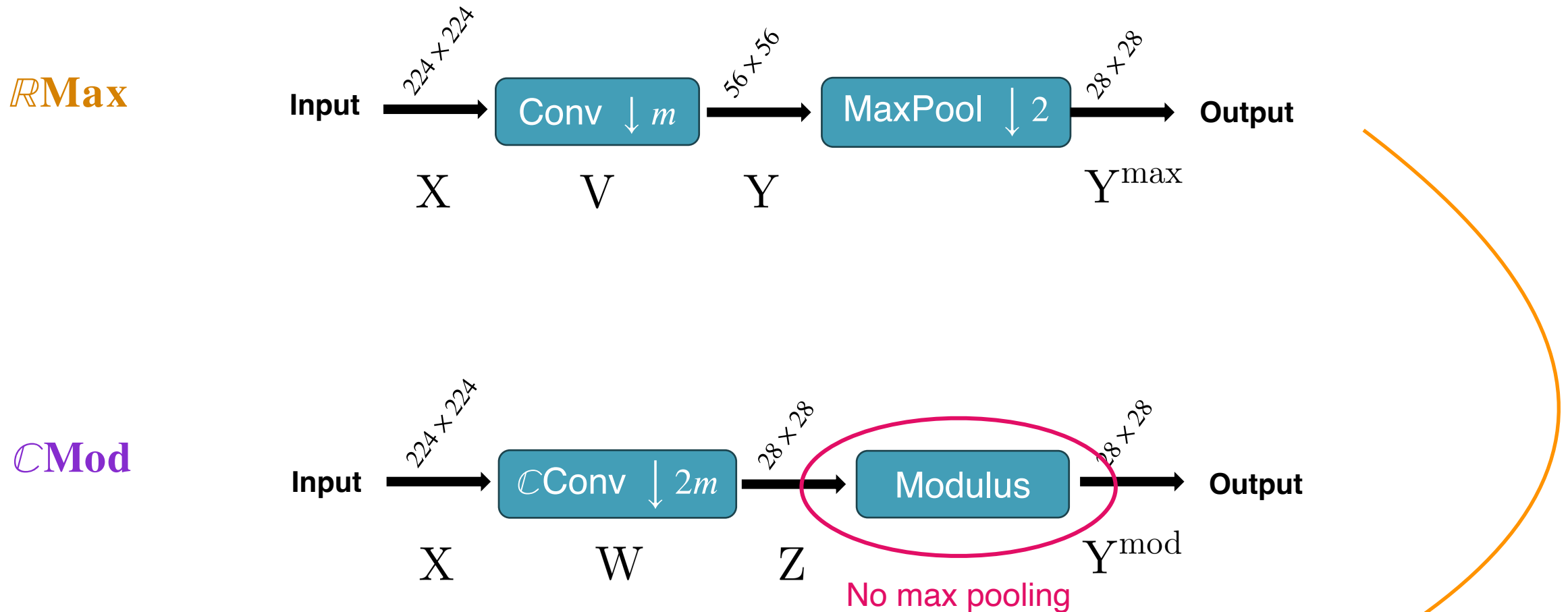


Two operators to compare



■ $U_{m,q}^{\max}[W] : X \mapsto \text{MaxPool}_q \left((X * \overline{\text{Re}W}) \downarrow m \right)$

Two operators to compare

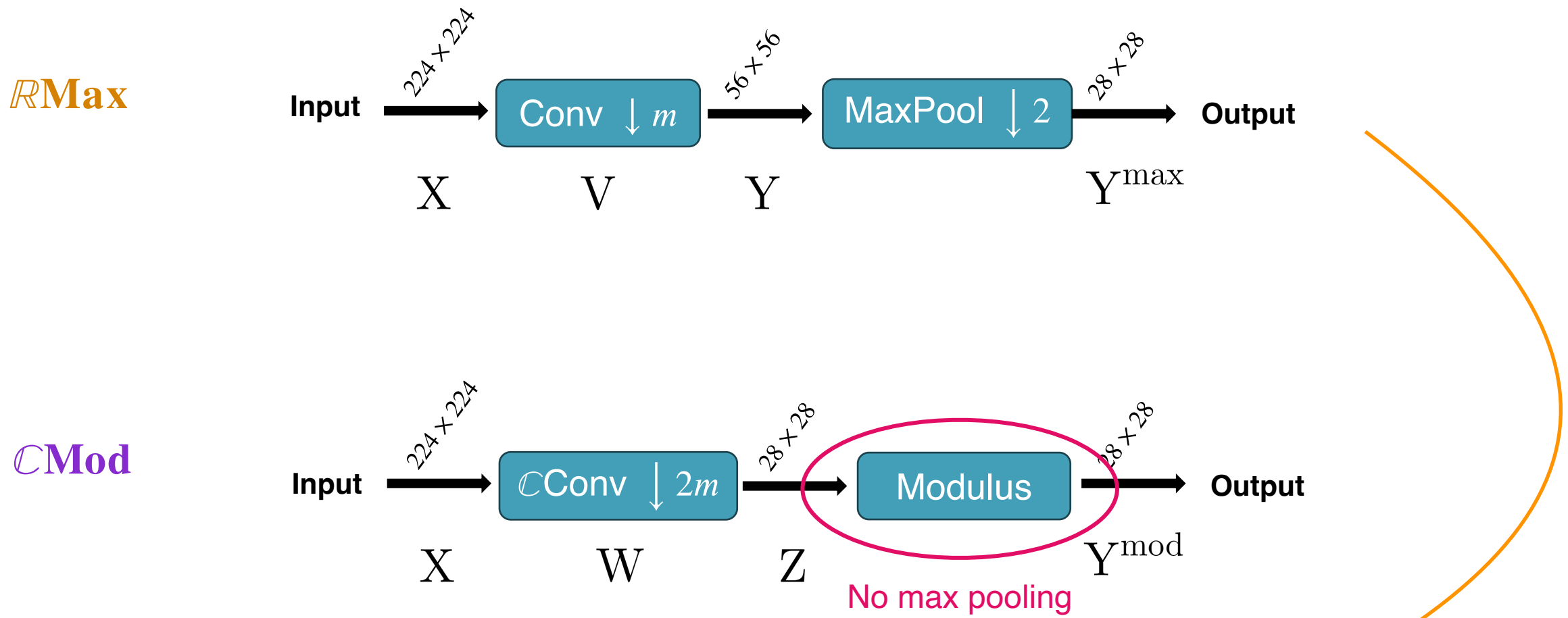


■ $U_{m,q}^{\max}[W] : X \mapsto \text{MaxPool}_q((X * \overline{\text{Re}W}) \downarrow m)$

$$(X * \overline{V})[\mathbf{n}] := \sum_{\mathbf{p} \in \mathbb{Z}^2} X[\mathbf{p}] \overline{V}[\mathbf{n} - \mathbf{p}] \quad \overline{V}[\mathbf{n}] := V[-\mathbf{n}]$$

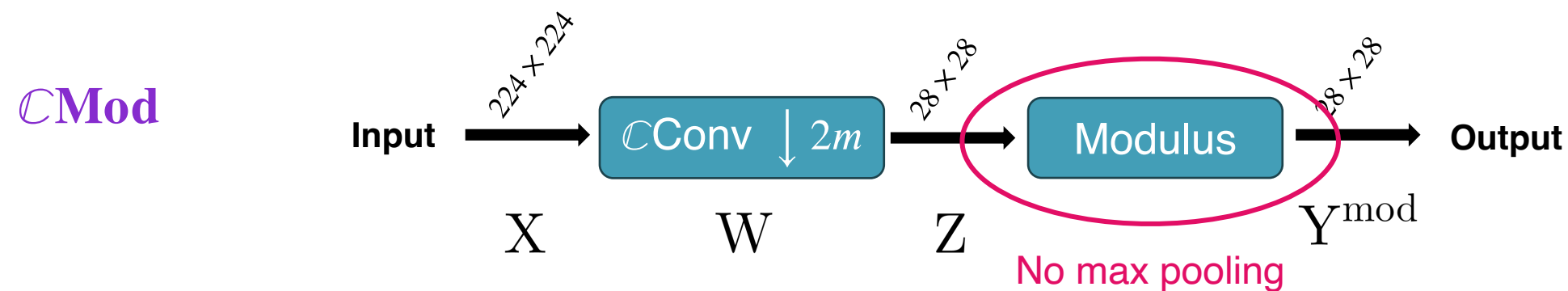
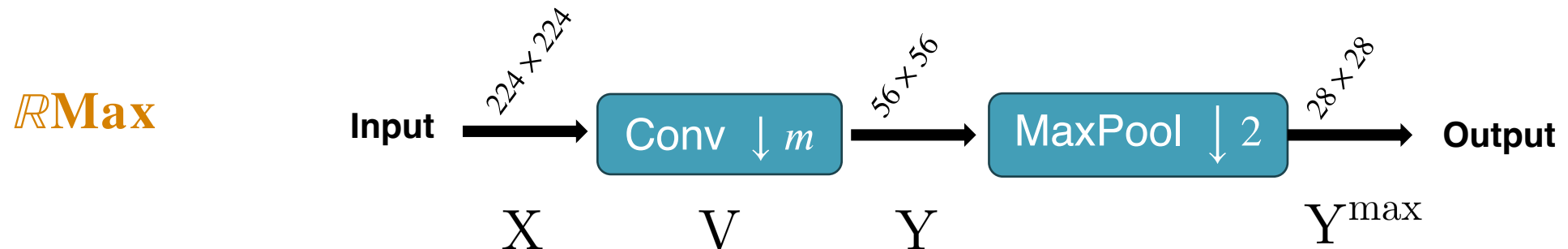
$$\text{MaxPool}_q(Y)[\mathbf{n}] := \max_{\|\mathbf{p}\|_\infty \leq q} Y[2\mathbf{n} + \mathbf{p}] \quad (Y \downarrow m)[\mathbf{n}] := Y[m\mathbf{n}]$$

Two operators to compare



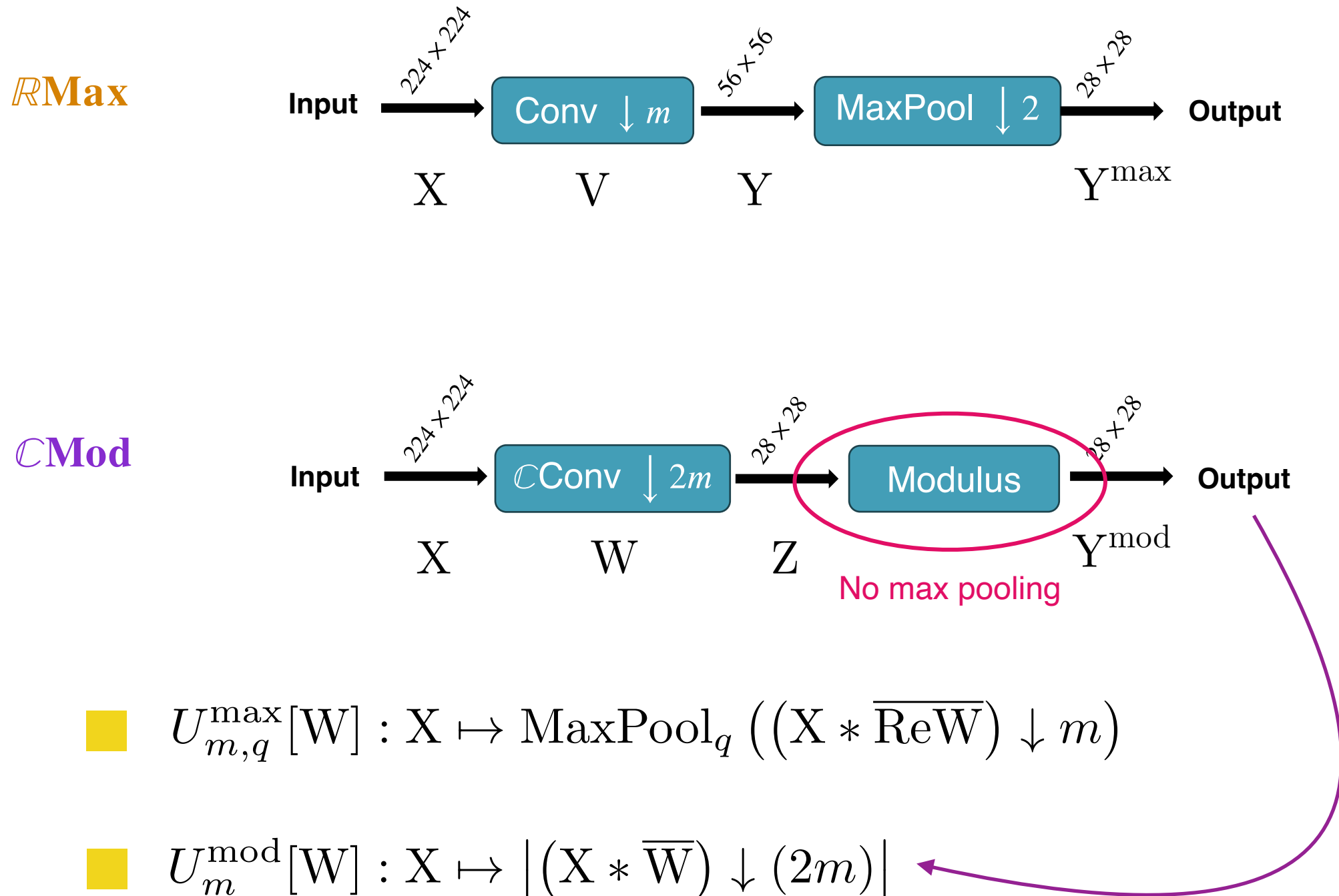
■ $U_{m,q}^{\max}[W] : X \mapsto \text{MaxPool}_q \left((X * \overline{\text{Re}W}) \downarrow m \right)$

Two operators to compare



■ $U_{m,q}^{\max}[W] : X \mapsto \text{MaxPool}_q \left((X * \overline{\text{Re}W}) \downarrow m \right)$

Two operators to compare



Roadmap

Roadmap

- Show that, **under the Gabor hypothesis**, $\mathcal{C}\text{Mod}$ is **stable** with respect to small input shifts

Roadmap

- Show that, **under the Gabor hypothesis**, CMod is **stable** with respect to small input shifts
- **Establish conditions** on the filter's frequency and orientation under which RMax and CMod **produce comparable outputs**:

$$U_{m,q}^{\max}[W](X) \approx U_m^{\text{mod}}[W](X)$$

Roadmap

- Show that, **under the Gabor hypothesis**, CMod is **stable** with respect to small input shifts
- **Establish conditions** on the filter's frequency and orientation under which RMax and CMod **produce comparable outputs**:

$$U_{m,q}^{\max}[W](X) \approx U_m^{\text{mod}}[W](X)$$

- Deduce a **measure of shift invariance** for RMax operator, which benefits from the stability of CMod

Roadmap

- Show that, **under the Gabor hypothesis**, **CMod** is **stable** with respect to small input shifts
- **Establish conditions** on the filter's frequency and orientation under which **RMax** and **CMod** **produce comparable outputs**:

$$U_{m,q}^{\max}[W](X) \approx U_m^{\text{mod}}[W](X)$$

- Deduce a **measure of shift invariance** for **RMax** operator, which benefits from the stability of **CMod**
- Extend our results to **multichannel operators** (RGB images), such as implemented in conventional CNN architectures

Roadmap

- Show that, **under the Gabor hypothesis**, **CMod** is **stable** with respect to small input shifts
- **Establish conditions** on the filter's frequency and orientation under which **RMax** and **CMod** **produce comparable outputs**:

$$U_{m,q}^{\max}[W](X) \approx U_m^{\text{mod}}[W](X)$$

- Deduce a **measure of shift invariance** for **RMax** operator, which benefits from the stability of **CMod**
- Extend our results to **multichannel operators** (RGB images), such as implemented in conventional CNN architectures
- Experimental validation on a deterministic setting based on the **dual-tree complex wavelet packet transform** (DT-CWPT)

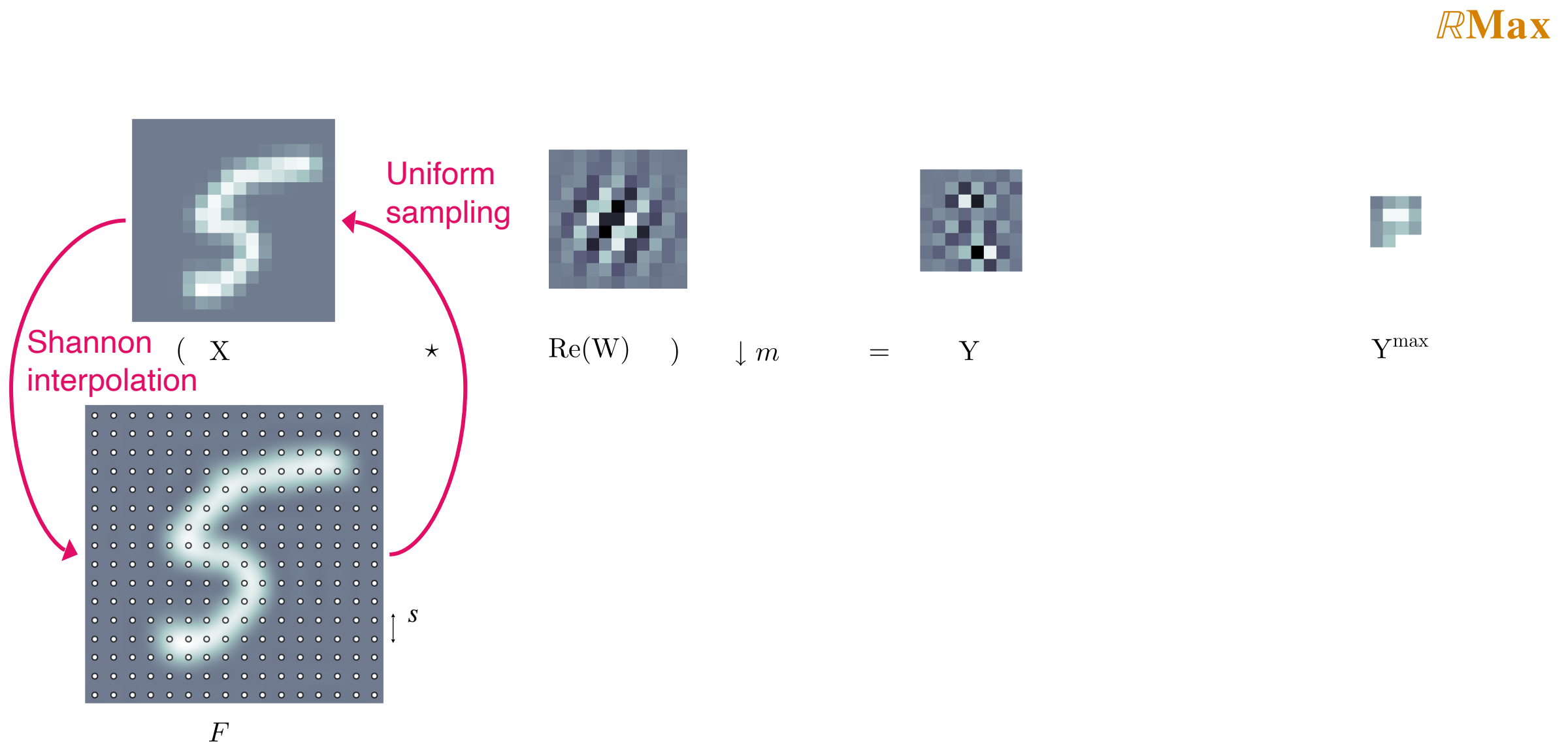
Detour via the continuous framework

■ Using the **Shannon-Whittaker sampling theorem**

$$\text{RMax}$$
$$\begin{matrix} \text{S} \\ \text{X} \end{matrix} \star \begin{pmatrix} \text{Re}(W) \end{pmatrix} \downarrow m = \text{Y} \quad \text{Y}^{\max} \quad \text{P}$$

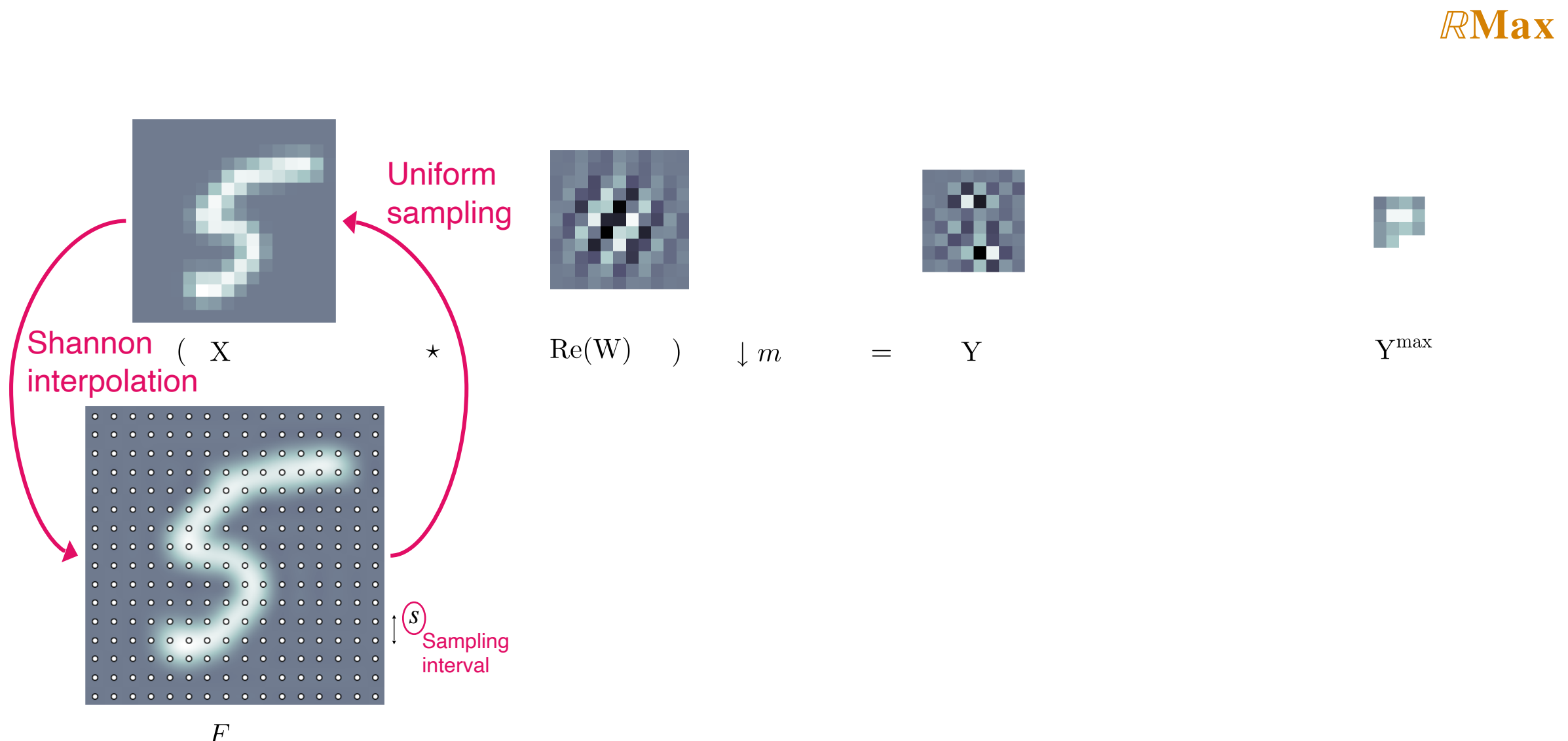

Detour via the continuous framework

■ Using the **Shannon-Whittaker sampling theorem**



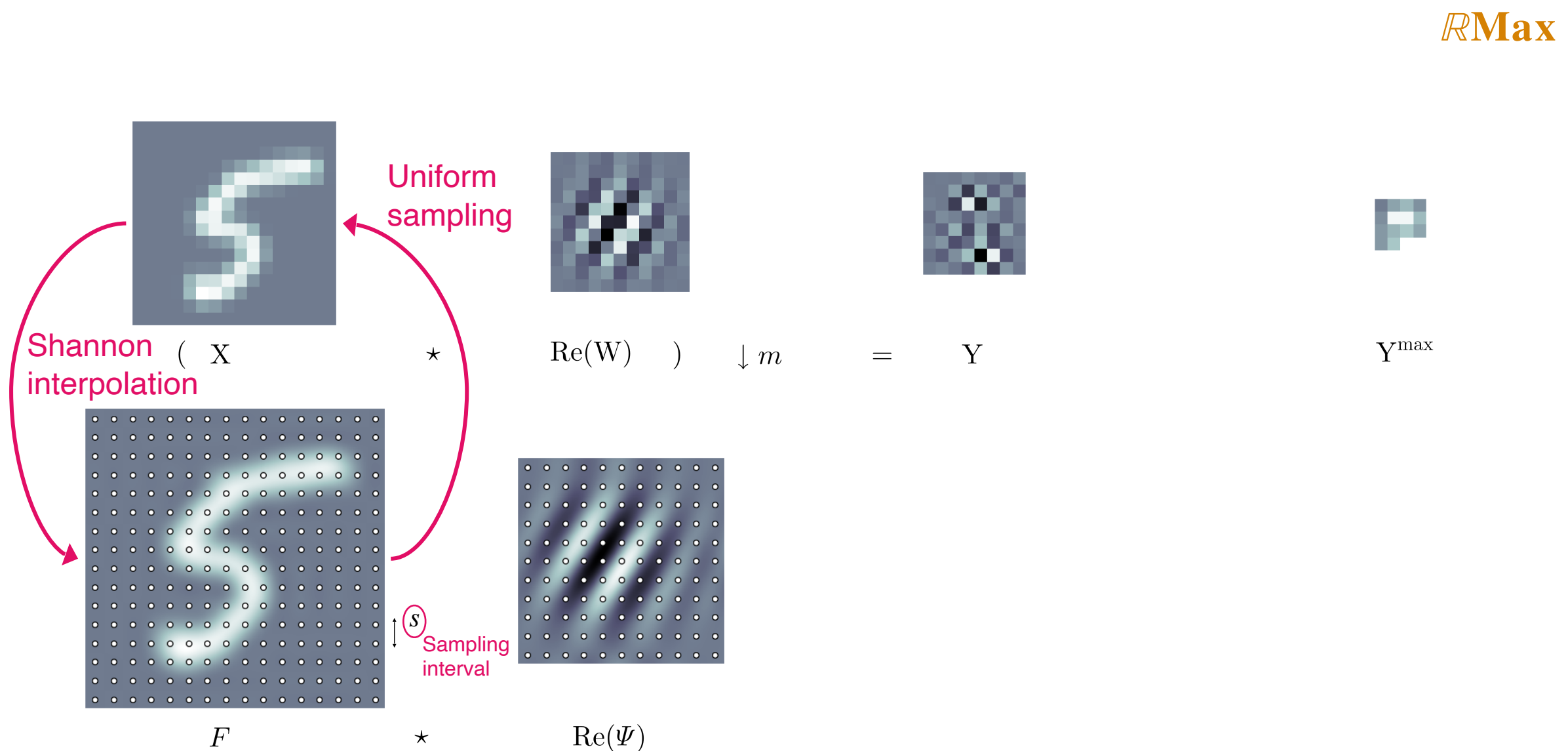
Detour via the continuous framework

■ Using the **Shannon-Whittaker sampling theorem**



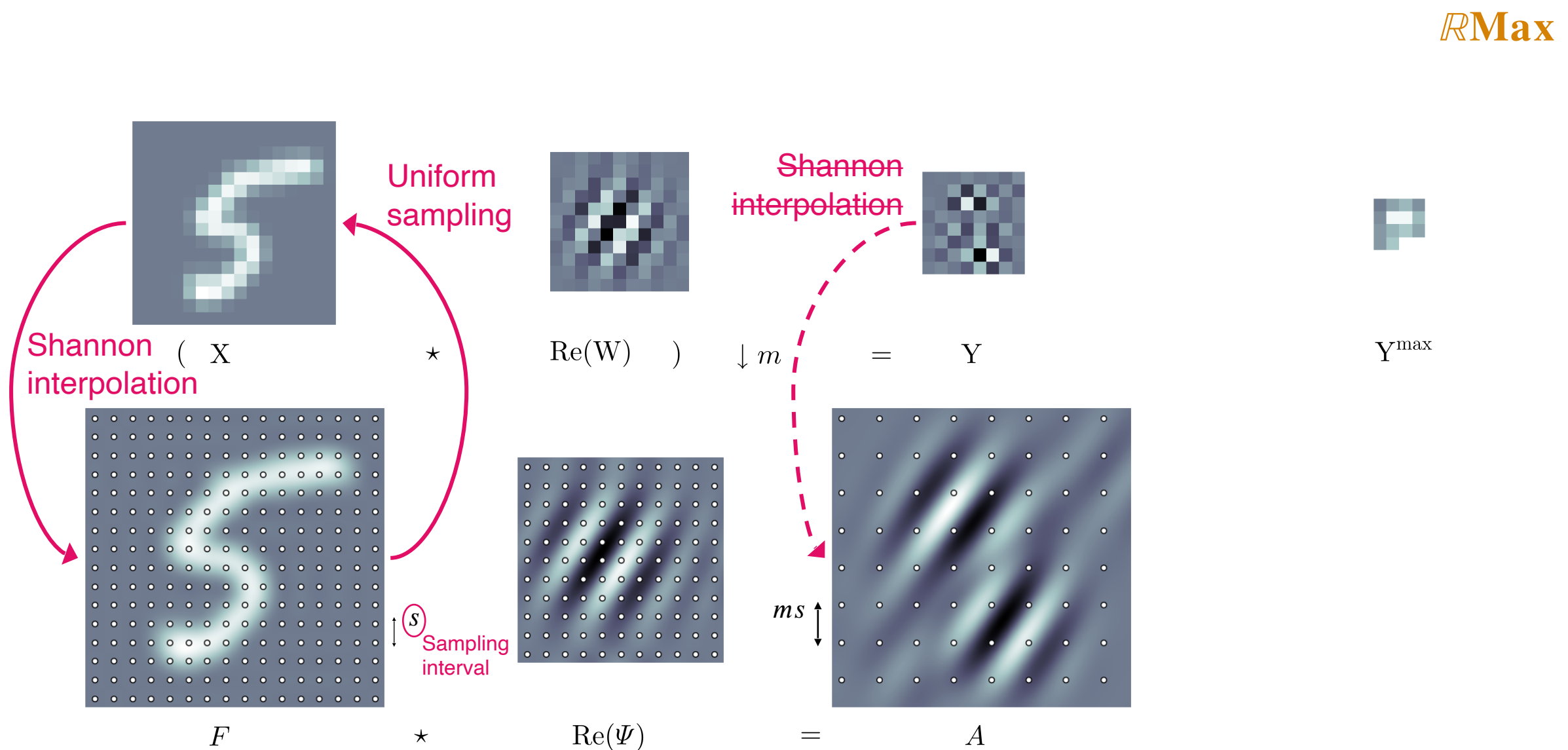
Detour via the continuous framework

■ Using the **Shannon-Whittaker sampling theorem**



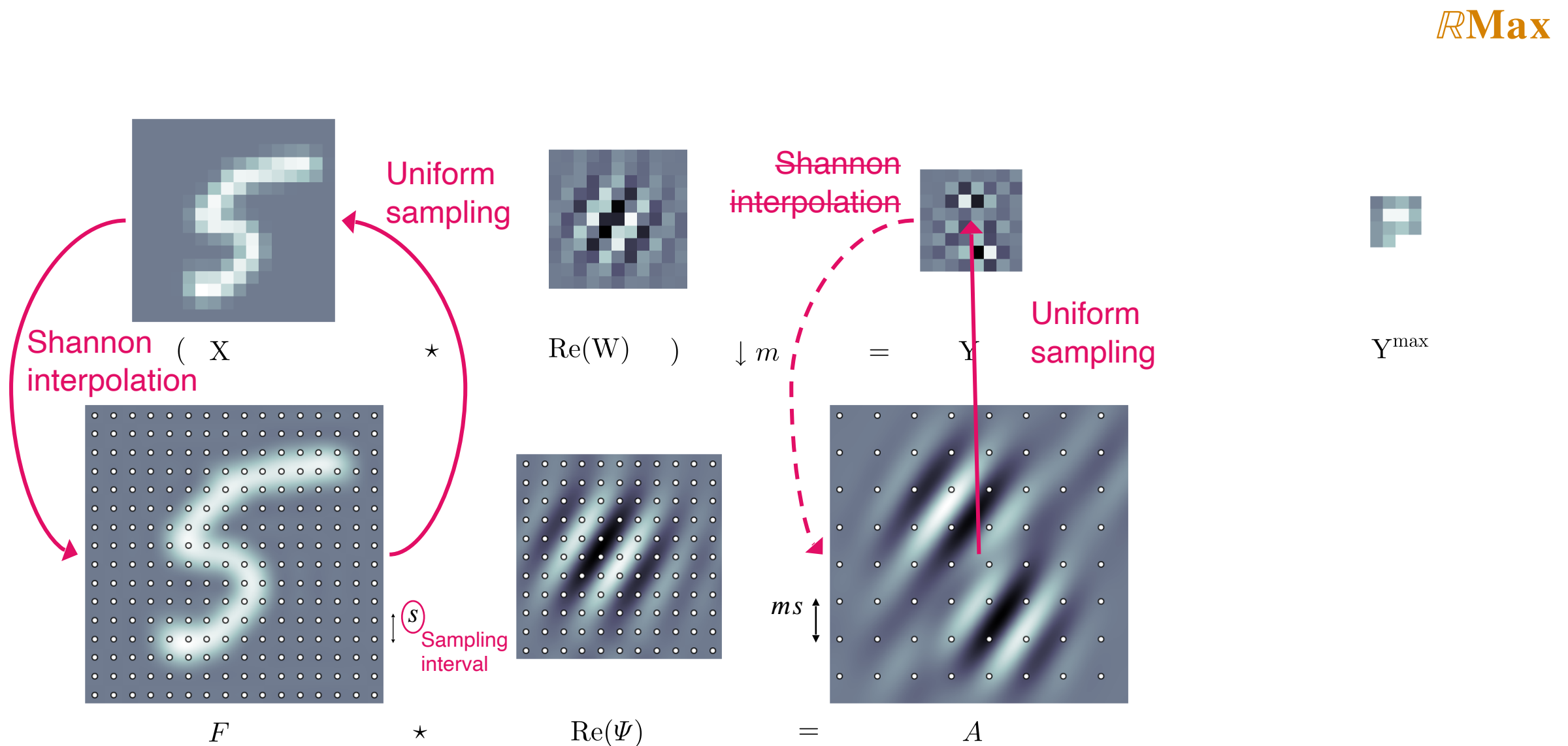
Detour via the continuous framework

Using the **Shannon-Whittaker sampling theorem**



Detour via the continuous framework

Using the **Shannon-Whittaker sampling theorem**

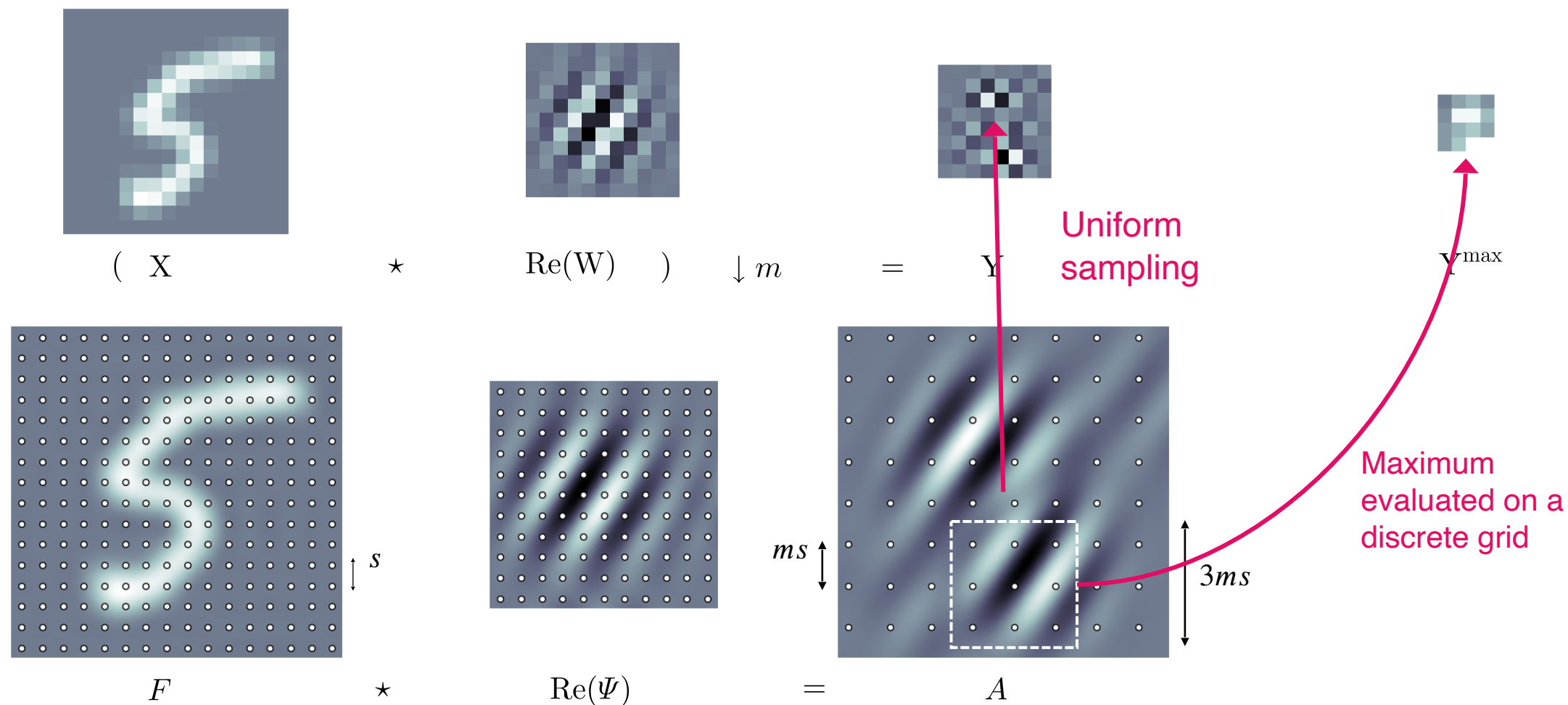


Detour via the continuous framework

Using the **Shannon-Whittaker sampling theorem**

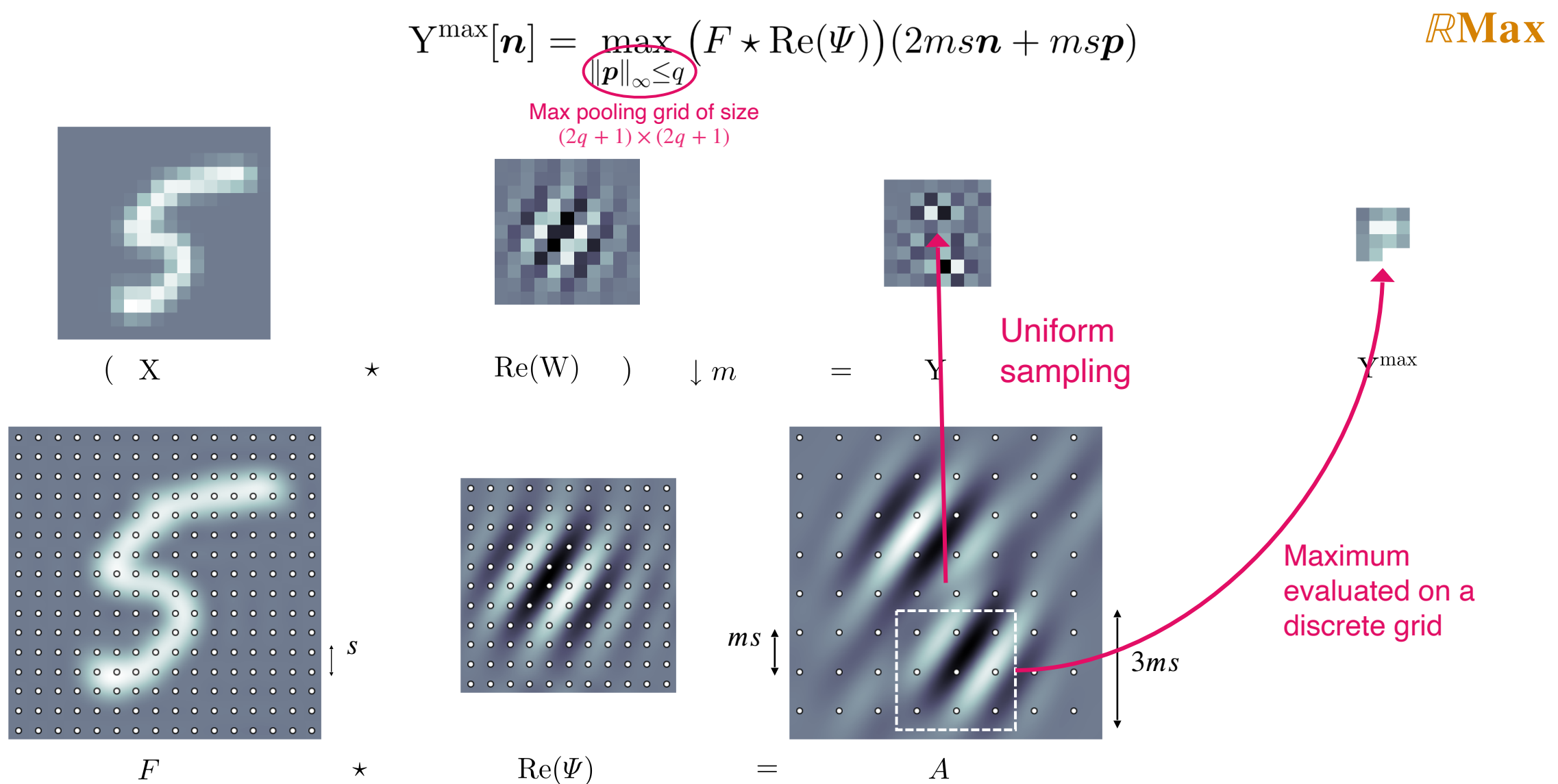
$$Y^{\max}[n] = \max_{\|p\|_\infty \leq q} (F * \text{Re}(\Psi))(2msn + msp)$$

RMax



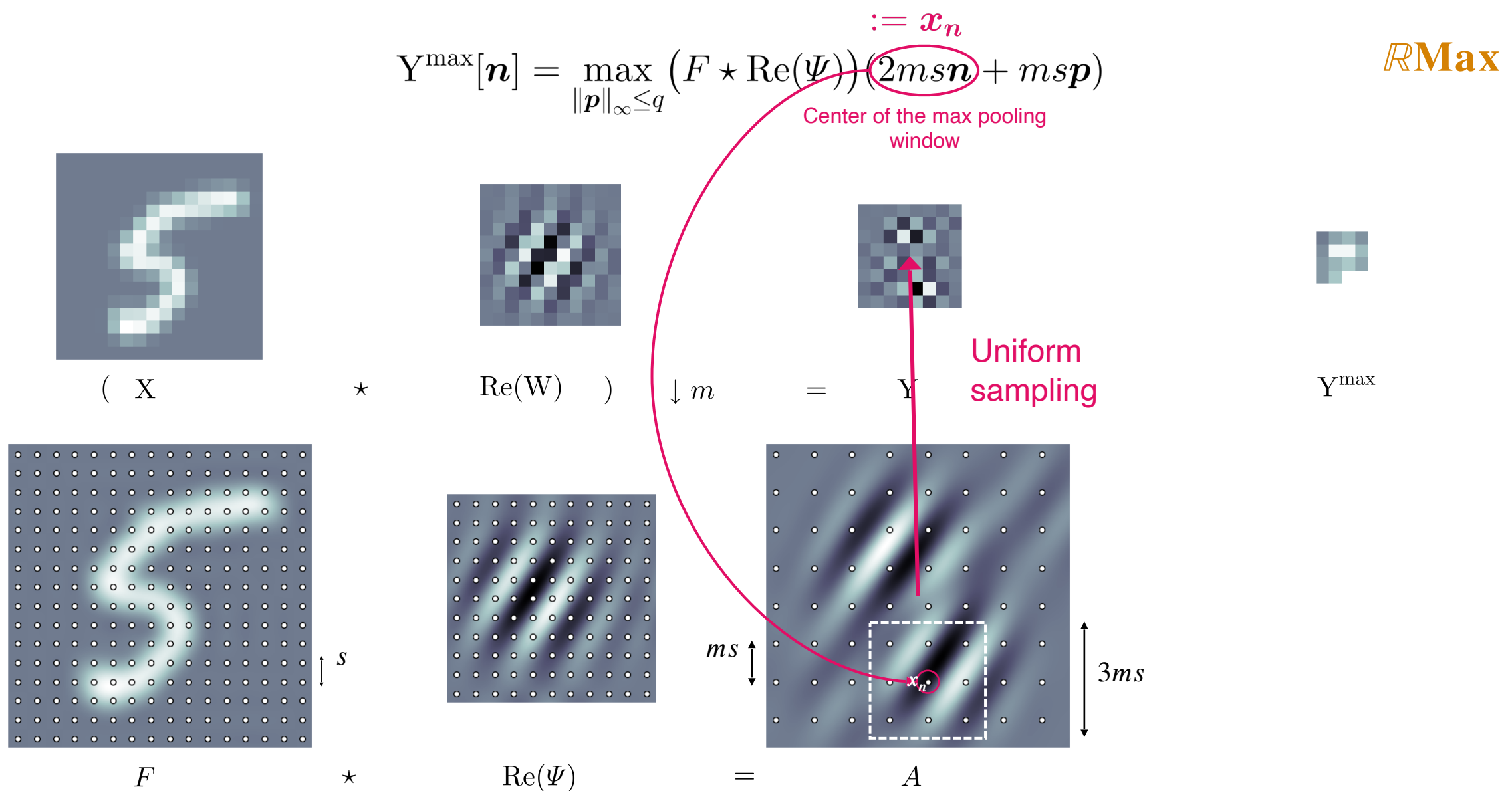
Detour via the continuous framework

Using the Shannon-Whittaker sampling theorem



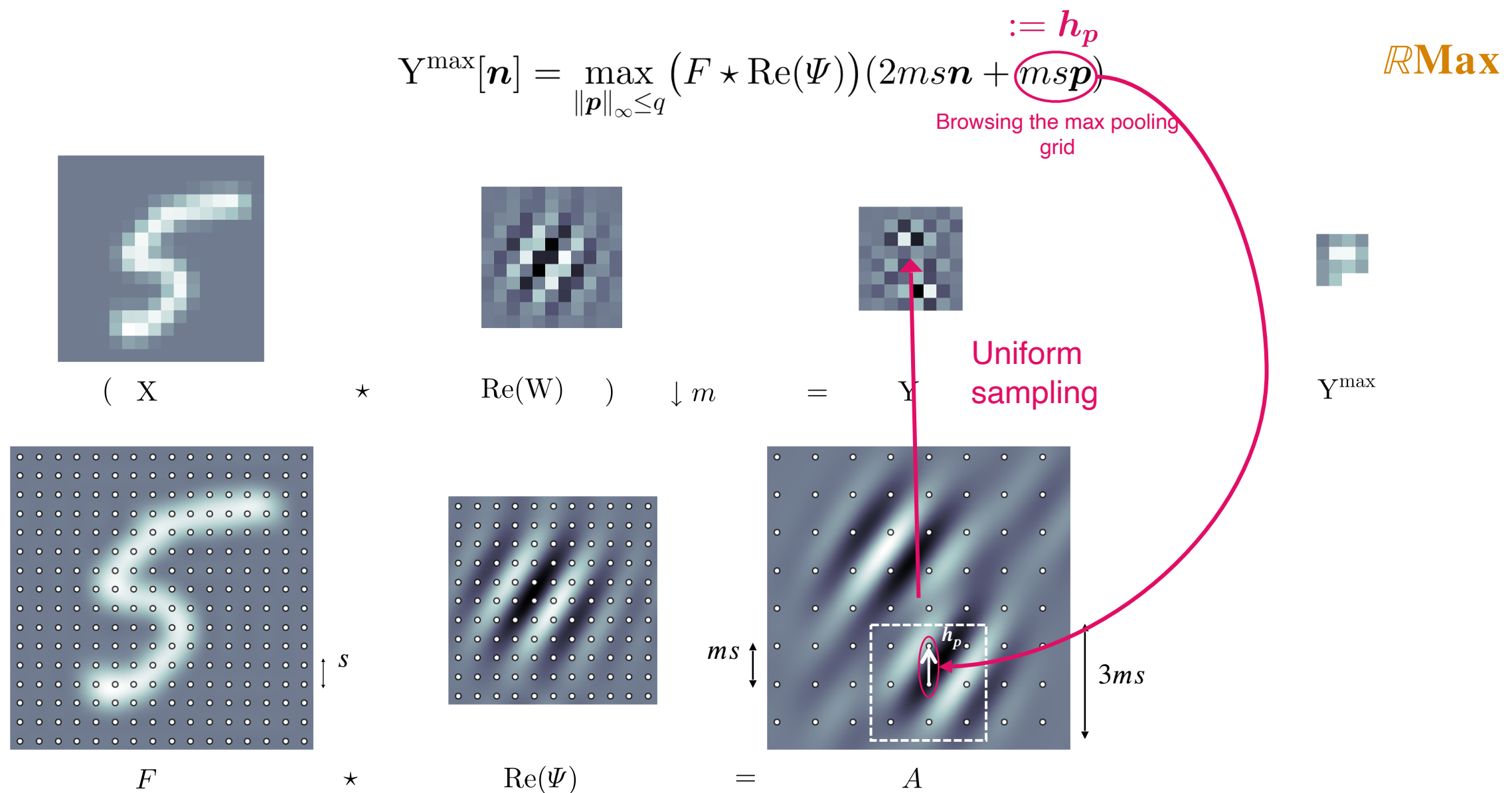
Detour via the continuous framework

Using the Shannon-Whittaker sampling theorem



Detour via the continuous framework

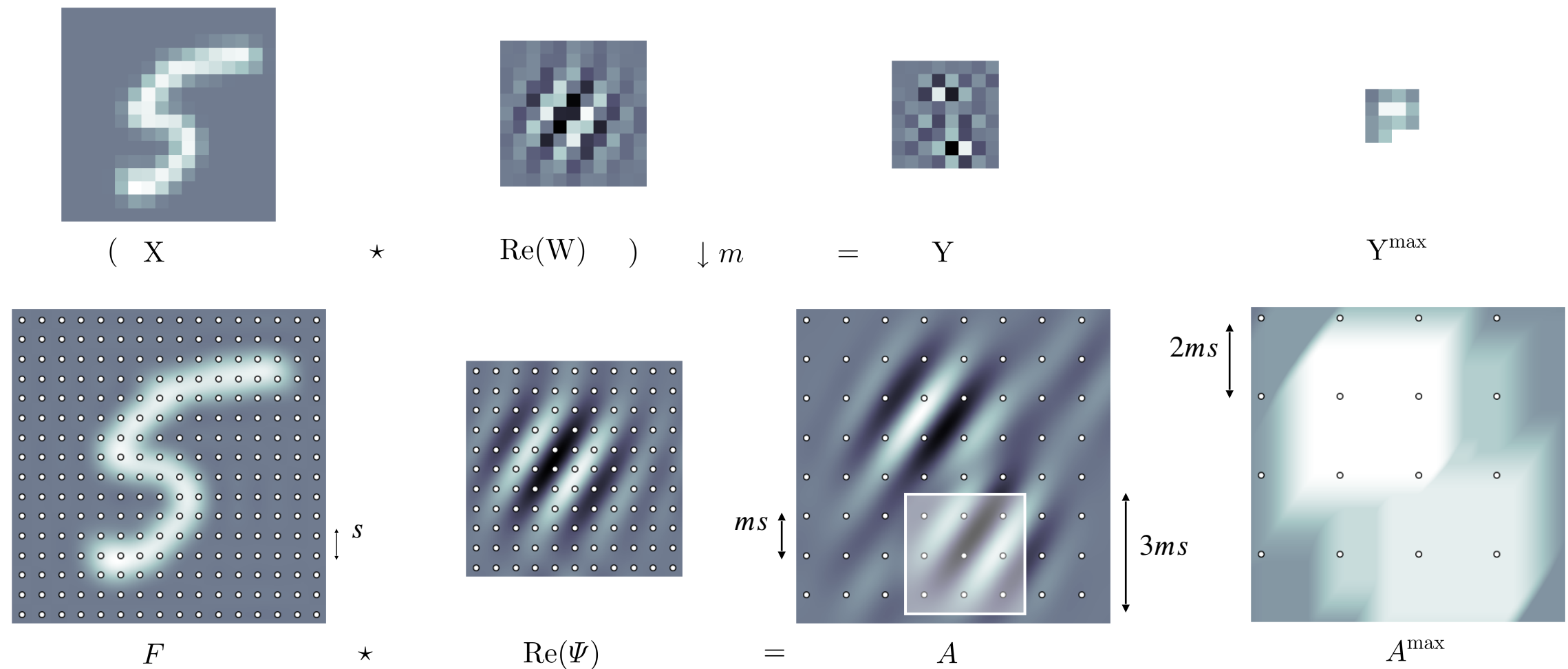
Using the Shannon-Whittaker sampling theorem



Detour via the continuous framework

■ What if we search for the maximum **continuously** in the window?

$$Y_0^{\max}[n] = \max_{\|h\|_\infty \leq \frac{3ms}{2}} (F \star \text{Re}(\Psi))(x_n + h) \approx Y^{\max}[n]? \quad \text{RMax}_0$$

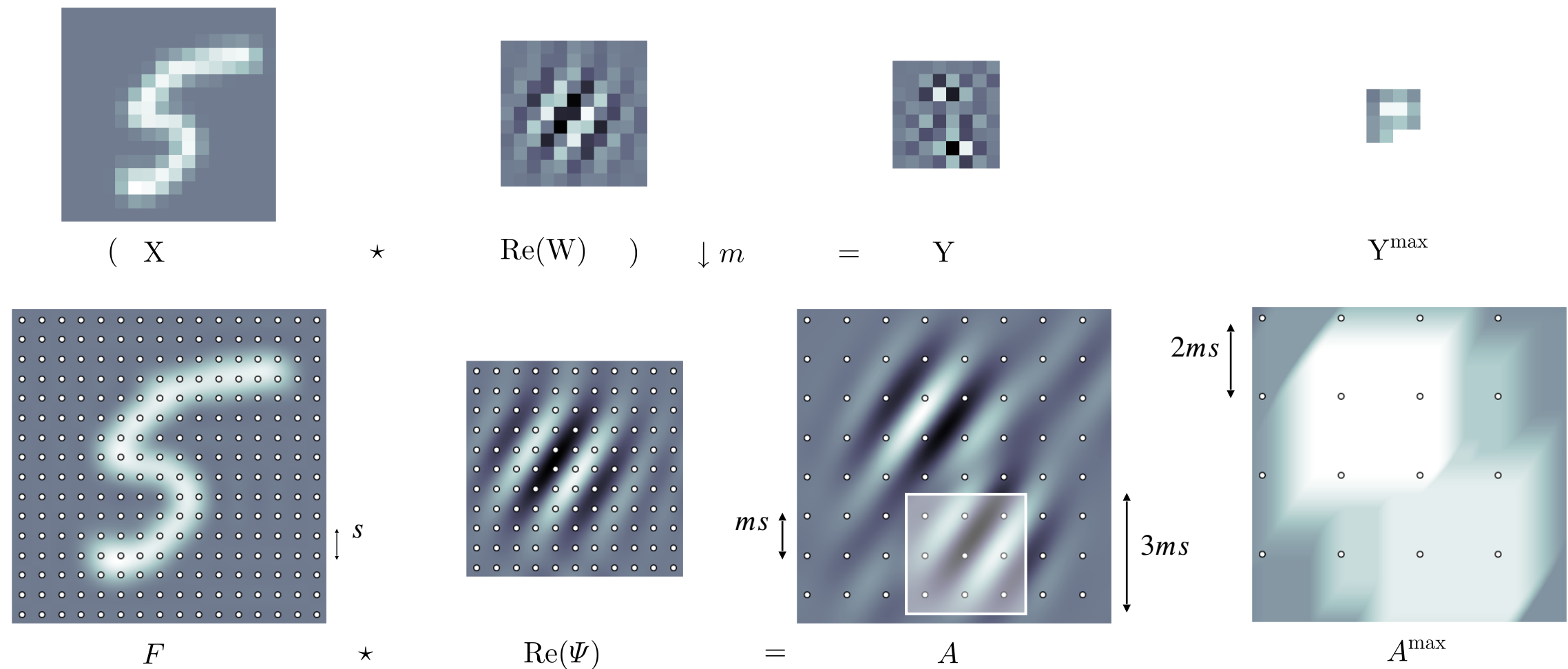


Detour via the continuous framework

■ What if we search for the maximum **continuously** in the window?

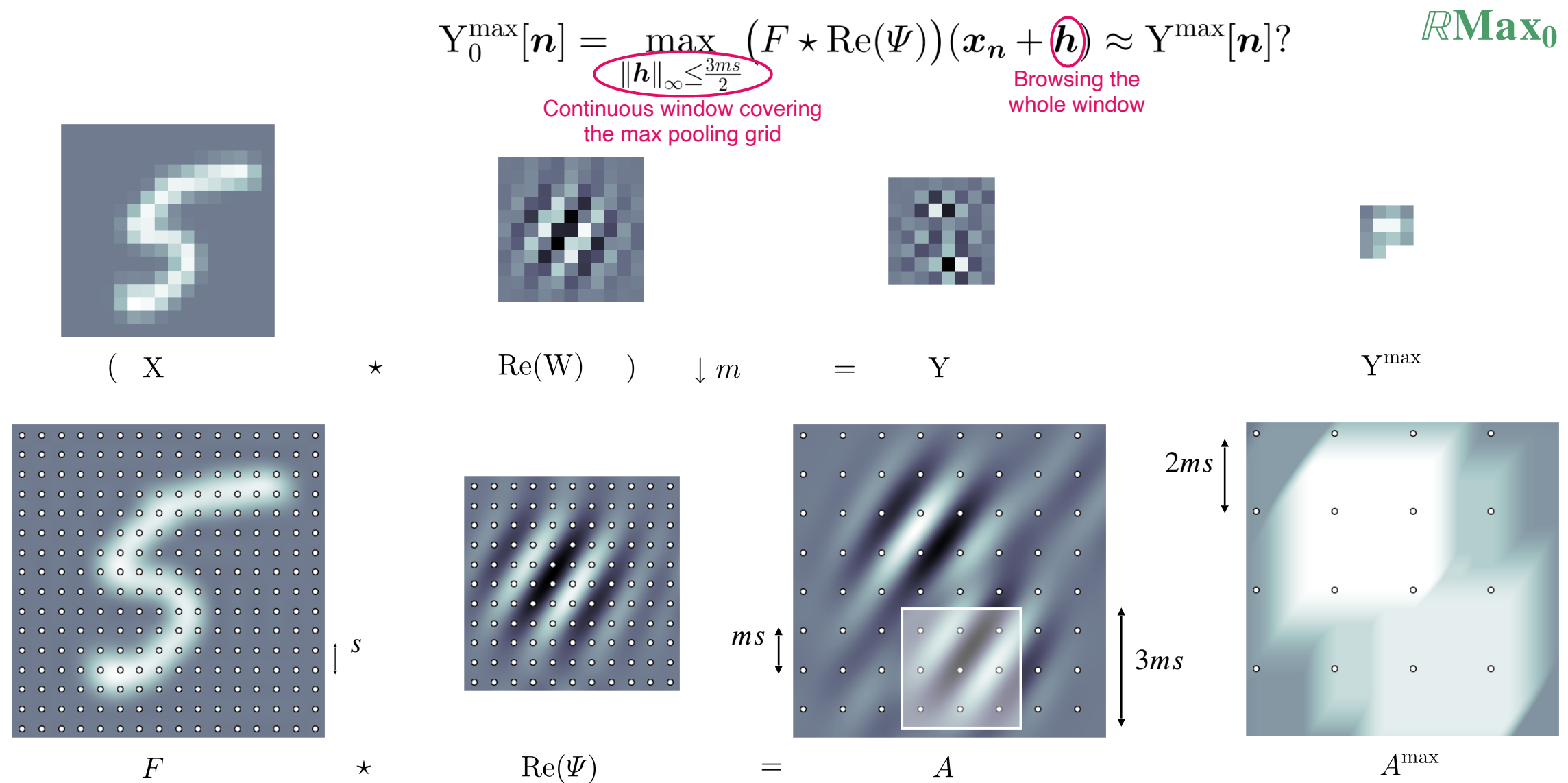
$$Y_0^{\max}[n] = \max_{\|h\|_\infty \leq \frac{3ms}{2}} (F \star \text{Re}(\Psi))(x_n + h) \approx Y^{\max}[n]?$$

RMax₀



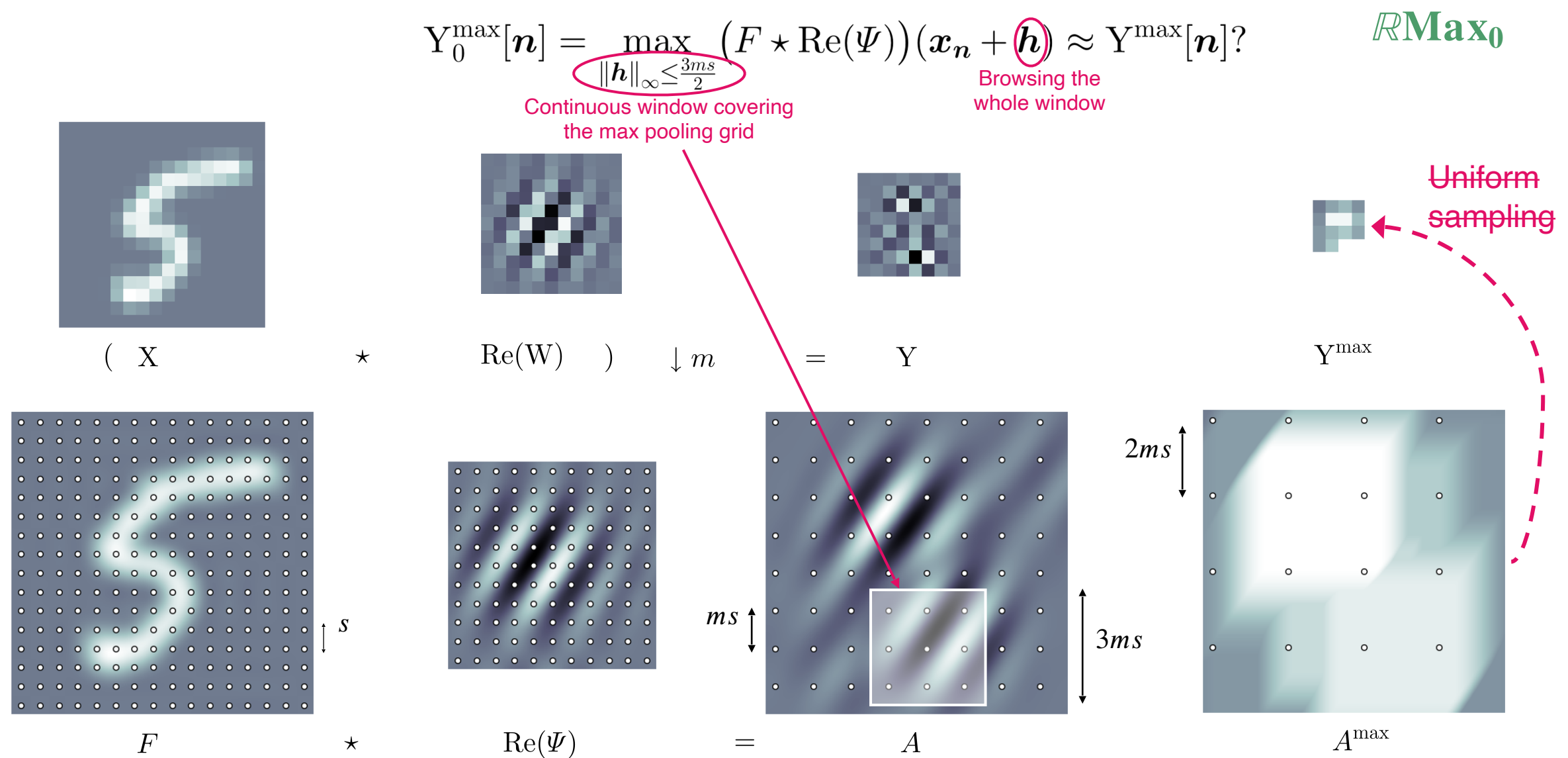
Detour via the continuous framework

■ What if we search for the maximum **continuously** in the window?



Detour via the continuous framework

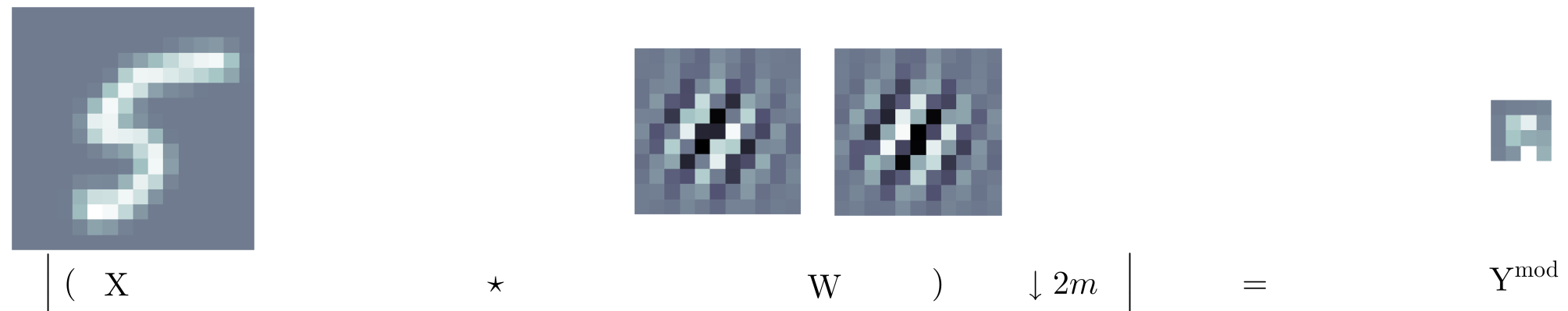
- What if we search for the maximum **continuously** in the window?



Detour via the continuous framework

- The output \mathbf{Y}^{mod} can be obtained by a uniform sampling of $|F * \Psi|$

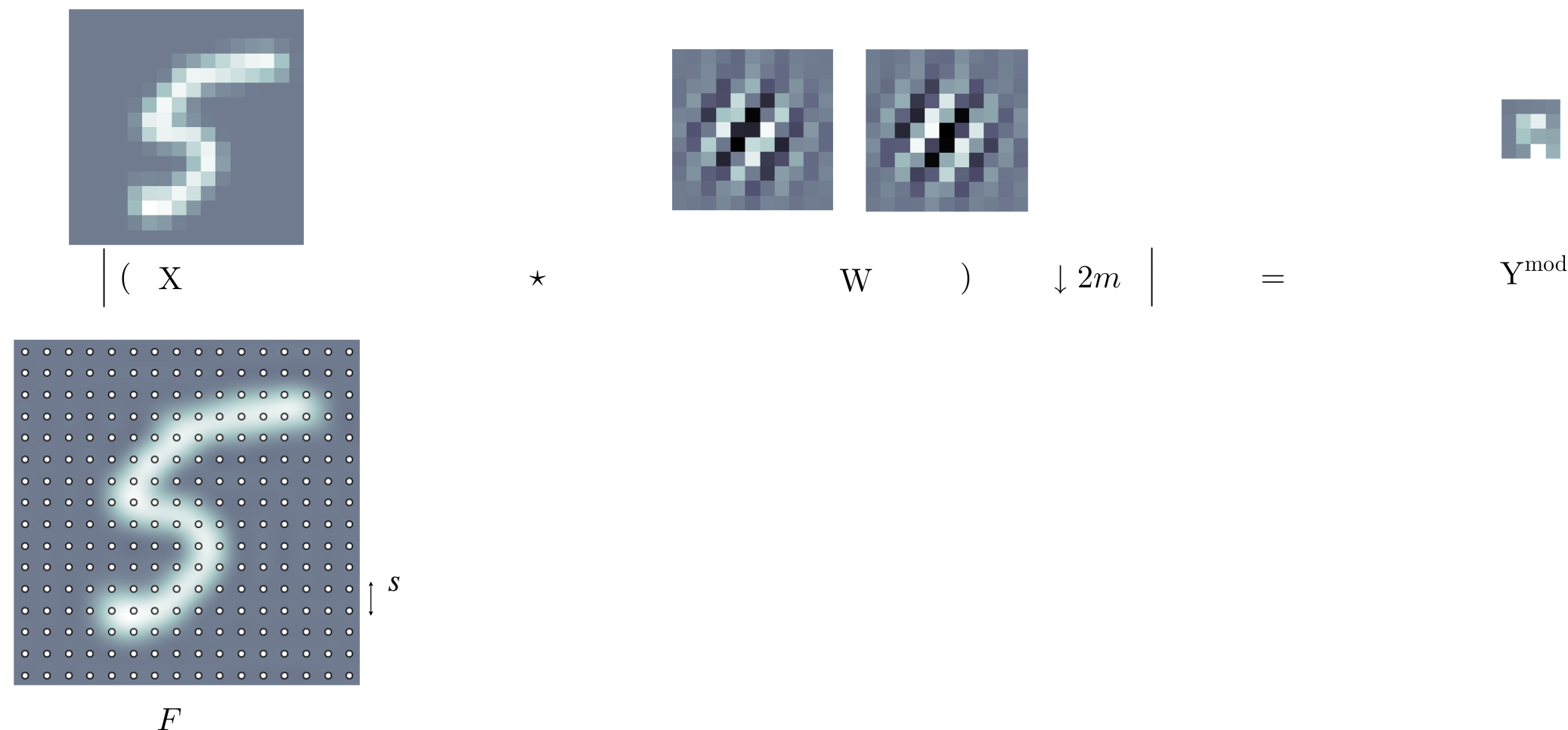
$\mathcal{C}\mathbf{Mod}$

$$\left| \begin{array}{c} \text{Input Image} \\ | \\ (\quad \mathbf{X} \\ \star \\ \mathbf{W} \\) \\ \downarrow 2m \\ | \\ = \end{array} \right| = \mathbf{Y}^{\text{mod}}$$


Detour via the continuous framework

- The output \mathbf{Y}^{mod} can be obtained by a uniform sampling of $|F * \Psi|$

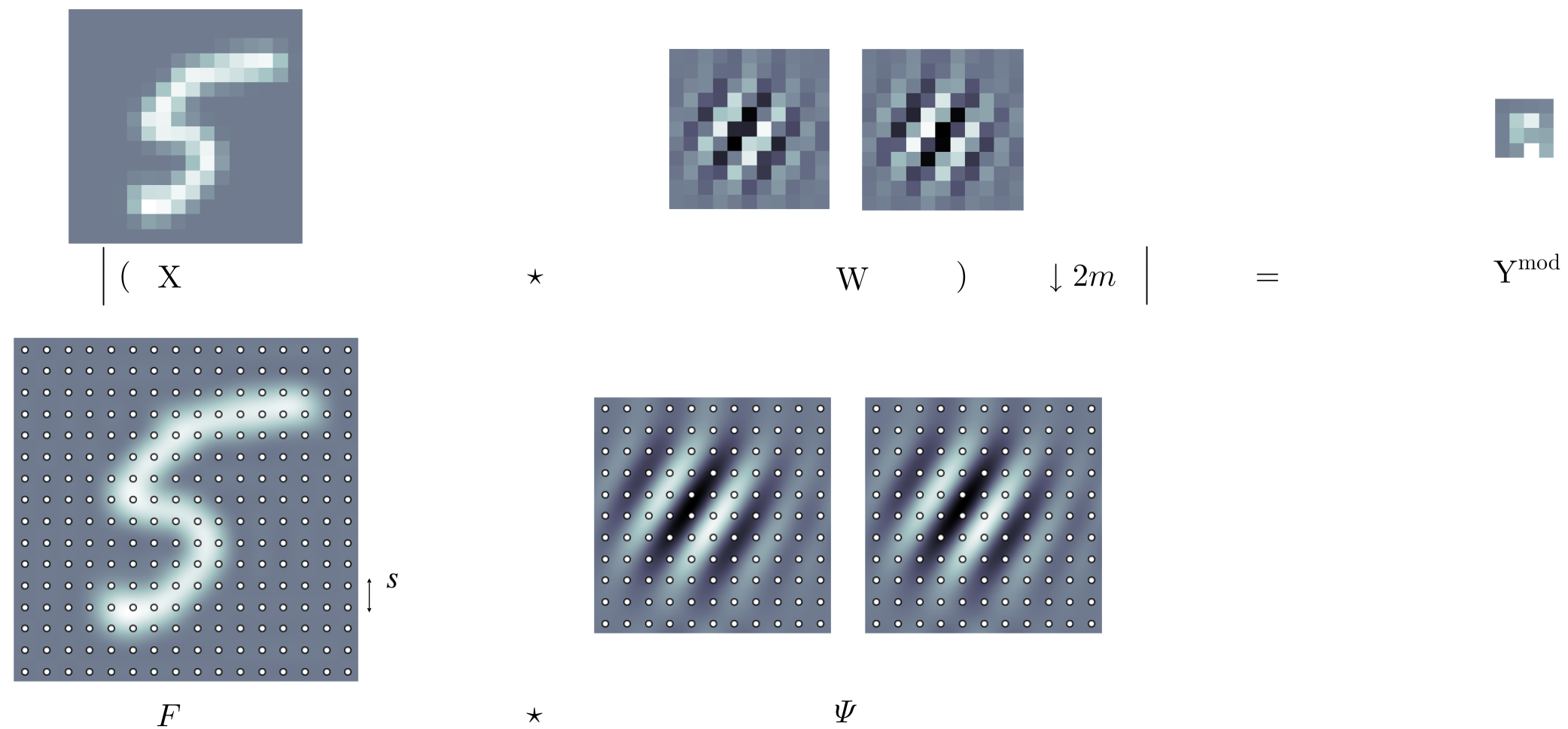
$\mathcal{C}\mathbf{Mod}$



Detour via the continuous framework

- The output \mathbf{Y}^{mod} can be obtained by a uniform sampling of $|F * \Psi|$

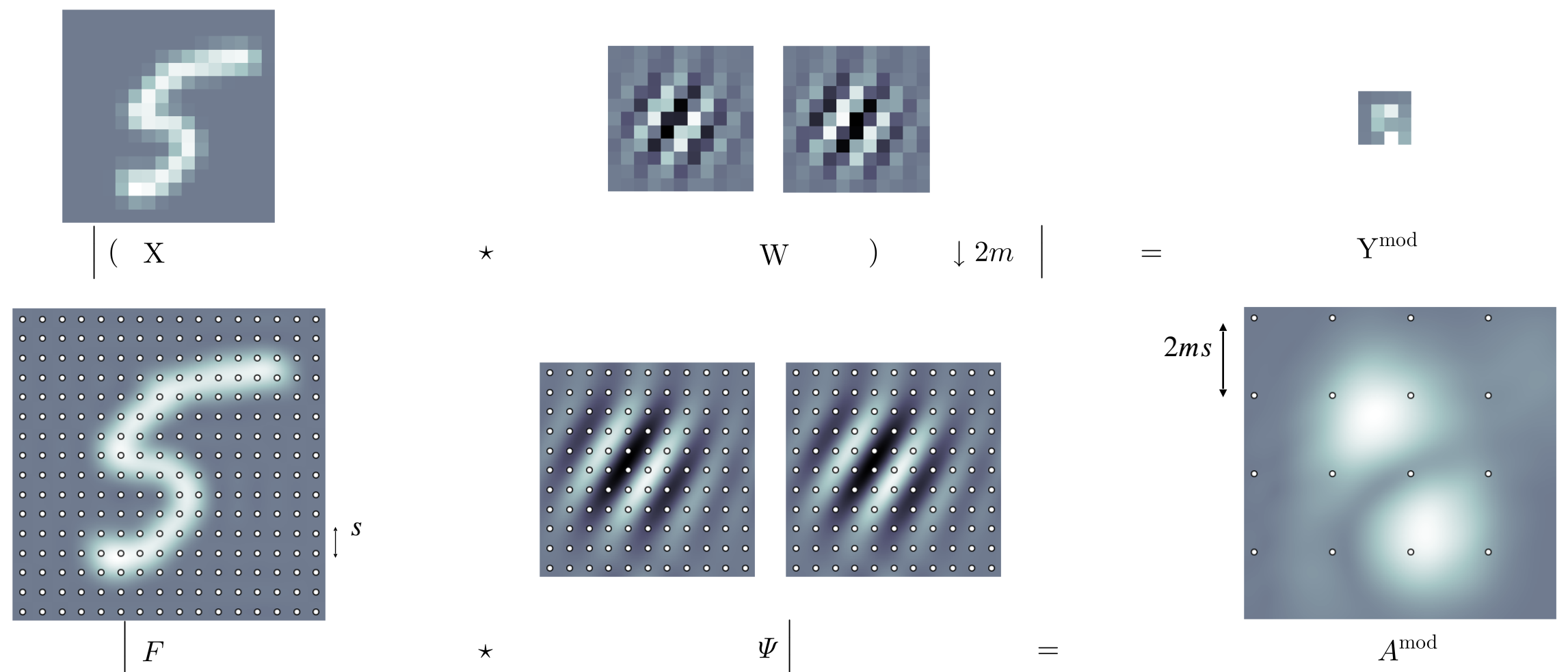
$\mathcal{C}\mathbf{Mod}$



Detour via the continuous framework

- The output \mathbf{Y}^{mod} can be obtained by a uniform sampling of $|F * \Psi|$

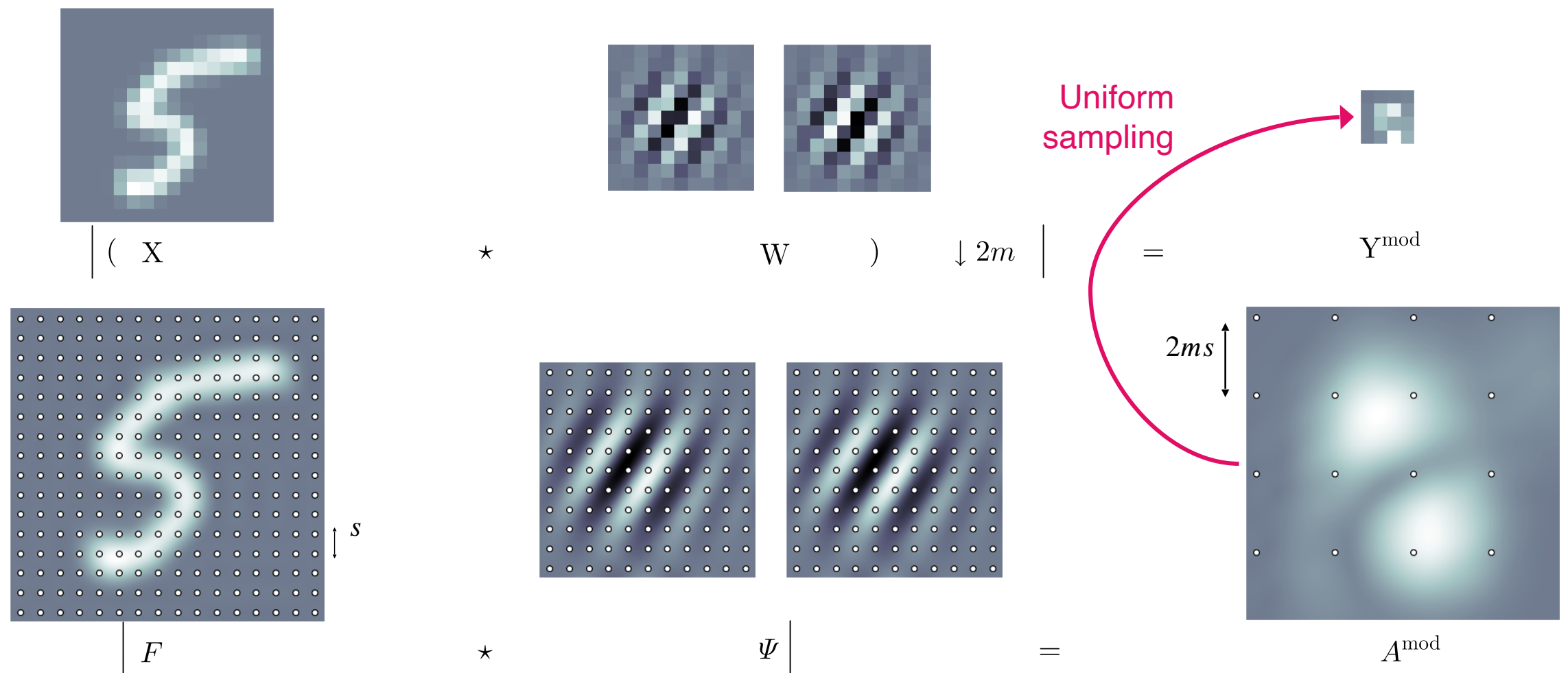
$\mathcal{C}\mathbf{Mod}$



Detour via the continuous framework

- The output \mathbf{Y}^{mod} can be obtained by a uniform sampling of $|F * \Psi|$

$\mathcal{C}\text{Mod}$

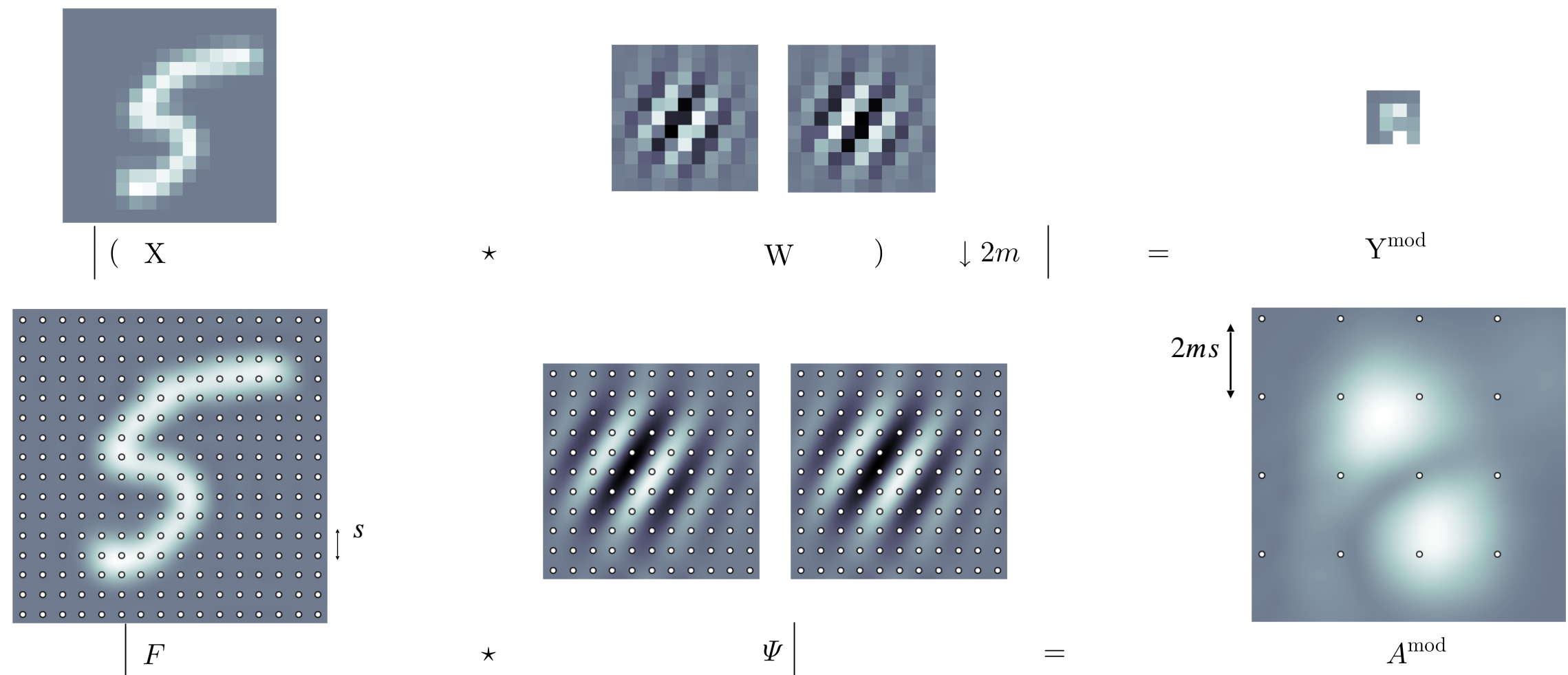


Detour via the continuous framework

- The output \mathbf{Y}^{mod} can be obtained by a uniform sampling of $|F * \Psi|$

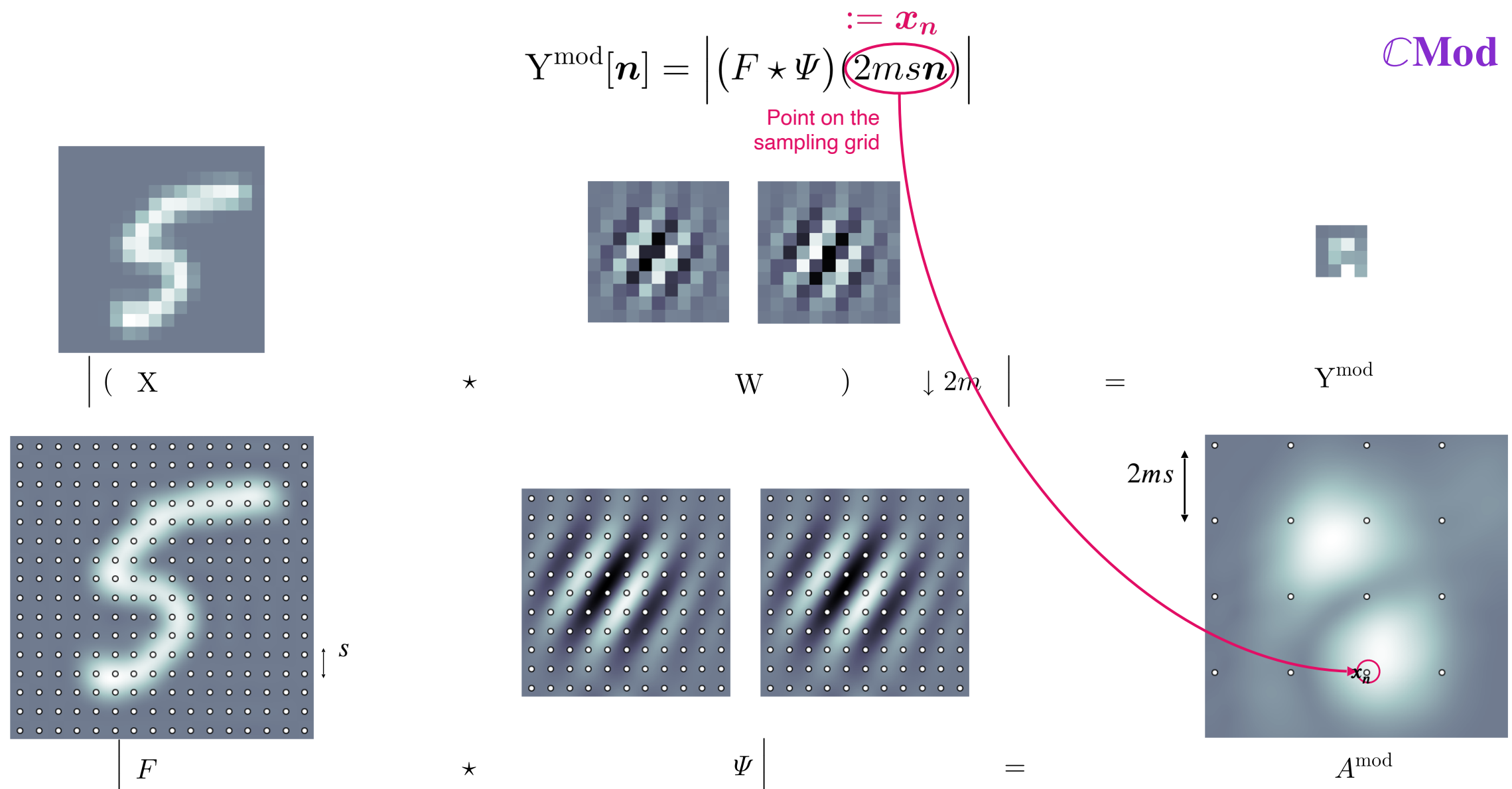
$$\mathbf{Y}^{\text{mod}}[\mathbf{n}] = |(F * \Psi)(2ms\mathbf{n})|$$

CMod



Detour via the continuous framework

- The output \mathbf{Y}^{mod} can be obtained by a uniform sampling of $|F * \Psi|$



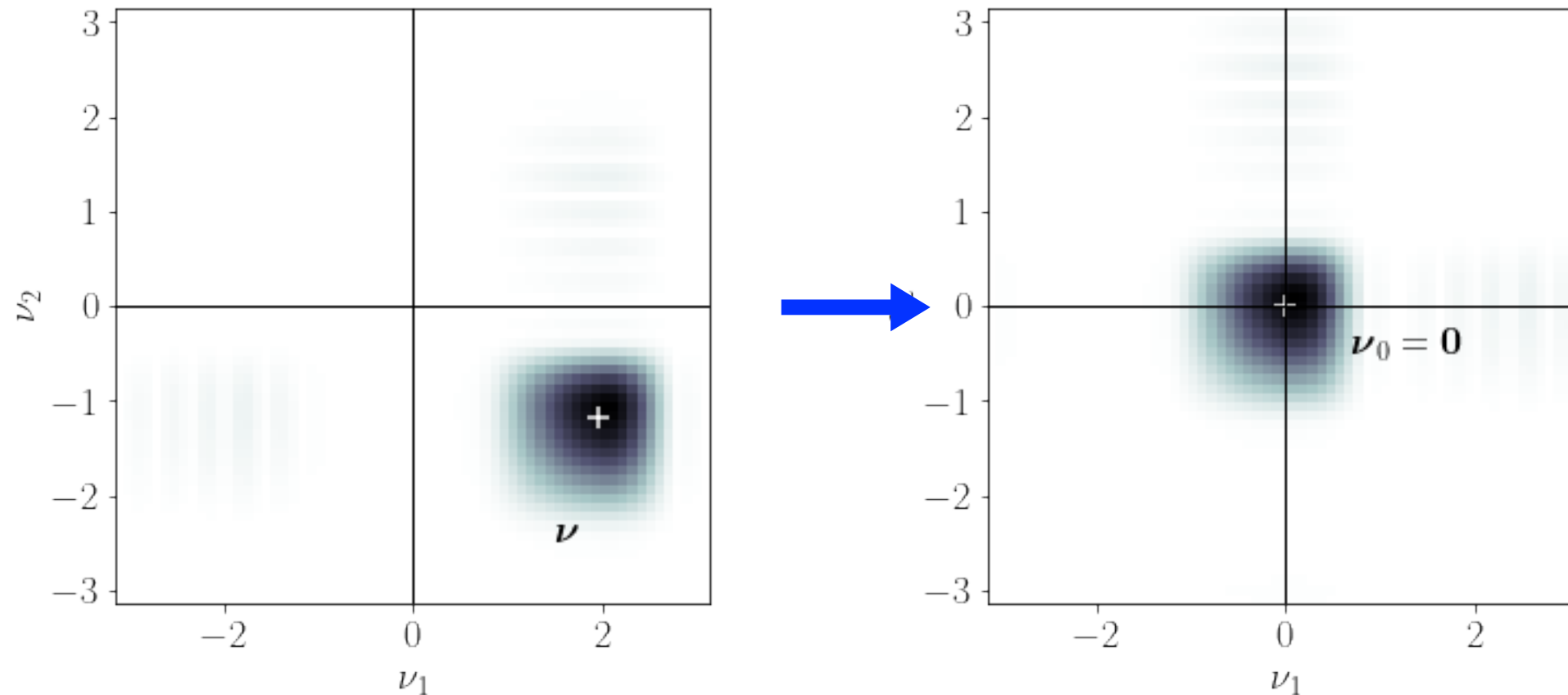
From high to low-frequency

From high to low-frequency

- $\mathcal{V}(\nu, \varepsilon) := \left\{ \Psi \in L^2_{\mathbb{C}}(\mathbb{R}^2) \mid \text{supp } \widehat{\Psi} \subset B_{\infty}(\nu, \varepsilon/2) \right\}.$

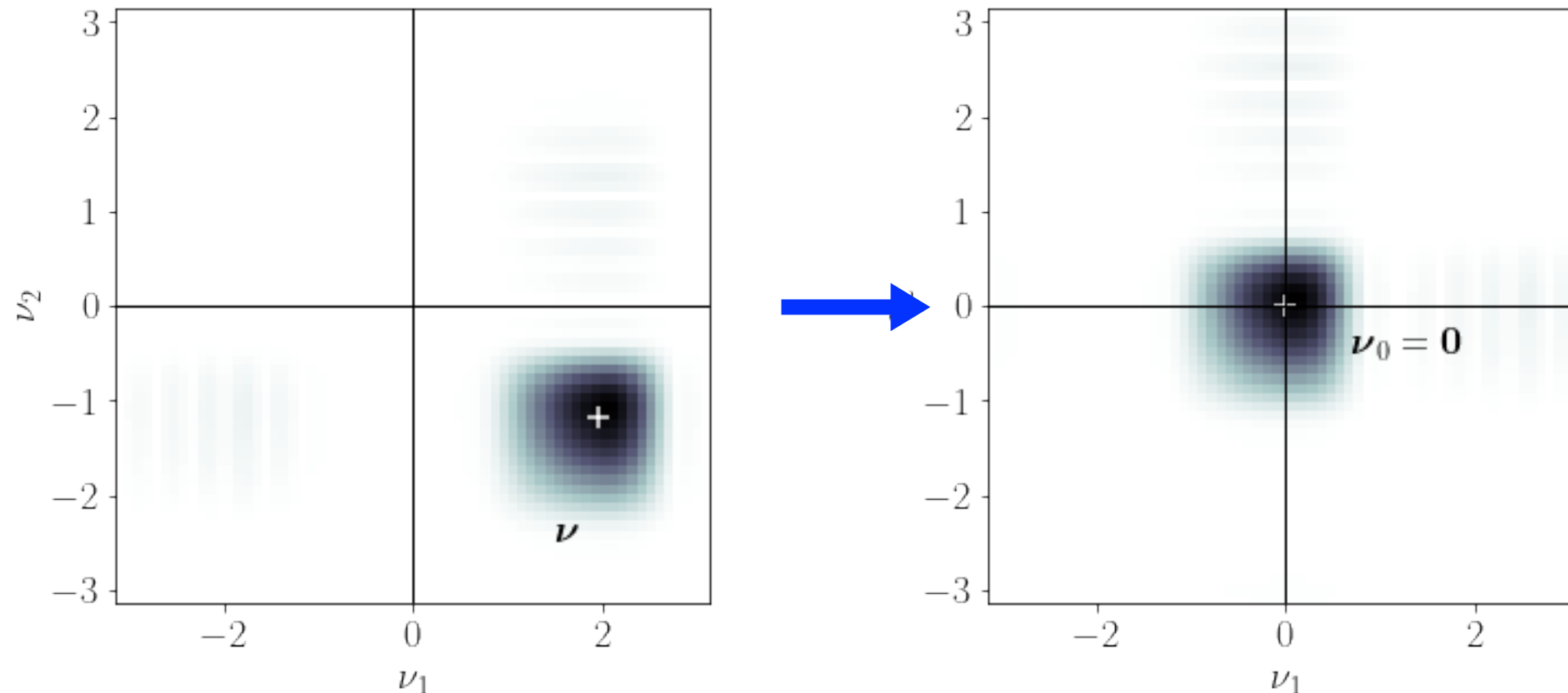
From high to low-frequency

- $\mathcal{V}(\boldsymbol{\nu}, \varepsilon) := \left\{ \Psi \in L^2_{\mathbb{C}}(\mathbb{R}^2) \mid \text{supp } \widehat{\Psi} \subset B_{\infty}(\boldsymbol{\nu}, \varepsilon/2) \right\}.$
- $F_0 : \mathbf{x} \mapsto (F * \overline{\Psi})(\mathbf{x}) e^{i\langle \boldsymbol{\nu}, \mathbf{x} \rangle} \xrightarrow{\Psi \in \mathcal{V}(\boldsymbol{\nu}, \varepsilon)} \text{supp } \widehat{F}_0 \subset B_{\infty}(\varepsilon/2)$



From high to low-frequency

- $\mathcal{V}(\boldsymbol{\nu}, \varepsilon) := \left\{ \Psi \in L^2_{\mathbb{C}}(\mathbb{R}^2) \mid \text{supp } \widehat{\Psi} \subset B_{\infty}(\boldsymbol{\nu}, \varepsilon/2) \right\}.$
- $F_0 : \mathbf{x} \mapsto (F * \overline{\Psi})(\mathbf{x}) e^{i\langle \boldsymbol{\nu}, \mathbf{x} \rangle} \xrightarrow{\Psi \in \mathcal{V}(\boldsymbol{\nu}, \varepsilon)} \text{supp } \widehat{F}_0 \subset B_{\infty}(\varepsilon/2)$



- **Shift-invariance bound** for low-frequency functions:

$$\|\mathcal{T}_{\mathbf{h}} F_0 - F_0\|_{L^2} \leq \alpha(\varepsilon \mathbf{h}) \|F_0\|_{L^2} \quad \alpha : \boldsymbol{\tau} \mapsto \frac{\|\boldsymbol{\tau}\|_1}{2}$$

Shift-invariance of CMod in the discrete framework

Shift-invariance of CMod in the discrete framework

- $W \in \mathcal{J}(\theta, \kappa)$

Shift-invariance of CMod in the discrete framework

- $W \in \mathcal{J}(\theta, \kappa)$
- $F_0 : x \mapsto (F_X * \overline{\Psi}_W)(x) e^{i\langle \theta/s, x \rangle} \xrightarrow{\kappa \leq \pi/m} F_0 \in \mathcal{V}(0, 2\pi/s)$

Shift-invariance of CMod in the discrete framework

- $W \in \mathcal{J}(\theta, \kappa)$
- $F_0 : \mathbf{x} \mapsto (F_X * \overline{\Psi}_W)(\mathbf{x}) e^{i\langle \theta/s, \mathbf{x} \rangle} \xrightarrow{\kappa \leq \pi/m} F_0 \in \mathcal{V}(\mathbf{0}, 2\pi/s)$
- $\sum_{\mathbf{n} \in \mathbb{Z}^2} \left| \mathcal{T}_h F_0(s' \mathbf{n}) - F_0(s' \mathbf{n}) \right|^2 = \frac{1}{s'^2} \|\mathcal{T}_h F_0 - F_0\|_{L^2}^2 \quad s' := 2ms$

Shift-invariance of CMod in the discrete framework

- $W \in \mathcal{J}(\theta, \kappa)$
- $F_0 : \mathbf{x} \mapsto (F_X * \overline{\Psi}_W)(\mathbf{x}) e^{i\langle \theta/s, \mathbf{x} \rangle} \xrightarrow{\kappa \leq \pi/m} F_0 \in \mathcal{V}(\mathbf{0}, 2\pi/s)$
- $\sum_{\mathbf{n} \in \mathbb{Z}^2} \left| \mathcal{T}_h F_0(s' \mathbf{n}) - F_0(s' \mathbf{n}) \right|^2 = \frac{1}{s'^2} \| \mathcal{T}_h F_0 - F_0 \|_{L^2}^2 \quad s' := 2ms$
- $\| U_m^{\text{mod}} X \|_2 = \frac{1}{s'} \| F_0 \|_{L^2}$

Shift-invariance of CMod in the discrete framework

- $W \in \mathcal{J}(\theta, \kappa)$
- $F_0 : \mathbf{x} \mapsto (F_X * \overline{\Psi}_W)(\mathbf{x}) e^{i\langle \theta/s, \mathbf{x} \rangle} \xrightarrow{\kappa \leq \pi/m} F_0 \in \mathcal{V}(\mathbf{0}, 2\pi/s)$
- $\sum_{\mathbf{n} \in \mathbb{Z}^2} \left| \mathcal{T}_h F_0(s' \mathbf{n}) - F_0(s' \mathbf{n}) \right|^2 = \frac{1}{s'^2} \| \mathcal{T}_h F_0 - F_0 \|_{L^2}^2 \quad s' := 2ms$
- $\| U_m^{\text{mod}} X \|_2 = \frac{1}{s'} \| F_0 \|_{L^2}$

Theorem (Shift invariance of $\mathcal{C}\text{Mod}$)

If $W \in \mathcal{J}(\theta, \kappa)$ and $\kappa \leq \pi/m$

then for any input image with finite support $X \in l_{\mathbb{R}}^2(\mathbb{Z}^2)$

$$\| U_m^{\text{mod}}(\mathcal{T}_u X) - U_m^{\text{mod}} X \|_2 \leq \alpha(\kappa u) \| U_m^{\text{mod}} X \|_2$$

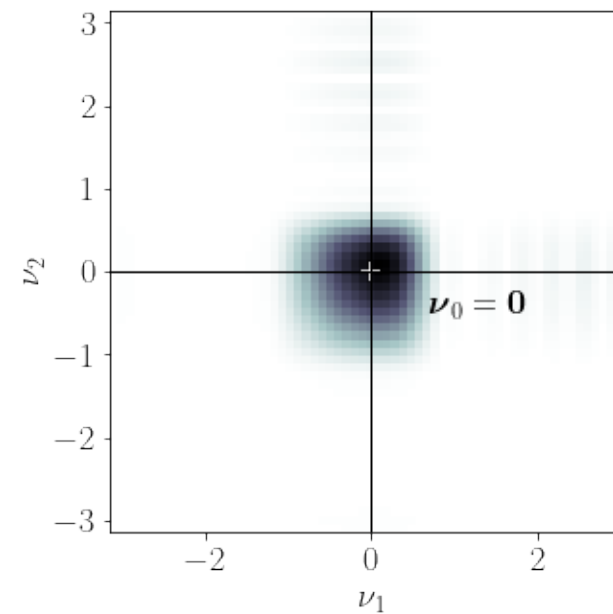
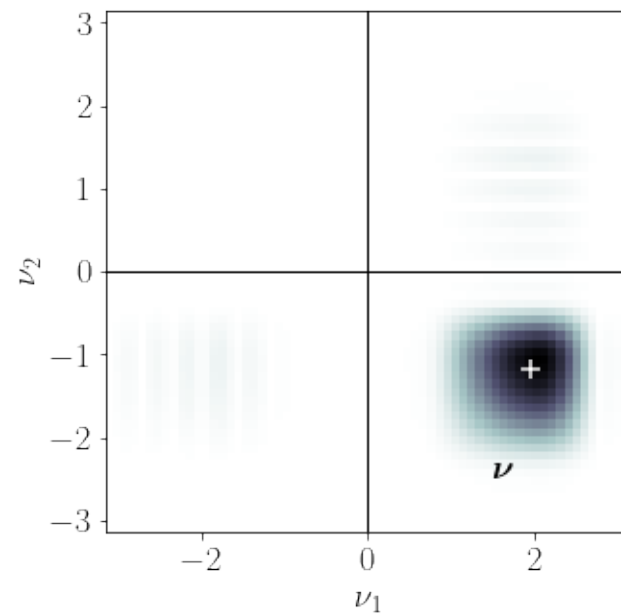
From CMod to RMax in the continuous framework

■ I. Waldspurger intuition linking the two operators:

From CMod to RMax in the continuous framework

I. Waldspurger intuition linking the two operators:

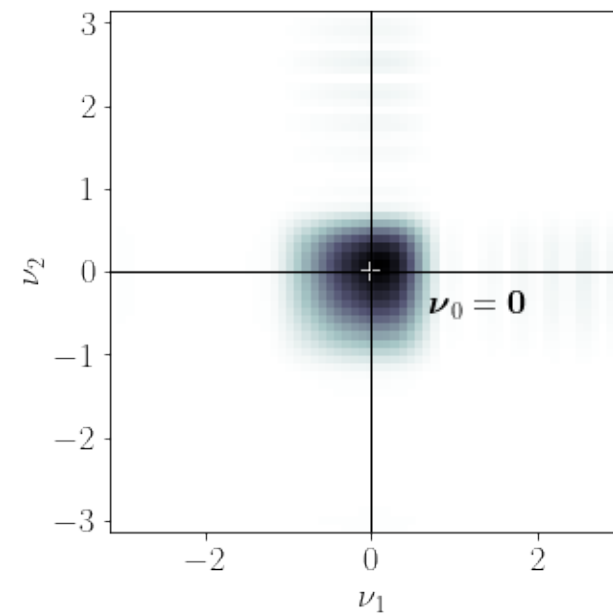
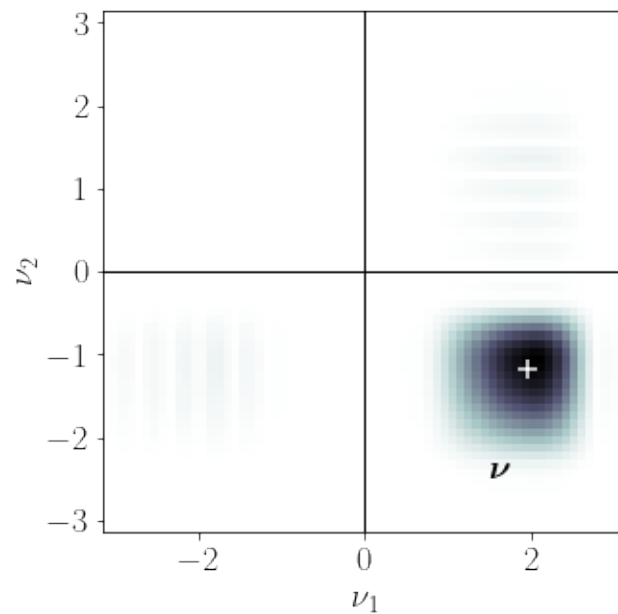
$$F_0 : \mathbf{x} \mapsto (F * \overline{\Psi})(\mathbf{x}) e^{i\langle \boldsymbol{\nu}, \mathbf{x} \rangle} \xrightarrow{\Psi \in \mathcal{V}(\boldsymbol{\nu}, \varepsilon)} \text{supp } \widehat{F_0} \subset B_\infty(\varepsilon/2)$$



From CMod to RMax in the continuous framework

I. Waldspurger intuition linking the two operators:

$$F_0 : \mathbf{x} \mapsto (F * \overline{\Psi})(\mathbf{x}) e^{i\langle \boldsymbol{\nu}, \mathbf{x} \rangle} \xrightarrow{\Psi \in \mathcal{V}(\boldsymbol{\nu}, \varepsilon)} \text{supp} \widehat{F_0} \subset B_\infty(\varepsilon/2)$$

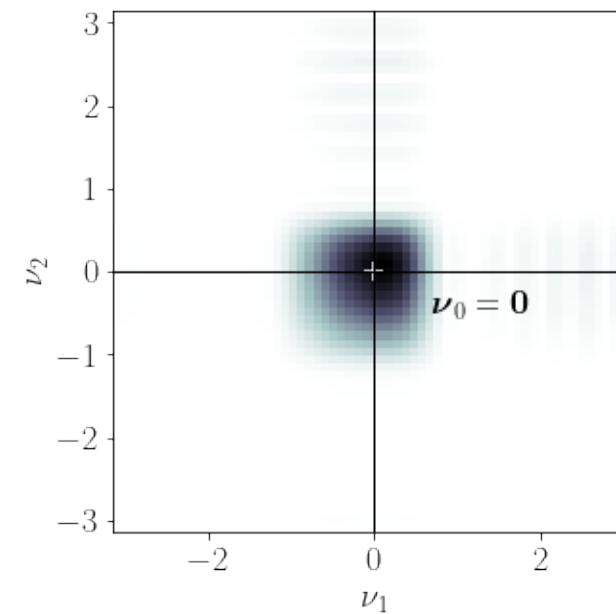
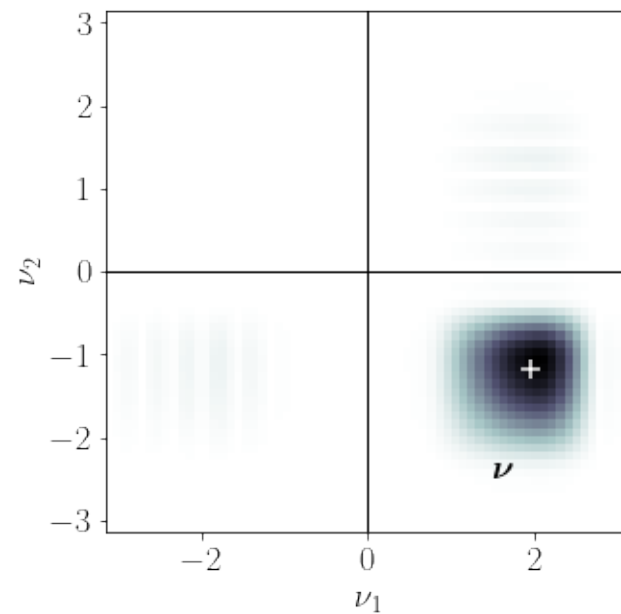


$$(F * \text{Re } \overline{\Psi})(\mathbf{x}) = \text{Re}((F * \overline{\Psi})(\mathbf{x})) = \text{Re}(F_0(\mathbf{x}) e^{-i\langle \boldsymbol{\nu}, \mathbf{x} \rangle})$$

From CMod to RMax in the continuous framework

I. Waldspurger intuition linking the two operators:

$$F_0 : \mathbf{x} \mapsto (F * \overline{\Psi})(\mathbf{x}) e^{i\langle \boldsymbol{\nu}, \mathbf{x} \rangle} \xrightarrow{\Psi \in \mathcal{V}(\boldsymbol{\nu}, \varepsilon)} \text{supp} \widehat{F_0} \subset B_\infty(\varepsilon/2)$$



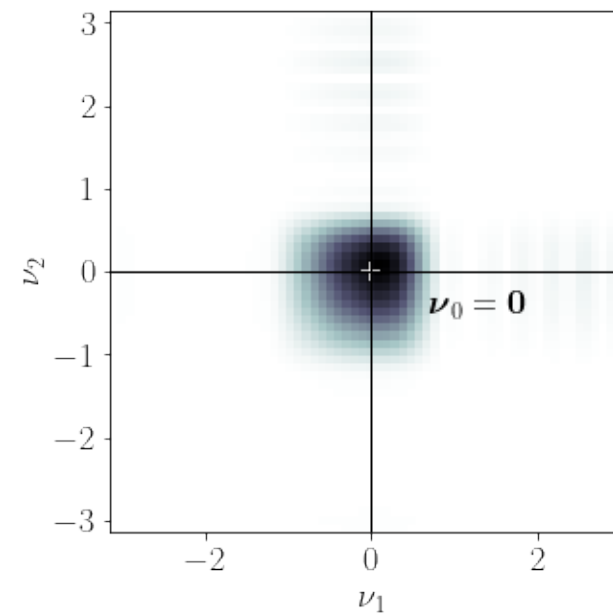
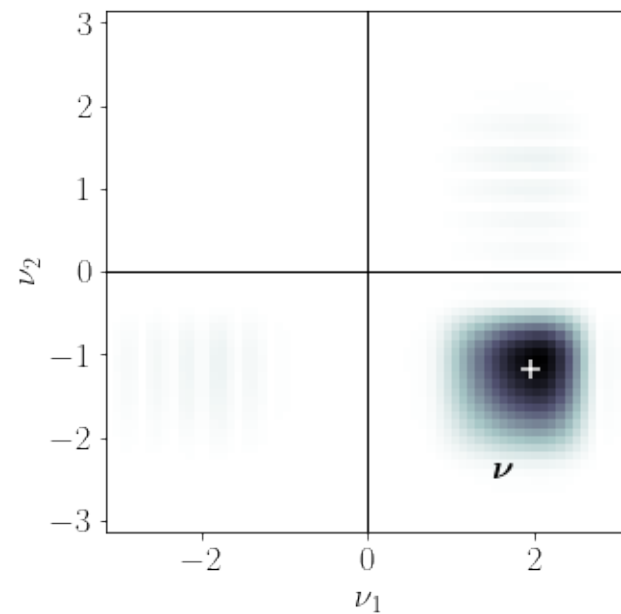
$$(F * \text{Re } \overline{\Psi})(\mathbf{x}) = \text{Re}((F * \overline{\Psi})(\mathbf{x})) = \text{Re}(F_0(\mathbf{x}) e^{-i\langle \boldsymbol{\nu}, \mathbf{x} \rangle})$$

$$(F * \text{Re } \overline{\Psi})(\mathbf{x} + \mathbf{h}) \approx \text{Re}(F_0(\mathbf{x}) e^{-i\langle \boldsymbol{\nu}, \mathbf{x} + \mathbf{h} \rangle}) = \text{Re}((F * \overline{\Psi})(\mathbf{x}) e^{-i\langle \boldsymbol{\nu}, \mathbf{h} \rangle})$$

From CMod to RMax in the continuous framework

I. Waldspurger intuition linking the two operators:

$$F_0 : \mathbf{x} \mapsto (F * \overline{\Psi})(\mathbf{x}) e^{i\langle \boldsymbol{\nu}, \mathbf{x} \rangle} \xrightarrow{\Psi \in \mathcal{V}(\boldsymbol{\nu}, \varepsilon)} \text{supp } \widehat{F_0} \subset B_\infty(\varepsilon/2)$$



$$\|\mathbf{h}\|_2 \ll 2\pi/\varepsilon \implies F_0(\mathbf{x} + \mathbf{h}) \approx F_0(\mathbf{x})$$

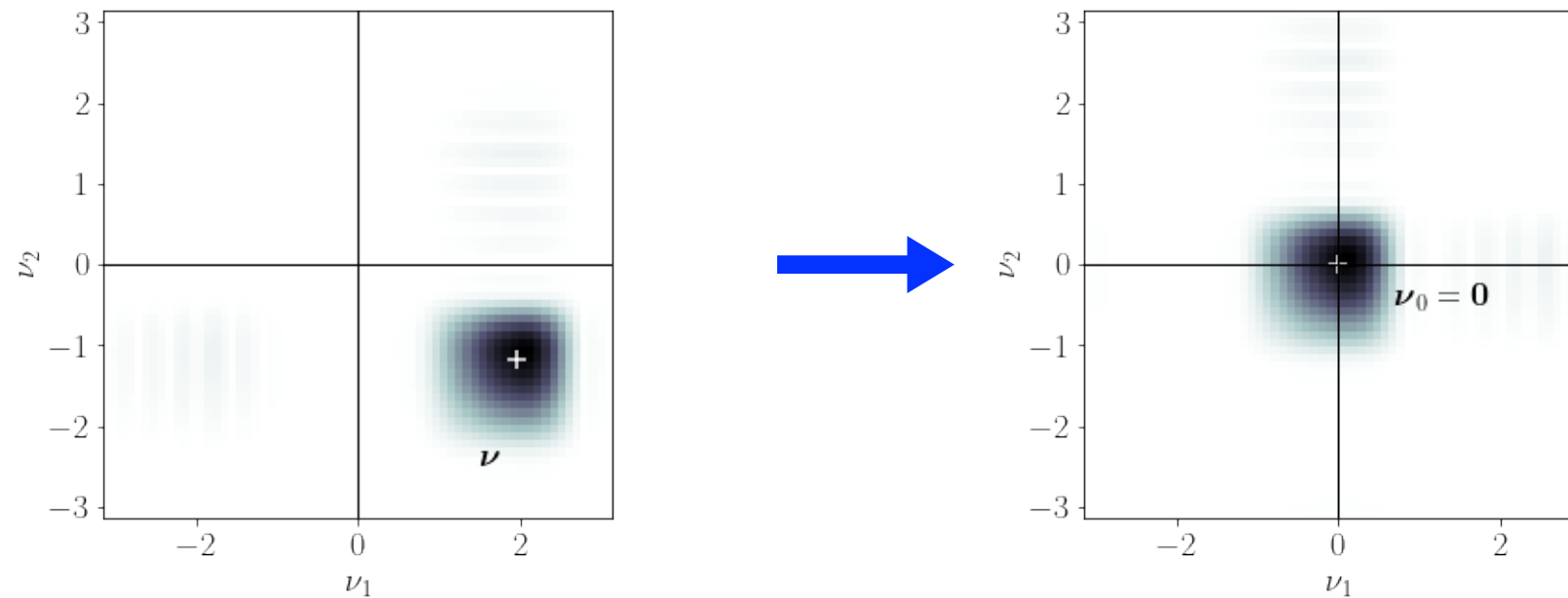
$$(F * \text{Re } \overline{\Psi})(\mathbf{x}) = \text{Re}((F * \overline{\Psi})(\mathbf{x})) = \text{Re}(F_0(\mathbf{x}) e^{-i\langle \boldsymbol{\nu}, \mathbf{x} \rangle})$$

$$(F * \text{Re } \overline{\Psi})(\mathbf{x} + \mathbf{h}) \approx \text{Re}(F_0(\mathbf{x}) e^{-i\langle \boldsymbol{\nu}, \mathbf{x} + \mathbf{h} \rangle}) = \text{Re}((F * \overline{\Psi})(\mathbf{x}) e^{-i\langle \boldsymbol{\nu}, \mathbf{h} \rangle})$$

From CMod to RMax in the continuous framework

I. Waldspurger intuition linking the two operators:

$$F_0 : \mathbf{x} \mapsto (F * \overline{\Psi})(\mathbf{x}) e^{i\langle \boldsymbol{\nu}, \mathbf{x} \rangle} \xrightarrow{\Psi \in \mathcal{V}(\boldsymbol{\nu}, \varepsilon)} \text{supp} \widehat{F_0} \subset B_\infty(\varepsilon/2)$$



$$(F * \overline{\Psi})(\mathbf{x}) = |(F * \overline{\Psi})(\mathbf{x})| e^{-iH(\mathbf{x})} \quad \|h\|_2 \ll 2\pi/\varepsilon \implies F_0(\mathbf{x} + \mathbf{h}) \approx F_0(\mathbf{x})$$

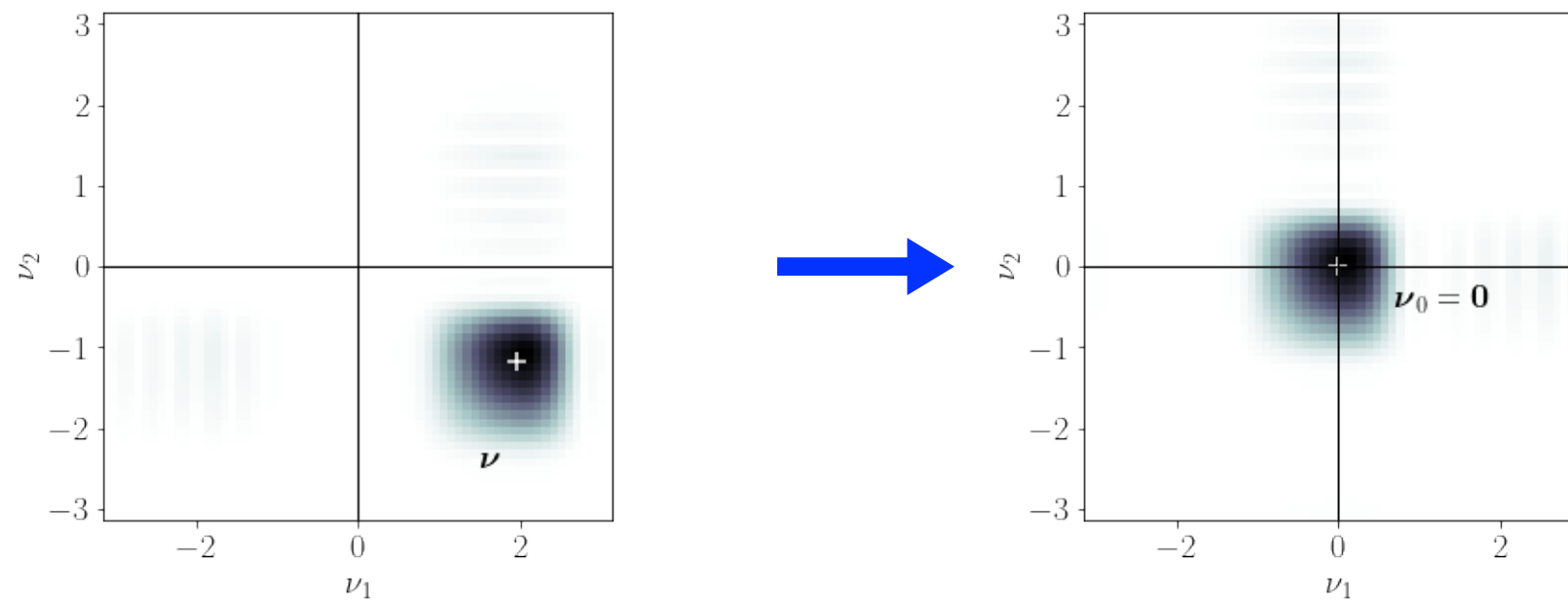
$$(F * \text{Re } \overline{\Psi})(\mathbf{x}) = \text{Re}((F * \overline{\Psi})(\mathbf{x})) = \text{Re}(F_0(\mathbf{x}) e^{-i\langle \boldsymbol{\nu}, \mathbf{x} \rangle})$$

$$(F * \text{Re } \overline{\Psi})(\mathbf{x} + \mathbf{h}) \approx \text{Re}(F_0(\mathbf{x}) e^{-i\langle \boldsymbol{\nu}, \mathbf{x} + \mathbf{h} \rangle}) = \text{Re}((F * \overline{\Psi})(\mathbf{x}) e^{-i\langle \boldsymbol{\nu}, \mathbf{h} \rangle})$$

From CMod to RMax in the continuous framework

I. Waldspurger intuition linking the two operators:

$$F_0 : \mathbf{x} \mapsto (F * \overline{\Psi})(\mathbf{x}) e^{i\langle \boldsymbol{\nu}, \mathbf{x} \rangle} \xrightarrow{\Psi \in \mathcal{V}(\boldsymbol{\nu}, \varepsilon)} \text{supp} \widehat{F_0} \subset B_\infty(\varepsilon/2)$$



$$(F * \overline{\Psi})(\mathbf{x}) = |(F * \overline{\Psi})(\mathbf{x})| e^{-iH(\mathbf{x})} \quad \|h\|_2 \ll 2\pi/\varepsilon \implies F_0(\mathbf{x} + \mathbf{h}) \approx F_0(\mathbf{x})$$

$$(F * \text{Re } \overline{\Psi})(\mathbf{x}) = \text{Re}((F * \overline{\Psi})(\mathbf{x})) = \text{Re}(F_0(\mathbf{x}) e^{-i\langle \boldsymbol{\nu}, \mathbf{x} \rangle})$$

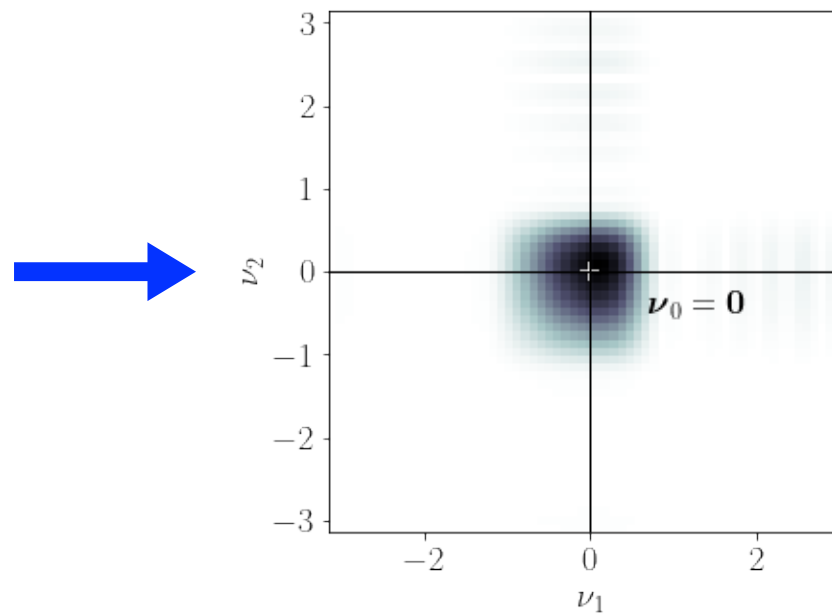
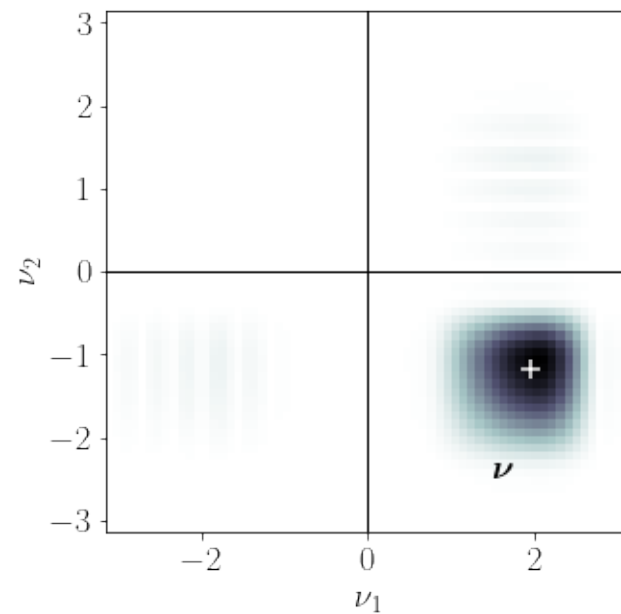
$$(F * \text{Re } \overline{\Psi})(\mathbf{x} + \mathbf{h}) \approx \text{Re}(F_0(\mathbf{x}) e^{-i\langle \boldsymbol{\nu}, \mathbf{x} + \mathbf{h} \rangle}) = \text{Re}((F * \overline{\Psi})(\mathbf{x}) e^{-i\langle \boldsymbol{\nu}, \mathbf{h} \rangle})$$

$$(F * \text{Re } \overline{\Psi})(\mathbf{x} + \mathbf{h}) \approx |(F * \overline{\Psi})(\mathbf{x})| \cos(\langle \boldsymbol{\nu}, \mathbf{h} \rangle - H(\mathbf{x}))$$

From CMod to RMax in the continuous framework

I. Waldspurger intuition linking the two operators:

$$F_0 : \mathbf{x} \mapsto (F * \overline{\Psi})(\mathbf{x}) e^{i\langle \boldsymbol{\nu}, \mathbf{x} \rangle} \xrightarrow{\Psi \in \mathcal{V}(\boldsymbol{\nu}, \varepsilon)} \text{supp } \widehat{F_0} \subset B_\infty(\varepsilon/2)$$



$$(F * \overline{\Psi})(\mathbf{x}) = |(F * \overline{\Psi})(\mathbf{x})| e^{-iH(\mathbf{x})} \quad \|h\|_2 \ll 2\pi/\varepsilon \implies F_0(\mathbf{x} + \mathbf{h}) \approx F_0(\mathbf{x})$$

$$(F * \text{Re } \overline{\Psi})(\mathbf{x}) = \text{Re}((F * \overline{\Psi})(\mathbf{x})) = \text{Re}(F_0(\mathbf{x}) e^{-i\langle \boldsymbol{\nu}, \mathbf{x} \rangle})$$

$$(F * \text{Re } \overline{\Psi})(\mathbf{x} + \mathbf{h}) \approx \text{Re}(F_0(\mathbf{x}) e^{-i\langle \boldsymbol{\nu}, \mathbf{x} + \mathbf{h} \rangle}) = \text{Re}((F * \overline{\Psi})(\mathbf{x}) e^{-i\langle \boldsymbol{\nu}, \mathbf{h} \rangle})$$

$$(F * \text{Re } \overline{\Psi})(\mathbf{x} + \mathbf{h}) \approx |(F * \overline{\Psi})(\mathbf{x})| \cos(\langle \boldsymbol{\nu}, \mathbf{h} \rangle) - H(\mathbf{x}) \xleftarrow{G(\mathbf{x}, \mathbf{h})}$$

From CMod to RMax in the continuous framework

■ I. Waldspurger intuition linking the two operators:

$$(F * \text{Re } \bar{\Psi})(\mathbf{x} + \mathbf{h}) \approx |(F * \bar{\Psi})(\mathbf{x})| \cos(\langle \boldsymbol{\nu}, \mathbf{h} \rangle - H(\mathbf{x}))$$

From CMod to RMax in the continuous framework

■ I. Waldspurger intuition linking the two operators:

$$(F * \operatorname{Re} \bar{\Psi})(\mathbf{x} + \mathbf{h}) \approx |(F * \bar{\Psi})(\mathbf{x})| \cos(\langle \boldsymbol{\nu}, \mathbf{h} \rangle - H(\mathbf{x}))$$

- $U^{\text{mod}}[\Psi](F) : \mathbf{x} \mapsto |(F * \bar{\Psi})(\mathbf{x})|$
- $U_r^{\max}[\Psi](F) : \mathbf{x} \mapsto \max_{\|\mathbf{h}\|_\infty \leq r} (F * \operatorname{Re} \bar{\Psi})(\mathbf{x} + \mathbf{h})$

From CMod to RMax in the continuous framework

■ I. Waldspurger intuition linking the two operators:

$$(F * \operatorname{Re} \bar{\Psi})(\mathbf{x} + \mathbf{h}) \approx |(F * \bar{\Psi})(\mathbf{x})| \cos(\langle \boldsymbol{\nu}, \mathbf{h} \rangle - H(\mathbf{x}))$$

- $U^{\text{mod}}[\Psi](F) : \mathbf{x} \mapsto |(F * \bar{\Psi})(\mathbf{x})|$
- $U_r^{\max}[\Psi](F) : \mathbf{x} \mapsto \max_{\|\mathbf{h}\|_\infty \leq r} (F * \operatorname{Re} \bar{\Psi})(\mathbf{x} + \mathbf{h})$

$$r \ll 2\pi/\varepsilon \implies U_r^{\max} F(\mathbf{x}) \approx U^{\text{mod}} F(\mathbf{x}) \max_{\|\mathbf{h}\|_\infty \leq r} G(\mathbf{x}, \mathbf{h})$$

Max

From CMod to RMax in the continuous framework

■ I. Waldspurger intuition linking the two operators:

$$(F * \operatorname{Re} \bar{\Psi})(\mathbf{x} + \mathbf{h}) \approx |(F * \bar{\Psi})(\mathbf{x})| \cos(\langle \boldsymbol{\nu}, \mathbf{h} \rangle - H(\mathbf{x}))$$

- $U^{\text{mod}}[\Psi](F) : \mathbf{x} \mapsto |(F * \bar{\Psi})(\mathbf{x})|$
 - $U_r^{\max}[\Psi](F) : \mathbf{x} \mapsto \max_{\|\mathbf{h}\|_\infty \leq r} (F * \operatorname{Re} \bar{\Psi})(\mathbf{x} + \mathbf{h})$
- Max
- $$r \ll 2\pi/\varepsilon \implies U_r^{\max} F(\mathbf{x}) \approx U^{\text{mod}} F(\mathbf{x}) \max_{\|\mathbf{h}\|_\infty \leq r} G(\mathbf{x}, \mathbf{h})$$
- For $r \geq \frac{\pi}{\|\boldsymbol{\nu}\|_2}$ the cosine $\mathbf{h} \mapsto G(\mathbf{x}, \mathbf{h})$ reaches 1 on $B_\infty(r)$

From CMod to RMax in the continuous framework

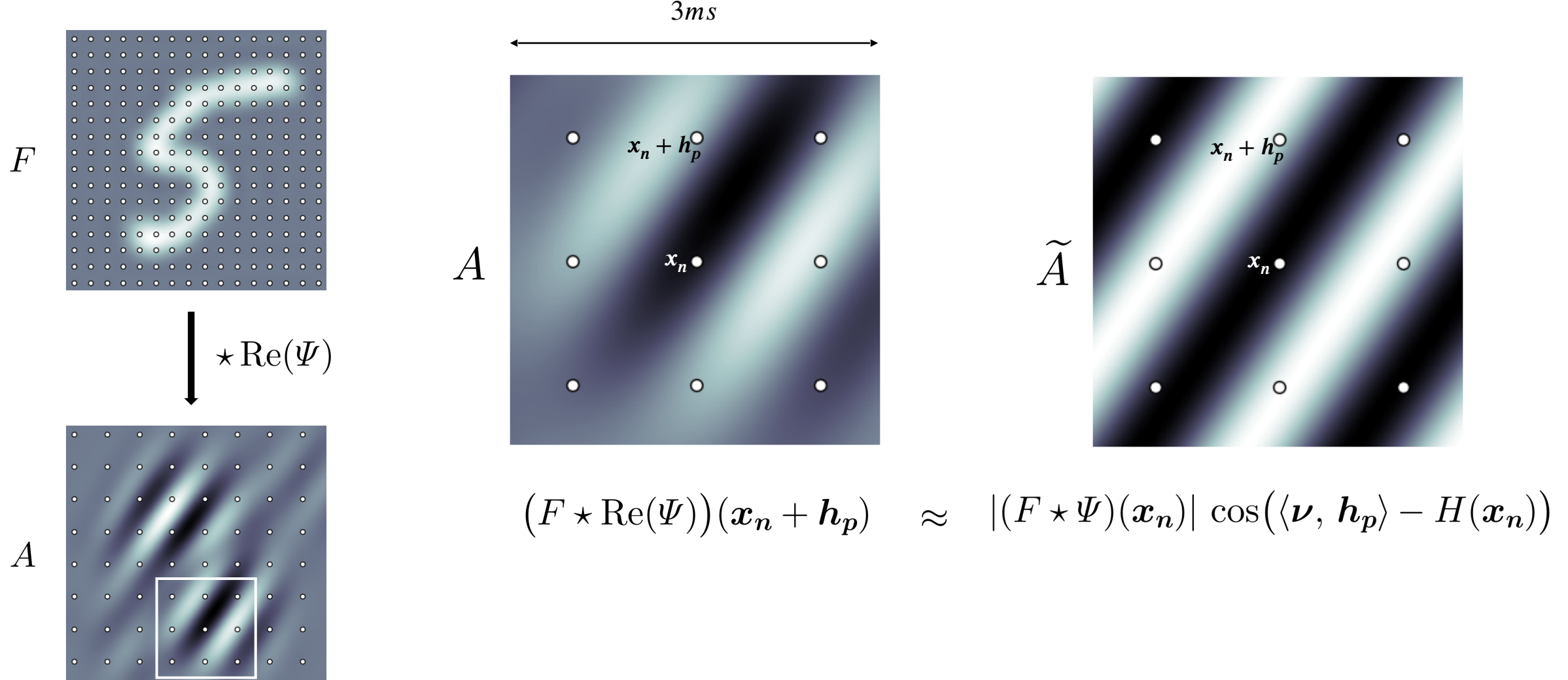
■ I. Waldspurger intuition linking the two operators:

$$(F * \operatorname{Re} \bar{\Psi})(\mathbf{x} + \mathbf{h}) \approx |(F * \bar{\Psi})(\mathbf{x})| \cos(\langle \boldsymbol{\nu}, \mathbf{h} \rangle - H(\mathbf{x}))$$

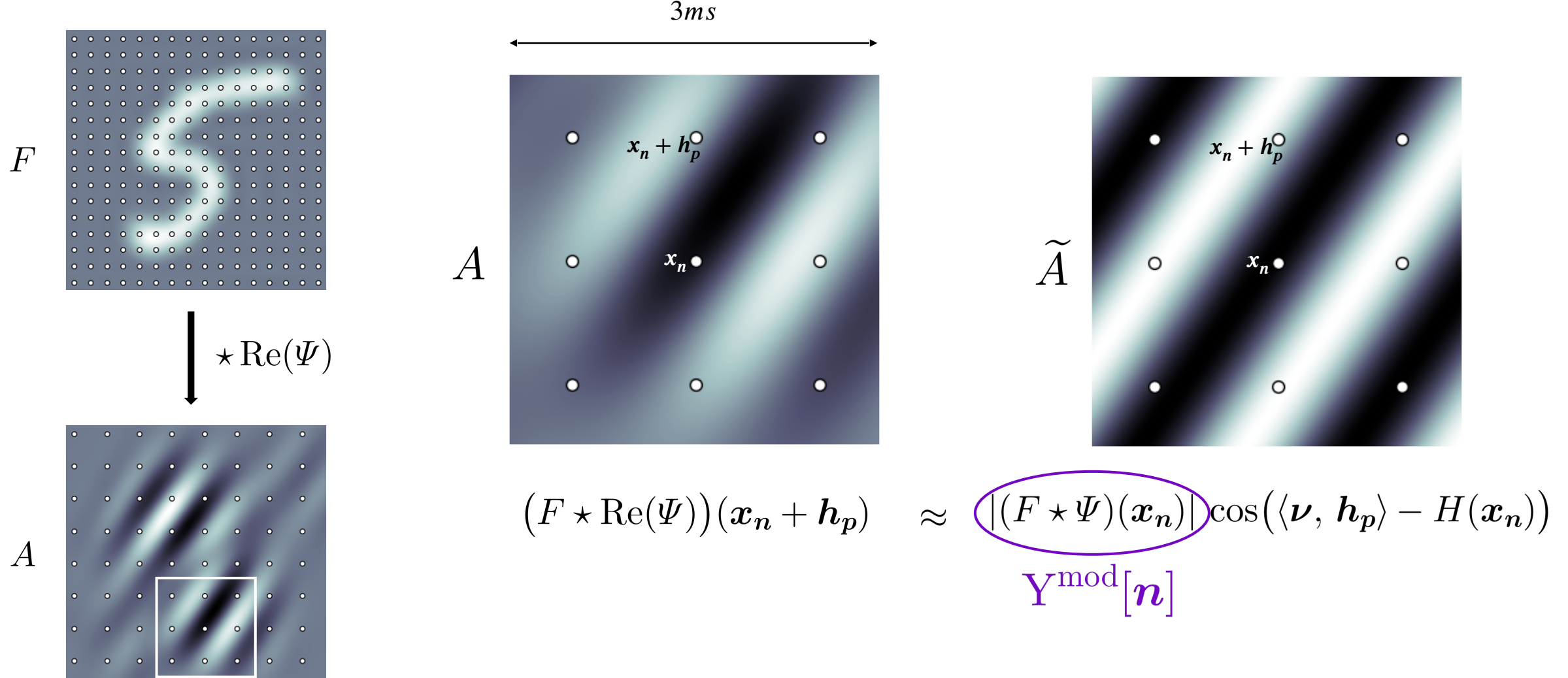
- $U^{\text{mod}}[\Psi](F) : \mathbf{x} \mapsto |(F * \bar{\Psi})(\mathbf{x})|$
 - $U_r^{\max}[\Psi](F) : \mathbf{x} \mapsto \max_{\|\mathbf{h}\|_\infty \leq r} (F * \operatorname{Re} \bar{\Psi})(\mathbf{x} + \mathbf{h})$
- Max
- $$r \ll 2\pi/\varepsilon \implies U_r^{\max} F(\mathbf{x}) \approx U^{\text{mod}} F(\mathbf{x}) \max_{\|\mathbf{h}\|_\infty \leq r} G(\mathbf{x}, \mathbf{h})$$
- For $r \geq \frac{\pi}{\|\boldsymbol{\nu}\|_2}$ the cosine $\mathbf{h} \mapsto G(\mathbf{x}, \mathbf{h})$ reaches 1 on $B_\infty(r)$

$$\frac{\pi}{\|\boldsymbol{\nu}\|_2} \leq r \ll \frac{2\pi}{\varepsilon} \implies U_r^{\max} F(\mathbf{x}) \approx U^{\text{mod}} F(\mathbf{x})$$

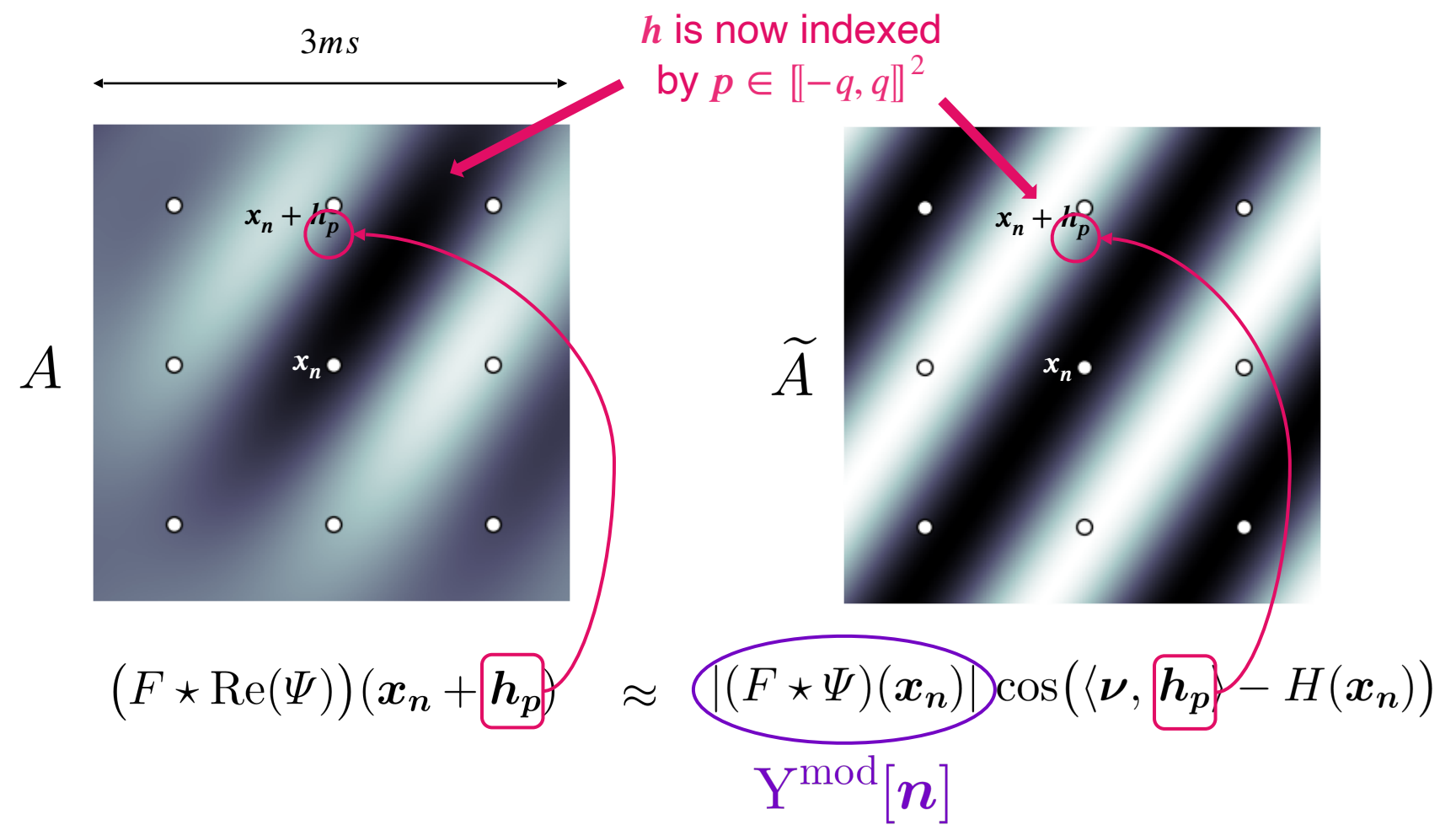
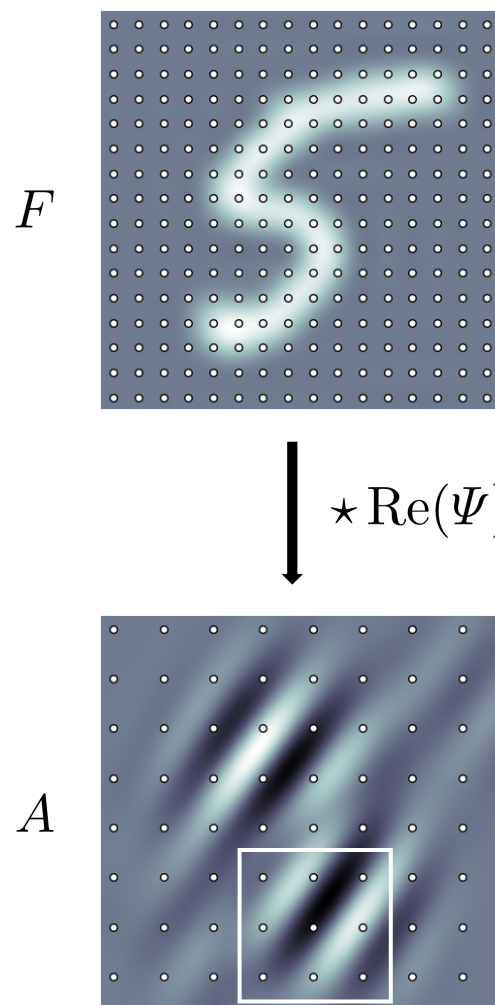
Adaptation to the discrete case



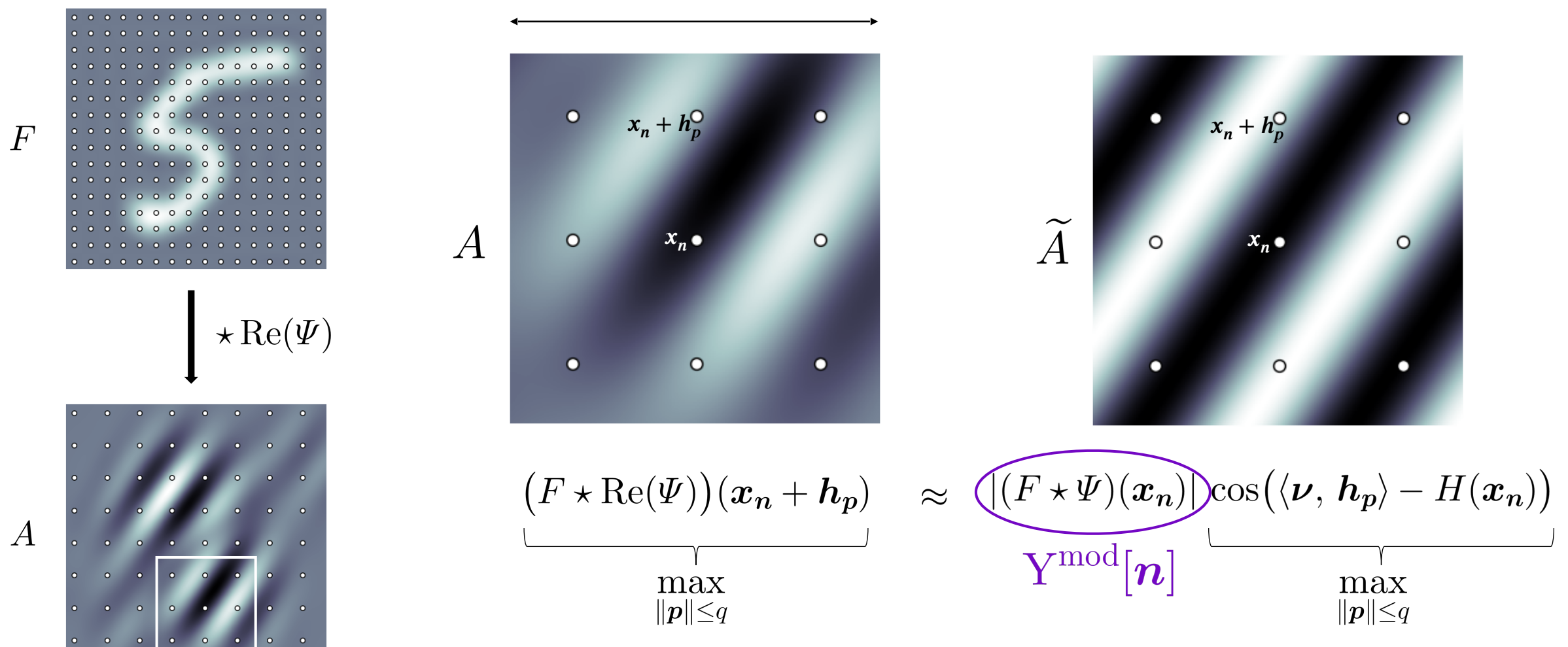
Adaptation to the discrete case



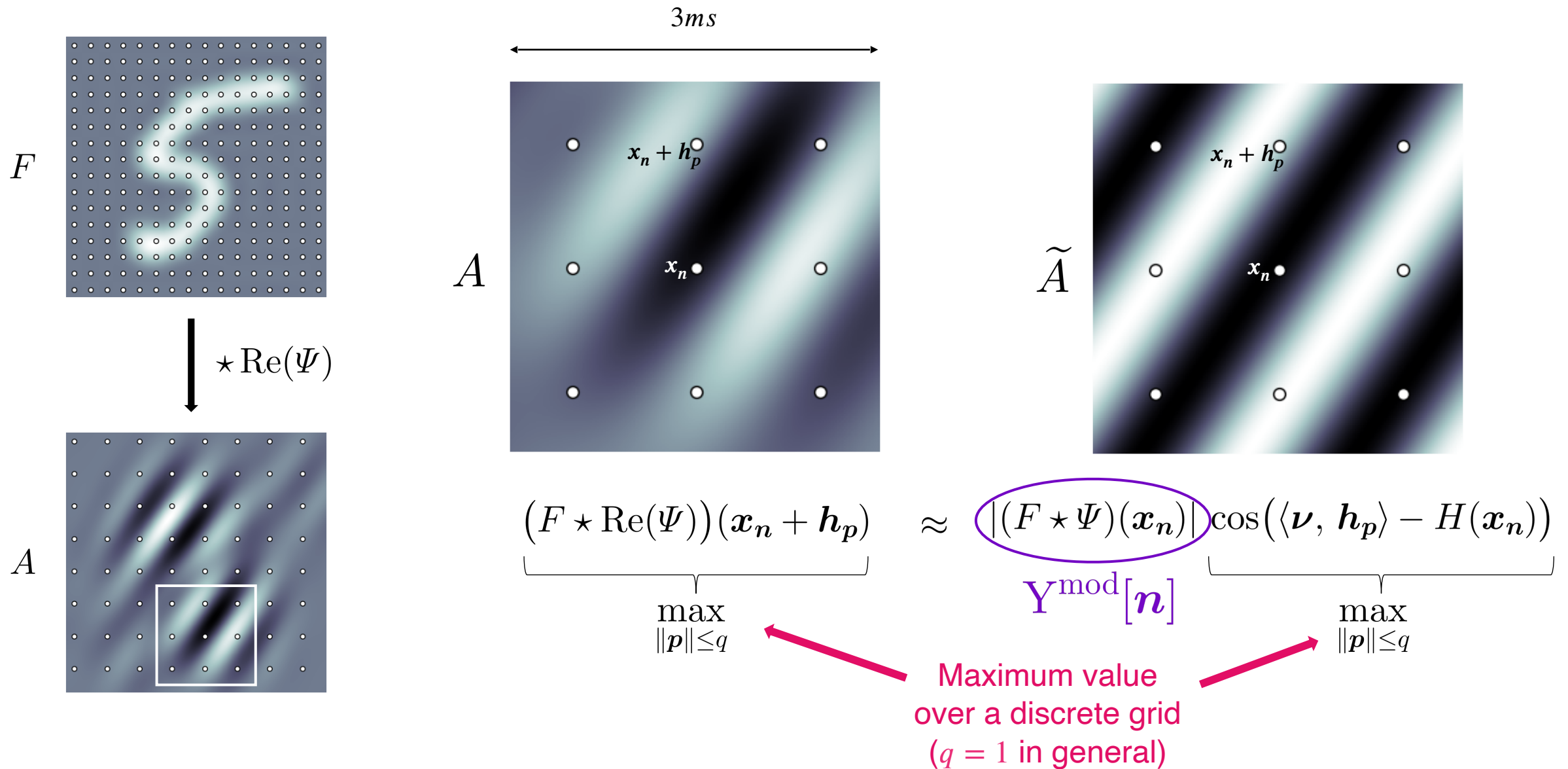
Adaptation to the discrete case



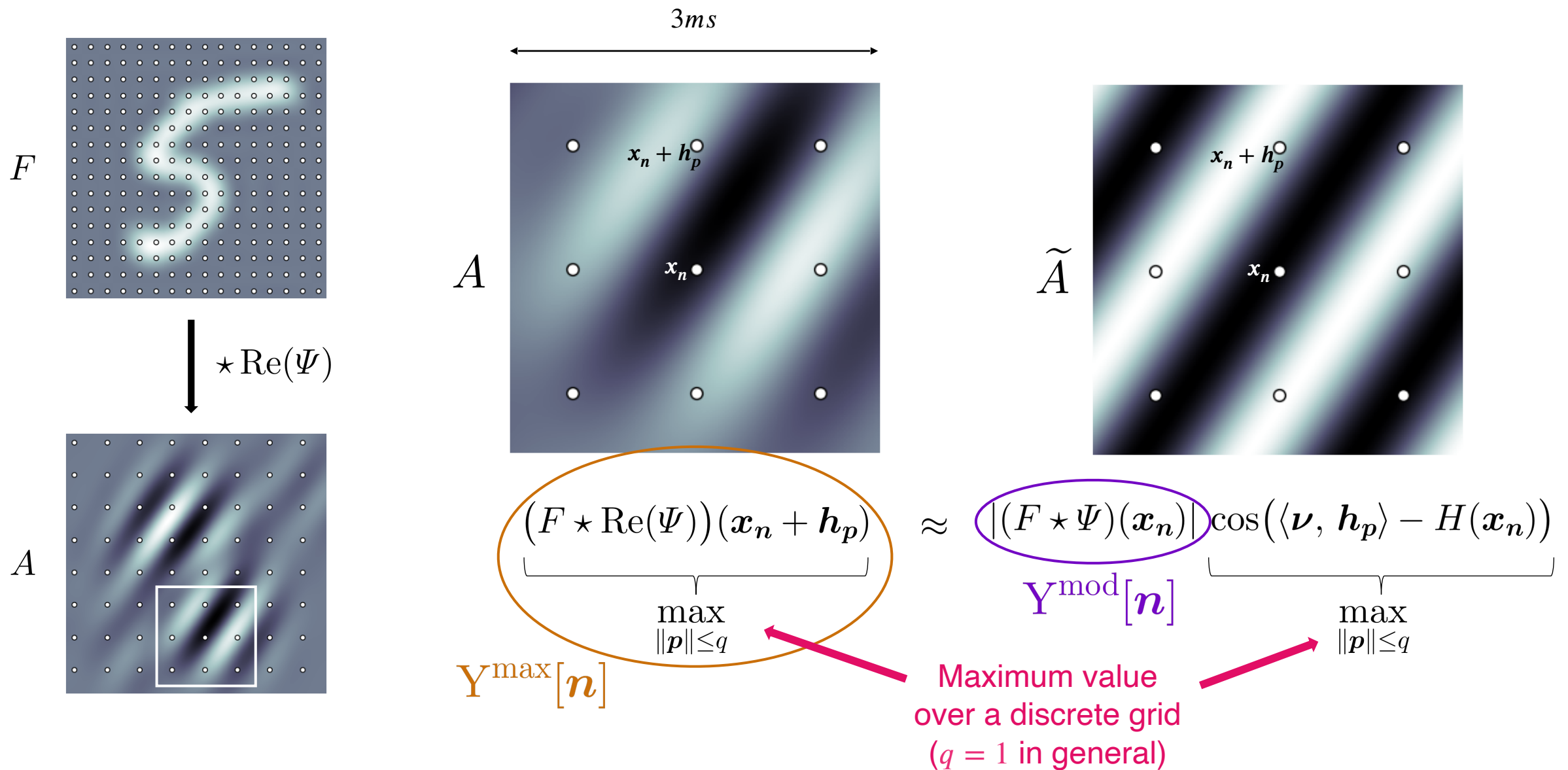
Adaptation to the discrete case



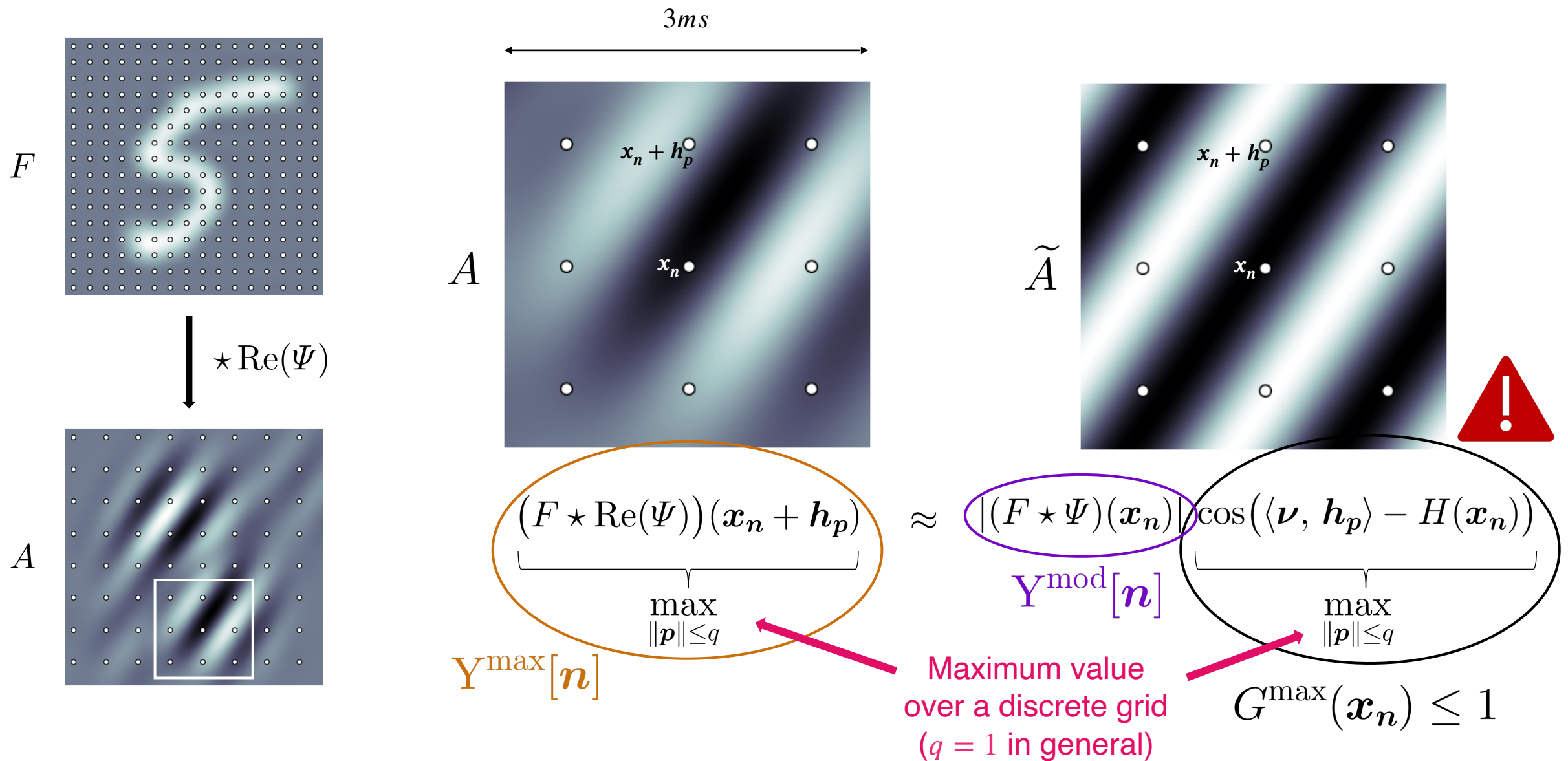
Adaptation to the discrete case



Adaptation to the discrete case



Adaptation to the discrete case



Adaptation to the discrete case

$$q \ll 2\pi/(m\kappa) \quad \Rightarrow \quad U_{m,q}^{\max} X[\mathbf{n}] \approx U_{2m}^{\text{mod}} X[\mathbf{n}] \max_{\|\mathbf{p}\|_\infty \leq q} G_X(\mathbf{x}_n, \mathbf{h}_p),$$

Adaptation to the discrete case

$$q \ll 2\pi/(m\kappa) \implies U_{m,q}^{\max} X[\mathbf{n}] \approx U_{2m}^{\text{mod}} X[\mathbf{n}] \max_{\|\mathbf{p}\|_\infty \leq q} G_X(\mathbf{x}_n, h_p),$$

Not necessarily reaches 1

Adaptation to the discrete case

$$q \ll 2\pi/(m\kappa) \implies U_{m,q}^{\max} X[\mathbf{n}] \approx U_{2m}^{\text{mod}} X[\mathbf{n}] \max_{\|\mathbf{p}\|_\infty \leq q} G_X(\mathbf{x}_n, h_p),$$

$$q \ll 2\pi/(m\kappa) \implies \|U_{2m}^{\text{mod}} X - U_{m,q}^{\max} X\|_2 \approx \|\delta_{m,q} X\|_2$$

Not necessarily reaches 1

Adaptation to the discrete case

$$q \ll 2\pi/(m\kappa) \implies U_{m,q}^{\max} X[\mathbf{n}] \approx U_{2m}^{\text{mod}} X[\mathbf{n}] \max_{\|\mathbf{p}\|_\infty \leq q} G_X(\mathbf{x}_n, h_p),$$

$$q \ll 2\pi/(m\kappa) \implies \|U_{2m}^{\text{mod}} X - U_{m,q}^{\max} X\|_2 \approx \|\delta_{m,q} X\|_2$$

Not necessarily reaches 1

$$\delta_{m,q} X[\mathbf{n}] := U_{2m}^{\text{mod}} X[\mathbf{n}] \left(1 - \max_{\|\mathbf{p}\|_\infty \leq q} G_X(\mathbf{x}_n, h_p) \right)$$

Adaptation to the discrete case

$$q \ll 2\pi/(m\kappa) \implies U_{m,q}^{\max} X[\mathbf{n}] \approx U_{2m}^{\text{mod}} X[\mathbf{n}] \max_{\|\mathbf{p}\|_\infty \leq q} G_X(\mathbf{x}_n, h_p),$$

$$q \ll 2\pi/(m\kappa) \implies \|U_{2m}^{\text{mod}} X - U_{m,q}^{\max} X\|_2 \approx \|\delta_{m,q} X\|_2$$

Not necessarily reaches 1

$$\delta_{m,q} X[\mathbf{n}] := U_{2m}^{\text{mod}} X[\mathbf{n}] \left(1 - \max_{\|\mathbf{p}\|_\infty \leq q} G_X(\mathbf{x}_n, h_p) \right)$$

Theorem (Bound on the difference of $\mathbb{C}\text{Mod}$ and $\mathbb{R}\text{Max}$)

If $\kappa \leq \pi/m$ and under another reasonable hypothesis

$$\|U_{2m}^{\text{mod}} X - U_{m,q}^{\max} X\|_2 \leq \|\delta_{m,q} X\|_2 + \beta_q(m\kappa) \|U_{2m}^{\text{mod}} X\|_2$$

Adaptation to the discrete case

$$q \ll 2\pi/(m\kappa) \implies U_{m,q}^{\max} X[\mathbf{n}] \approx U_{2m}^{\text{mod}} X[\mathbf{n}] \max_{\|\mathbf{p}\|_\infty \leq q} G_X(\mathbf{x}_n, \mathbf{h}_p),$$

$$q \ll 2\pi/(m\kappa) \implies \|U_{2m}^{\text{mod}} X - U_{m,q}^{\max} X\|_2 \approx \|\delta_{m,q} X\|_2$$

Not necessarily reaches 1

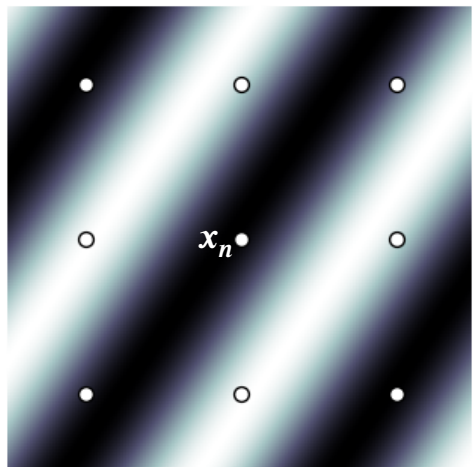
$$\delta_{m,q} X[\mathbf{n}] := U_{2m}^{\text{mod}} X[\mathbf{n}] \left(1 - \max_{\|\mathbf{p}\|_\infty \leq q} G_X(\mathbf{x}_n, \mathbf{h}_p) \right) \quad \beta_q : \kappa' \mapsto q\kappa'.$$

Theorem (Bound on the difference of $\mathbb{C}\text{Mod}$ and $\mathbb{R}\text{Max}$)

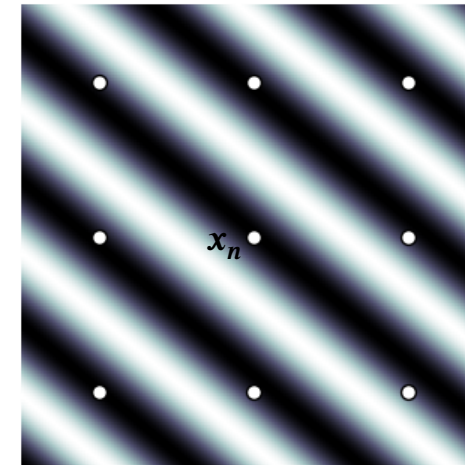
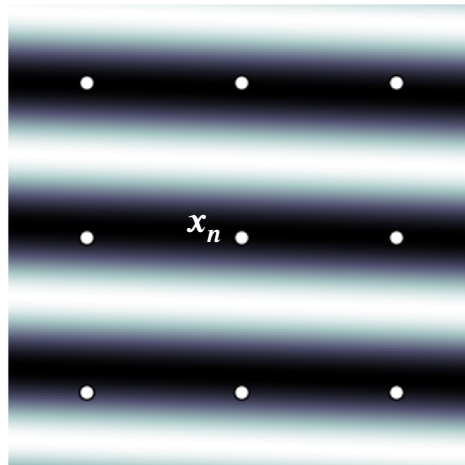
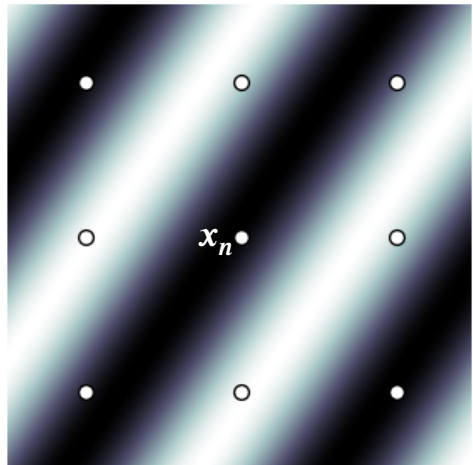
If $\kappa \leq \pi/m$ and under another reasonable hypothesis

$$\|U_{2m}^{\text{mod}} X - U_{m,q}^{\max} X\|_2 \leq \|\delta_{m,q} X\|_2 + \beta_q(m\kappa) \|U_{2m}^{\text{mod}} X\|_2$$

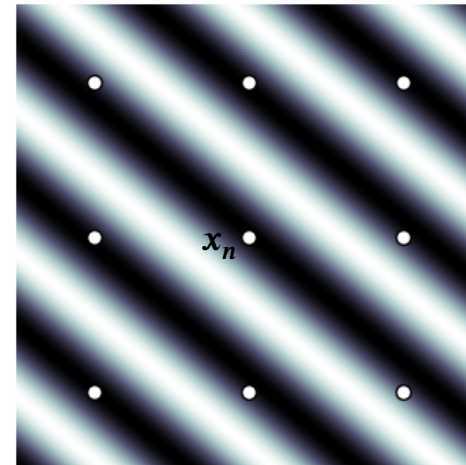
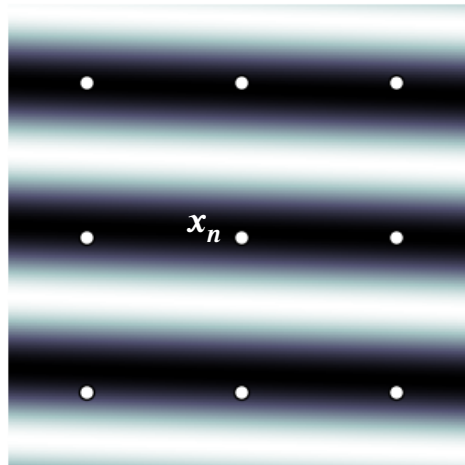
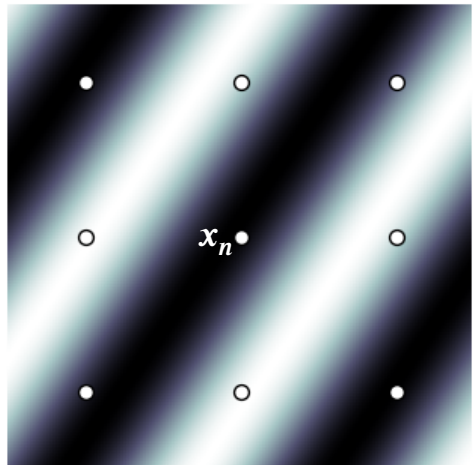
Pathological frequencies



Pathological frequencies

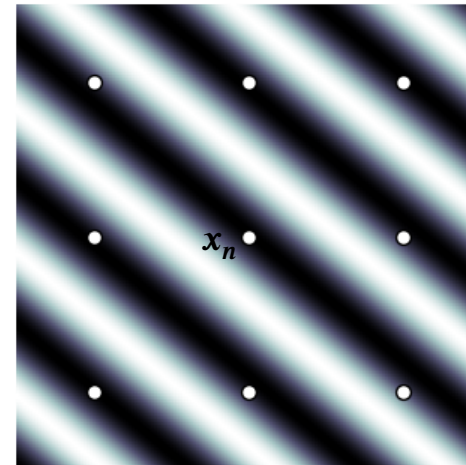
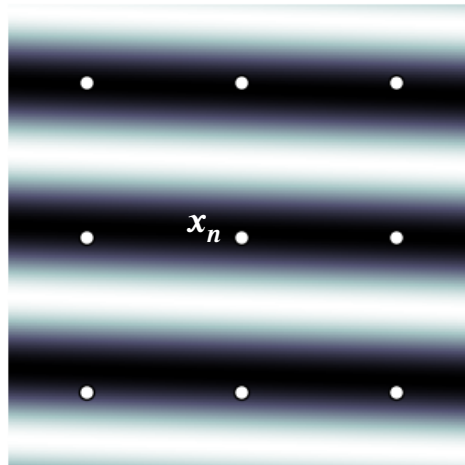
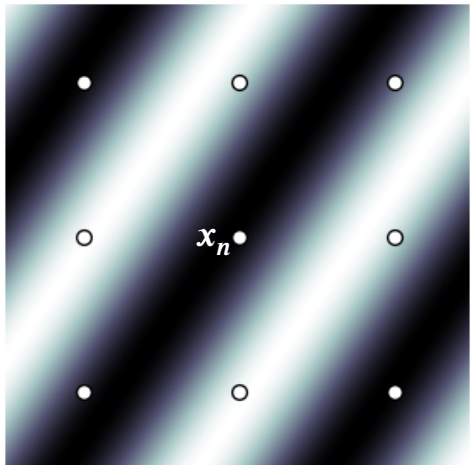


Pathological frequencies



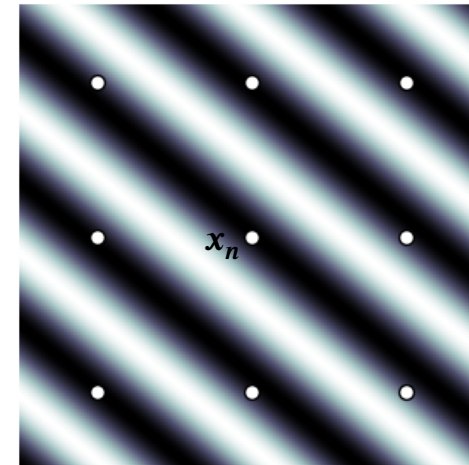
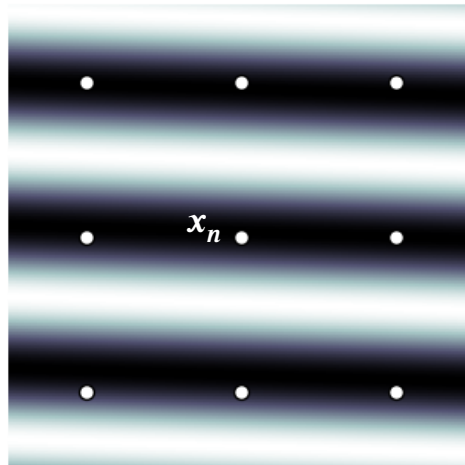
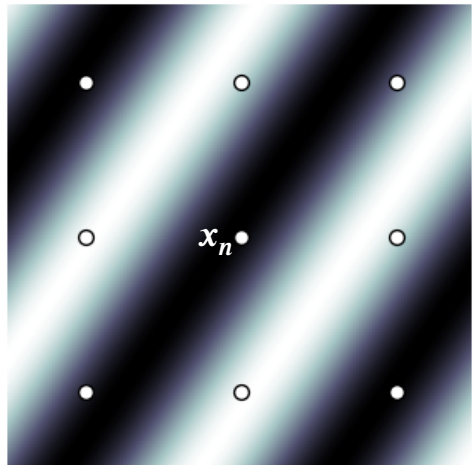
- Need for a probabilistic framework where X (resp. F) is seen as a discrete (resp. continuous) stochastic process on \mathbb{Z}^2 (resp. \mathbb{R}^2)

Pathological frequencies



- Need for a probabilistic framework where X (resp. F) is seen as a discrete (resp. continuous) stochastic process on \mathbb{Z}^2 (resp. \mathbb{R}^2)
- Quantity of interest: $\mathbb{E}\left[\left(1 - G^{\max}(x_n)\right)^2\right]$

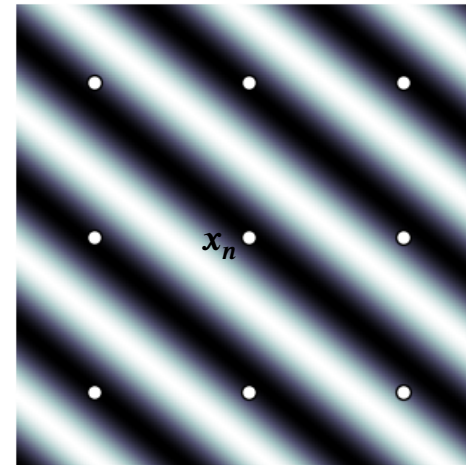
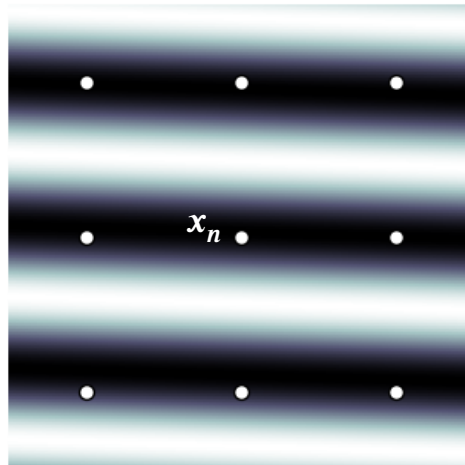
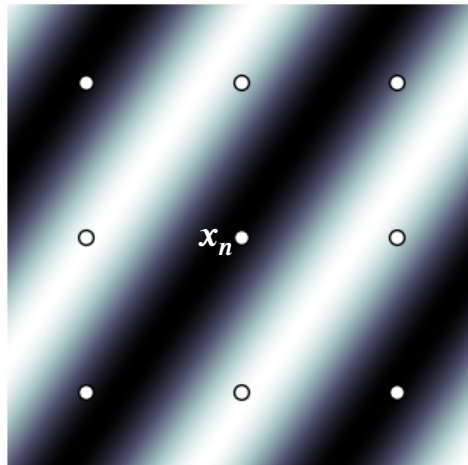
Pathological frequencies



- Need for a probabilistic framework where X (resp. F) is seen as a discrete (resp. continuous) stochastic process on \mathbb{Z}^2 (resp. \mathbb{R}^2)
- Quantity of interest: $\mathbb{E}\left[\left(1 - G^{\max}(x_n)\right)^2\right]$

with $G^{\max}(x_n) = \max_{\|p\|_\infty \leq 1} \cos(\langle \nu, h_p \rangle - H(x_n))$

Pathological frequencies



- Need for a probabilistic framework where X (resp. F) is seen as a discrete (resp. continuous) stochastic process on \mathbb{Z}^2 (resp. \mathbb{R}^2)

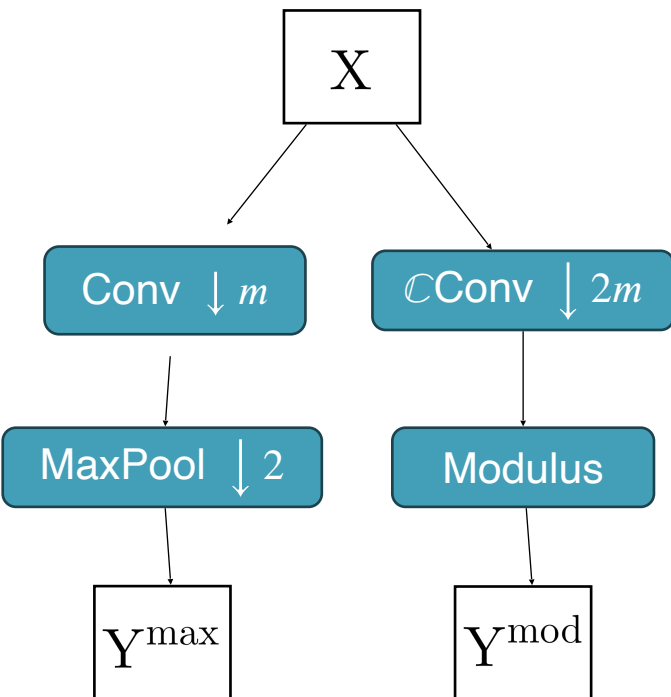
- Quantity of interest: $\mathbb{E}\left[\left(1 - G^{\max}(x_n)\right)^2\right]$

Hypothesis: uniformly distributed

with $G^{\max}(x_n) = \max_{\|p\|_\infty \leq 1} \cos(\langle \nu, h_p \rangle - H(x_n))$

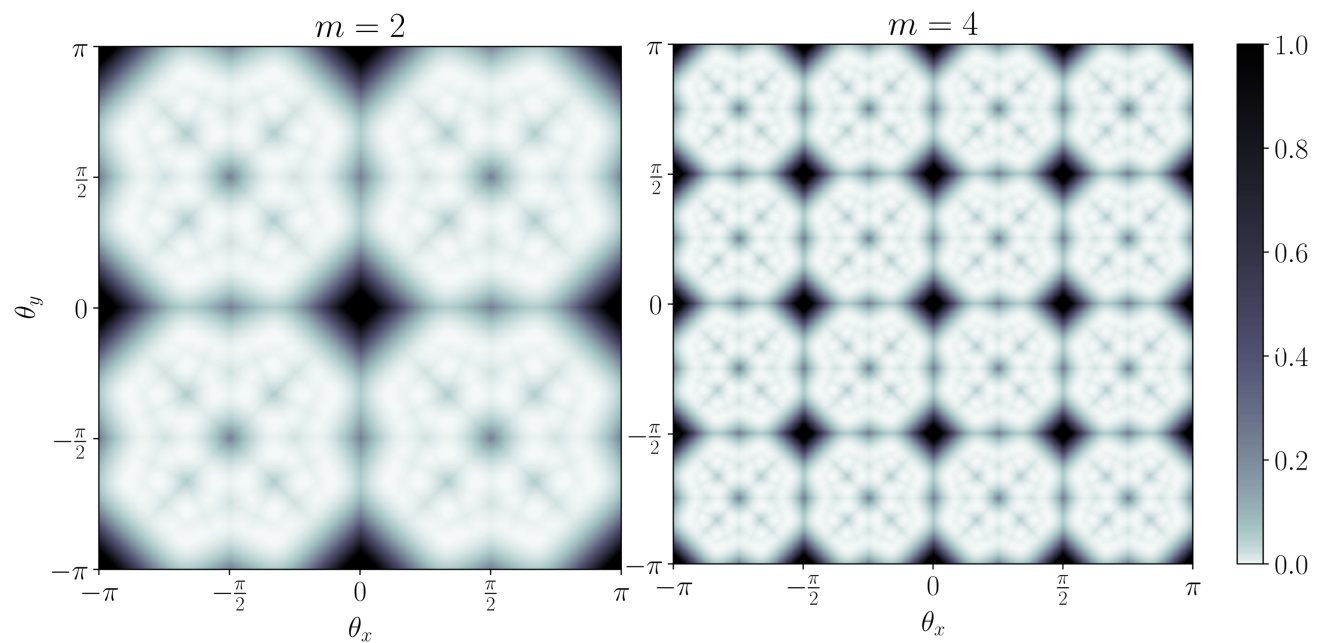
Main result

- MSE between CMod and RMax output



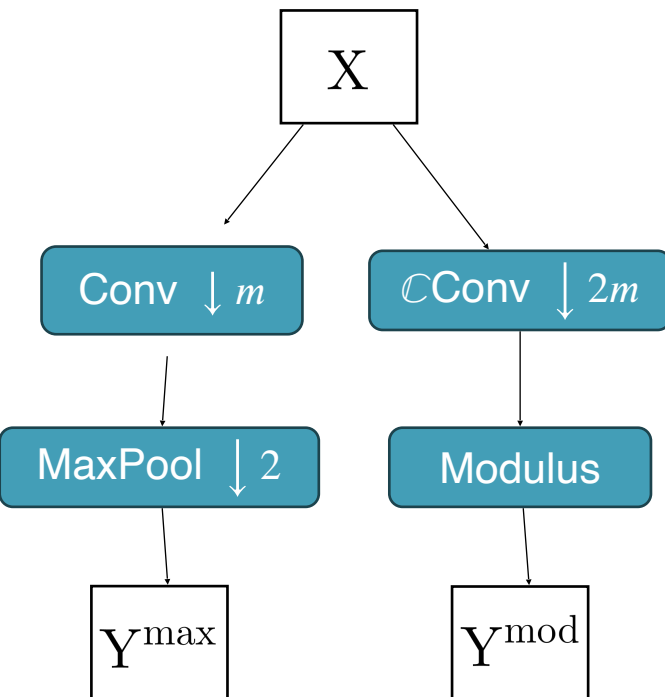
$$\mathbb{E} \left[\frac{\|Y^{\text{max}} - Y^{\text{mod}}\|_2^2}{\|Y^{\text{mod}}\|_2^2} \right] \leq (\beta_q(m\kappa) + \gamma_q(m\theta))^2$$

$$\theta \mapsto \gamma_q(m\theta)^2$$
$$q = 1$$



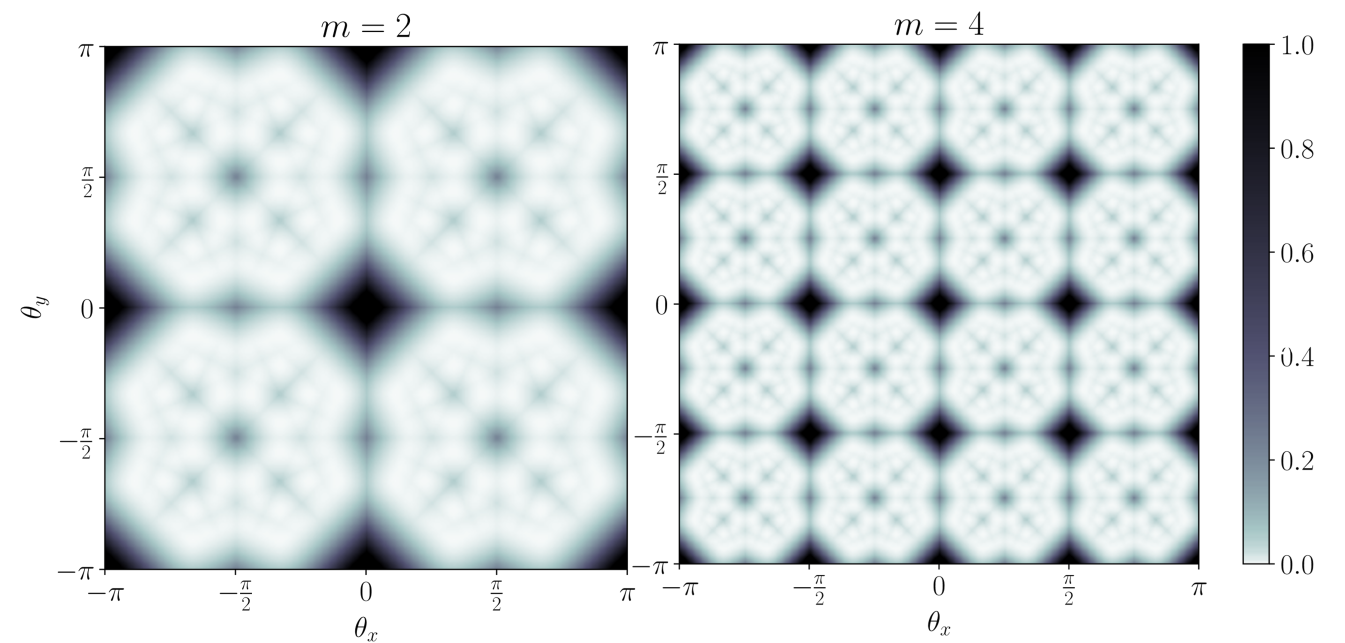
Main result

MSE between CMod and RMax output



$$\mathbb{E} \left[\frac{\|Y^{\max} - Y^{\text{mod}}\|_2^2}{\|Y^{\text{mod}}\|_2^2} \right] \leq (\beta_q(m\kappa) + \gamma_q(m\theta))^2$$

Upper bound under hypothesis $G^{\max} = 1$

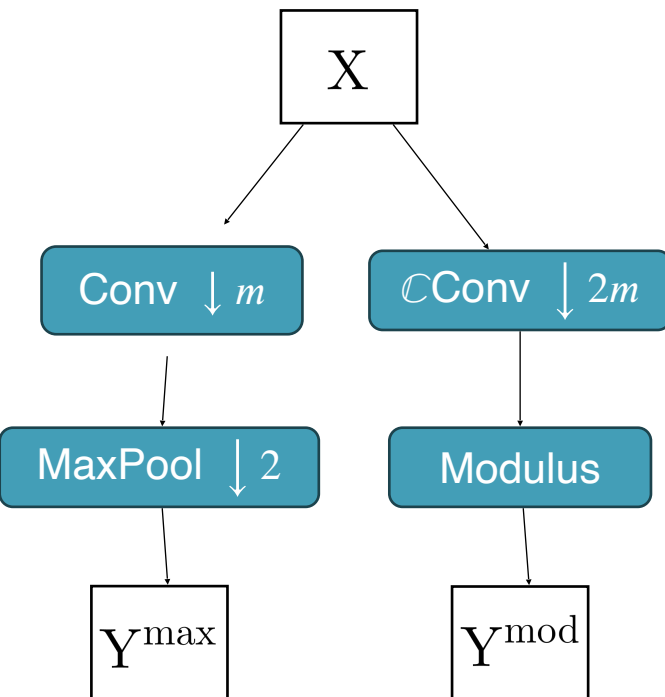


$$\theta \mapsto \gamma_q(m\theta)^2$$

$$q = 1$$

Main result

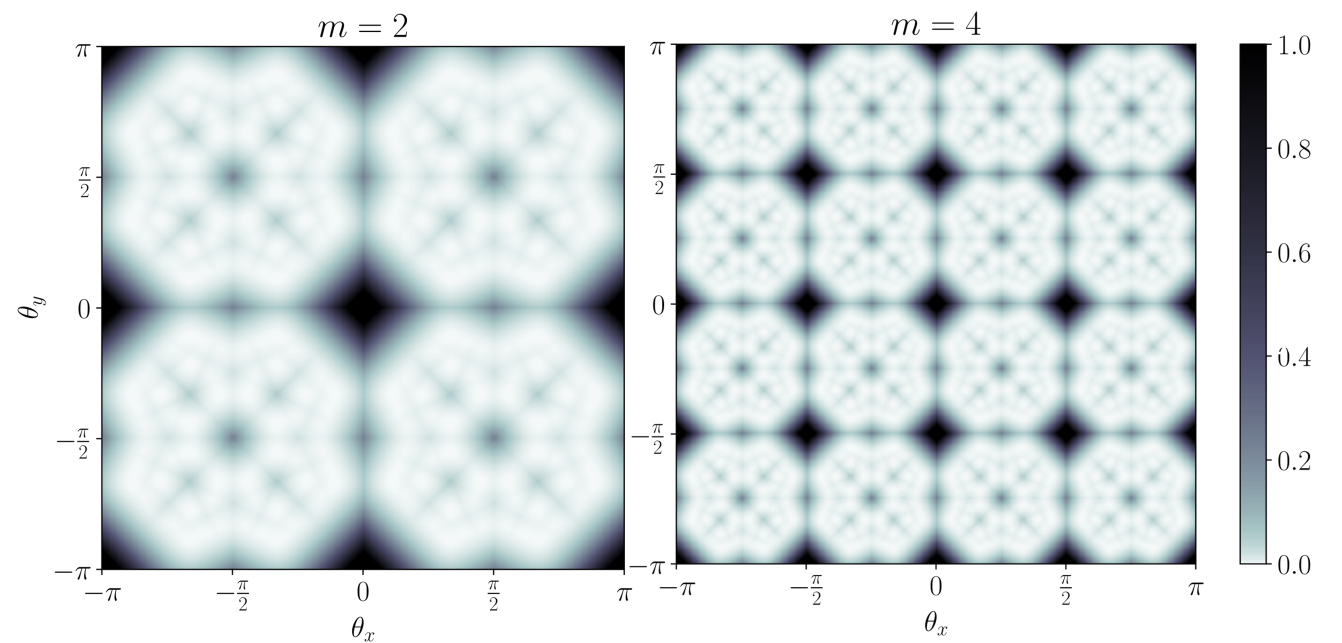
MSE between CMod and RMax output



$$\mathbb{E} \left[\frac{\|Y^{\max} - Y^{\text{mod}}\|_2^2}{\|Y^{\text{mod}}\|_2^2} \right] \leq (\beta_q(m\kappa) + \gamma_q(m\theta))^2$$

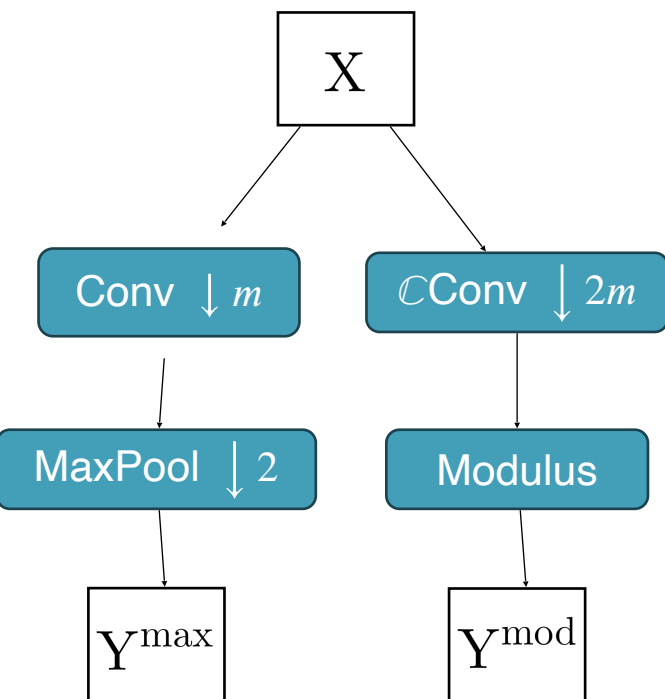
Discrete nature of the max pooling grid

$$\mathbb{E} \left[(1 - G^{\max}(\mathbf{x}_n))^2 \right] \xrightarrow{\theta \mapsto \gamma_q(m\theta)^2} q = 1$$



Main result

MSE between CMod and RMax output

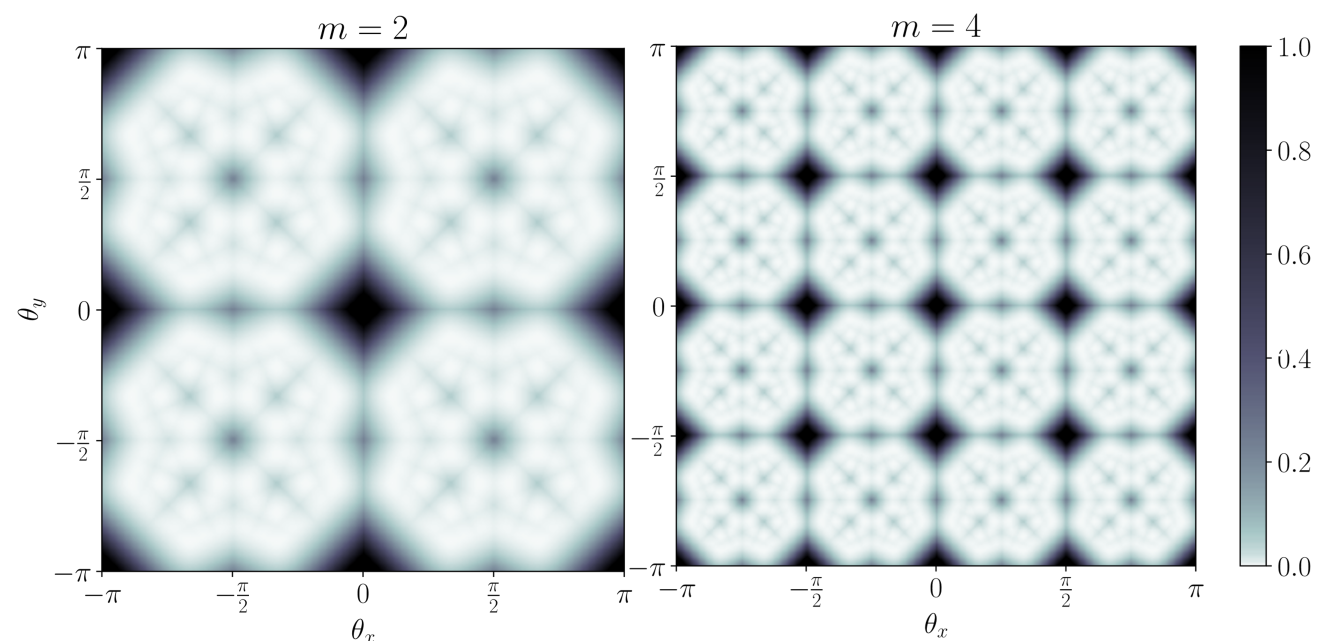


$$\mathbb{E} \left[\frac{\|Y^{\max} - Y^{\text{mod}}\|_2^2}{\|Y^{\text{mod}}\|_2^2} \right] \leq (\beta_q(m\kappa) + \gamma_q(m\theta))^2$$

Discrete nature of the max pooling grid

$$\mathbb{E} \left[(1 - G^{\max}(\mathbf{x}_n))^2 \right] \xrightarrow[q=1]{\theta \mapsto \gamma_q(m\theta)^2}$$

$$\gamma_q(\boldsymbol{\omega}) = \sqrt{\frac{3}{2} + \frac{1}{4\pi} \sum_{i=0}^{n_q-1} \left(\sin \delta H_i^{(q)}(\boldsymbol{\omega}) - 8 \sin \frac{\delta H_i^{(q)}(\boldsymbol{\omega})}{2} \right)}$$



Sketch of the proof

- **Reformulation** of the problem on the unit circle $\mathbb{S}^1 \subset \mathbb{C}$

Sketch of the proof

■ **Reformulation** of the problem on the unit circle $\mathbb{S}^1 \subset \mathbb{C}$

$[z, z']_{\mathbb{S}^1} \subset \mathbb{S}^1$ arc on the unit circle going from z to z'

Sketch of the proof

■ Reformulation of the problem on the unit circle $\mathbb{S}^1 \subset \mathbb{C}$

$[z, z']_{\mathbb{S}^1} \subset \mathbb{S}^1$ arc on the unit circle going from z to z'

$$Z_X : x \mapsto e^{i H_X(x)} \quad \text{and} \quad Z_p : \omega \mapsto e^{i \langle \omega, p \rangle}$$

Sketch of the proof

- **Reformulation** of the problem on the unit circle $\mathbb{S}^1 \subset \mathbb{C}$

$[z, z']_{\mathbb{S}^1} \subset \mathbb{S}^1$ arc on the unit circle going from z to z'

$$Z_X : x \mapsto e^{i H_X(x)} \quad \text{and} \quad Z_p : \omega \mapsto = e^{i \langle \omega, p \rangle}$$

$$\blacksquare G_X(x_n, h_p) = \operatorname{Re}(Z_X^*(x_n) Z_p(m\theta)) \quad \longrightarrow \quad \cos(\langle \nu, h_p \rangle - H(x_n))$$

Sketch of the proof

- **Reformulation** of the problem on the unit circle $\mathbb{S}^1 \subset \mathbb{C}$

$[z, z']_{\mathbb{S}^1} \subset \mathbb{S}^1$ arc on the unit circle going from z to z' $h_p = msp$

$$Z_X : x \mapsto e^{i H_X(x)} \quad \text{and} \quad Z_p : \omega \mapsto e^{i \langle \omega, p \rangle}$$

■ $G_X(x_n, h_p) = \operatorname{Re}(Z_X^*(x_n) Z_p(m\theta)) \quad \longrightarrow \quad \cos(\langle \nu, h_p \rangle - H(x_n))$

Sketch of the proof

- **Reformulation** of the problem on the unit circle $\mathbb{S}^1 \subset \mathbb{C}$

$[z, z']_{\mathbb{S}^1} \subset \mathbb{S}^1$ arc on the unit circle going from z to z' $h_p = msp$

$$Z_X : x \mapsto e^{i H_X(x)} \quad \text{and} \quad Z_p : \omega \mapsto e^{i \langle \omega, p \rangle} \quad \nu = \theta/s$$

■ $G_X(x_n, h_p) = \operatorname{Re}(Z_X^*(x_n) Z_p(m\theta)) \quad \longrightarrow \quad \cos(\langle \nu, h_p \rangle - H(x_n))$

Sketch of the proof

■ Reformulation of the problem on the unit circle $\mathbb{S}^1 \subset \mathbb{C}$

$[z, z']_{\mathbb{S}^1} \subset \mathbb{S}^1$ arc on the unit circle going from z to z' $h_p = msp$

$$Z_X : x \mapsto e^{i H_X(x)} \quad \text{and} \quad Z_p : \omega \mapsto e^{i \langle \omega, p \rangle} \quad \nu = \theta/s$$

- $G_X(x_n, h_p) = \operatorname{Re}(Z_X^*(x_n) Z_p(m\theta)) \rightarrow \cos(\langle \nu, h_p \rangle - H(x_n))$
- Sort $\{Z_p(\omega)\}_{p \in \{-q..q\}^2} \rightarrow (Z_i^{(q)}(\omega))_{i \in \{0..n_q-1\}}$ $n_q := (2q + 1)^2$

Sketch of the proof

■ Reformulation of the problem on the unit circle $\mathbb{S}^1 \subset \mathbb{C}$

$[z, z']_{\mathbb{S}^1} \subset \mathbb{S}^1$ arc on the unit circle going from z to z' $h_p = msp$

$$Z_X : x \mapsto e^{i H_X(x)} \quad \text{and} \quad Z_p : \omega \mapsto e^{i \langle \omega, p \rangle} \quad \nu = \theta/s$$

- $G_X(x_n, h_p) = \operatorname{Re}(Z_X^*(x_n) Z_p(m\theta)) \rightarrow \cos(\langle \nu, h_p \rangle - H(x_n))$
- Sort $\{Z_p(\omega)\}_{p \in \{-q..q\}^2} \rightarrow (Z_i^{(q)}(\omega))_{i \in \{0..n_q-1\}}$ $n_q := (2q + 1)^2$

in ascending order of their argument:

$$0 = H_0^{(q)}(\omega) \leq \dots \leq H_{n_q-1}^{(q)}(\omega) < 2\pi$$

Sketch of the proof

■ Reformulation of the problem on the unit circle $\mathbb{S}^1 \subset \mathbb{C}$

$[z, z']_{\mathbb{S}^1} \subset \mathbb{S}^1$ arc on the unit circle going from z to z' $h_p = msp$

$$Z_X : x \mapsto e^{i H_X(x)} \quad \text{and} \quad Z_p : \omega \mapsto e^{i \langle \omega, p \rangle} \quad \nu = \theta/s$$

- $G_X(x_n, h_p) = \operatorname{Re}(Z_X^*(x_n) Z_p(m\theta)) \rightarrow \cos(\langle \nu, h_p \rangle - H(x_n))$
- Sort $\{Z_p(\omega)\}_{p \in \{-q..q\}^2} \rightarrow (Z_i^{(q)}(\omega))_{i \in \{0..n_q-1\}}$ $n_q := (2q+1)^2$

in ascending order of their argument:

$$0 = H_0^{(q)}(\omega) \leq \dots \leq H_{n_q-1}^{(q)}(\omega) < 2\pi$$

$$H_{n_q}^{(q)}(\omega) := 2\pi$$

$$Z_{n_q}^{(q)}(\omega) := 1$$

Sketch of the proof

■ Reformulation of the problem on the unit circle $\mathbb{S}^1 \subset \mathbb{C}$

$[z, z']_{\mathbb{S}^1} \subset \mathbb{S}^1$ arc on the unit circle going from z to z' $h_p = msp$

$$Z_X : x \mapsto e^{i H_X(x)} \quad \text{and} \quad Z_p : \omega \mapsto e^{i \langle \omega, p \rangle} \quad \nu = \theta/s$$

- $G_X(x_n, h_p) = \operatorname{Re}(Z_X^*(x_n) Z_p(m\theta)) \rightarrow \cos(\langle \nu, h_p \rangle - H(x_n))$
- Sort $\{Z_p(\omega)\}_{p \in \{-q..q\}^2} \rightarrow (Z_i^{(q)}(\omega))_{i \in \{0..n_q-1\}}$ $n_q := (2q+1)^2$

in ascending order of their argument:

$$H_{n_q}^{(q)}(\omega) := 2\pi$$

$$0 = H_0^{(q)}(\omega) \leq \dots \leq H_{n_q-1}^{(q)}(\omega) < 2\pi$$

$$Z_{n_q}^{(q)}(\omega) := 1$$

- Split \mathbb{S}^1 into n_q arcs delimited by the $Z_i^{(q)}(\omega)$

$$\mathfrak{A}_i^{(q)}(\omega) := \begin{cases} [Z_i^{(q)}(\omega), Z_{i+1}^{(q)}(\omega)]_{\mathbb{S}^1} & \text{if } H_{i+1}^{(q)}(\omega) - H_i^{(q)}(\omega) < 2\pi; \\ \mathbb{S}^1 & \text{otherwise.} \end{cases}$$

Sketch of the proof

■ Reformulation of the problem on the unit circle $\mathbb{S}^1 \subset \mathbb{C}$

$[z, z']_{\mathbb{S}^1} \subset \mathbb{S}^1$ arc on the unit circle going from z to z' $h_p = msp$

$$Z_X : x \mapsto e^{i H_X(x)} \quad \text{and} \quad Z_p : \omega \mapsto e^{i \langle \omega, p \rangle} \quad \nu = \theta/s$$

- $G_X(x_n, h_p) = \operatorname{Re}(Z_X^*(x_n) Z_p(m\theta)) \rightarrow \cos(\langle \nu, h_p \rangle - H(x_n))$
- Sort $\{Z_p(\omega)\}_{p \in \{-q..q\}^2} \rightarrow (Z_i^{(q)}(\omega))_{i \in \{0..n_q-1\}}$ $n_q := (2q+1)^2$

in ascending order of their argument:

$$H_{n_q}^{(q)}(\omega) := 2\pi$$

$$0 = H_0^{(q)}(\omega) \leq \dots \leq H_{n_q-1}^{(q)}(\omega) < 2\pi$$

$$Z_{n_q}^{(q)}(\omega) := 1$$

- Split \mathbb{S}^1 into n_q arcs delimited by the $Z_i^{(q)}(\omega)$

$$\mathfrak{A}_i^{(q)}(\omega) := \begin{cases} [Z_i^{(q)}(\omega), Z_{i+1}^{(q)}(\omega)]_{\mathbb{S}^1} & \text{if } H_{i+1}^{(q)}(\omega) - H_i^{(q)}(\omega) < 2\pi; \\ \mathbb{S}^1 & \text{otherwise.} \end{cases}$$

$$\delta H_i^{(q)}(\omega)$$

Sketch of the proof

■ Reformulation of the problem on the unit circle $\mathbb{S}^1 \subset \mathbb{C}$

$[z, z']_{\mathbb{S}^1} \subset \mathbb{S}^1$ arc on the unit circle going from z to z' $h_p = msp$

$Z_X : x \mapsto e^{i H_X(x)}$ and $Z_p : \omega \mapsto e^{i \langle \omega, p \rangle}$ $\nu = \theta/s$

■ $G_X(x_n, h_p) = \operatorname{Re}(Z_X^*(x_n) Z_p(m\theta)) \quad \rightarrow \quad \cos(\langle \nu, h_p \rangle - H(x_n))$

Sketch of the proof

■ Reformulation of the problem on the unit circle $\mathbb{S}^1 \subset \mathbb{C}$

$[z, z']_{\mathbb{S}^1} \subset \mathbb{S}^1$ arc on the unit circle going from z to z' $h_p = msp$

$$Z_X : x \mapsto e^{i H_X(x)} \quad \text{and} \quad Z_p : \omega \mapsto e^{i \langle \omega, p \rangle} \quad \nu = \theta/s$$

- $G_X(x_n, h_p) = \operatorname{Re}(Z_X^*(x_n) Z_p(m\theta)) \quad \longrightarrow \quad \cos(\langle \nu, h_p \rangle - H(x_n))$
- $G_X^{\max}(x) = g_{\max}(Z_X(x)) \quad \longrightarrow \quad g_{\max} : z \mapsto \max_{\|p\|_\infty \leq q} \operatorname{Re}(z^* Z_p)$

Sketch of the proof

■ Reformulation of the problem on the unit circle $\mathbb{S}^1 \subset \mathbb{C}$

$[z, z']_{\mathbb{S}^1} \subset \mathbb{S}^1$ arc on the unit circle going from z to z' $h_p = msp$

$$Z_X : x \mapsto e^{i H_X(x)} \quad \text{and} \quad Z_p : \omega \mapsto e^{i \langle \omega, p \rangle} \quad \nu = \theta/s$$

- $G_X(x_n, h_p) = \operatorname{Re}(Z_X^*(x_n) Z_p(m\theta)) \rightarrow \cos(\langle \nu, h_p \rangle - H(x_n))$
- $G_X^{\max}(x) = g_{\max}(Z_X(x)) \rightarrow g_{\max} : z \mapsto \max_{\|p\|_\infty \leq q} \operatorname{Re}(z^* Z_p)$
- $Z_X(x)$ uniformly distributed on the unit circle (Hypothesis)

Sketch of the proof

■ Reformulation of the problem on the unit circle $\mathbb{S}^1 \subset \mathbb{C}$

$[z, z']_{\mathbb{S}^1} \subset \mathbb{S}^1$ arc on the unit circle going from z to z' $h_p = msp$

$$Z_X : x \mapsto e^{i H_X(x)} \quad \text{and} \quad Z_p : \omega \mapsto e^{i \langle \omega, p \rangle} \quad \nu = \theta/s$$

- $G_X(x_n, h_p) = \operatorname{Re}(Z_X^*(x_n) Z_p(m\theta)) \rightarrow \cos(\langle \nu, h_p \rangle - H(x_n))$
- $G_X^{\max}(x) = g_{\max}(Z_X(x)) \rightarrow g_{\max} : z \mapsto \max_{\|p\|_\infty \leq q} \operatorname{Re}(z^* Z_p)$
- $Z_X(x)$ uniformly distributed on the unit circle (Hypothesis)
- The p-th moment is given by

$$\mathbb{E}[G_X^{\max}(x)^p] = \frac{1}{2\pi} \int_{\mathbb{S}^1} g_{\max}(z)^p d\vartheta(z) = \frac{1}{2\pi} \sum_{i=0}^{n_q-1} \int_{\mathfrak{A}_i^{(q)}} g_{\max}(z)^p d\vartheta(z).$$

Sketch of the proof

■ Reformulation of the problem on the unit circle $\mathbb{S}^1 \subset \mathbb{C}$

$[z, z']_{\mathbb{S}^1} \subset \mathbb{S}^1$ arc on the unit circle going from z to z' $h_p = msp$

$$Z_X : x \mapsto e^{i H_X(x)} \quad \text{and} \quad Z_p : \omega \mapsto e^{i \langle \omega, p \rangle} \quad \nu = \theta/s$$

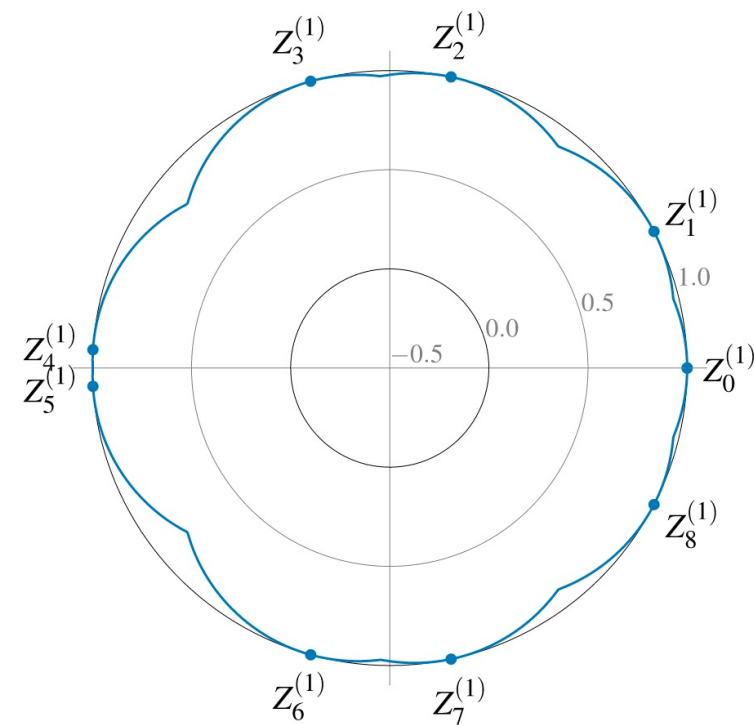
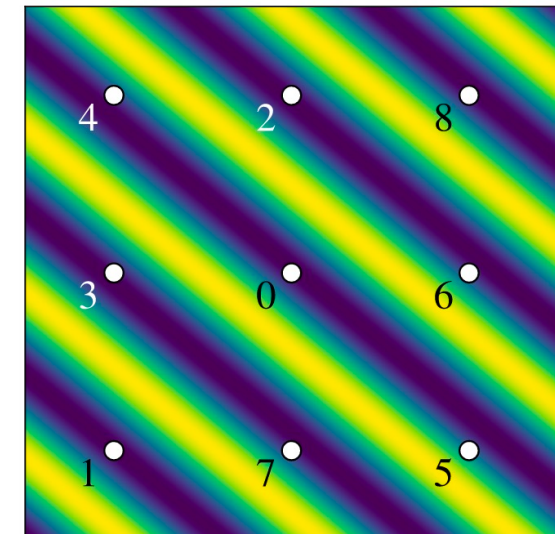
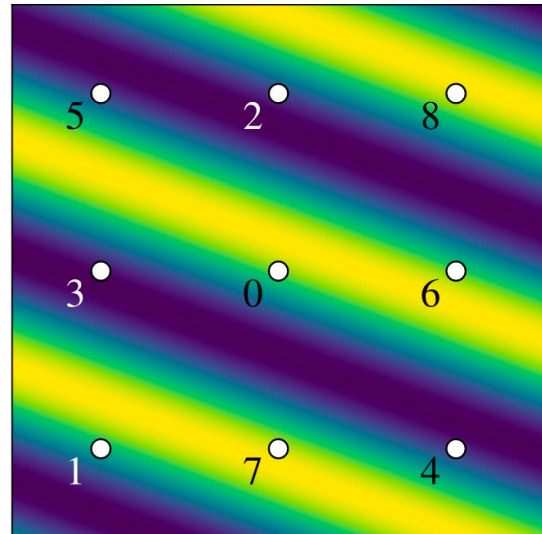
- $G_X(x_n, h_p) = \operatorname{Re}(Z_X^*(x_n) Z_p(m\theta)) \rightarrow \cos(\langle \nu, h_p \rangle - H(x_n))$
- $G_X^{\max}(x) = g_{\max}(Z_X(x)) \rightarrow g_{\max} : z \mapsto \max_{\|p\|_\infty \leq q} \operatorname{Re}(z^* Z_p)$
- $Z_X(x)$ uniformly distributed on the unit circle (Hypothesis)
- The p-th moment is given by

$$\mathbb{E}[G_X^{\max}(x)^p] = \frac{1}{2\pi} \int_{\mathbb{S}^1} g_{\max}(z)^p d\vartheta(z) = \frac{1}{2\pi} \sum_{i=0}^{n_q-1} \int_{\mathfrak{A}_i^{(q)}} g_{\max}(z)^p d\vartheta(z).$$

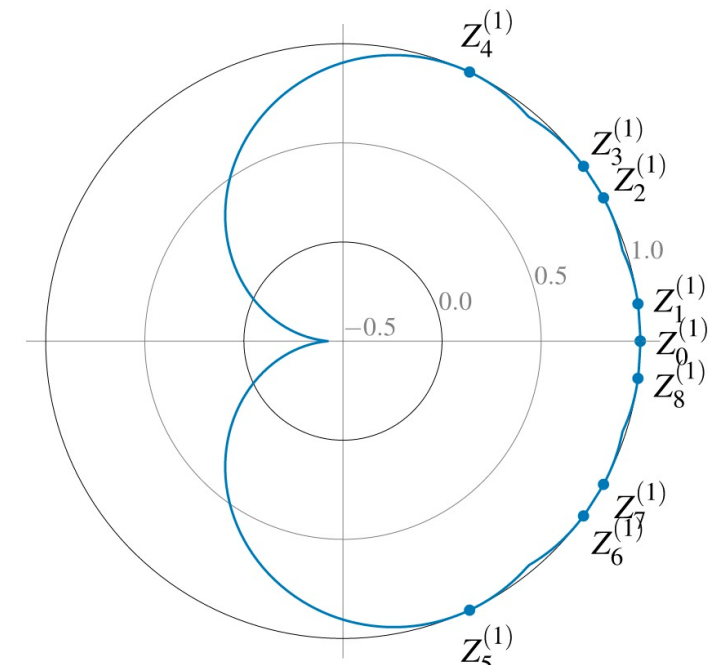
- $\forall z \in \mathfrak{A}_i^{(q)}, g_{\max}(z) = \max(\operatorname{Re}(z^* Z_i^{(q)}), \operatorname{Re}(z^* Z_{i+1}^{(q)}))$

Sketch of the proof

$$g_{\max} : z \mapsto \max_{\|p\|_\infty \leq q} \operatorname{Re}(z^* Z_p)$$



(a) General case



(b) Pathological case

Sketch of the proof

■ Reformulation of the problem on the unit circle $\mathbb{S}^1 \subset \mathbb{C}$

- $\forall z \in \mathfrak{A}_i^{(q)}, g_{\max}(z) = \max \left(\operatorname{Re}(z^* Z_i^{(q)}), \operatorname{Re}(z^* Z_{i+1}^{(q)}) \right)$

Sketch of the proof

■ Reformulation of the problem on the unit circle $\mathbb{S}^1 \subset \mathbb{C}$

- $\forall z \in \mathfrak{A}_i^{(q)}, g_{\max}(z) = \max \left(\operatorname{Re}(z^* Z_i^{(q)}), \operatorname{Re}(z^* Z_{i+1}^{(q)}) \right)$
- $\forall z \in \overline{\mathfrak{A}}_i^{(q)}, g_{\max}(z) = \operatorname{Re}(z^* Z_i^{(q)})$

Sketch of the proof

■ Reformulation of the problem on the unit circle $\mathbb{S}^1 \subset \mathbb{C}$

- $\forall z \in \mathfrak{A}_i^{(q)}, g_{\max}(z) = \max \left(\operatorname{Re}(z^* Z_i^{(q)}), \operatorname{Re}(z^* Z_{i+1}^{(q)}) \right)$
- $\forall z \in \overline{\mathfrak{A}}_i^{(q)}, g_{\max}(z) = \operatorname{Re}(z^* Z_i^{(q)})$

$$\begin{aligned}\int_{\mathfrak{A}_i^{(q)}} g_{\max}(z)^p d\vartheta(z) &= 2 \int_{\overline{\mathfrak{A}}_i^{(q)}} \operatorname{Re}(z^* Z_i^{(q)})^p d\vartheta(z) \\ &= 2 \int_{H_i^{(q)}}^{\overline{H}_i^{(q)}} \cos^p(\eta - H_i^{(q)}) d\eta \\ &= 2 \int_0^{\delta H_i^{(q)}/2} \cos^p \eta' d\eta'\end{aligned}$$

Sketch of the proof

■ Reformulation of the problem on the unit circle $\mathbb{S}^1 \subset \mathbb{C}$

- $\forall z \in \mathfrak{A}_i^{(q)}, g_{\max}(z) = \max \left(\operatorname{Re}(z^* Z_i^{(q)}), \operatorname{Re}(z^* Z_{i+1}^{(q)}) \right)$
- $\forall z \in \overline{\mathfrak{A}}_i^{(q)}, g_{\max}(z) = \operatorname{Re}(z^* Z_i^{(q)})$

$$\begin{aligned}\int_{\mathfrak{A}_i^{(q)}} g_{\max}(z)^p d\vartheta(z) &= 2 \int_{\overline{\mathfrak{A}}_i^{(q)}} \operatorname{Re}(z^* Z_i^{(q)})^p d\vartheta(z) && z \leftarrow e^{i\eta} \\ &= 2 \int_{H_i^{(q)}}^{\overline{H}_i^{(q)}} \cos^p(\eta - H_i^{(q)}) d\eta \\ &= 2 \int_0^{\delta H_i^{(q)}/2} \cos^p \eta' d\eta'\end{aligned}$$

Sketch of the proof

■ Reformulation of the problem on the unit circle $\mathbb{S}^1 \subset \mathbb{C}$

- $\forall z \in \mathfrak{A}_i^{(q)}, g_{\max}(z) = \max \left(\operatorname{Re}(z^* Z_i^{(q)}), \operatorname{Re}(z^* Z_{i+1}^{(q)}) \right)$
- $\forall z \in \overline{\mathfrak{A}}_i^{(q)}, g_{\max}(z) = \operatorname{Re}(z^* Z_i^{(q)})$

$$\begin{aligned}\int_{\mathfrak{A}_i^{(q)}} g_{\max}(z)^p d\vartheta(z) &= 2 \int_{\overline{\mathfrak{A}}_i^{(q)}} \operatorname{Re}(z^* Z_i^{(q)})^p d\vartheta(z) && z \leftarrow e^{i\eta} \\ &= 2 \int_{H_i^{(q)}}^{\overline{H}_i^{(q)}} \cos^p(\eta - H_i^{(q)}) d\eta && \overline{H}_i^{(q)} := (H_i^{(q)} + H_{i+1}^{(q)})/2 \\ &= 2 \int_0^{\delta H_i^{(q)}/2} \cos^p \eta' d\eta'\end{aligned}$$

Sketch of the proof

■ Reformulation of the problem on the unit circle $\mathbb{S}^1 \subset \mathbb{C}$

- $\forall z \in \mathfrak{A}_i^{(q)}, g_{\max}(z) = \max \left(\operatorname{Re}(z^* Z_i^{(q)}), \operatorname{Re}(z^* Z_{i+1}^{(q)}) \right)$
- $\forall z \in \overline{\mathfrak{A}}_i^{(q)}, g_{\max}(z) = \operatorname{Re}(z^* Z_i^{(q)})$

$$\begin{aligned} \int_{\mathfrak{A}_i^{(q)}} g_{\max}(z)^p d\vartheta(z) &= 2 \int_{\overline{\mathfrak{A}}_i^{(q)}} \operatorname{Re}(z^* Z_i^{(q)})^p d\vartheta(z) && z \leftarrow e^{i\eta} \\ &= 2 \int_{H_i^{(q)}}^{\overline{H}_i^{(q)}} \cos^p(\eta - H_i^{(q)}) d\eta && \overline{H}_i^{(q)} := (H_i^{(q)} + H_{i+1}^{(q)})/2 \\ &= 2 \int_0^{\delta H_i^{(q)}/2} \cos^p \eta' d\eta' && \eta' \leftarrow \eta - H_i^{(q)} \end{aligned}$$

Sketch of the proof

Sketch of the proof

- $\mathbb{E} [\mathbf{G}_X^{\max}(\mathbf{x})] = \frac{1}{\pi} \sum_{i=0}^{n_q-1} \sin \frac{\delta H_i^{(q)}}{2};$
- $\mathbb{E} [\mathbf{G}_X^{\max}(\mathbf{x})^2] = \frac{1}{2} + \frac{1}{4\pi} \sum_{i=0}^{n_q-1} \sin \delta H_i^{(q)}.$

Sketch of the proof

- $\mathbb{E} [G_X^{\max}(\boldsymbol{x})] = \frac{1}{\pi} \sum_{i=0}^{n_q-1} \sin \frac{\delta H_i^{(q)}}{2};$
- $\mathbb{E} [G_X^{\max}(\boldsymbol{x})^2] = \frac{1}{2} + \frac{1}{4\pi} \sum_{i=0}^{n_q-1} \sin \delta H_i^{(q)}.$
- $Q_X := 1 - G_X^{\max}$

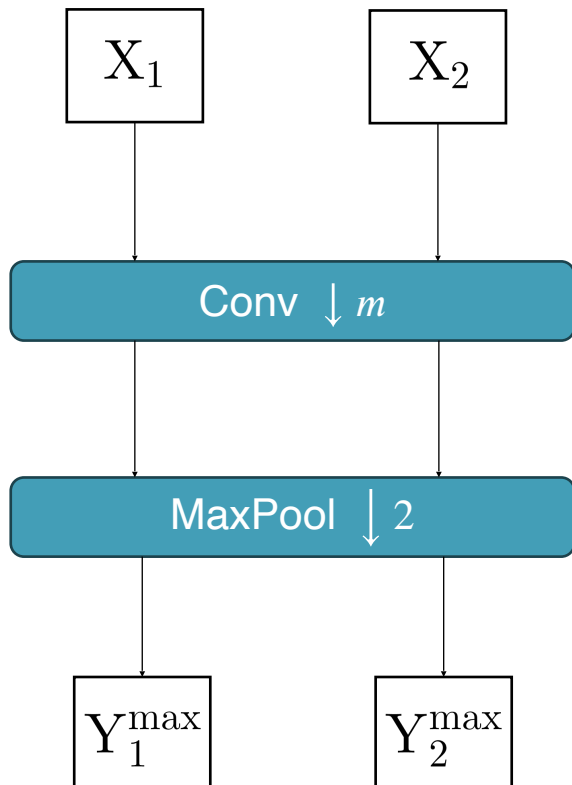
Sketch of the proof

- $\mathbb{E} [G_X^{\max}(\mathbf{x})] = \frac{1}{\pi} \sum_{i=0}^{n_q-1} \sin \frac{\delta H_i^{(q)}}{2};$
- $\mathbb{E} [G_X^{\max}(\mathbf{x})^2] = \frac{1}{2} + \frac{1}{4\pi} \sum_{i=0}^{n_q-1} \sin \delta H_i^{(q)}.$
- $Q_X := 1 - G_X^{\max}$
- By linearity of the expected value

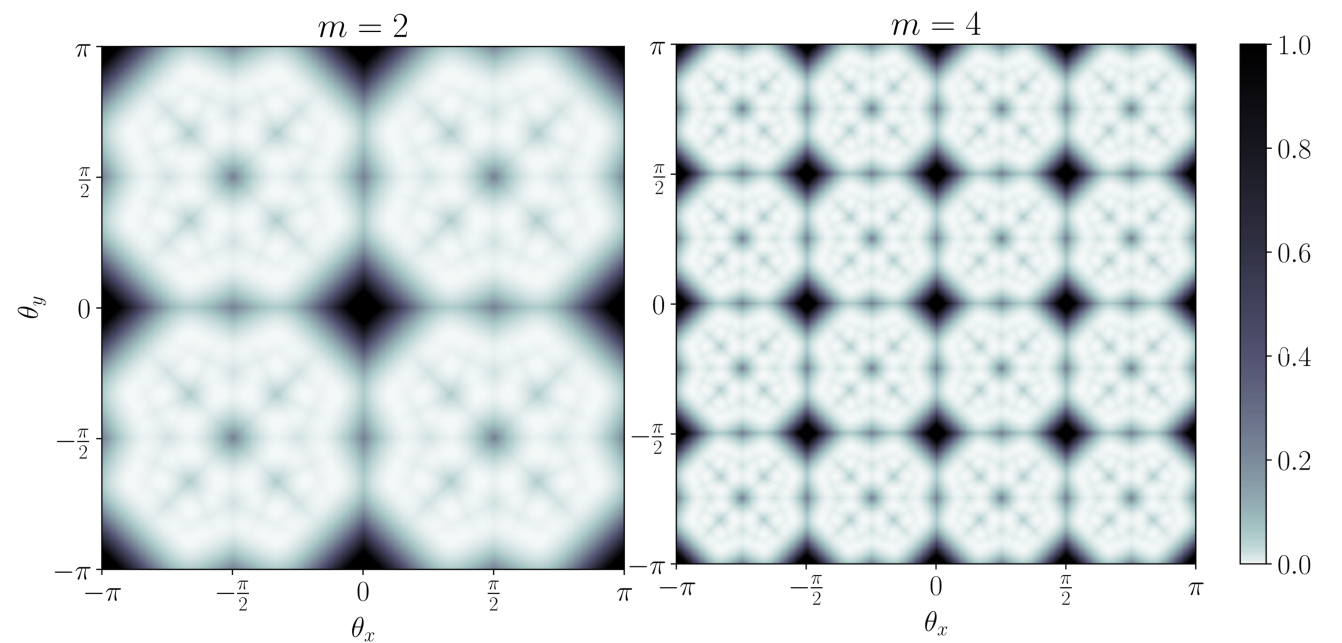
$$\mathbb{E} [Q_X(\mathbf{x})^2] := \frac{3}{2} + \frac{1}{4\pi} \sum_{i=0}^{n_q-1} \left(\sin \delta H_i^{(q)} - 8 \sin \frac{\delta H_i^{(q)}}{2} \right)$$

Main result

- MSE between CMod and RMax output

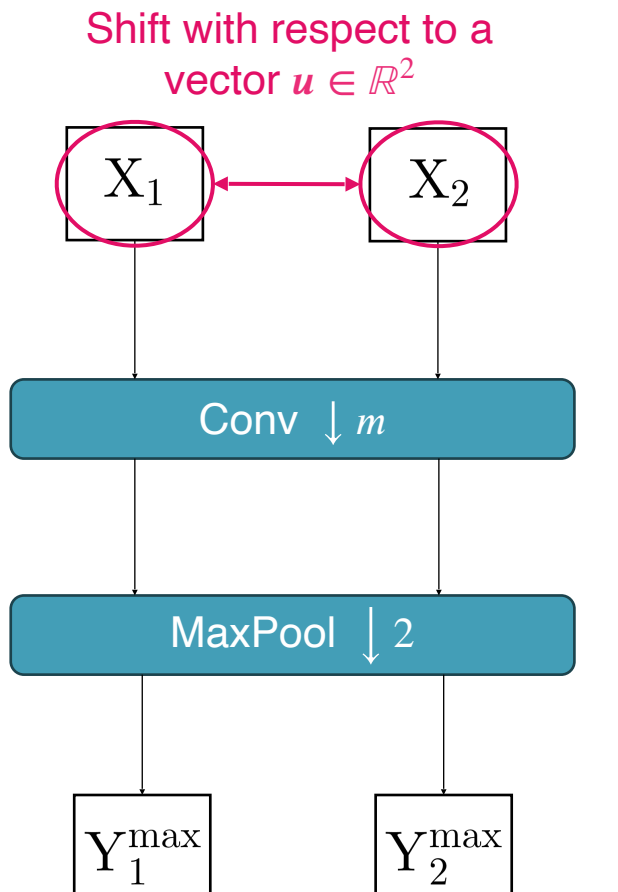


$$\boldsymbol{\theta} \mapsto \gamma_q (m\boldsymbol{\theta})^2$$
$$q = 1$$

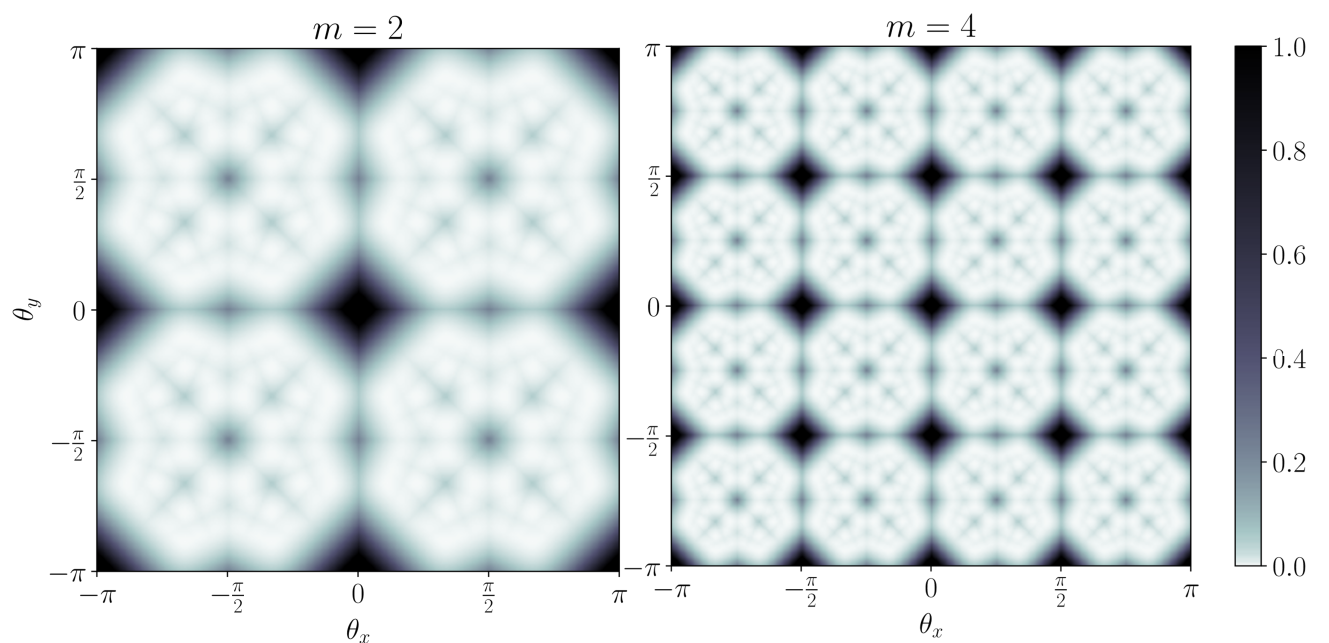


Main result

MSE between CMod and RMax output

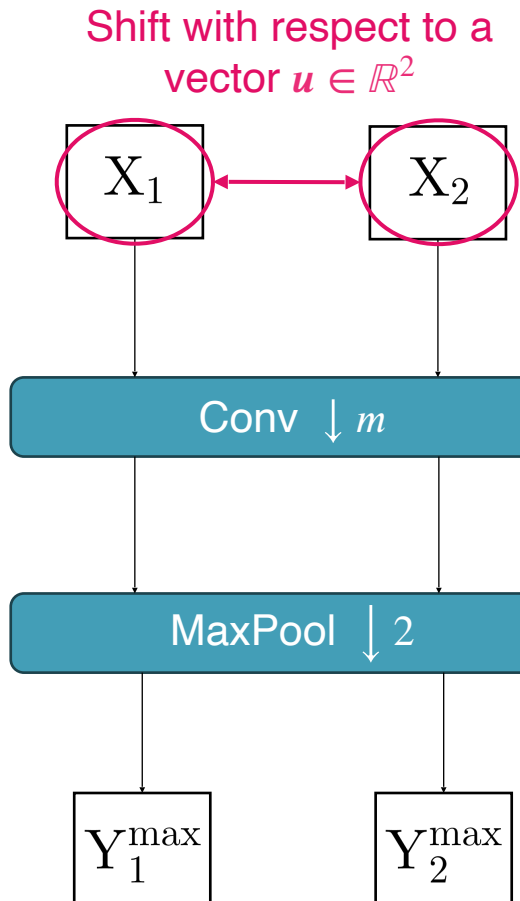


$$\theta \mapsto \gamma_q (m\theta)^2$$
$$q = 1$$



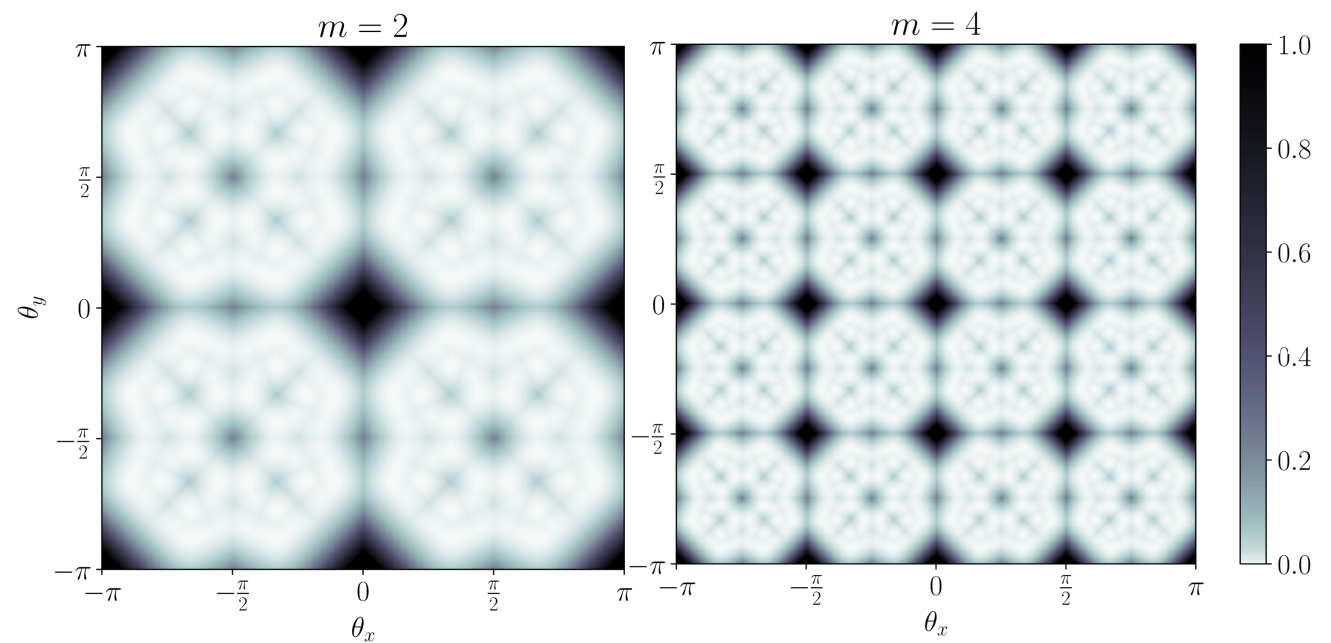
Main result

MSE between CMod and RMax output



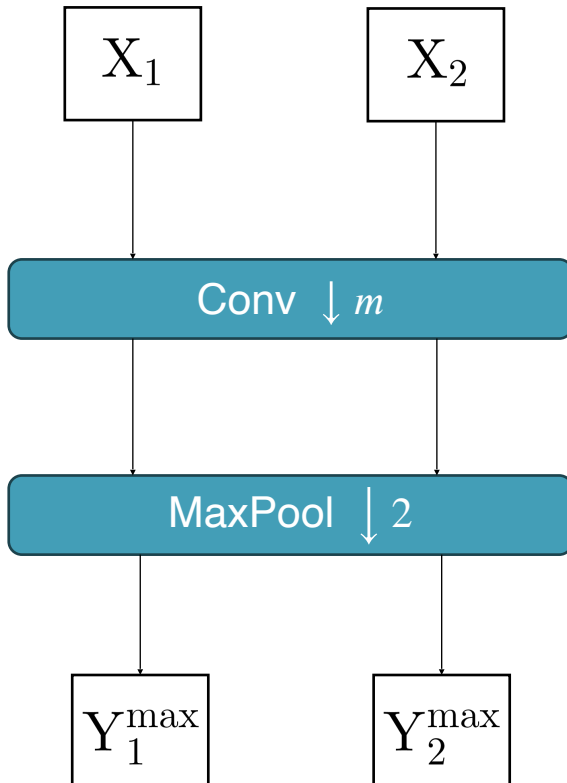
$$\mathbb{E} \left[\frac{\|\mathbf{Y}_1^{\max} - \mathbf{Y}_2^{\max}\|_2}{\|\mathbf{Y}_1^{\text{mod}}\|_2} \right] \leq 2(\beta_q(m\kappa) + \gamma_q(m\theta)) + \alpha(\kappa u)$$

$$\theta \mapsto \gamma_q(m\theta)^2$$
$$q = 1$$



Main result

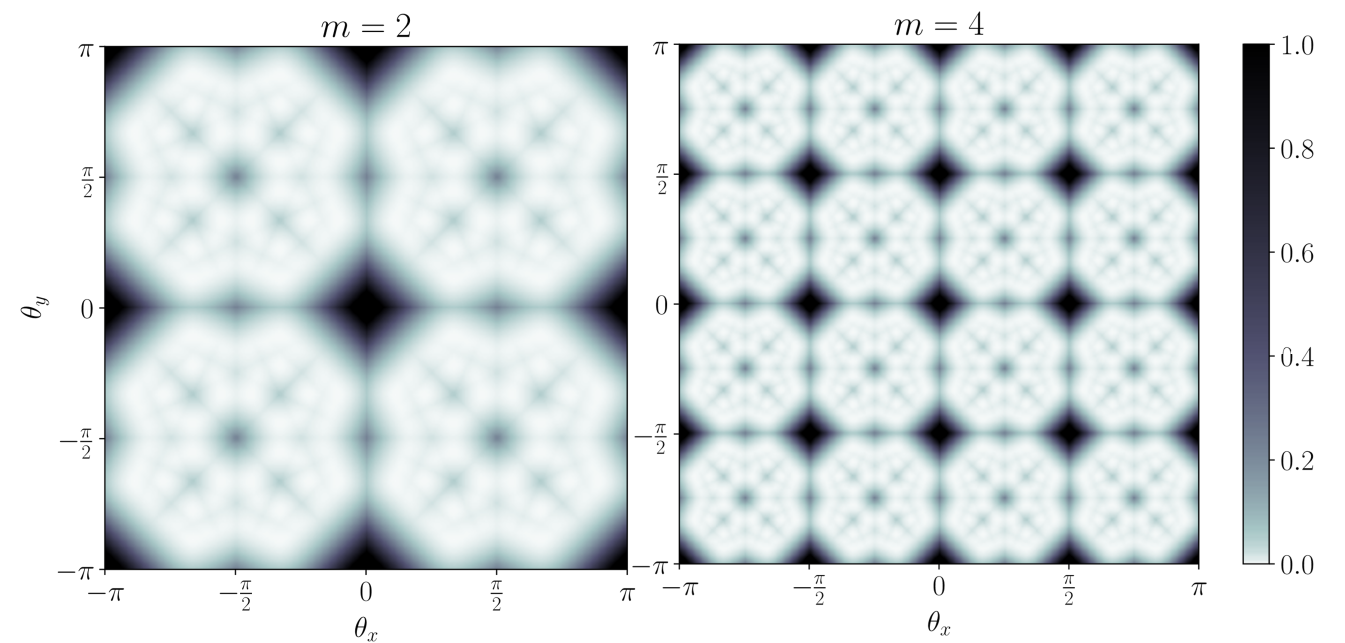
MSE between CMod and RMax output



$$\mathbb{E} \left[\frac{\|\mathbf{Y}_1^{\max} - \mathbf{Y}_2^{\max}\|_2}{\|\mathbf{Y}_1^{\text{mod}}\|_2} \right] \leq 2(\beta_q(m\kappa) + \gamma_q(m\theta)) + \alpha(\kappa u)$$

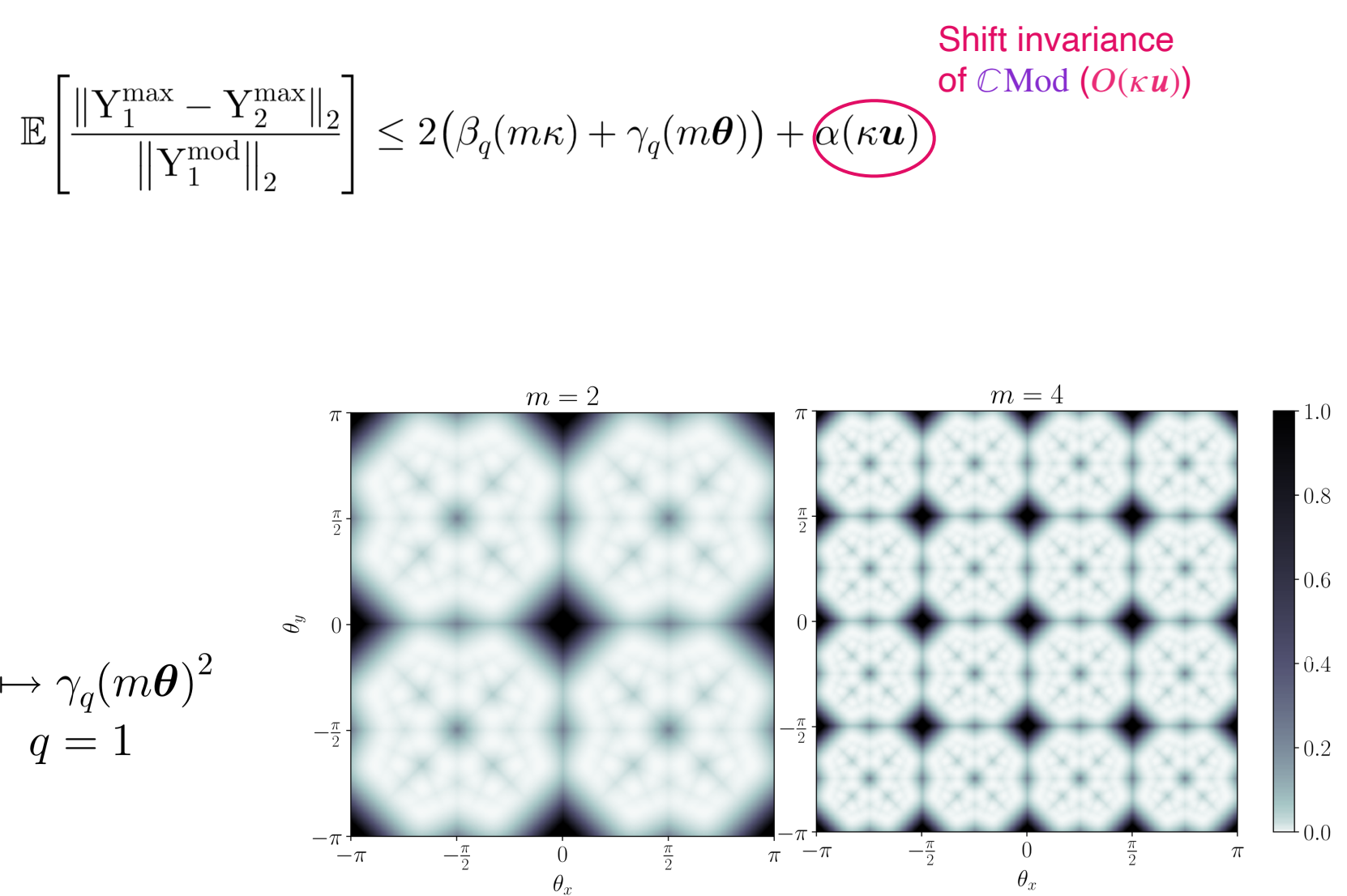
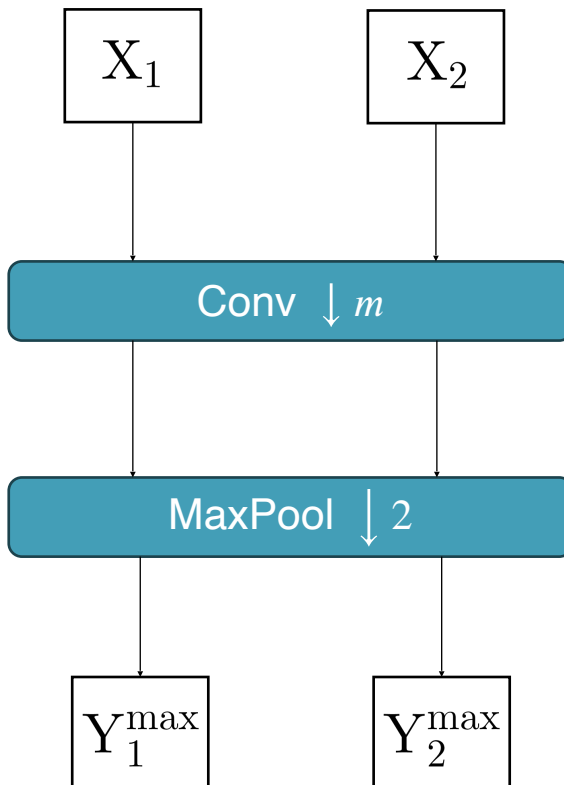
Divergence RMax-CMod

$$\theta \mapsto \gamma_q(m\theta)^2$$
$$q = 1$$



Main result

MSE between $\mathcal{C}\text{Mod}$ and $\mathcal{R}\text{Max}$ output



Experimental validation

Experimental validation

■ What we need:

Experimental validation

■ What we need:

- A fully deterministic model with predefined convolution kernels

Experimental validation

■ What we need:

- A fully deterministic model with predefined convolution kernels
- A set of **Gabor-like filters** tiling the entire frequency plane and a unique bandwidth share across all filters

Experimental validation

■ What we need:

- A fully deterministic model with predefined convolution kernels
- A set of **Gabor-like filters** tiling the entire frequency plane and a unique bandwidth share across all filters
- No prediction, only the first layers are implemented

Experimental validation

■ What we need:

- A fully deterministic model with predefined convolution kernels
- A set of **Gabor-like filters** tiling the entire frequency plane and a unique bandwidth share across all filters
- No prediction, only the first layers are implemented
- Dataset: **ImageNet-1K**, validation set (50 000 images)

Experimental validation

■ What we need:

- A fully deterministic model with predefined convolution kernels
- A set of **Gabor-like filters** tiling the entire frequency plane and a unique bandwidth share across all filters
- No prediction, only the first layers are implemented
- Dataset: **ImageNet-1K**, validation set (50 000 images)

■ Proposed solution:

Experimental validation

■ What we need:

- A fully deterministic model with predefined convolution kernels
- A set of **Gabor-like filters** tiling the entire frequency plane and a unique bandwidth share across all filters
- No prediction, only the first layers are implemented
- Dataset: **ImageNet-1K**, validation set (50 000 images)

■ Proposed solution:

- The **dual-tree complex wavelet packet transform** (DT-CWPT)

Experimental validation

■ What we need:

- A fully deterministic model with predefined convolution kernels
- A set of **Gabor-like filters** tiling the entire frequency plane and a unique bandwidth share across all filters
- No prediction, only the first layers are implemented
- Dataset: **ImageNet-1K**, validation set (50 000 images)

■ Proposed solution:

- The **dual-tree complex wavelet packet transform** (DT-CWPT)

I. Bayram and I. W. Selesnick, "On the Dual-Tree Complex Wavelet Packet and M-Band Transforms," IEEE TSP, 2008.

Experimental validation

■ What we need:

- A fully deterministic model with predefined convolution kernels
- A set of **Gabor-like filters** tiling the entire frequency plane and a unique bandwidth share across all filters
- No prediction, only the first layers are implemented
- Dataset: **ImageNet-1K**, validation set (50 000 images)

■ Proposed solution:

- The **dual-tree complex wavelet packet transform** (DT-CWPT)
- The bandwidth and subsampling are controlled by the depth J

I. Bayram and I. W. Selesnick, "On the Dual-Tree Complex Wavelet Packet and M-Band Transforms," IEEE TSP, 2008.

Experiments

■ Filters generated by the DT-CWPT

Case $J = 2$ (two levels of dual-tree decomposition):

$\kappa = \pi/2$;

$m = 2$;

32 filters + complex conjugates.

Experiments

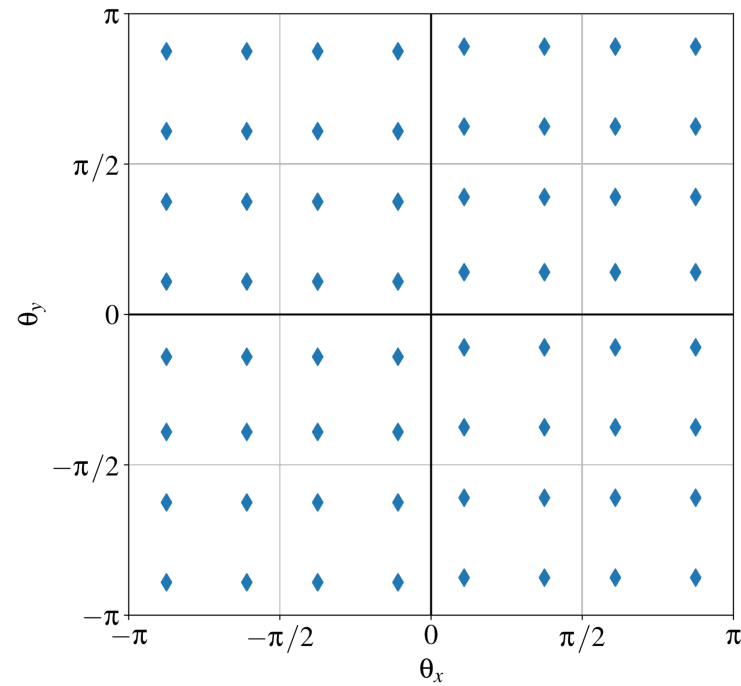
■ Filters generated by the DT-CWPT

Case $J = 2$ (two levels of dual-tree decomposition):

$$\kappa = \pi/2;$$

$$m = 2;$$

32 filters + complex conjugates.



Experiments

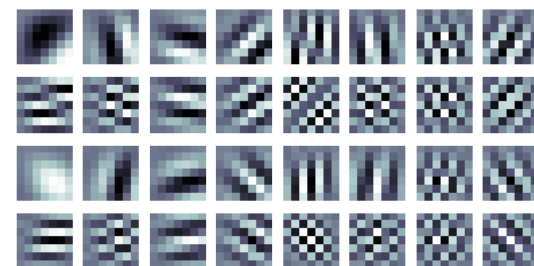
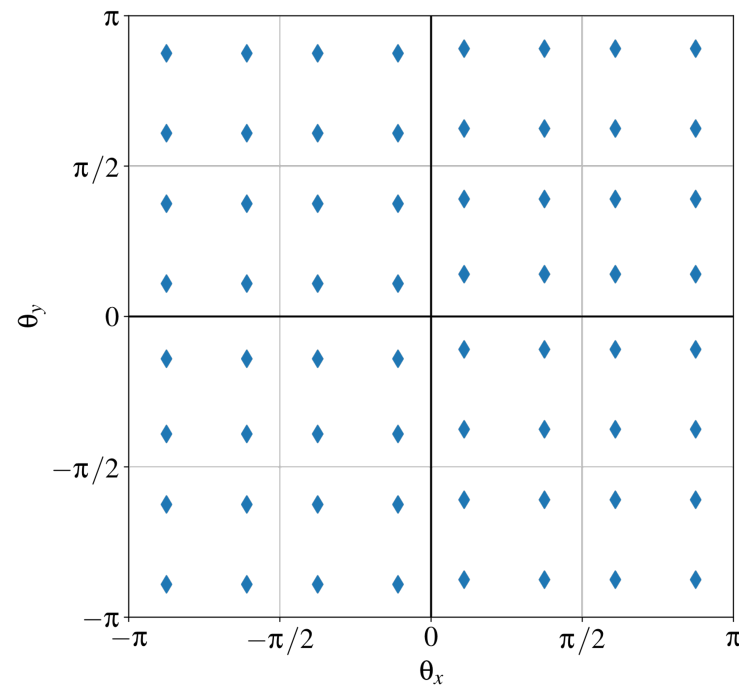
Filters generated by the DT-CWPT

Case $J = 2$ (two levels of dual-tree decomposition):

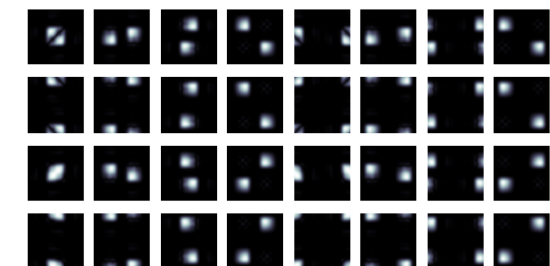
$$\kappa = \pi/2;$$

$$m = 2;$$

32 filters + complex conjugates.



Spatial domain



Fourier domain

DT- \mathcal{C} WPT
(real part only)

Experiments

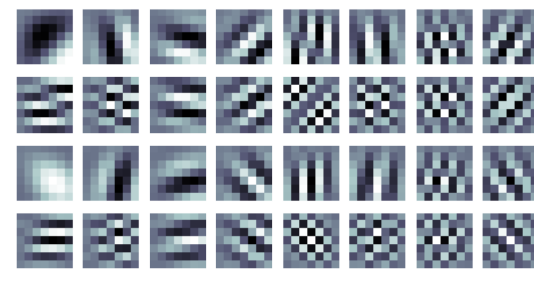
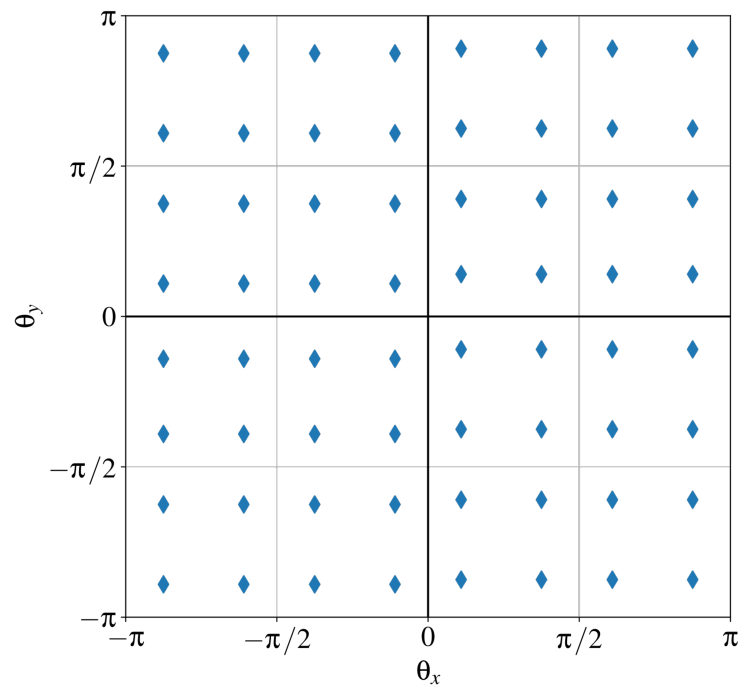
Filters generated by the DT-CWPT

Case $J = 2$ (two levels of dual-tree decomposition):

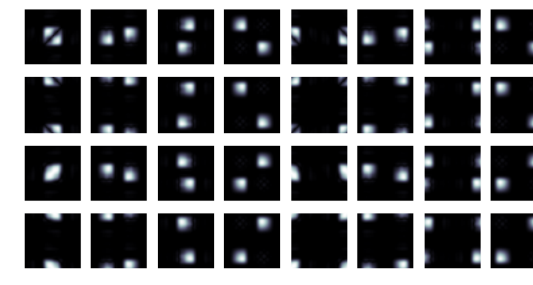
$$\kappa = \pi/2;$$

$$m = 2;$$

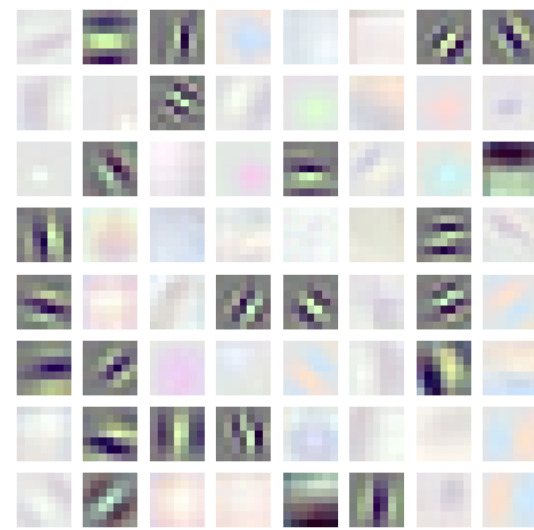
32 filters + complex conjugates.



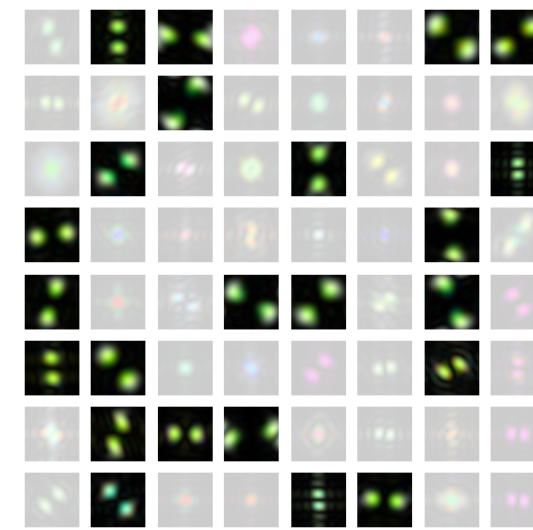
Spatial domain



Fourier domain



DT-CWPT
(real part only)



ResNet-34

Experiments

■ Filters generated by the DT-CWPT

Case $J = 3$ (three levels of dual-tree decomposition):

$\kappa = \pi/4$;

$m = 4$;

128 filters + complex conjugates.

Experiments

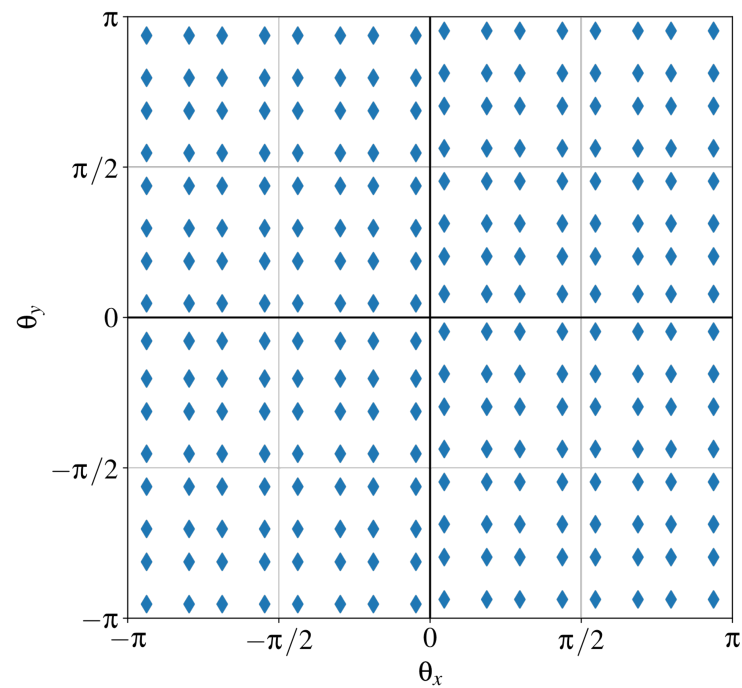
■ Filters generated by the DT-CWPT

Case $J = 3$ (three levels of dual-tree decomposition):

$$\kappa = \pi/4;$$

$$m = 4;$$

128 filters + complex conjugates.



Experiments

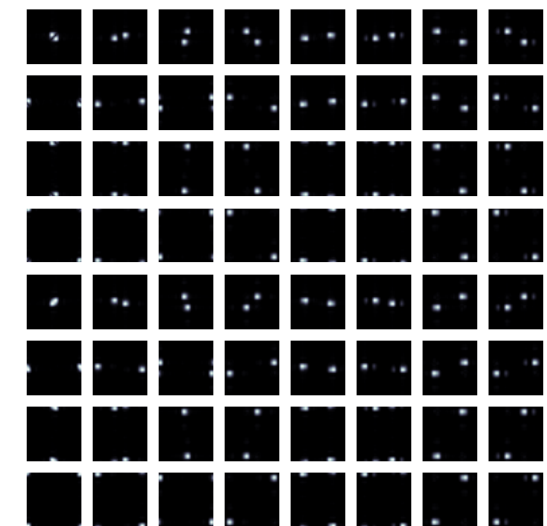
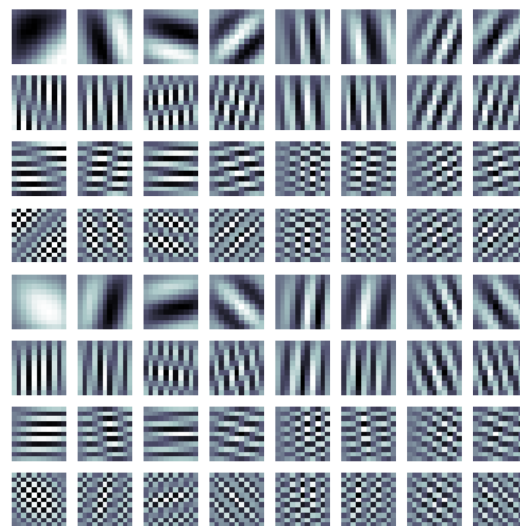
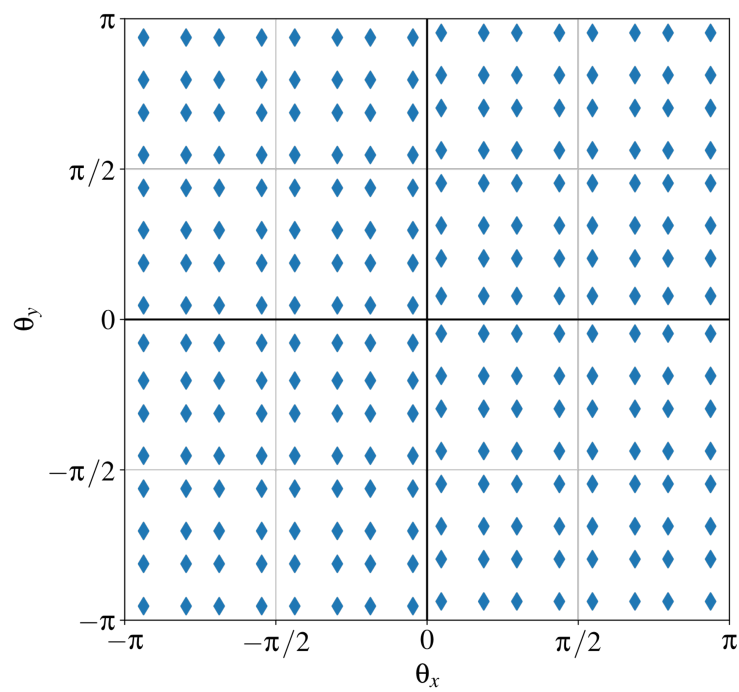
Filters generated by the DT-CWPT

Case $J = 3$ (three levels of dual-tree decomposition):

$$\kappa = \pi/4;$$

$$m = 4;$$

128 filters + complex conjugates.



DT-CWPT
(subset, real
part only)

Experiments

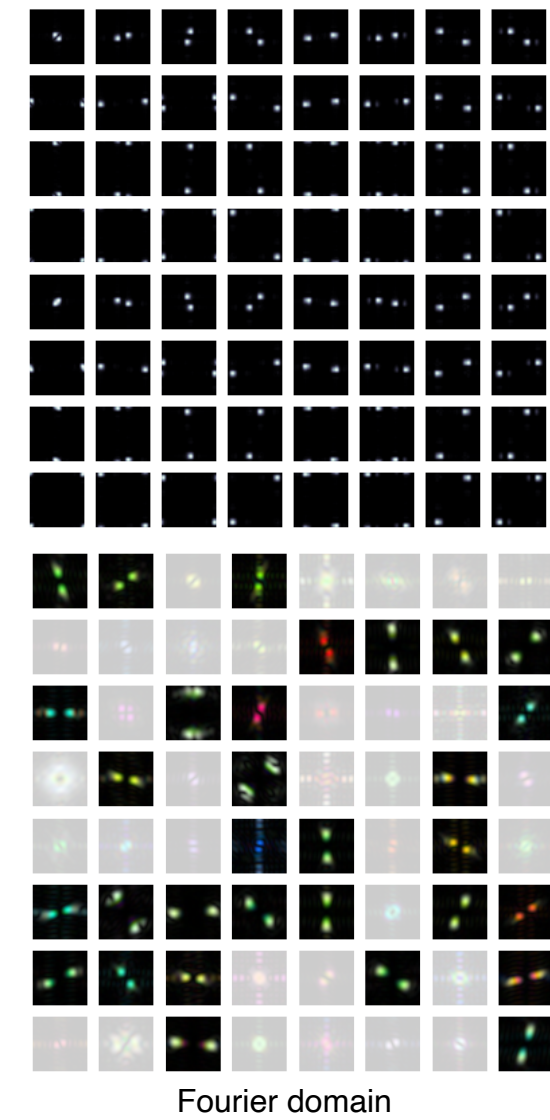
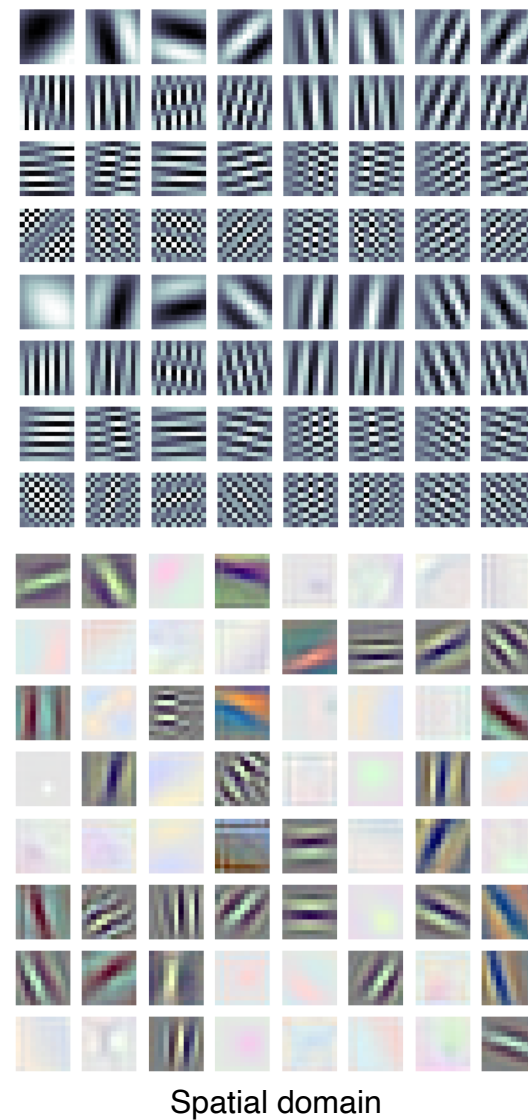
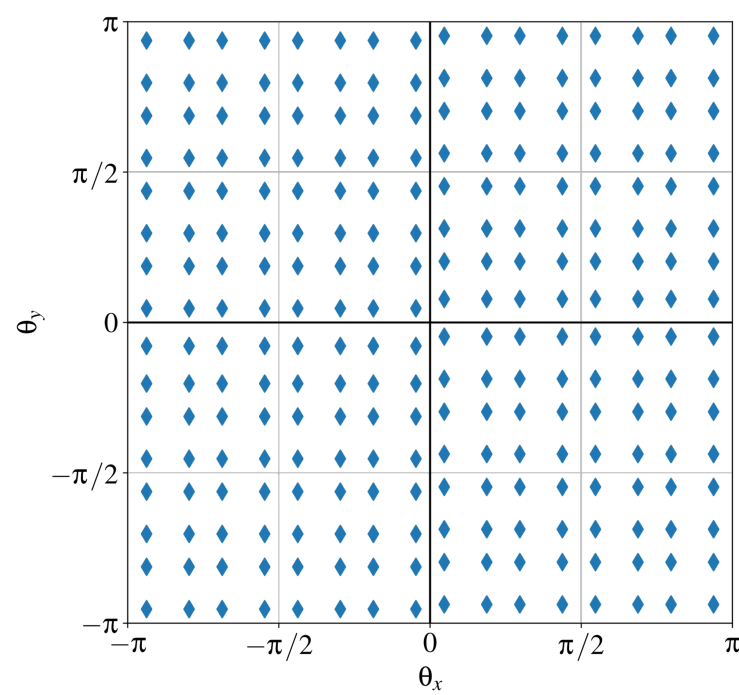
Filters generated by the DT-CWPT

Case $J = 3$ (three levels of dual-tree decomposition):

$$\kappa = \pi/4;$$

$$m = 4;$$

128 filters + complex conjugates.

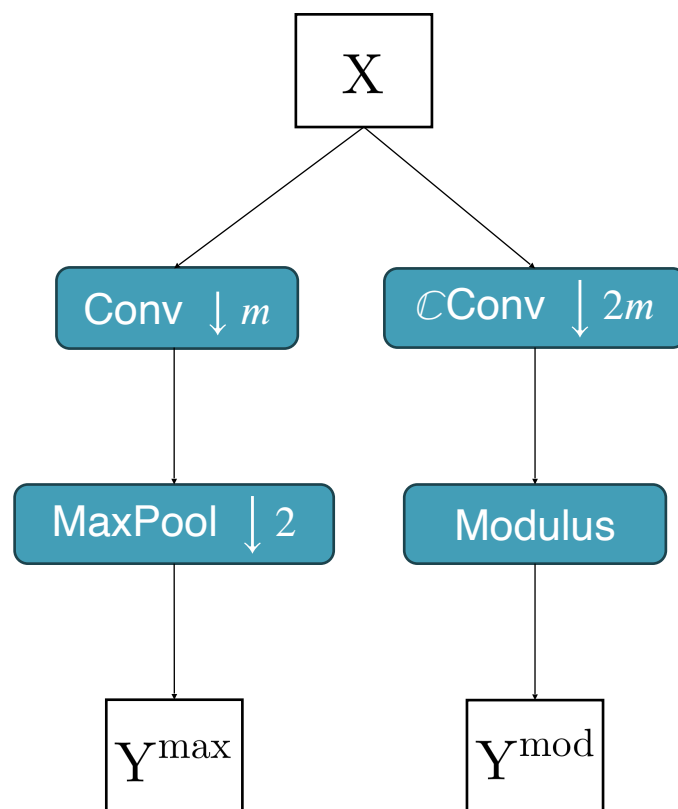


DT-CWPT
(subset, real part only)

AlexNet

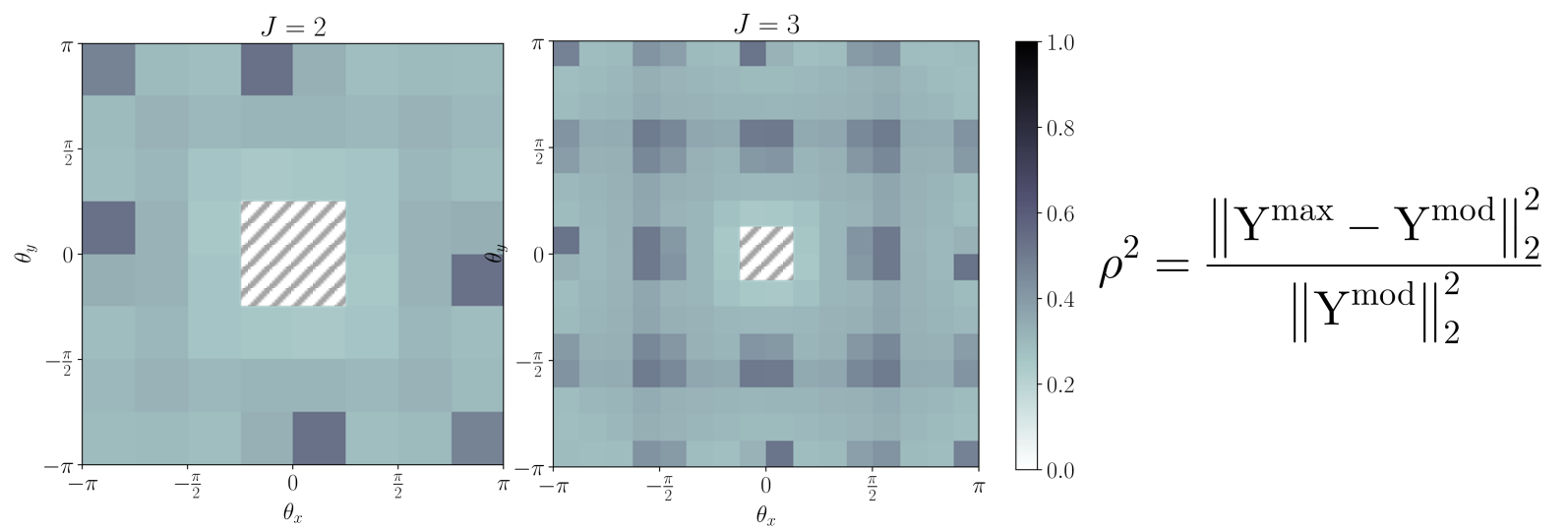
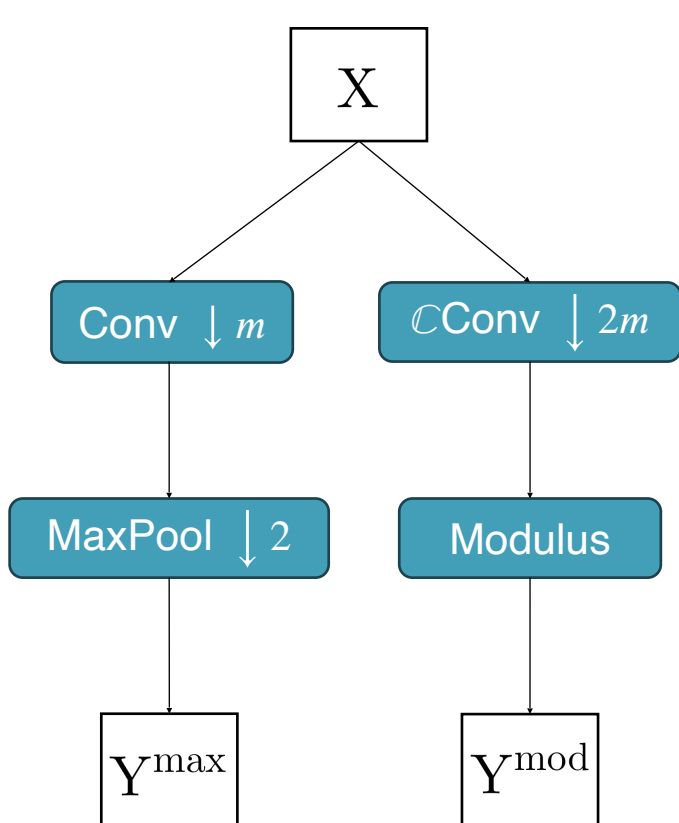
Experiments

- Normalized MSE between $\text{\textit{CMod}}$ and $\text{\textit{RMax}}$



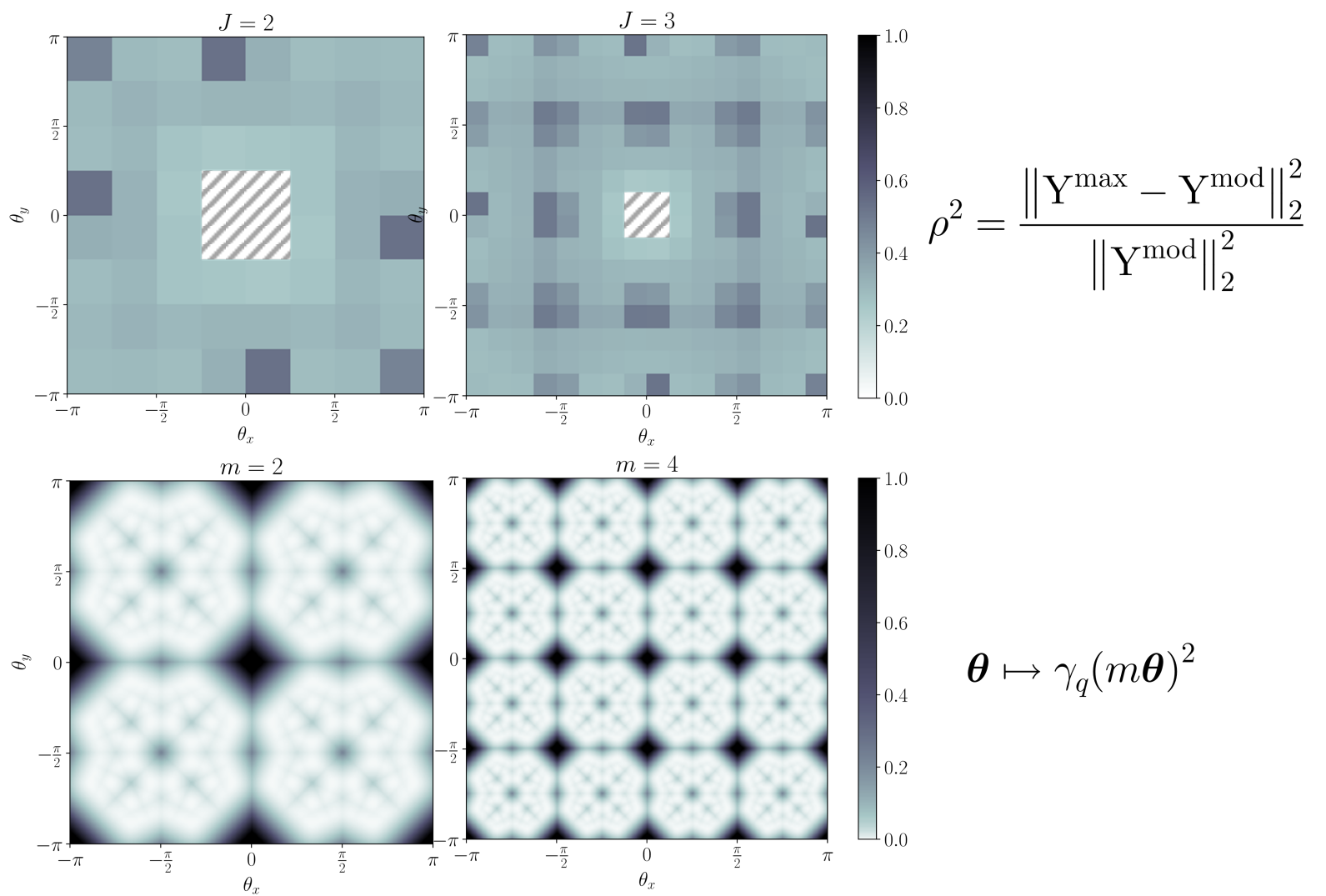
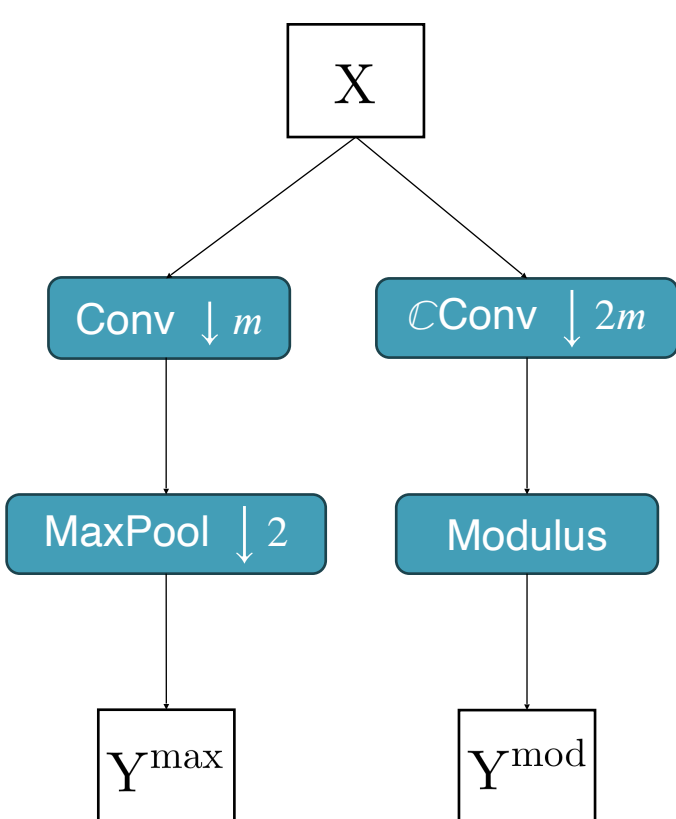
Experiments

Normalized MSE between $\mathcal{C}\text{Mod}$ and $\mathcal{R}\text{Max}$



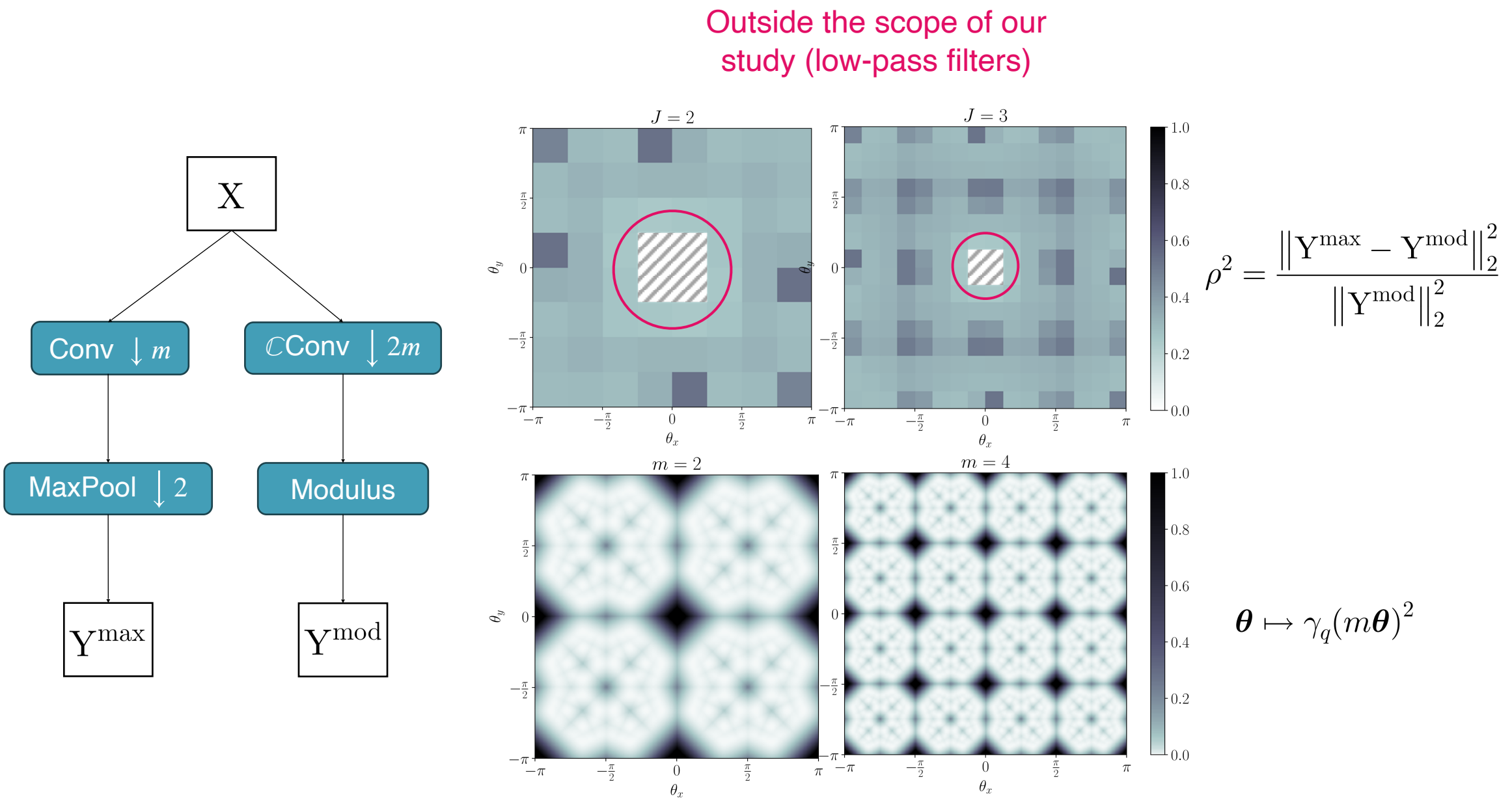
Experiments

Normalized MSE between $\mathcal{C}\text{Mod}$ and $\mathcal{R}\text{Max}$



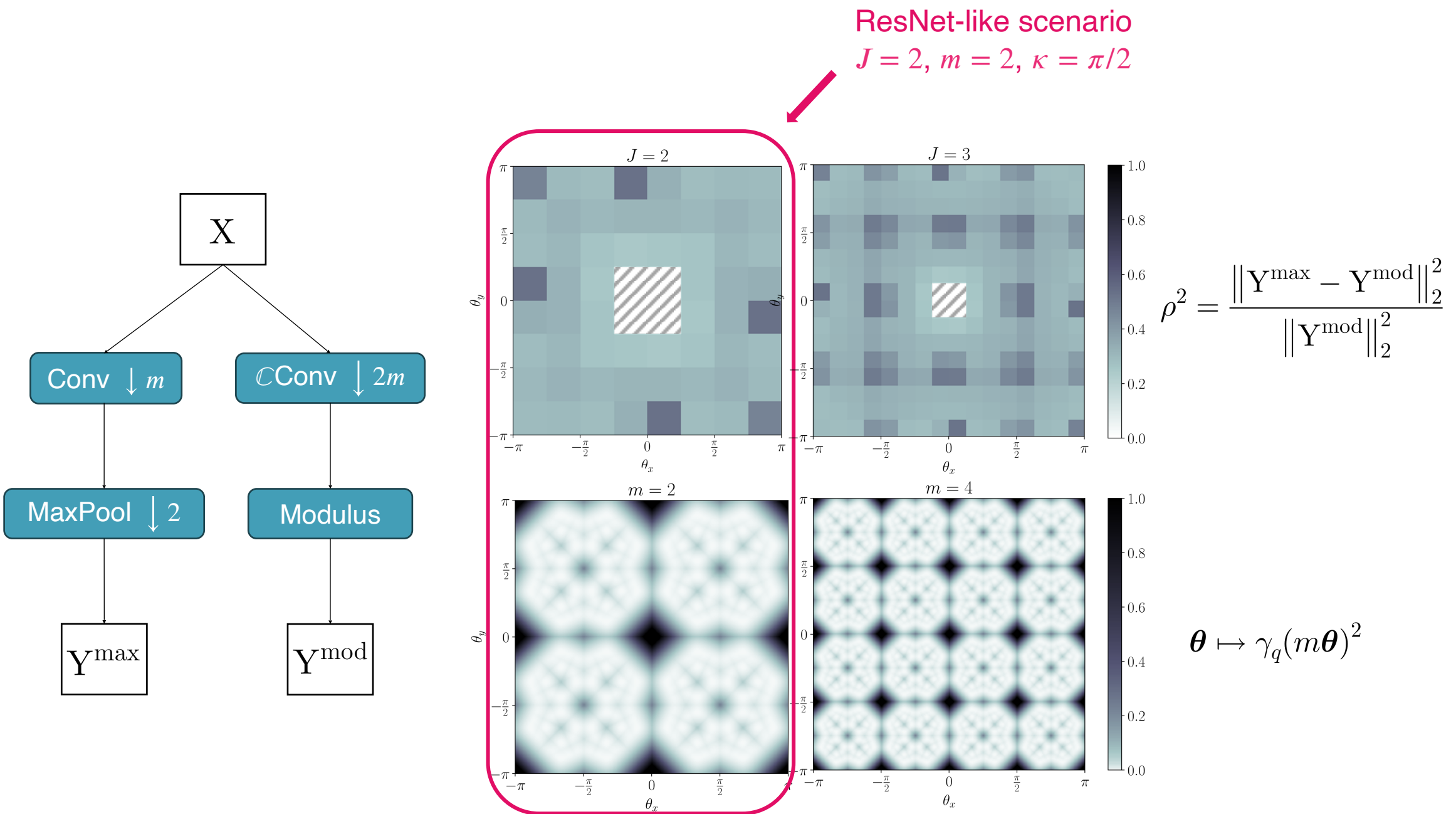
Experiments

Normalized MSE between $\mathcal{C}\text{Mod}$ and $\mathcal{R}\text{Max}$



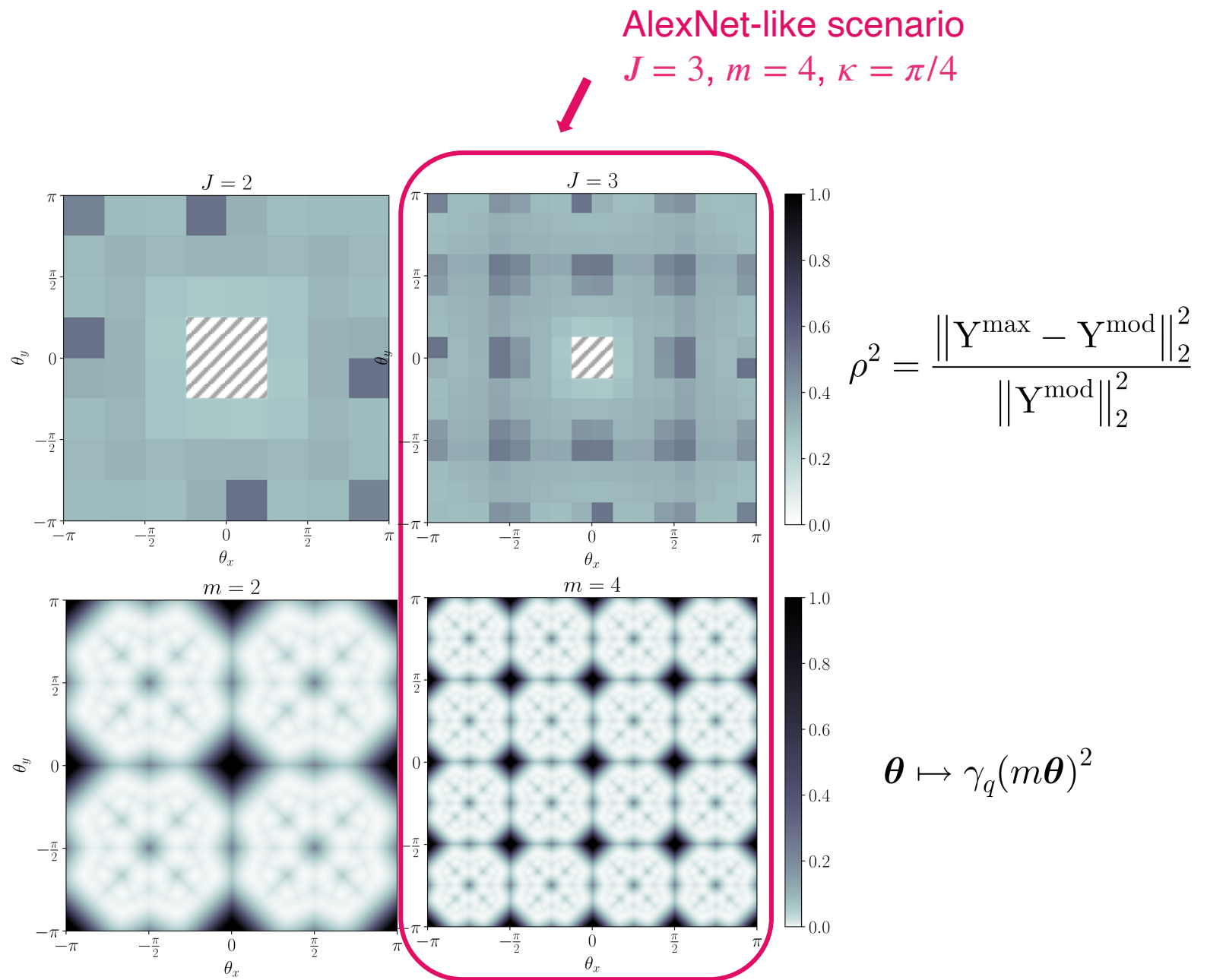
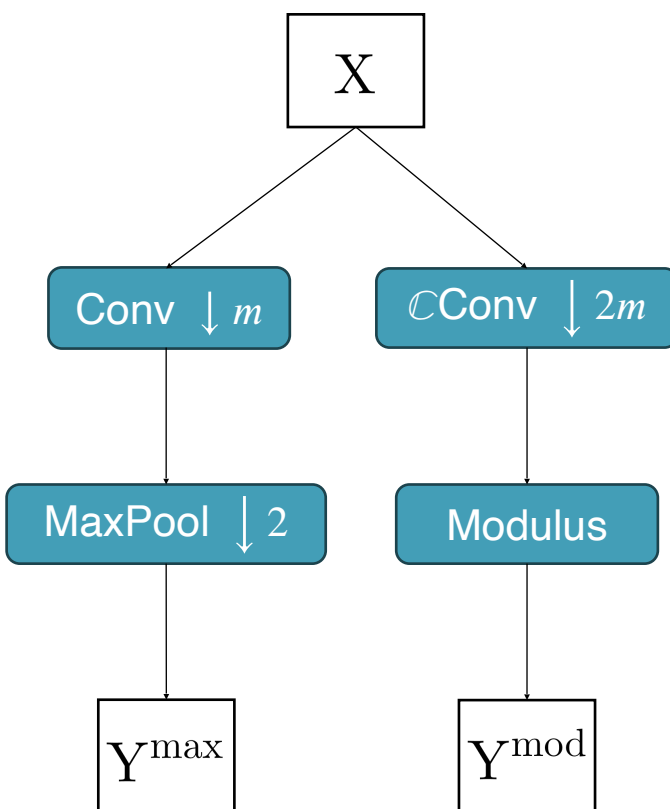
Experiments

Normalized MSE between $\mathcal{C}\text{Mod}$ and $\mathcal{R}\text{Max}$



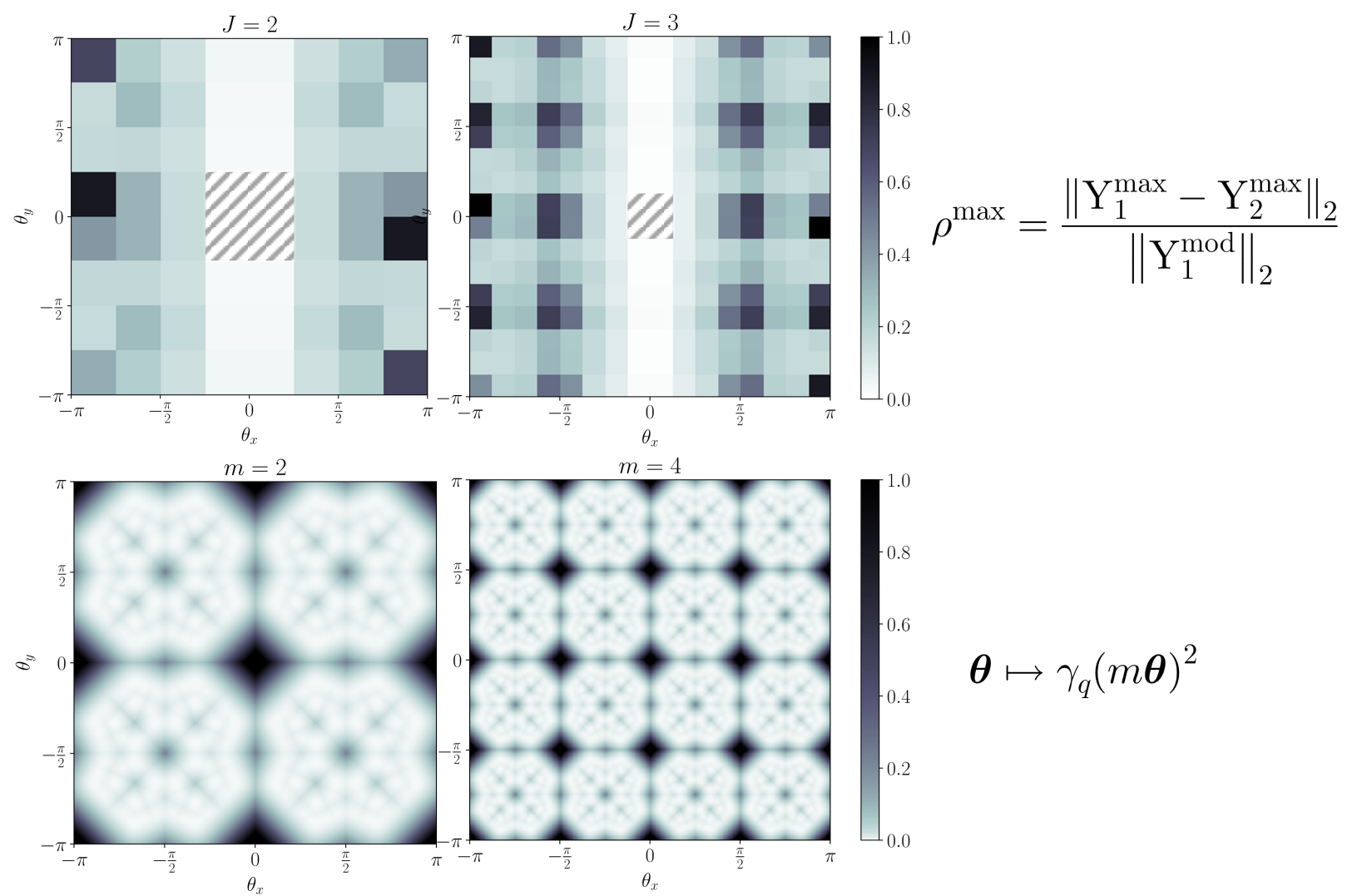
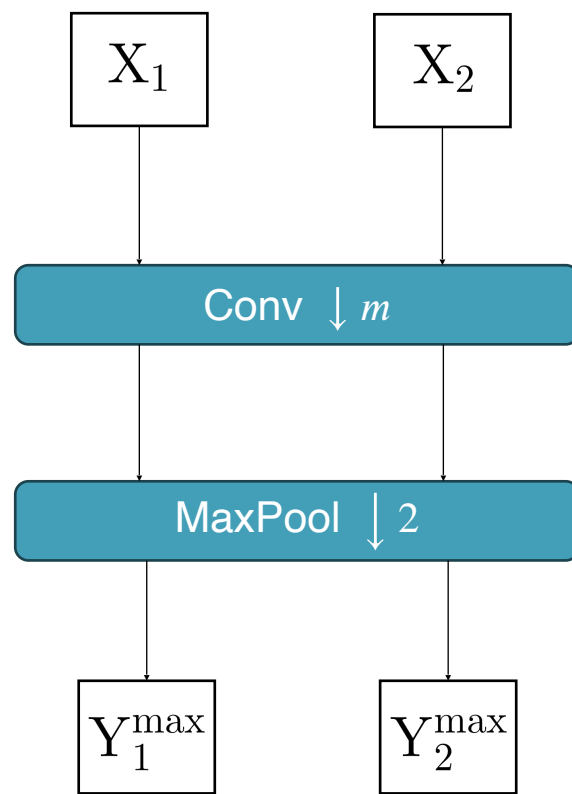
Experiments

Normalized MSE between $\mathcal{C}\text{Mod}$ and $\mathcal{R}\text{Max}$



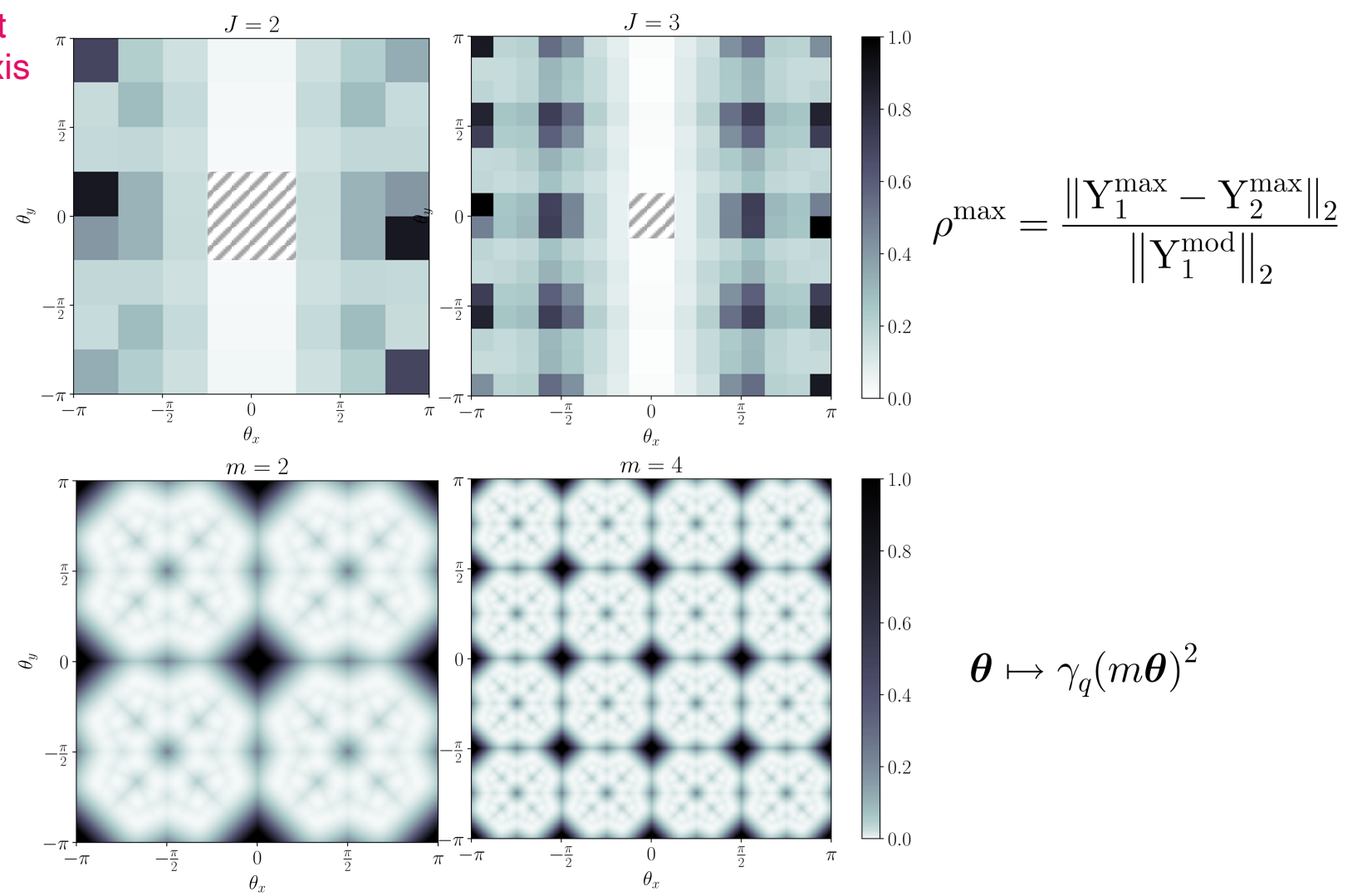
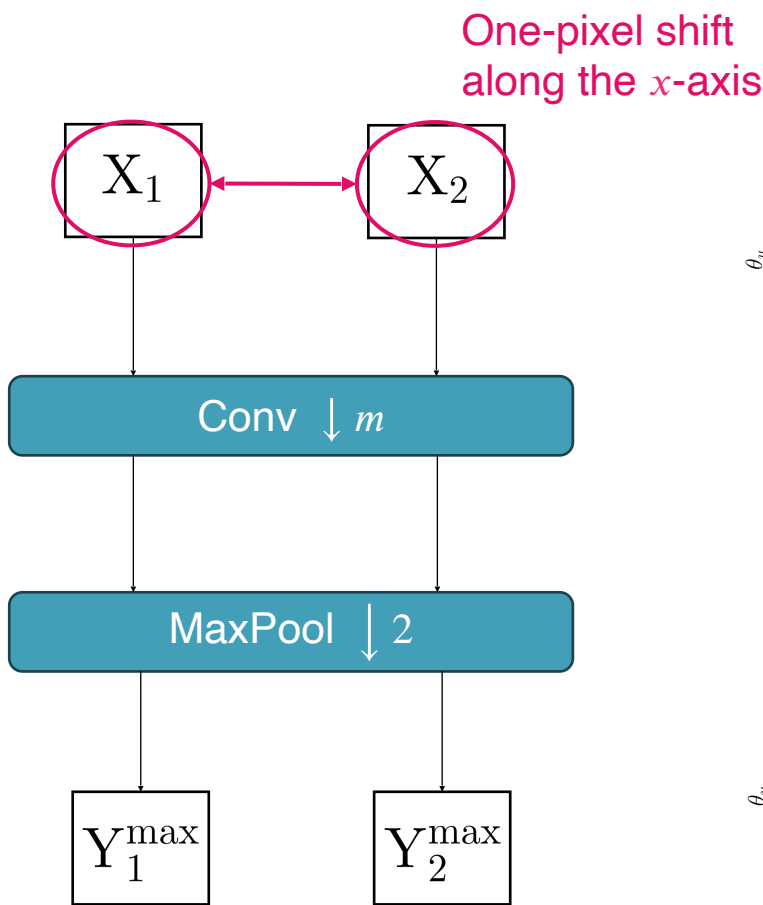
Experiments

■ Shift-invariance of **RMax** outputs



Experiments

Shift-invariance of **RMax** outputs



Conclusion

Conclusion

- Exploration of the **shift invariance** properties captured by the **max pooling** operator, when applied on the **first layer**.

Conclusion

- Exploration of the **shift invariance** properties captured by the **max pooling** operator, when applied on the **first layer**.
- Bridge between **complex** and standard **real CNNs**.

Conclusion

- Exploration of the **shift invariance** properties captured by the **max pooling** operator, when applied on the **first layer**.
- Bridge between **complex** and standard **real CNNs**.
- Study of the **discrete** case in a **probabilist** framework.

Conclusion

- Exploration of the **shift invariance** properties captured by the **max pooling** operator, when applied on the **first layer**.
- Bridge between **complex** and standard **real CNNs**.
- Study of the **discrete** case in a **probabilist** framework.
- Establish a **validity domain** for near-shift invariance.

Conclusion

- Exploration of the **shift invariance** properties captured by the **max pooling** operator, when applied on the **first layer**.
- Bridge between **complex** and standard **real** CNNs.
- Study of the **discrete** case in a **probabilist** framework.
- Establish a **validity domain** for near-shift invariance.
- **Experimental setting** based on the **dual-tree complex** wavelet packet transform

Conclusion

- Exploration of the **shift invariance** properties captured by the **max pooling** operator, when applied on the **first layer**.
- Bridge between **complex** and standard **real** CNNs.
- Study of the **discrete** case in a **probabilist** framework.
- Establish a **validity domain** for near-shift invariance.
- **Experimental setting** based on the **dual-tree complex** wavelet packet transform
- **CMod** operator can serve as a **stable proxy** for **RMax** enabling to **improve shift invariance** in CNNs architecture while preserving high-frequency information.

Publications

- Hubert Leterme, Kévin Polisano, Valérie Perrier, Karteek Alahari. **Modélisation Parcimonieuse de CNNs avec des Paquets d'Ondelettes Dual-Tree.** ORASIS 2021 - Journées francophones des jeunes chercheurs en vision par ordinateur, Centre National de la Recherche Scientifique [CNRS], Sep 2021, Saint Ferréol, France. pp.1-9. <hal-03339792v2>
- Hubert Leterme, Kévin Polisano, Valérie Perrier, Karteek Alahari. **On the Shift Invariance of Max Pooling Feature Maps in Convolutional Neural Networks.** 2023. <hal-03779434v2>
- Hubert Leterme, Kévin Polisano, Valérie Perrier, Karteek Alahari. **From CNNs to Shift-Invariant Twin Models Based on Complex Wavelets.** 2023. <hal-03880520v2>

Thank you!